Development of a Random Time-Frequency Access Protocol for M2M Communication

Submitted for the Degree of Doctor of Philosophy
At the University of Northampton

2019

Riyadh Abedraba Abbas

Dedication

To my parents

For their sacrifices and ceaseless prayers, encouragement and endless love.

To my wife
Sana Adel Majeed

For her endless love and support.

To my children
Rana, Ali, Mohammed, and Hasan

May God bless them.

To my brothers and sister
Amer, Alaa, and Khawla

The hidden strength behind my ever success.

Declaration

I hereby declare that the work described in this thesis is original work undertaken by me for the degree of Doctor of Philosophy, at the Department of Electrical Engineering – University of Northampton, United Kingdom. No part of the material described in this thesis has been submitted for any award of any other degree or qualification in this or any other University or College of advanced education.

Riyadh A. Abbas

Acknowledgements

First and foremost, I thank Allah Almighty for giving me the strength and patience to accomplish this research.

The splendid and challenging journey of my doctoral study would not have been possible without the guidance and kind support of several individuals. I owe my sincerest gratitude and deepest appreciation to my supervisor Dr Ali Al-Sherbaz for his endless support, and for providing me with the freedom and independence that have been essential to the making of this thesis. I also greatly appreciate his care and concern throughout my PhD study.

I am truly indebted and thankful to Prof. Phil Picton and Dr Abdeldjalil Bennecer for their thoughtful and valuable guidance, insightful suggestions in the research work and constant encouragement. Their feedback and constructive criticism have been a great asset to me.

My great appreciation goes to the Iraqi Ministry of Higher Education and Scientific Research who provided me with the financial support needed to complete this research. I would like also to express my grateful thanks to Wasit University for their continuous encouragements and moral support.

I am also very grateful to all my colleagues and the staff at the University of Northampton, especially Dr Ameer Al-Sadi, Dr Naktal Edan, Dr Marwan Aldabbagh, and Dr Hayder Al-Jelawy for their cooperative work and moral support.

My special gratitude is due to my parents for their endless support. Their prayers and blessings were no doubt the true reason behind any success I have realised in my life.

Finally, I should always remember the support and endless wishes of my wife Sana and my lovely children Rana, Ali, Mohammed, and Hasan. I owe sincere and earnest thankfulness to my dearest Brothers Mr. Amer and Mr. Alaa, and my sister Mrs. Khawla for their encouragement and support.

Publications

During the 4-years of the research study, the following papers were published within the Faculty of Arts, Science and Technology at The University of Northampton.

1. 2017, "A new channel selection algorithm for the weightless-n frequency hopping with lower collision probability", Published in *8th International Conference on the Network of the Future (NOF)*, London, UK.
2. 2019, "Collision Evaluation in Low Power Wide Area Networks", Accepted in *the 19th IEEE International Conference on Scalable Computing and Communications (ScalCom 2019),* Leicester, UK.
3. 2019, "Collision Modelling for Random Time-Frequency Access in LPWANs", submitted to Digital Communications and Networks Journal.

Abstract

This thesis focuses on the design and development of the random time-frequency access protocol in Machine-to-Machine (M2M) communication systems and covers different aspects of the data collision problem in these systems.

The randomisation algorithm, used to access channels in the frequency domain, represents the key factor that affects data collisions. This thesis presents a new randomisation algorithm for the channel selection process for M2M technologies. The new algorithm is based on a uniform randomisation distribution and is called the Uniform Randomisation Channel Selection Technique (URCST). This new channel selection algorithm improves system performance and provides a low probability of collision with minimum complexity, power consumption, and hardware resources. Also, URCST is a general randomisation technique which can be utilised by different M2M technologies. The analysis presented in this research confirms that using URCST improves system performance for different M2M technologies, such as Weightless-N and Sigfox, with a massive number of devices.

The thesis also provides a rigorous and flexible mathematical model for the random time-frequency access protocol which can precisely describe the performance of different M2M technologies. This model covers various scenarios with multiple groups of devices that employ different transmission characteristics like the number of connected devices, the number of message copies, the number of channels, the payload size, and transmission time.

In addition, new and robust simulation testbeds have been built and developed in this research to evaluate the performance of different M2M technologies that utilise the random time-frequency access protocol. These testbeds cover the channel histogram, the probability of collisions, and the mathematical model. The testbeds were designed to support the multiple message copies approach with various groups of devices that are connected to the same base station and employ different transmission characteristics.

Utilising the newly developed channel selection algorithm, mathematical model, and testbeds, the research offers a detailed and thorough analysis of the performance of Weightless-N and Sigfox in terms of the message lost ratio (MLR) and power consumption. The analysis shows some useful insights into the performance of M2M systems. For instance, while using multiple message copies improves the system performance, it might degrade the reliability of the system as the number of devices increases beyond a specific limit. Therefore, increasing the number of message copies can be disadvantageous to M2M communication performance.

Table of contents

List of Figures

List of Tables

List of Abbreviations

3GPP	3rd Generation Partnership Group
6LoWPAN	Internet Protocol Version 6 (IPv6) Over Low-Power Wireless Personal Area Networks
AFH	Adaptive Frequency Hopping
AIND	Adaptive Increase No Division
AMI	Advanced Metering Infrastructure
AP	Access Point
ASK	Amplitude Shift Keying
BER	Bit Error Rate
BLAST	Bursty, Light, Asynchronous, Stealth, and Transitional
BLE	Bluetooth Low Energy
bps	Bit Per Second
BPSK	Binary Phase Shift Keying
CE	Coverage Enhancement
CRC	Cyclic Redundancy Check
CSMA	Carrier Sense Multiple Access
CSMA/CA	Carrier Sense Multiple Access with Collision Avoidance
CSS	Chirp Spread Spectrum
dBm	Decibels with reference to one milliwatt
DBPSK	Differential Binary Phase Shift keying
DS-OFDM	Direct Sequence Orthogonal Frequency Division Multiplexing
DSSS	Direct Sequence Spread Spectrum
eMTC	Enhanced Machine Type Communication
FCC	Federal Communications Commission
FCS	Frame-Check Sequence
FDMA	Frequency Division Multiple Access
FEC	Forward Error Correction
FFD	Full Function Devices

FH	Frequency hopping
FSK	Frequency Shift Keying
GFSK	Gaussian Frequency Shift Keying
GMSK	Gaussian Minimum Shift Keying
GSM	Global System for Mobile
GUI	Graphical User Interface
IDB	Inter-Domain Bridges
ID	Identifier
IEC	International Electrotechnical Commission
IoT	Internet of Things
IR-UWB	Impulse Radio Ultra-Wide Band
ISM	Industrial, Scientific, and Medical
ISO	International Organization for Standardization
ITU-T	International Telecommunications Union - Telecommunication Standardization Sector
LBT	Listen Before Talk
LPWA	Low Power Wide Area
LPWANs	Low Power Wide Area Networks
LTE	Long-Term Evolution
LTE-M	Long-Term Evolution - category M (machine type communication)
M2M	Machine-to-Machine
MAC	Medium Access Control
MB-OFDM	Multiband Orthogonal Frequency Division Multiplexing
MCL	Maximum Coupling Loss
MLR	Message Lost Ratio
MPDCCH	Machine-type Physical Download Control Channel
MT19937	Mersenne Twister Algorithm
MTC	Machine Type Communication
NB-IoT	Narrowband Internet of Things
NPRACH	Narrowband Physical Random Access Channel

NPUSCH	Narrowband Physical Uplink Shared Channel
NRMSE	Normalised Root Mean Square Error
NSE	Nash-Sutcliffe Coefficient of Efficiency
OFDM	Orthogonal Frequency Division Multiplexing
OFDMA	Orthogonal Frequency-Division Multiple Access
OQPSK	Offset Quadrature Phase Shift Keying
PHY	Physical
PPM	Pulse Position Modulation
PRAW	Periodically Restricted Access Window
PRBs	Physical Resource Blocks
PSD	Power Spectral Density
PUSCH	Physical Upload Shared Channel
QAM	Quadrature Amplitude Modulation
QoS	Quality of Service
QPSK	Quadrature Phase Shift Keying
RAIND	Random Adaptive Increase No Division
RAM	Random-Access Memory
RAW	Restricted Access Window
RF	Radio Frequency
RFD	Reduced Function Devices
RFID	Radio Frequency Identification
RIGD	Random Increase Geometric Division
RPMA	Random Phase Multiple Access
SCADA	Supervisory Control and Data Acquisition
SC-FDMA	Single-Carrier Frequency Division Multiple Access
SF	Spreading Factors
SINR	Signal-to-Interference-Plus-Noise Ratio
STAs	Stations
TDD	Time Division Duplex

TDMA	Time Division Multiple Access
TH-UWB	Time hopping - Ultra-Wide Band
TIM	Traffic Indication Map
UNB	Ultra-Narrow Band
URCST	Uniform Randomisation Channel Selection Technique
UWB	Ultra-Wide Band
WSN	Wireless Sensor Network
WSP	Wireless Short-Packet
ZC	ZigBee Coordinator
ZED	ZigBee End Device
ZR	ZigBee Router

Chapter 1

Introduction

1.1 Introduction

Wireless communication has grown tremendously over the last decade, especially now that the Internet has become an essential part of many peoples' lives, and billions of devices are using wireless communication to connect to the Internet. Although it seems that it is mainly human use, such as mobile phones and laptops, there is another significant form of wireless communication which is entirely different. This class of communication is called Machine-to-Machine (M2M) communication (or Machine Type Communication MTC), which is based on applications for devices that can work autonomously and do not require human intervention during the operation phase. M2M communications are not initiated by people but occur according to the function of the device. M2M communication has unique characteristics which need to be considered in the design and implementation of wireless systems (Al-Shammari *et al.*, 2018; Webb, 2015; Anton-Haro and Dohler, 2015; Webb, 2012c).

1.2 M2M Communication Architecture and Features

The importance of M2M communication systems has been increasing recently, especially with the emergence of the Internet of Things (IoT) and smart cities. IoT refers to the connectivity of any physical object to the internet so that it can send and receive data and information. M2M communication represents the cornerstone of the IoT and smart cities, where most of the connected devices comprise sensors and actuators (Ding *et al.*, 2019; Jia *et al.*, 2019; Al-Shammari *et al.*, 2018).

M2M systems are mainly based on short messages/low rate communication between devices. In general, the architecture of M2M systems is principally comprised of three domains: M2M device domain, M2M Network domain, and M2M application domain. Devices in the M2M device domain can either communicate directly to the base station or communicate with each other to form a device area network. Communication technologies used to connect devices in this domain should be aware of the individual requirements of M2M communication. Therefore, many M2M communication technologies have been proposed in the last couple of decades with distinctive design consideration to fulfil these requirements. Figure 1.1 illustrates an overview of a typical M2M communication system where devices can send and receive data to the network via the base station (Al-Shammari

et al., 2018; Verma *et al.*, 2016; Ghavimi and Chen, 2015; Webb, 2015; Anton-Haro and Dohler, 2015).

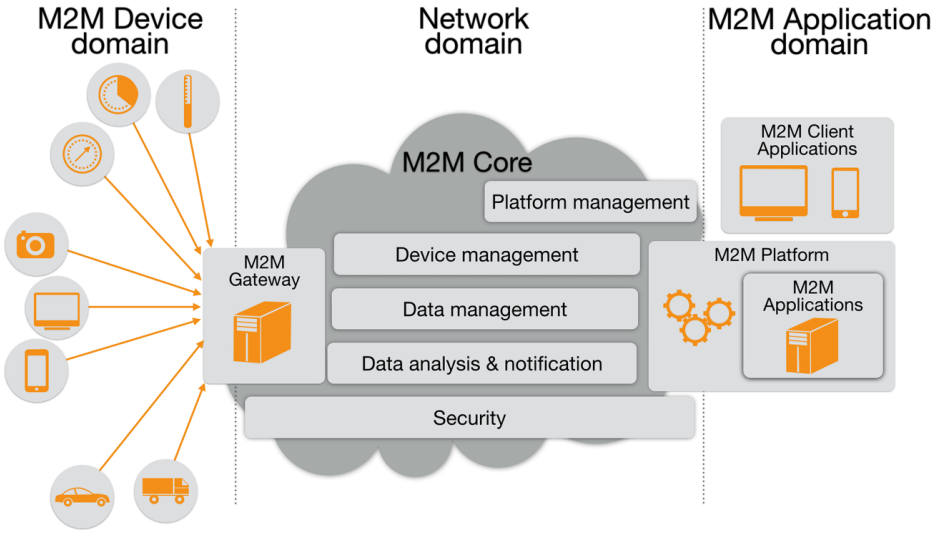

Figure 1.1: An overview of a typical M2M communication system (Digital Technology Poland, 2019).

M2M communication should provide ubiquitous connectivity between devices with a broad range of applications. Therefore, M2M communication should offer unique features and characteristics which can be summarised as follows (Webb, 2015; Anton-Haro and Dohler, 2015; Webb, 2012c):

- ***Support of a massive number of nodes***. Each base station can serve hundreds of thousands of devices.
- ***Excellent coverage***. Each base station should offer communication for all devices connected to the M2M device domain. Some M2M technologies provide a communication range of 2-5 km in urban areas with 100% outdoor and indoor coverage.
- ***Ultra-low power consumption***. Devices should work with minimum power consumption so that a network lifetime of 10 years on a single battery can be offered.
- ***Low cost***. The total cost should be within $2- $5 for terminal devices with only a few dollars a year for a network subscription.

- ***Diverse Quality-of-Service (QoS)***. Some applications required high quality of service (QoS) with guaranteed message delivery while other applications allow lossy communication. M2M technologies should offer services for both types of applications.
- ***Low data rate***. M2M communication is quite distinct from human communications and can be accomplished using only a few hundreds to several thousand bits per second (bps).
- ***Low message rate***. Most M2M communication requires a low message rate within the range of several messages per day up to one message per minute.
- ***Short messages***. Most of the information exchanged between M2M devices can be achieved with short messages that only have several bytes of data.

These special attributes pose some critical challenges to the design and implementation of M2M technologies, especially supporting a massive number of devices with minimum power consumption.

1.3 Problem Statement

M2M communication is a very promising paradigm especially with the extension of Internet into physical objects. Many M2M communication technologies have been proposed to meet the unique set of requirements and characteristics of M2M systems. With the wide diversity of applications in the IoT and smart cities, a massive number of devices is expected to be connected to each base station (Mekki *et al.*, 2019; Al-Shammari *et al.*, 2018; Goursaud and Gorce, 2015; Pereira and Aguiar, 2014). This represents the most critical challenge to the M2M communication systems, where data collisions become an inevitable problem that substantially affect message delivery and system performance and reliability (Li *et al.*, 2017; Centenaro *et al.*, 2017; Vejlgaard *et al.*, 2017; Lauridsen *et al.*, 2016). The process of designing a communication technology that can support such an enormous number of devices and maintain other M2M system requirements, such as low power consumption and low cost, is quite challenging. Although the use of acknowledgements, synchronisation, and channel sense mechanisms can improve system performance, it significantly increases power consumption and the cost of terminal devices. Therefore, most M2M technologies rely on the random time-frequency access protocol (ALOHA-based random access protocol) with the frequency hopping technique to reduce the probability of collisions while retaining the other virtues of the M2M communication. In addition, some M2M technologies utilise a multiple-message copies approach in order to increase the rate of successful message delivery and improve system performance. This

can significantly improve system performance within specific limits which are related to other system characteristics, like the number of connected devices, the number of channels, and the payload size. Using this approach poses some other challenges to the evaluation and modelling of M2M communication technologies.

With the random time-frequency access protocol, the randomisation algorithm used to access channels is the key factor that affects the probability of collisions and system performance. Using high performance randomisation algorithms, like Mersenne Twister algorithm, can significantly reduce the probability of collisions. However, such algorithms are highly complex and require high computational time and hardware resources. This can significantly increase the cost and power consumption of terminal devices. Therefore, it is crucial to develop a random channel selection protocol that offers the lowest probability of collisions with minimum complexity, power consumption, and hardware resources.

It is also essential to evaluate how efficient the designed technique is. This step is vital during the early stages of system design to ensure its reliability and represents another major challenge for the design and implementation of M2M communication systems. This is due to the high complexity and cost of conducting such evaluation in real systems with a massive number of devices. Therefore, it is crucial to provide a reliable evaluation environment for such systems by developing simulation testbeds and mathematical models.

The work presented in this thesis covers different aspects of the data collision problem in M2M systems. It provides a novel channel selection technique, simulation testbeds, and a mathematical model for M2M technologies that employ random time-frequency access protocol with the frequency hopping technique and the multiple message copies method.

1.4 Aims and Objectives

Data collisions represent the most important challenge for the IoT and M2M communication technologies due to the interference between the enormous number of connected devices. Although collisions are directly related to the number of nodes, it is also dependent on other system characteristics. Therefore, the aims of this research are:

- Design a new channel selection technique that can provide a low probability of collisions for M2M communication technologies that utilise the random time-frequency access protocol with minimum power consumption, complexity, and hardware resources.

- Develop a reliable evaluation environment (rigorous mathematical model and robust testbeds) to study the effect of different transmission characteristics on the collisions in M2M communication technologies that employ the random time-frequency access protocol.

The objectives of this research are:

1. Investigate the existing M2M communication technologies and explore the collision mitigation techniques that are implemented in these technologies.
2. Design and develop new simulation testbeds (called URCST simulators) that can be used to evaluate the effect of different transmission characteristics on the performance of M2M systems in terms of collisions. These new developed simulators are capable of analysing system performance involving multiple groups of devices with variant transmission characteristics and the multiple message copies approach.
3. Provide a mathematical model that can accurately describe the performance of M2M technologies that utilise the random time-frequency access protocol with multiple groups of devices and the multiple message copies approach including different transmission characteristics.
4. Evaluate the performance of the newly developed channel selection algorithm in comparison with the standard algorithm and other prominent randomisation algorithms using some well known M2M technologies.
5. Study the effects of various transmission characteristics, such as the number of message copies and the payload size, on the performance of different M2M technologies with the presence of a massive number of devices.
6. Evaluate the performance of different M2M technologies in terms of collisions and power consumption using a practical IoT application that requires a vast number of devices like smart meters.

1.5 Research Contributions

The research contributions presented in this thesis cover different aspects of the data collision problem in M2M communication. The key outcomes of this work can be summarised as follows:

1. An extensive study of a broad range of M2M communication technologies with a particular focus on collision avoidance techniques.

2. Design and development of a novel random channel selection technique that provides a low probability of collisions with minimum complexity, power consumption, and hardware resources.
3. Design and development of robust simulation testbeds for M2M technologies which utilise the random time-frequency access protocol. These testbeds support multiple groups, multiple message copies, and diverse system parameters.
4. Derivation of a rigorous mathematical model for the random time-frequency access protocol with the support of multiple groups of devices and multiple message copies.
5. A thorough and comprehensive analysis of two prominent M2M technologies in terms of collisions and power consumption, which offers some fresh insights into the performance of ALOHA-based M2M technologies and the effect of different transmission characteristics on the collisions problem.

1.6 Scope of Work

Supporting millions of connected devices in the IoT and smart cities inevitably creates a competition over the transmission channel for the existing M2M technologies. Many of them have been specifically developed to resolve these challenges and fulfil M2M communication requirements. Most of these technologies utilise the random time-frequency access protocol to maintain low complexity, low cost, low power consumption, and low probability of collisions. In general, the incumbent protocols only work to optimise one parameter such as message interference at the expense of other equally important requirements of power consumption and cost. On the other hand, the novel communication channel access randomisation algorithm developed in this thesis offers superior performance for each criterion.

In order to evaluate the performance of the newly developed channel selection technique and the newly developed mathematical model, it is vital to select appropriate M2M technologies. In general, short-range M2M technologies, like Zigbee and Bluetooth, are mainly designed for home and residential IoT applications with several tens to several hundreds of devices per cell over distances of less than 100 m. This may not put a significant strain on the communication channel, as explained in Chapter 2. Therefore, Low Power Wide Area (LPWA) technologies are the most proper choice for this intention.

To study the collision problem with the massive number of devices that are required in the IoT and smart cities, two candidate LPWA M2M technologies, namely Weightless-N and Sigfox, are nominated as case studies for this research. Both technologies utilise the

ALOHA-based random time-frequency access protocol without acknowledgements, synchronisation, or any channel sense mechanism. In addition, these two technologies employ the frequency hopping technique with a large number of ultra-narrow band (UNB) channels to extend the wireless system capability and support a massive number of nodes. Furthermore, both technologies utilise multiple message copies to mitigate the effect of collisions on the system performance and reduce the probability of lost messages (Weightless-SIG, 2015c; Abbas *et al.*, 2017; Sigfox, 2019a; Sigfox, 2017b; Sigfox, 2017a; Sigfox, 2017c). Both technologies claim to support an extremely large number of connected devices within the range of several hundreds of thousands up to one million devices, as described in Chapter 2. Therefore, Weightless-N and Sigfox represent the preferred wireless technologies to study the effect of collisions and assess the developed technique and model.

1.7 Thesis Structure

This thesis is structured into six chapters. Following the general introduction presented in this chapter, the rest of the thesis is organised as follows:

- ***Chapter 2***. This chapter provides a detailed study of the characteristics of M2M communication. Various M2M technologies are presented in this chapter with a detailed description of each technology specifications with a focus on the number of connected devices and the collisions avoidance techniques utilised by these technologies.
- ***Chapter 3***. This chapter presents the novel developed channel selection technique called Uniform Randomisation Channel Selection Technique (URCST), which provides a low probability of collision with minimum complexity and power consumption. The chapter also offers a comparison of system performance using the Weightless-N standard algorithm, the URCST algorithm, and the standard uniform random distribution algorithm called Mersenne Twister (MT19937).
- ***Chapter 4***. The newly derived mathematical model for the random time-frequency access protocol is described in this chapter. First, previous contributions in the mathematical modelling of ALOHA-based wireless communication systems are presented. Second, a thorough description of the mathematical derivation of the new model is demonstrated for different system scenarios including multiple groups of devices and multiple message copies. Third, model validation is presented using

Weightless-N and Sigfox M2M technologies with different working scenarios. Finally, the chapter demonstrates the limitations of the presented model.

- ***Chapter 5***. In this chapter, an evaluation of the performance of Weightless-N and Sigfox technologies is demonstrated in terms of the message lost ratio and power consumption. The analysis presented in this chapter is based on the newly developed channels selection technique and the newly developed mathematical model. The evaluation considers various scenarios and studies the effect of different transmission parameters on system performance including the number of devices, the number of message copies, the payload size, the transmission time, and the number of utilised channels. Also, this chapter offers a detailed analysis of smart meters as a case study for IoT and smart cities applications.
- ***Chapter 6***. This chapter concludes the study presented in this thesis and offers recommendations for future research directions.

Chapter 2

M2M Technologies and Collisions Avoidance Techniques

2.1 Introduction

The internet of things (IoT) and smart cities represent the new revolutionary era in internet technology and telecommunication systems. IoT is aimed at the ability of connecting everyone and every physical device in the world to the internet (Ding *et al.*, 2019; Jia *et al.*, 2019; Bao *et al.*, 2018; Farooq and Zhu, 2018; Xu *et al.*, 2018; Esfahani *et al.*, 2017; Centenaro *et al.*, 2017; Waidner and Kasper, 2016). This poses several critical challenges to wireless communication technologies like the coverage range, the number of connected devices, the power consumption, and the cost of the network. However, with such a wide diversity of applications, a massive number of devices is expected to be connected to each base station (Mekki *et al.*, 2019; Goursaud and Gorce, 2015; Pereira and Aguiar, 2014). Consequently, the data collision problem becomes a vital factor that affects system performance and reliability. This represents one of the most important challenges that face the design and implementation of wireless communication technologies. This chapter provides a general background of diverse wireless communication technologies that are mainly designed for IoT applications. It focuses on the data collision problem and discusses the collision avoidance techniques utilised by different wireless technologies to mitigate its effect on system performance.

In general, the IoT is mainly based on the machine type communication (MTC), or machine-to-machine (M2M) communication systems, where sensors and actuators represent most of the connected devices to the IoT (Ding *et al.*, 2019; Al-Shammari *et al.*, 2018; Xu *et al.*, 2018; Esfahani *et al.*, 2017; Qian *et al.*, 2017; Goursaud and Gorce, 2015; Biral *et al.*, 2015; Pereira and Aguiar, 2014). A machine-to-machine communication system denotes the communication technologies between devices that work autonomously without the interaction of humans during the operation phase (Al-Shammari *et al.*, 2018; Anton-Haro and Dohler, 2015; Kim *et al.*, 2014; Pereira and Aguiar, 2014; Laya *et al.*, 2014; Chen, 2013). M2M systems can be considered as to have evolved from the classic Wireless Sensor Networks (WSN), which can provide reliable communication for monitoring and control applications. Supervisory control and data acquisition (SCADA) systems can be assumed as a primitive form of M2M communication, which is based on controlling multiple separated systems via a central control unit (Kim *et al.*, 2014; Lien *et al.*, 2011). However, with the massive number of connected devices that are required in

smart cities and the IoT, it is not feasible to use such a system. The total number of connected devices will increase significantly in the next few years, and it is predicted that there will be 50 billion devices connected to the IoT by the end of 2020 (Zhang *et al.*, 2019; Mekki *et al.*, 2019; Jia *et al.*, 2019; Al-Shammari *et al.*, 2018; Xu *et al.*, 2018; Evans, 2011; Webb, 2015; Ghavimi and Chen, 2015; Vermesan and Friess, 2014; Ofcom, 2014).

M2M communication systems are mainly built on a short message low rate exchange approach between devices (Webb, 2015; Anton-Haro and Dohler, 2015; Webb, 2012c). For instance, a smart meter sends more than a few messages per a day, considering it typically reports to the utility every 15 minutes (Andreadou *et al.*, 2018; Wang *et al.*, 2018; Barai *et al.*, 2015; Karimi *et al.*, 2015; Balachandran *et al.*, 2014; Budka *et al.*, 2014). On the other hand, some M2M systems should maintain high reliability and Quality of Service (QoS) with minimum power consumption, which requires special technical consideration and improvements to the design of these systems. This creates the need for new communication systems with unique characteristics that are entirely different from the available human communication systems. Figure 2.1 shows a typical M2M communication system architecture in which devices can send and receive data to the database via the base station (Webb, 2015; Anton-Haro and Dohler, 2015).

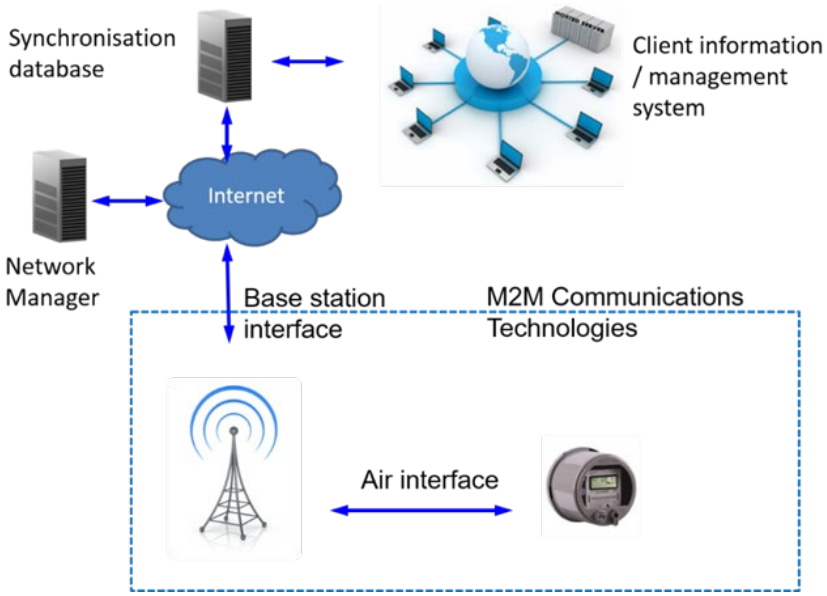

Figure 2.1: M2M communication system architecture (Webb, 2015).

This chapter provides a general background of M2M communication systems and describes in detail the prominent M2M technologies and the collision mitigation

techniques utilised by them. In this chapter, the M2M communication technologies are divided into two main categories: short-range M2M technologies, which are described in section 2.3, and long-range M2M technologies, which are discussed in section 2.4. In addition, the chapter provides a summary of each category, as presented in sections 2.3.8 and 2.4.9 respectively. Finally, a general summary of the M2M communication technologies is presented in section 2.5.

2.2 Machine-To-Machine Technologies and Collision Avoidance Techniques

A number of platforms and architectures have been proposed in the last couple of decades to meet the special requirements of M2M communication, particularly the communication range, the supported data rate, the power consumption, and the number of connected devices. These characteristics will be outlined and discussed in the next sections. A detailed comparison between the well-known M2M technologies is provided with a particular focus on the problem of interference between devices and the data collision and the techniques that are used to mitigate this problem.

Various channel access schemes are utilised by different M2M technologies to mitigate the data collision problem and improve the successful packet transmission. A few examples include the ALOHA random access protocol, Listen Before Talk (LBT) mechanism, and the carrier sense multiple access with collision avoidance (CSMA/CA) mechanism. The ALOHA protocol was developed in 1968 at the University of Hawaii to connect computers from different locations and form a radio-linked computer network as an alternative to the conventional wire communication system (Abramson, 2009). It is based on a random time-frequency access scheme where devices send data at any time using available channels without checking the status of channel occupancy (Goursaud and Mo, 2016; Abramson, 2009; Abramson, 1970). In contrast, Listen Before Talk (LBT) is a sort of carrier sense mechanism that was first designed to deal with the coexistence issue. It is used in wireless communication systems whereby a wireless transmitter first senses its wireless environment before starting a transmission. If the channel is occupied, the sensing process will be continuously repeated until the channel is clear (Yin *et al.*, 2016; Centenaro *et al.*, 2016; Enocean Alliance, 2017). On the other hand, CSMA/CA is a media access control (MAC) protocol developed in 1985 at Xerox Palo Alto Research Centre with a similar channel access approach but with backoff time. In a CSMA/CA network, if a node tries to transmit, it checks the channel status first. If there is another transmission on the network, the node will refrain from transmitting for a selected amount of time (backoff) in

order to avoid packet collisions and then try to access the channel again (Umar and Gupta, 2016; Khan *et al.*, 2010; IEEE 802.3, 2008).

In this chapter, M2M technologies are divided into two main categories: short-range M2M technologies and long-range M2M technologies. Although there is no specific definition for short-range wireless communication (Centenaro *et al.*, 2016; Webb, 2012c; Guvenc *et al.*, 2011; Kraemer and Katz, 2009), in this chapter it will be defined as the technologies that can cover a communication range of shorter than 100 metres from any router or base station (Webb, 2012c). Other technologies will be assumed as long-range technologies. This distinction includes the coverage of both indoor and outdoor devices. First, section 2.3 clarifies the main characteristics of short-range M2M technologies and provides a comparison between their features. Second, section 2.4 explores the main characteristics of low-power long-range M2M technologies (or Low Power Wide Area Networks LPWANs) and provides a comparison of these technologies.

2.3 Short-Range Technologies

Short-range M2M technologies are mainly intended for Wireless Personal Area Networks (WPANs) and home IoT applications (Zhang *et al.*, 2019; Zhang and Hu, 2017; Pan *et al.*, 2018; Webb, 2012c). The terminal devices communicate with a specified M2M technology router which forwards terminals' data to a cloud database for later access. The characteristics of the main short-range M2M technologies are described in the following sections.

2.3.1 Zigbee

ZigBee is a low-power, low rate, and narrowband M2M wireless communication technology that is based on the IEEE 802.15.4 standard. In 2004, ZigBee Alliance published the first ZigBee specifications standard, which was based on IEEE 802.15.4-2003 physical (PHY) layer and medium access control (MAC) layer, as shown in Figure 2.2 (Ajah *et al.*, 2015; Sivasankari *et al.*, 2014; M Chen *et al.*, 2013; Usman and Shami, 2013; Gratton, 2013; Lavric *et al.*, 2012; ZigBee Alliance, 2012; Abouzar *et al.*, 2011; Gomez and Paradells, 2010; Hunn, 2010b).

In 2007, ZigBee Alliance utilised the IEEE 802.15.4-2006 PHY and MAC layers and produced two ZigBee standards: the ZigBee-2007, which is simply just called ZigBee, and the ZigBee Pro. ZigBee is specialised for simple applications with limited memory and processing capabilities. On the other hand, ZigBee Pro was designed to fulfil large networks

requirements with high processing capability and up to 30 hops across the network. Another major improvement of this version is the frequency agility function, which provides the ability to move the network between different channels if high noise is detected. In 2009, ZigBee Alliance adopted the use of IPv6 over low-power wireless personal area networks (6LoWPAN) above the MAC layer to simplify the connection to web-based applications with the maintenance of the low power and low cost requirements of M2M communication systems (Kumar and Mane, 2016; Sivasankari *et al.*, 2014; ZigBee Alliance, 2014; Gomez and Paradells, 2010; Huq and Islam, 2010; Hunn, 2010b; Hauer *et al.*, 2009; Lee *et al.*, 2007).

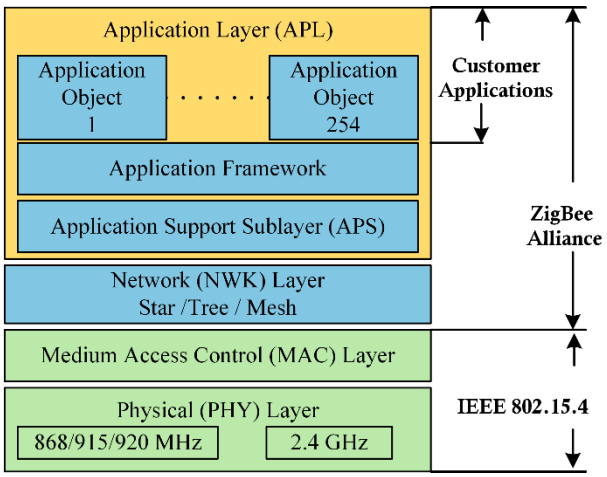

Figure 2.2: ZigBee technology architecture.

ZigBee utilises the Industrial, Scientific, and Medical (ISM) bands of 868 MHz, 915/920 MHz, and 2.4 GHz with maximum data rates of 20 kbps, 40 kbps, and 250 kbps respectively. ZigBee supports a maximum payload size of 104 bytes with a maximum message size of 127 bytes. In addition, ZigBee employs the direct sequence spread spectrum (DSSS) as a spreading technique, and uses Binary Phase Shift Keying (BPSK) or Offset Quadrature Phase Shift Keying (OQPSK) as a modulation scheme (Punj and Kumar, 2019; Zhang and Hu, 2017; ZigBee Alliance, 2012; Gomez and Paradells, 2010; Hunn, 2010b; Adame *et al.*, 2014; Sivasankari *et al.*, 2014; ZigBee Alliance, 2014; ZigBee Alliance, 2016; Watteyne, 2015; García-Hernando *et al.*, 2008; Severino, 2008; Lee, 2005; Insteon, 2013b; Gratton, 2013). Table 2.1 and Figure 2.3 below show the general radio specifications of ZigBee and the number of channels used in each band (Hunn, 2010b; ZigBee Alliance, 2016; Adame *et al.*, 2014; Lee *et al.*, 2007; Severino, 2008; Sahinoglu and Guvenc, 2011).

Table 2.1: ZigBee radio specifications.

Frequency	Channels	Channel bandwidth (MHz)	Data rate (kbps)	Region
868 MHz	1	0.3	20	Europe
915/920 MHz	10	0.6	40	USA/Japan
2.4 GHz	16	2	250	Worldwide

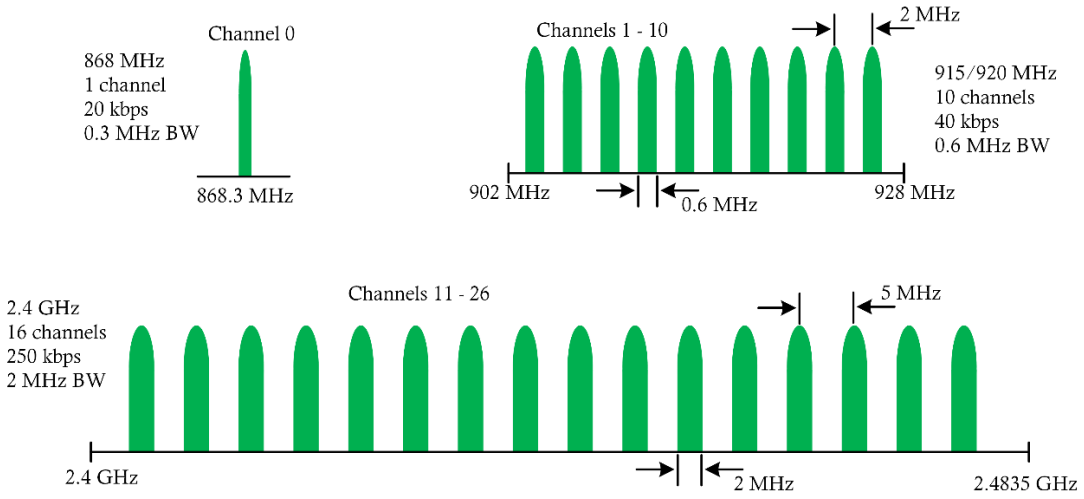

Figure 2.3: ZigBee Operating frequencies and bands.

ZigBee can provide a coverage range of 10 m – 100 m, reliant on environmen characteristics and terminal devices' power transmission. Although ZigBee end devices can work with an output power range from 1 mW up to 100 mW (0 dBm – 20 dBm), the typical output transmission power for ZigBee devices is maintained to be in the range 1 mW – 20 mW (Punj and Kumar, 2019; Zhang *et al.*, 2019; Kos *et al.*, 2019; Qadir *et al.*, 2018; Shende *et al.*, 2017; ZigBee Alliance, 2014; Hunn, 2010b; Ajah *et al.*, 2015; Watteyne, 2015; Adame *et al.*, 2014; Hazmi *et al.*, 2012; ZigBee Alliance, 2018; Fadlullah *et al.*, 2011; Lee *et al.*, 2007). Depending on the applications, the required intervals of transmissions, and the sleep mode period, ZigBee end devices can work on a single battery from months up to more than two years with a duty cycle of 1% (Hunn, 2010b; Ajah *et al.*, 2015; ZigBee Alliance, 2016; Watteyne, 2015; Rawat *et al.*, 2014).

ZigBee supports three network topologies; star, tree (or cluster-tree), and mesh. In addition, ZigBee defines three types of devices: ZigBee coordinator (ZC), ZigBee router (ZR), and ZigBee end device (ZED). These devices are divided into two categories according to their functionality: reduced function devices (RFD), or called child devices, and full function devices (FFD). In general, FFD refers to ZC and ZR (sometimes called sinks), which are usually powered from the main supply and are ready to receive and route packets. Each ZigBee network should contain only one ZC. On the contrary, ZR represents the intermediate routing layer of the network by relaying data from other devices to other ZR or the ZC. ZR is mainly implemented for network extension (Shende *et al.*, 2017; Kumar and Mane, 2016; Hunn, 2010b; Koubaa *et al.*, 2008; Usman and Shami, 2013; Severino, 2008; Gomez and Paradells, 2010; Gratton, 2013; García-Hernando *et al.*, 2008; Lee *et al.*, 2007; Lee, 2005; Cuomo *et al.*, 2008; Korte and Tumar, 2009). Each FFD device supports up to 240 ZigBee end devices, while ZigBee networks can support up to 20 FFDs. Consequently, the maximum number of end devices that can be connected to ZigBee is 240 devices with star network and up to 4800 devices with tree and mesh networks (Kumar and Mane, 2016; Hunn, 2010b; Park, 2011; Vlajic and Stevanovic, 2009; Cuomo *et al.*, 2008; Silicon LABS, 2018).

ZigBee employs the carrier sense multiple access with collision avoidance (CSMA/CA) channel access mechanism to mitigate the collision of messages from different devices. ZigBee implements the CSMA/CA as a simple "listen before talk" (LBT) strategy with a random exponential backoff time. To transmit data, each ZigBee node will listen to the channel activity and determine if it is idle or busy. If the channel is busy, the node will choose a random time to acquire the channel status again. If it is still occupied, the node will increase the random time exponentially and request the channel status again. This technique will fairly ensure that a minimum number of nodes will access the channel at the same time. Conversely, this escalates the latency time for large networks (Pan *et al.*, 2018; Hunn, 2010b; Gomez and Paradells, 2010; Severino, 2008; Cuomo *et al.*, 2008; Koubaa *et al.*, 2008; Thonet *et al.*, 2008). Moreover, ZigBee improves performance by using acknowledgements approach, which will ensure that all packets will reach their destinations. If the transmitter node does not receive the acknowledgement, it will retransmit the data again until a successful transmission is achieved or a failure is reported after a few tries (Severino, 2008; Koubaa *et al.*, 2008; ZigBee Alliance, 2012; Chen, 2013).

2.3.2 Bluetooth

Bluetooth is a low-power, low cost, and short-range communication technology based on the IEEE 802.15.1 standard. The original idea of Bluetooth was instigated by Ericsson Telecommunication in 1994 when it was looking for new wireless technology as a substitution for the wired connections between its mobiles and other accessories. In 1998, the Bluetooth Special Interest Group (Bluetooth SIG) was formed by Ericsson, Intel, IBM, Nokia, and Toshiba, and later in 1998 announced the first version of the Bluetooth standard. In 2010, Bluetooth SIG announced Bluetooth v4.0, which is called Bluetooth Low-Energy (BLE) or Bluetooth Smart that is aimed at the M2M communication systems with low power consumption and sleep capability. The Bluetooth protocol is based on the standard OSI layers, as shown in Figure 2.4 (Collotta *et al.*, 2018; Ray and Agarwal, 2016; Hunn, 2010a; Garg, 2007b; Ferro and Potorti, 2005; Bluetooth SIG, 2014a; Chang, 2014; Latvakoski *et al.*, 2014; Gratton, 2013; Bluetooth SIG, 2014b).

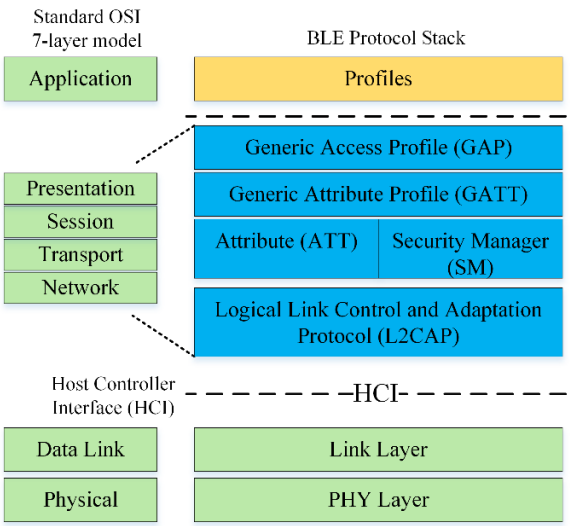

Figure 2.4: BLE protocol stack.

In 2016, the Bluetooth SIG announced a new version of the Bluetooth low energy called Bluetooth 5, which is intended especially for the IoT applications. Bluetooth 5 offers some important advantageous over the BLE to fulfil the broad requirements for IoT applications. Bluetooth 5 adds two new physical (PHY) layers to the specified Bluetooth 4 PHY layers to keep compatibility with old devices. On the other hand, this provides new features for Bluetooth 5 like supporting higher data throughput and providing longer distance connections. Bluetooth 5 quadruples the coverage range of BLE with up to 200 meters outdoors and about 40 meters indoors with transmission power of 10 mW (10 dBm). In

addition, it offers a data rate of up to 2 Mbps with a payload of 255 and forward error correction (FEC). Also, Bluetooth 5 supports mesh network topology with multiple hop approach which can support up 1000 devices (Qadir *et al.*, 2018; Collotta *et al.*, 2018; Pau *et al.*, 2017; Ray and Agarwal, 2016).

BLE and Bluetooth 5 operate in the 2.4 GHz ISM band with 40 channels each of 2 MHz width and utilise the Gaussian Frequency Shift Keying (GFSK) modulation scheme. These channels are distributed in the range 2400 – 2483.5 MHz with the first channel centre frequency of 2402 MHz, as shown in Figure 2.5. Three of these channels are called advertising channels, which are used to detect devices and initialise the connection between them. The advertising channels located at specific frequencies that avoid the interference with WiFi channels. The remaining 37 channels are called data channels and are used to send and receive data with a maximum payload size of 31 bytes (Collotta *et al.*, 2018; Pau *et al.*, 2017; Chang, 2014; Adame *et al.*, 2014; Latvakoski *et al.*, 2014; Rawat *et al.*, 2014; Fan and Tan, 2012; Bluetooth SIG, 2014b; Gratton, 2013).

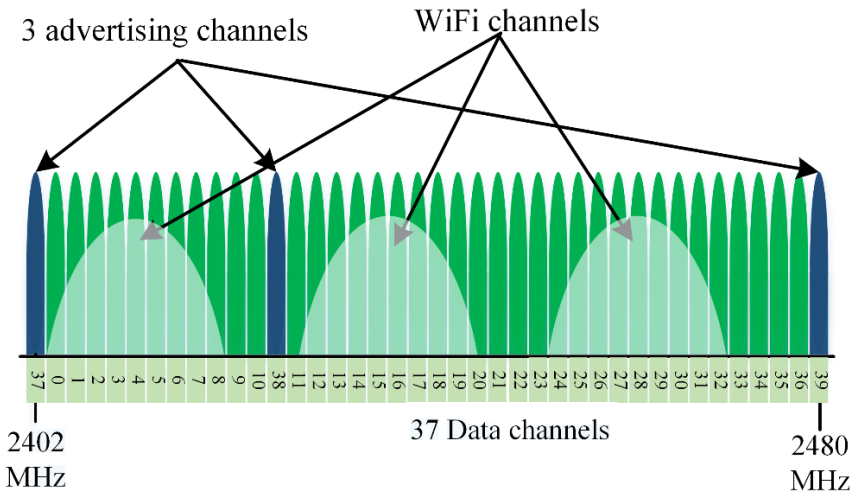

Figure 2.5: BLE operating channels.

Bluetooth employs the adaptive frequency hopping spread spectrum (AFH) technique to reduce data collision and interference between connected devices. Figure 2.6a illustrates the general block diagram for the demodulation process utilised by BLE with the frequency hopping technique. The hopping sequence is based on the ID number and the internal timer of the master device with a hopping speed of 1600 hops/sec. The sequencing scheme is composed by generating a pseudorandom sequence based on the 27 LSBs (Least Significant Bits) of the timer and the 28 LSBs of the address of each device, as shown in Figure 2.6b (M Chen *et al.*, 2013; Gratton, 2013; Song *et al.*, 2007; Wu and Shi, 2007;

Bluetooth SIG, 2014c; Alghamdi *et al.*, 2015). Moreover, Bluetooth utilises acknowledgements technique to improve the probability of successful transmission, where transmitters forced to retransmit unacknowledged packets (Pau *et al.*, 2017; Ray and Agarwal, 2016).

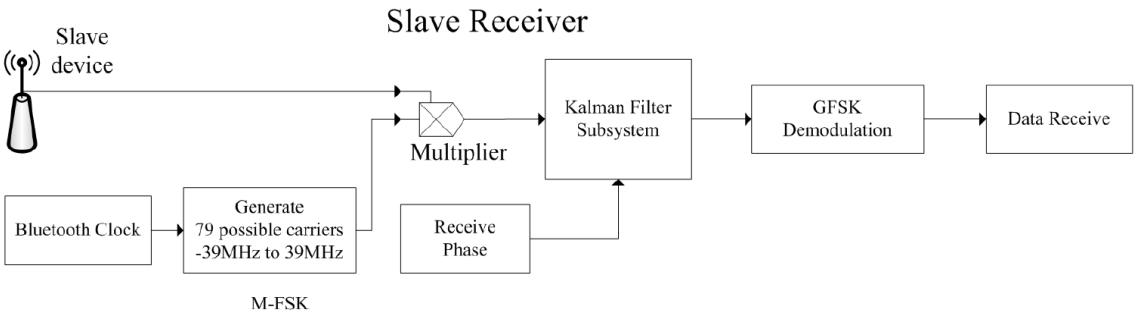

a) General demodulation black diagram.

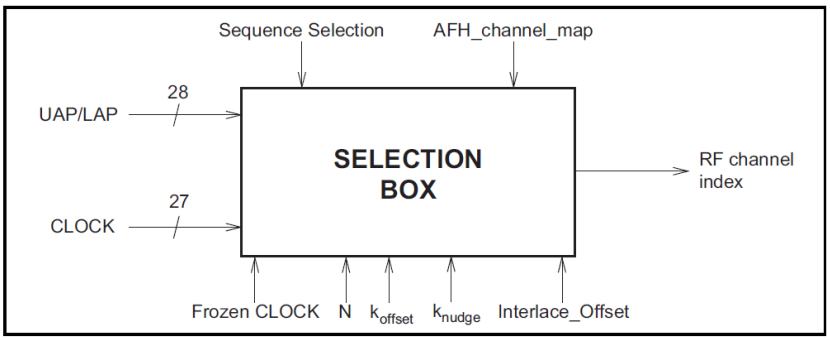

b) Basic hop selection kernel for the hop system (selection box).

Figure 2.6: BLE hop system (Bluetooth SIG, 2014c).

2.3.3 Ultra-Wide Band (UWB)

Although UWB technology was first used in 1901 by Guglielmo Marconi in spark gap radio, it was restricted for military use only until 2002 when the Federal Communications Commission (FCC) approved the commercial use of it. The FCC determines the frequency range of 3.1–10.6 GHz for the UWB with a total bandwidth of 7.5 GHz and a minimum channel bandwidth of 500 MHz. The FCC also restrict the power emission of the UWB signals by a maximum power spectral density (PSD) of (-41.3 dBm/MHz or 75 nW/MHz), which requires a transmission power of around 0.5 mW (-3 dBm). Nowadays, UWB technology is mostly used in Micro-location and real time location tracking applications (Jia *et al.*, 2019; Amini *et al.*, 2019; Rashid *et al.*, 2019; Kshetrimayum, 2009; Kartsakli *et al.*, 2014; Sahinoglu *et al.*, 2009; Garg, 2007a).

UWB is based on the IEEE 802.15.3a standard which designed to provide a high data rate of up to 110 Mbps at a distance of 10 m and up to 480 Mbps at 2 m using the Multiband Orthogonal Frequency Division Multiplexing (MB-OFDM) or direct sequence OFDM (DS-OFDM) (Punj and Kumar, 2019; Garg, 2007a; Obaidat and Misra, 2014; Lee *et al.*, 2007). However, in 2007 IEEE task group 4a (TG4a) proposed a new standard for the UWB technology named IEEE 802.15.4a, which is specialised for a low rate and low-power wireless sensor networks (WSNs) with data rates between 110 kbps and 27 Mbps with a maximum payload of 4095 bytes. According to the IEEE 802.15.4a specifications, the UWB signals can be transmitted using ultra-short duration pulses (in nanosecond range) called Impulse Radio UWB (IR-UWB) with either pulse position modulation (PPM) or the polarity of the pulses (Amini *et al.*, 2019; Kshetrimayum, 2009; Sahinoglu *et al.*, 2009; Sahinoglu and Guvenc, 2011).

IR-UWB utilises three frequency bands as specified by the IEEE 802.15.4a standard: the sub-1GHz band in the frequency range 250–750 MHz, the low band in the frequency range 3.244 – 4.742 GHz, and the high band in the frequency range of 5.944 – 10.234 GHz. A total number of 16 overlapped channels are supported on these bands, as shown in Figure 2.7 and Table 2.2 (Sahinoglu and Guvenc, 2011; Sahinoglu *et al.*, 2009). Channels 0, 3, and 9 are mandatory channels for each band respectively, while other channels are optional, and each device working in one of these bands should support mandatory channel of the working band.

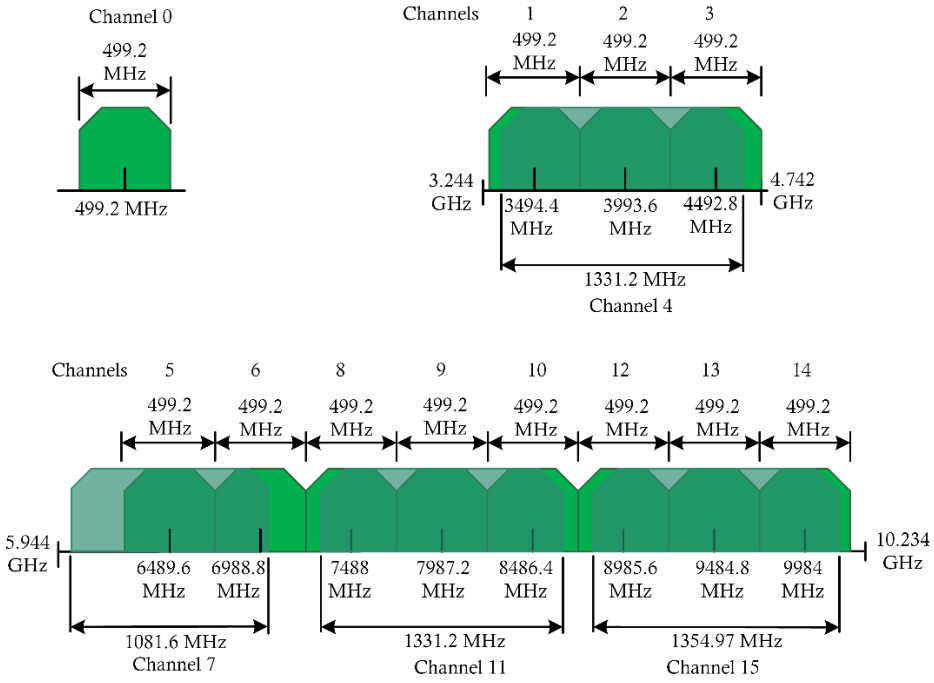

Figure 2.7: IR-UWB channels.

Table 2.2: IR-UWB channels.

Channel No.	Centre frequency (MHz)	Channel bandwidth (MHz)	Band	Mandatory
0	499.2	499.2	Sub-GHz	Yes
1	3494.4	499.2	Low band	No
2	3993.6	499.2	Low band	No
3	4492.8	499.2	Low band	Yes
4	3993.6	1331.2	Low band	No
5	6489.6	499.2	High band	No
6	6988.8	499.2	High band	No
7	6489.6	1081.6	High band	No
8	7488.0	499.2	High band	No
9	7987.2	499.2	High band	Yes
10	8486.4	499.2	High band	No
11	7987.2	1331.2	High band	No
12	8985.6	499.2	High band	No
13	9484.8	499.2	High band	No
14	9984.0	499.2	High band	No
15	9484.8	1354.97	High band	No

Low power consumption and use of the Impulse radio technique enable terminal devices to work for years using a single battery (Rawat *et al.*, 2014). However, one of the main drawbacks of the low power requirements of the UWB technology is the interference from other higher power signals in the same frequency range, especially the IEEE 802.11a which works in the frequency range 5.725–8.825 GHz with a bandwidth of 100 MHz (Sahinoglu *et al.*, 2009; Garg, 2007a).

IR-UWB is based on a peer-to-peer piconet network topology with a maximum number of eight connected devices (Lee *et al.*, 2007). IR-UWB employs an ALOHA-based channel access mechanism which is aimed at the random time access approach without inspecting if the channel is busy or not. To reduce the probability of packets collisions, IR-UWB employs a special time hopping technique (TH-UWB) that is achieved by adding a pseudorandom time shift to each pulse, which enables channel sharing for multi-devices. Moreover, it utilises acknowledgements to ensure the reception of each transmission. If the transmitter does not receive the acquired acknowledgement, it will resend the data after a random backoff (Wang Chen *et al.*, 2013; Shao and Beaulieu, 2011; Sahinoglu and Guvenc, 2011; Sahinoglu *et al.*, 2009; Kshetrimayum, 2009; Zhang *et al.*, 2007; Win and Scholtz, 2000).

2.3.4 Z-Wave

In 2005, the company ZenSys developed the former version of the Z-Wave technology, which is a low power wireless communication technology tailored for residential automation and remote-control applications. In 2008, ZenSys became a division of Sigma Designs which promoted the formation of Z-Wave Alliance. In 2013, it announced the new version of the Z-Wave technology that is based on ITU-T Recommendation G.9959 (2012) physical and MAC layers (Fuller *et al.*, 2017; Badenhop *et al.*, 2017; Z-Wave Alliance, 2019; Gomez and Paradells, 2010; Rawat *et al.*, 2014; Spadacini *et al.*, 2014; International Telecommunication Union, 2012; Insteon, 2013b; Rohini and Venkatasubramanian, 2015).

Z-Wave uses the sub-1GHz band with two main frequency bands of 868 MHz and 900 MHz in different regions around the globe (Z-Wave Alliance, 2019; Z-Wave Alliance, 2016; Tuna *et al.*, 2013). It might utilise one, two, or three channels, each with a bandwidth of 300 kHz and FSK modulation scheme to provide a data rate of 9.6 kbps and 40 kbps. On the other hand, it employs the GFSK modulation and a bandwidth of 400 kHz to provide a data rate of 100 kbps. The length of the Z-Wave message is variable between 14 bytes in standard mode and 28 bytes in extended mode, with a payload size between 4 and 6 bytes (Punj and Kumar, 2019; Fuller *et al.*, 2017; Badenhop *et al.*, 2017; Ghamari *et al.*, 2016; Mendes *et al.*, 2015; Fadel *et al.*, 2015; Sharma and Sharma, 2014; Z-Wave Alliance, 2018; Rohini and Venkatasubramanian, 2015; Insteon, 2013b).

Z-Wave can offer an indoor coverage range of 30 m based on a mesh network topology with a source routing approach. This means that the message route is determined and attached to each frame by the source with a maximum number of 4 hops. The Z-Wave network is divided into domains, where each domain represents a set of nodes that are connected to the same medium. Each domain is identified by a 32-bit ID while each node is identified by an 8-bit ID with up to 232 nodes in each domain. In each domain, there is only one controller, which is called the domain master, that can send control messages and commands to other devices in the domain. Other devices called slaves which are responsible for executing commands or replying to the controller. In addition, controllers perform the function of inter-domain bridges (IDB), which ensures communication between nodes in different domains, as shown in Figure 2.8. The Z-Wave network is a self-organising network, which means that all nodes can dynamically detect neighbour nodes and update the routing table and inform the controller about any of these nodes (Gomez

and Paradells, 2010; Huq and Islam, 2010; Spadacini *et al.*, 2014; Insteon, 2013b; International Telecommunication Union, 2012).

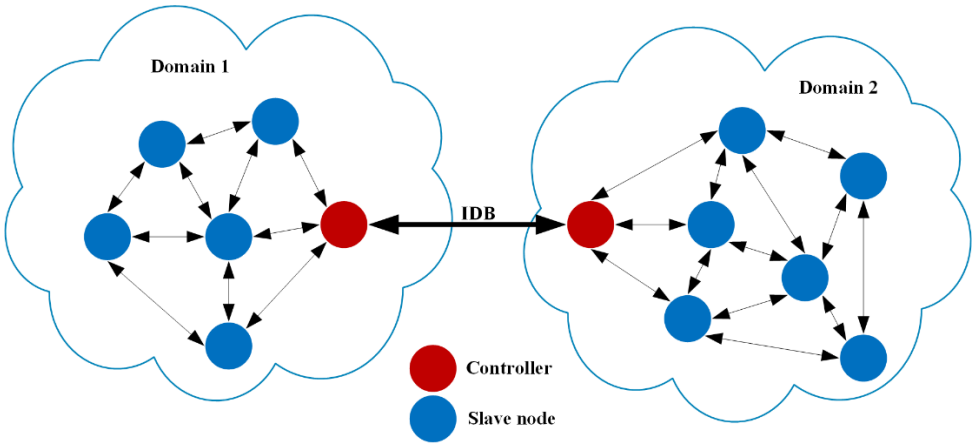

Figure 2.8: Z-Wave network architecture.

The maximum transmission power of Z-Wave devices is restricted by the local regulations and is not specified by the ITU-T G.9959 recommendations. In general, Z-Wave devices work with a typical transmission power of 2 mW (3 dBm) (Baviskar *et al.*, 2015). Furthermore, most Z-Wave devices are powered by a single battery, and the low power consumption with the use of the periodic sleep technique expands the battery life span to several years (Rawat *et al.*, 2014).

Z-Wave employs the CSMA/CA channel access mechanism with a random backoff algorithm to reduce the probability of collisions and ensure a clear channel for transmission. The backoff time is determined by the ITU-T G.9959 recommendations to be in the range of 10 – 40 milliseconds. Furthermore, Z-Wave utilises other mechanisms like frame acknowledgement, data verification, and frame retransmission to achieve better system robustness and ensure message delivery (Gomez and Paradells, 2010; Insteon, 2013b; International Telecommunication Union, 2012).

2.3.5 INSTEON

INSTEON is a short-range, low-power, low cost, and low data rate M2M technology developed by SmartLabs Inc. in 2005 for home automation applications. INSTEON provides an individual feature among other M2M technologies by supporting two communication schemes to connect devices: RF and powerline. INSTEON RF communication employ three ISM sub-1GHz frequencies: 915 MHz in the US, 869.85 MHz in Europe, and 921 MHz in Australia. It provides an unobstructed line-of-sight coverage area of up to 45 m with 12 dBm (≈ 16 mW) transmission power, which is reduced

by the presence of obstacles. INSTEON RF communication provide a data rate of 38.4 kbps with the FSK modulation scheme and a channel bandwidth of 64 kHz (Punj and Kumar, 2019; Talbot *et al.*, 2018; Ervin *et al.*, 2018; Lumpkins, 2015; Gomez and Paradells, 2010; Spadacini *et al.*, 2014; Baviskar *et al.*, 2015; Insteon, 2013b; Insteon, 2013a; Irwin *et al.*, 2011). On the other hand, powerline uses BPSK modulation with a carrier frequency of 131.65 kHz and can provide a maximum data rate of 13.165 kbps for instantaneous packets, and 2.88 kbps for sustained packets (Punj and Kumar, 2019; Lumpkins, 2015; Mendes *et al.*, 2015; Insteon, 2013b; Insteon, 2013a; Irwin *et al.*, 2011).

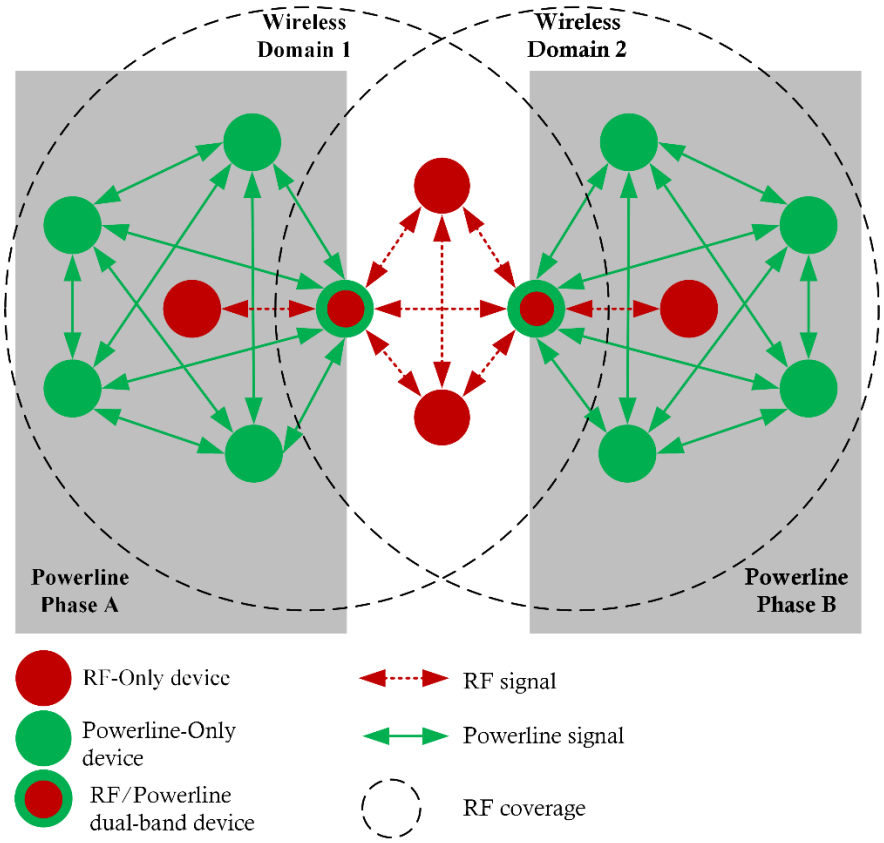

Figure 2.9: INSTEON network architecture.

INSTEON is based on a peer-to-peer dual-mesh (dual-band RF and powerline) network topology without a network controller or routing technique, as shown in Figure 2.9. Any INSTEON device can act as a sender, responder, or repeater by relaying messages. INSTEON supports multiple hops to achieve communication between devices located on different ranges or domains. The maximum number of hops is limited to three hops by two 2-bit fields in each message. One field represents the maximum hops permitted for the message, and the other field contains the number of hops remaining (Hops Left). Unless

the device is the destination of the message, it will retransmit it and decrease the remaining hops field by one. If this field of the received message is zero, the message will be neglected. The sender will automatically resend the message again when it does not receive an acknowledgement from the recipient. In general, each sender starts by sending the message with a zero hop and increases the maximum hops field with each transmission retry to increase the number of devices that relay the message and achieve a wider coverage range. If the sender does not receive the acknowledgement after five attempts, the message will be lost (Lumpkins, 2015; Insteon, 2013a; Irwin *et al.*, 2011).

INSTEON supports two message types: standard message with 10 bytes, and extended message with 24 bytes. The standard message does not contain any user data and is designed for direct commands and controls, which represent the two-bytes payload of the standard message. On the other hand, extended messages contain all standard message fields in addition to 14 bytes of user data payload. Since each INSTEON powerline packet contains only 24 bits, the standard message will be sent using five packets and the extended message will be sent using 11 packets, as shown in Figure 2.9 (Lumpkins, 2015; Insteon, 2013a; Insteon, 2013b; Irwin *et al.*, 2011).

INSTEON can support up to 1000 devices with a special collision avoidance and message synchronisation approach (Punj and Kumar, 2019; Baviskar *et al.*, 2015; Insteon, 2019). This is achieved by utilising the simulcasting technique, which means that all devices within the same range transmit the same message at the same time. Using simulcasting increases the probability of receiving the message by the intended recipient and improves system performance. All devices should be synchronised to avoid message collision and ensure that devices will not jam each other. INSTEON employs the powerline zero crossing for message synchronisation. To ensure synchronisation of prospective retransmitted messages by RF devices, a sender should wait for extra time after sending the last packet. This extra time is set to one zero crossing for the standard message and two zero crossing for the extended message. Therefore, 6 zero crossings are required to send a standard message, and 13 zero crossings are required to send an extended message. These periods are called timeslots, in which each message will be sent synchronously by all devices in the range, as shown in Figure 2.10. In addition, INSTEON dual-band devices will first retransmit any received message from powerline using RF immediately after receiving the last packet of the message. In the next timeslot, the message will be retransmitted on the powerline. If the message was received via RF, the dual-band devices will first send it on the powerline in the next timeslot, then it will be retransmitted using

RF instantly after sending the last packet on the powerline. This approach guarantees that any asynchronous RF message will be synchronised on the next timeslot (Insteon, 2013a; Insteon, 2013b).

Although simulcasting improves system performance and message delivery possibilities, there is a high probability of data collision due to synchronisation problems. RF-Only devices send messages asynchronously based on the ALOHA protocol and might collide with messages from other RF-Only devices or dual-band devices. Moreover, powerline devices might lose synchronisation due to a high level of noise caused by other electrical appliances and high amplitude spikes generated by motors, dimmers, and fluorescent lights (Insteon, 2013a; Insteon, 2013b; Irwin *et al.*, 2011).

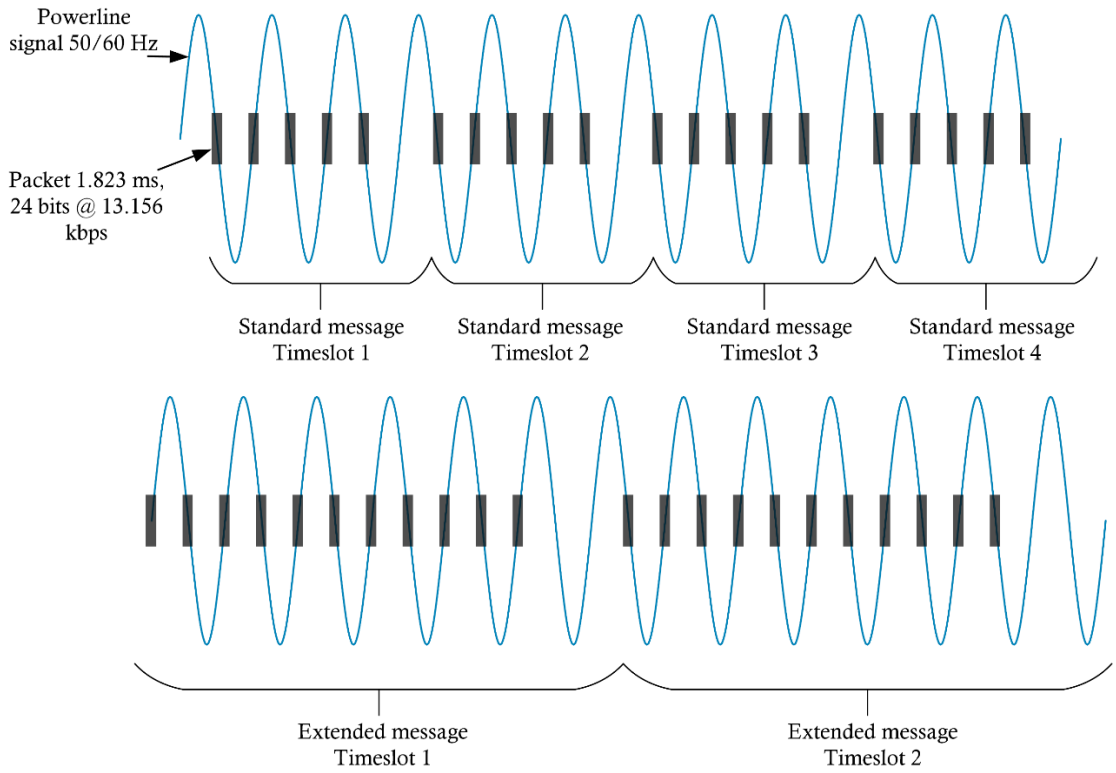

Figure 2.10: INSTEON standard and extended messages and timeslots.

2.3.6 EnOcean

EnOcean is an ultra-low power, short-range, and small packets wireless M2M communication system for residential and industrial applications. EnOcean sensors and switches are designed to work without batteries, which means that devices are self-powered. EnOcean is based on an innovative technique called energy harvesting where EnOcean devices derive energy from surrounding environment changes like light, temperature, vibration, and mechanical energy. EnOcean GmbH, which is a Germany

company located in Oberhaching, is the originator of the energy harvesting technique. It was founded in 2001 as an adjunct to Siemens Research and provided its first products to the market in 2002. In April 2008, EnOcean GmbH and several companies from Europe and the USA established the EnOcean Alliance to promote and develop the EnOcean technology worldwide. EnOcean Alliance announced its first official release of the EnOcean standard in 2009, which then modified in 2011 to support telegrams. In April 2012, the EnOcean wireless protocol standard was approved as an international standard by the International Organization for Standardization (ISO) and the International Electrotechnical Commission (IEC) and was titled ISO/IEC 14543-3-10 (Ghamari *et al.*, 2016; Mendes *et al.*, 2015; Xiaohui Li *et al.*, 2014; Rawat *et al.*, 2014; Gratton, 2013; Enocean Alliance, 2018a; Enocean Alliance, 2016d; Obaid *et al.*, 2014; Ploennigs *et al.*, 2010; Enocean Alliance, 2012; Enocean Alliance, 2015d; Enocean Alliance, 2019b; Enocean Alliance, 2019a; ISO and IEC, 2012).

The ISO/IEC 14543-3-10 standard is specially optimised for the ultra-low power Wireless Short-Packet (WSP) protocol and utilises two frequencies: 315 MHz and 868.3 MHz with a channel bandwidth of 280 kHz. In 2015, the ISO/IEC expanded the EnOcean standard and announced the new release ISO/IEC 14543-3-11, which supports the frequencies 902.875 MHz and 928.35 MHz with an FSK modulation for the USA and Japan respectively. At first, the Amplitude Shift Keying (ASK) modulation scheme was employed by EnOcean until 2017 where the Frequency Shift Keying (FSK) was also utilised by EnOcean. In both cases, EnOcean provides a data rate of 125 kbps (Purkovic *et al.*, 2019; Enocean Alliance, 2017; Xiaohui Li *et al.*, 2014; Enocean Alliance, 2016d; Enocean Alliance, 2015d; Enocean Alliance, 2016b; Enocean Alliance, 2016c; Enocean Alliance, 2015a; Enocean Alliance, 2015c; Enocean Alliance, 2016a; Enocean Alliance, 2019d; Enocean Alliance, 2019c; Enocean Alliance, 2011).

EnOcean WSP protocol, shown in Figure 2.11, can provide a coverage range of 30 m for indoor applications and up to 300 m in free field line-of-sight connections with maximum transmission power of 10 dBm (10 mW). However, it can attain the indoor coverage with only mere 50 μW (-13 dBm) of energy, which represents the typical output power of EnOcean devices (Arcari *et al.*, 2017; Xiaohui Li *et al.*, 2014; Enocean Alliance, 2016d; Rawat *et al.*, 2014; Obaid *et al.*, 2014; Enocean Alliance, 2015d; Enocean Alliance, 2015a; Enocean Alliance, 2016a; Enocean Alliance, 2018b; Enocean Alliance, 2011; ISO and IEC, 2012). On the other hand, the indoor range is significantly affected by the wall,

furniture, and other obstacles and might be reduced to 10 m in some buildings (Enocean Alliance, 2018b).

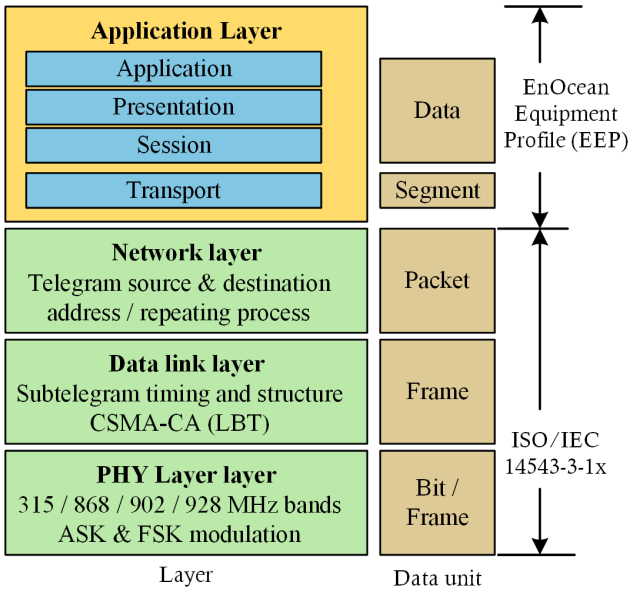

Figure 2.11: EnOcean protocol architecture.

EnOcean supports point-to-point and star network topologies, and by using repeaters, it can support mesh topology also. In addition, repeaters might be used for range extension with a maximum number of two repeaters for each network. The EnOcean network consists of switches, sensors, actuators, and a controller, and might include a gateway, which supports different types of wired protocols for remote monitoring and control, as shown in Figure 2.11. Each device in the EnOcean network is identified by a 32-bit ID number. Switches and sensors are self-powered devices, and all other devices in the network are powered from the power line. Switches and sensors work as unidirectional transmitters only, while actuators are unidirectional receivers with synchronisation functionality. The controller, the gateway, and repeaters are bidirectional devices and can support synchronisation and smart acknowledgements (ISO and IEC, 2012; Enocean Alliance, 2018b; Enocean Alliance, 2016d; Enocean Alliance, 2017).

In general, bidirectional devices support a message payload of 1 – 14 bytes that includes user data, acknowledgement, and control commands. On the other hand, sensors' messages support a payload of 1 – 4 bytes and switches support a payload of one byte only (Purkovic *et al.*, 2019; Arcari *et al.*, 2017; Enocean Alliance, 2017; Enocean Alliance, 2015b; Xiaohui Li *et al.*, 2014; Gratton, 2013; Enocean Alliance, 2016d; Enocean Alliance, 2011).

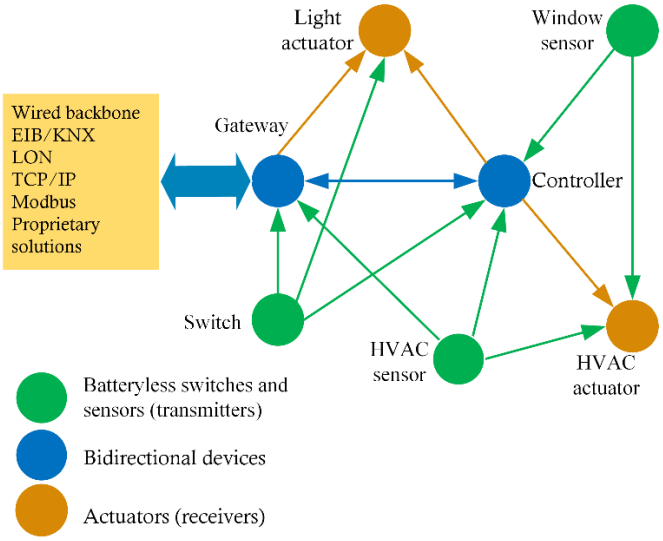

Figure 2.12: EnOcean system architecture.

To reduce the power consumption for unidirectional devices, EnOcean employs an ALOHA-based random access protocol without synchronisation, acknowledgement, and channel sensing mechanism. On the other hand, to increase the number of devices with a lower probability of collision, EnOcean sends each message using short sub-telegrams that last for less than one millisecond. In addition, EnOcean sends identical multi-copies of each sub-telegram on different time slots that selected by adding a random time delay. The total period of these time slots should not exceed a maximum transmission maturity period of 40 milliseconds. EnOcean sends three copies of the original sub-telegram within 40 milliseconds period and two copies of the repeated sub-telegram within 30 milliseconds time period. The 40 milliseconds transmission maturity period is divided into four 10 milliseconds windows each containing 10 time slots of one millisecond, as shown in Figure 2.13 and Table 2.3 (Yi-Chang Li *et al.*, 2014; Gratton, 2013; Ploennigs *et al.*, 2010; Enocean Alliance, 2017; Enocean Alliance, 2016d; Enocean Alliance, 2011; ISO and IEC, 2012).

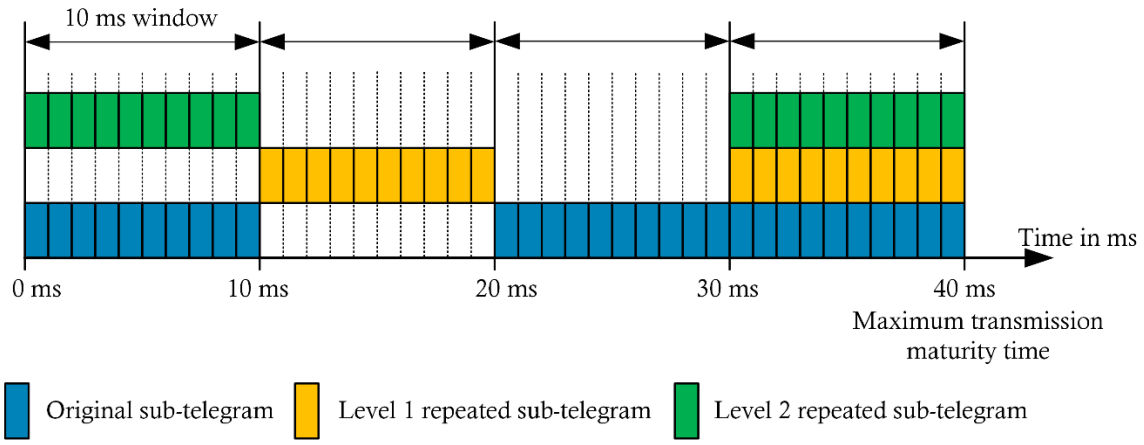

Figure 2.13: EnOcean sub-telegrams time slots.

Table 2.3: The appropriate allocation of time to the corresponding telegrams.

Status	1st sub-telegram	2nd sub-telegram	3rd sub-telegram
Original	0	1 … 9	20 … 39
Level 1 repeated	10 … 19	20 … 29	
Level 2 repeated	0 … 9	20 … 29	

Furthermore, to reduce the probability of collision, EnOcean supports the CSMA/CA technique for powered devices only (actuators, repeaters, gateways, and controllers). If the channel is occupied, the sender will add a delay of a random time range and check the channel again. If the sender finds that the calculated time delay exceeds the transmission maturity time, it sends the current sub-telegram despite the current channel status. Although the LBT technique is highly recommended, it is an optional feature of the EnOcean system (Gratton, 2013; Ploennigs *et al.*, 2010; Enocean Alliance, 2017; Enocean Alliance, 2016d; Enocean Alliance, 2011; ISO and IEC, 2012).

The optimal number of connected devices to each EnOcean network is 100 devices, which is suitable for most home automation applications. This number can be escalated up to 200 devices with a successful transmission probability of more than 99.9% for devices that transmit data once a minute, as shown in Figure 2.14. Increasing the number of connected device for more than 200 devices significantly affects the system performance and dramatically increases data collisions (Arcari *et al.*, 2017; Ploennigs *et al.*, 2010; Enocean Alliance, 2011).

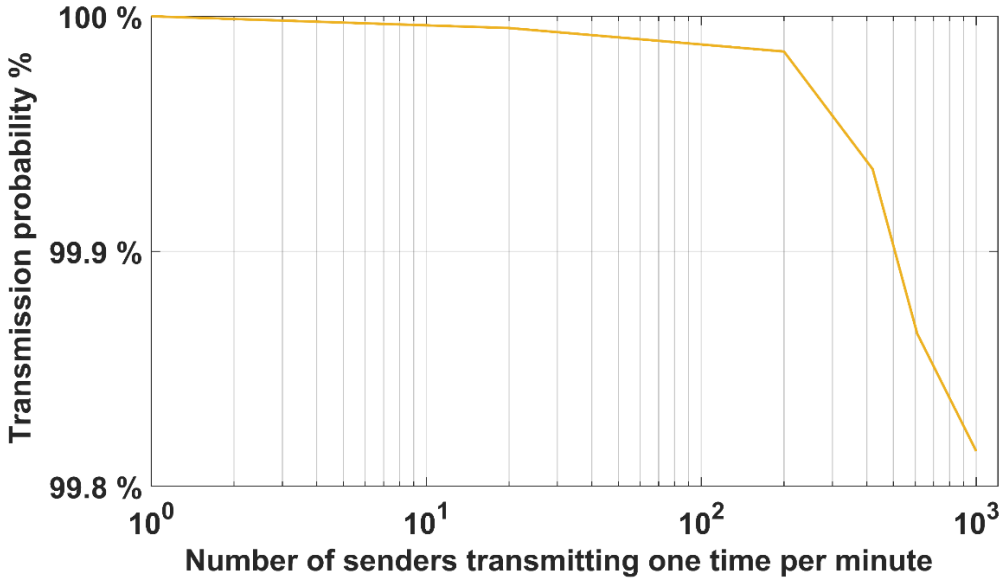

Figure 2.14: The transmission probability of EnOcean system versus the number of connected devices (Enocean Alliance, 2011).

2.3.7 ANT

ANT is an ultra-low power short-range wireless protocol that was initially developed by Dynastream Innovations Inc. in 2000 to solve the commercial problems of health and sports monitoring systems. In 2003, the ANT protocol was utilised by Nordic Semiconductor to create the first version of ANT devices that work in the 2.4 GHz ISM band, which then released in 2004. In 2005, the ANT+ Alliance was created to provide an international framework for the technology and to achieve better interoperability as a practical wireless sensor network (WSN). In December 2006, Dynastream became a wholly-owned subsidiary of Garmin Ltd (Rong and Xin, 2016; Kartsakli *et al.*, 2015; Gratton, 2013; ANT+ Alliance, 2019c; ANT+ Alliance, 2019b; ANT+ Alliance, 2019a; ANT+ Alliance, 2019d).

ANT supports different types of network topologies including peer-to-peer, tree, star, and mesh. ANT network can support up to 500 nodes that share the same channel using the Time Division Multiple Access (TDMA) technique. Each ANT powered node can act as a receiver, transmitter, or relay to ensure data routing without the need of a coordinator, especially as these nodes have the ability of channel sense and time slot selection. In addition, ANT devices might undertake different roles simultaneously on different channels (Dynastream Innovations Inc., 2018; Gratton, 2013; Dynastream Innovations Inc., 2014a; Dynastream Innovations Inc., 2015).

The ANT communication system is based on a channel connection scheme, which means that communications between any two devices are achieved by initialising a specific channel with special characteristics. Each channel must contain at least one master device and one slave device. There are two types of channels for any ANT communications: the independent channel, for a peer-to-peer connection, and the shared channel for a single master device and multiple slave devices. In general, ANT devices can work on more than one channel simultaneously, and some devices can support up to 15 channels. Three types of messages are defined for ANT devices, which are broadcast, acknowledgement, and burst messages. Broadcast messages are used by the master devices to initialise the connections with slave devices and to set the channel characteristics. On the other hand, burst transmission is used to send large message data or to increase the transmission speed. Sending data from the master device to the slave devices is mandatory and is called forward direction, while sending data from slave devices to the master device is optional and is called reverse direction, as shown in Figure 2.15. Each transmission should be held on a specific time slot based on a previously defined channel period (Tch). According to the

channel period, a frequency of 0.5 – 200 Hz can be achieved. ANT employs the GFSK modulation scheme with a data rate of 20 kbps in normal mode and up to 60 kbps with advanced burst mode. The payload of each ANT message is variable within the range of 1 – 8 bytes. In addition, ANT utilises 125 working channels in the frequency range of 2400 – 24125 MHz with a 1 MHz step and can provide a communication range of 5 – 10 metre with a maximum transmission power of 4 dBm (2.5 mW) (Mehmood *et al.*, 2016; Rong and Xin, 2016; Kartsakli *et al.*, 2015; Gratton, 2013; Dynastream Innovations Inc., 2014a; Dynastream Innovations Inc., 2015; Dynastream Innovations Inc., 2010; Dynastream Innovations Inc., 2016c; Dynastream Innovations Inc., 2016b; Dynastream Innovations Inc., 2016a; Dynastream Innovations Inc., 2011; Dynastream Innovations Inc., 2014b; Dynastream Innovations Inc., 2013).

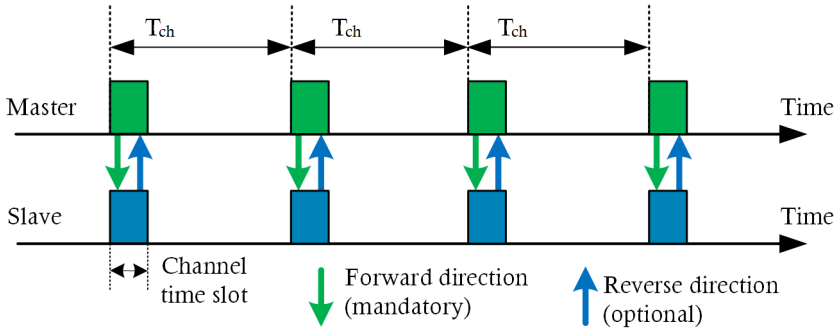

Figure 2.15: ANT transmission time slots.

Data collision in ANT system is known as "channel collisions", which occurs when two (or more) devices try to access the channel simultaneously. In such a case, one of the channels will be initialised correctly, and the other will be denied. If the data was sent by a slave device, the data will be lost while for the master channel, the data will be saved in the buffer until next channel period. If there is no new data, the master device will retransmit the data again. Otherwise, the data will be lost. In general, applications with 8 Hz channel period and higher are liable to provide collisions. The channel period is one of the vital factors that affect the probability of collisions. However, reducing the channel frequency is not suitable for all applications. Moreover, using a high number of simultaneous channels intensifies the probability of collisions as a consequence of decreasing the free radio bandwidth. In addition, dropping a slave channel into search mode will significantly increase the odds of collisions since it occupies the channel for a relatively long period. Consequently, channel collisions may drop slave devices into search mode and proliferates the probability of collisions again. Therefore, developers should be aware of this situation and avoid it at application design phase (Dynastream Innovations

Inc., 2014a; Dynastream Innovations Inc., 2015; Dynastream Innovations Inc., 2016c; Dynastream Innovations Inc., 2016a).

2.3.8 A comparative summary of short-range M2M technologies

The short-range M2M communication systems are mainly designed for industrial, health, and residential automation applications. The practical start of these systems was by developing the Bluetooth technology in 1998. However, several M2M technologies were developed in the next few years with different characteristics and specifications (see Figure 2.16). Over the last two decades, these technologies have been developed and enhanced to fulfil the requirements of the new applications and market.

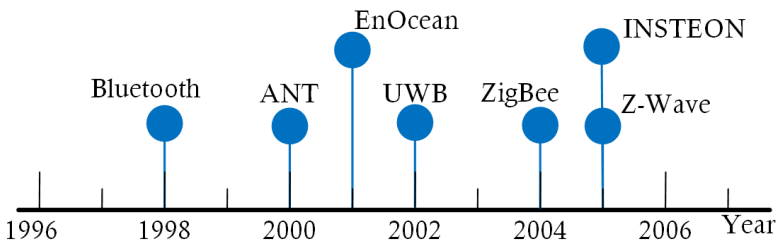

Figure 2.16: Short-range M2M communication technologies timeline.

In general, ZigBee provides the largest coverage range for short-range low-power M2M communication systems, but with the highest transmission power. On the other hand, the minimum power consumption can be achieved by EnOcean technology with only 50 µW transmission power as shown in Figure 2.17.

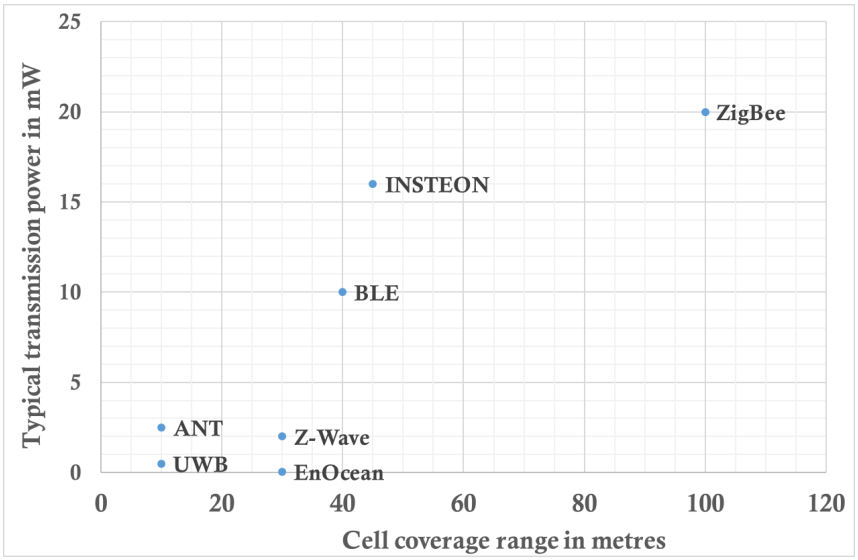

Figure 2.17: Short-range M2M technologies coverage range in metres versus the transmission power in mW.

Each M2M technology employs a certain collision avoidance technique to improve system performance and intensify the number of connected devices with a minimum collision probability. In general, ZigBee network offers the biggest number of terminal devices with up to 4800 nodes, while UWB technologies provide communication between 7 slave nodes. On the other hand, Bluetooth, EnOcean, Z-Wave, ANT, and INSTEON can support practically a few hundred to one thousand nodes with an acceptable probability of collision, as shown in Figure 2.18.

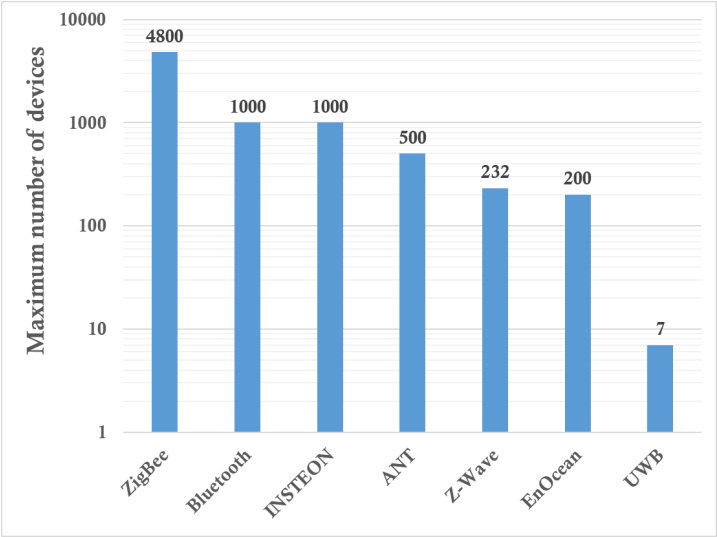

Figure 2.18: Short-range M2M technologies maximum number of connected devices.

UWB offers the highest data throughput of up to 27 Mbps, while Bluetooth provides a data rate of 2 Mbps, which allow these two technologies to be suitable for a wide range of applications including applications that require audio and video streaming. However, other technologies provide a data rate that is adequate for most M2M monitoring and control applications, as shown in Figure 2.19.

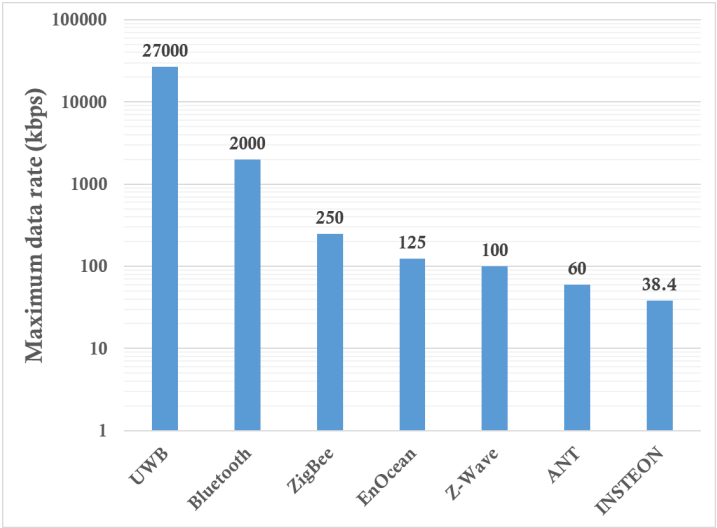

Figure 2.19: Short-range M2M technologies maximum data rate in kbps.

Table 2.4 and Figure 2.20 show a detailed comparison between the previous short-range M2M communication technologies.

Table 2.4: Summary of the short-range M2M technologies features and characteristics.

Characteristic	ZigBee	Bluetooth	UWB	Z-Wave	INSTEON	EnOcean	ANT
Operating frequency (MHz)	868.3, 915/920, 2400	2400	499.2, 3244 – 4742, 5944 – 10234	868, 900	869.85, 915, 921	315, 868.3, 902.875, 928.35	2400
Number of channels	1, 10, 16	40	1, 4, 11	1, 2, 3	1	1	125
Channel bandwidth (kHz)	300, 600, 2000	2000	499200, 1331200, 1081600, 1354970	300, 400	64	280	1000
Modulation scheme	BPSK, OQPSK	GFSK	Impulse	FSK, GFSK	FSK, BPSK	ASK/FSK	GFSK
Channel access/collision avoidance technique	CSMA/CA with random backoff	AFH	ALOHA with Time hopping	CSMA/CA with random backoff	Slotted simulcasting	Controllers / Gateways: Slotted CSMA/CA Sensors: ALOHA / 3 copies of telegrams	TDMA / CSMA/CA
Acknowledgement	Yes	Yes	Yes	Yes	Yes	Controllers / Gateways: Yes Sensors: NO	Yes
Network topology	Star, tree, mesh	Star, mesh	Peer-to-peer	Mesh	Peer-to-peer, dual-mesh	Peer-to-peer, start, mesh	Peer-to-peer, tree, start, mesh
Number of nodes	4800	1000	7	232	1000	200	500
Data rate (kbps)	20, 40, 250	2000	110, 27000	9.6, 40, 100	38.4, 13.165, 2.88	125	20, 60
Payload (Byte)	104	255	4095	6	14	4, 14	8
Coverage range (m)	10 – 100	1 – 40	10	30	45	30 – 300	5 - 10
Transmission power (dBm)	0 – 20 (13)	-20 – 10	-3	3	12	-13 – 10 (-13)	4

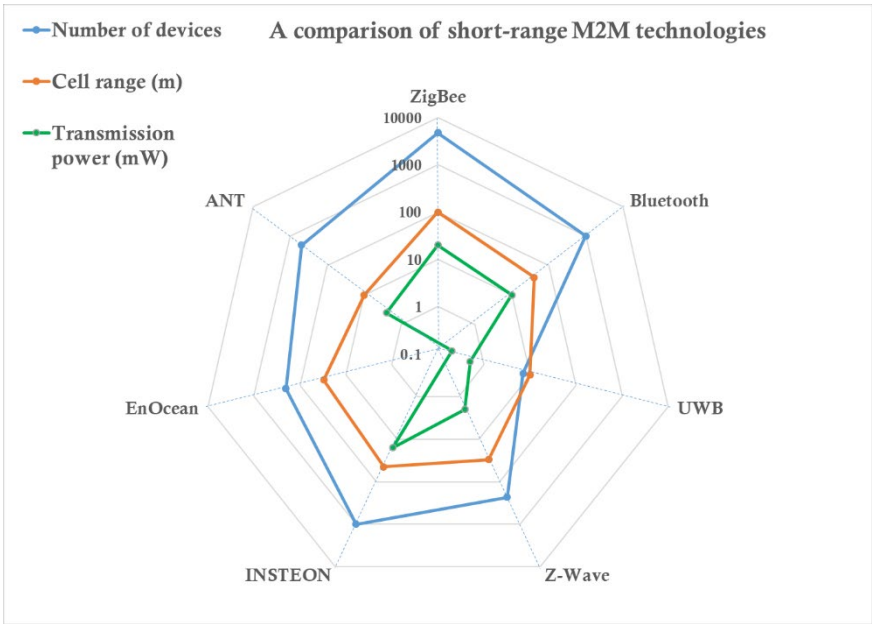

Figure 2.20: A comparison of short-range M2M technologies in terms of the number of connected devices, the coverage range, and the transmission power.

2.4 Long-Range Technologies (LPWANs)

Long-range M2M communication technologies (or LPWANs) are aimed at providing a robust communication system over a broad coverage area with a single base station and minimum network complexity. This wide coverage area should be achieved with minimum power consumption to fulfil the long battery life requirement of the M2M communication system. In addition, these technologies are designed to maintain high system reliability with low complexity and low cost even with a massive number of connected devices. To accomplish these objectives, some long-range technologies use different collision avoidance techniques without using synchronisation techniques or acknowledgements between the base station and end devices. In general, the most important characteristics of the long-range M2M communication systems can be summarised in four main points (Qadir *et al.*, 2018; Ayoub, Mroue, *et al.*, 2018; Webb, 2015; Anton-Haro and Dohler, 2015; Centenaro *et al.*, 2016; Xiong *et al.*, 2015; Webb, 2012c). First, supporting a vast number of terminals, so that each base station can support thousands to several hundreds of thousands of devices. Second, the low cost for both hardware and services such that the total cost of the terminal will be in a range of $2 to $5. Third, low power consumption so that terminals can work on a single battery for about ten years without any external power supply. Finally, excellent coverage that requires a 100% coverage for indoor and outdoor devices.

In the next sections, an outline of the characteristics of the main long-range M2M communication technologies with a detailed comparison between them is presented.

2.4.1 DASH7

The DASH7 Alliance protocol was first proposed in 2009 for radio frequency identification (RFID) and wireless sensors applications at a frequency of 433 MHz. In 2013, the DASH7 Alliance expanded the frequency range to sub-1GHz bands of 868 MHz and 915 MHz for Europe and the USA respectively. The Dash7 Alliance protocol is based on the ISO/IEC 18000-7 standard with seven OSI protocol layers, as shown in Figure 2.21 (Aravind *et al.*, 2018; Ayoub, Samhat, *et al.*, 2018; Ayoub, Nouvel, *et al.*, 2018; Ayoub, Mroue, *et al.*, 2018; Berkvens *et al.*, 2017; Grabia *et al.*, 2017; Shahid and Masud, 2015; Piromalis *et al.*, 2013; DASH7 Alliance, 2017; DASH7 Alliance, 2015; Weyn *et al.*, 2015; Tuset-Peiró *et al.*, 2014; Weyn *et al.*, 2013).

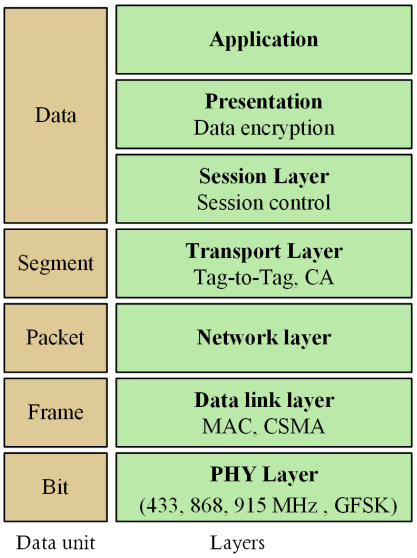

Figure 2.21: The DASH7 protocol stack.

DASH7 uses a BLAST network technology, which stands for Bursty, Light, Asynchronous, Stealth, and Transitional. "Bursty" means that data are sent as short sporadic packets according to the request-response topology. "Light" stands for the small packet size that is limited to a maximum size of 256 bytes with a payload of 0 – 250 bytes. "Asynchronous" means that there is no synchronisation between terminals and the base station. DASH7 is assumed to be "Transitional" because it is an upload-centric communication system where nodes send requests to the gateway at any time and wait for the gateway acknowledgement. Finally, the term "Stealth" refers to the fact that it does not support discovery beacons, so that endpoints can only respond to pre-approved devices (Aravind *et al.*, 2018; Ayoub, Samhat, *et al.*, 2018; Ayoub, Nouvel, *et al.*, 2018; Ayoub, Mroue, *et al.*, 2018; Piromalis *et al.*, 2013; DASH7 Alliance, 2017; Ghamari *et al.*, 2016; Weyn *et al.*, 2015; DASH7 Alliance, 2015; Vilajosana *et al.*, 2014; Weyn *et al.*, 2013; Lee *et al.*, 2013).

DASH7 employs the GFSK modulation scheme and supports three channel classes with different characteristics, namely lo-rate, normal, and hi-rate. The lo-rate class provides a data rate of 9.6 kbps with fifteen channels each with 108 kHz bandwidth and channel spacing of 25 kHz. The normal class provides a data rate of 55.555 kbps with eight channels each with 216 kHz bandwidth and 200 kHz channel spacing. Finally, the hi-rate class provides 166.667 kbps with four 432 kHz channels and 200 kHz channel spacing (Bembe *et al.*, 2019; Aravind *et al.*, 2018; Ayoub, Samhat, *et al.*, 2018; Ayoub, Nouvel, *et al.*, 2018; Ayoub, Mroue, *et al.*, 2018; Grabia *et al.*, 2017; DASH7 Alliance, 2017; Weyn *et al.*, 2015;

DASH7 Alliance, 2015; Ergeerts *et al.*, 2015; Vilajosana *et al.*, 2014; Tuset-Peiró *et al.*, 2014; Weyn *et al.*, 2013; Piromalis *et al.*, 2013; Lee *et al.*, 2013).

DASH7 supports three network topologies: star, tree with two hops, and mesh. It can achieve a coverage range between 1 to 3 km for each cell with transmission power of 0 – 16 dBm (1 – 40 mW). DASH7 is designed to support up to 10000 nodes by utilising a tag addressing scenario, rather than using the ID address, and tag collection scheme (Bembe *et al.*, 2019; Aravind *et al.*, 2018; Ayoub, Samhat, *et al.*, 2018; Grabia *et al.*, 2017; Shahid and Masud, 2015; Piromalis *et al.*, 2013; Lee *et al.*, 2013; Weyn *et al.*, 2013; DASH7 Alliance, 2014; Tuset-Peiró *et al.*, 2014).

In addition, DASH7 employs the slotted ALOHA protocol with the CSMA/CA technique to reduce the probability of collision. It supports three collision avoidance algorithms: Adaptive Increase No Division (AIND), Random Adaptive Increase No Division (RAIND), and Random Increase Geometric Division (RIGD), as shown in Figure 2.22 (Ayoub, Samhat, *et al.*, 2018; Grabia *et al.*, 2017; Lee *et al.*, 2013; DASH7 Alliance, 2017; Weyn *et al.*, 2015; DASH7 Alliance, 2015; Weyn *et al.*, 2013).

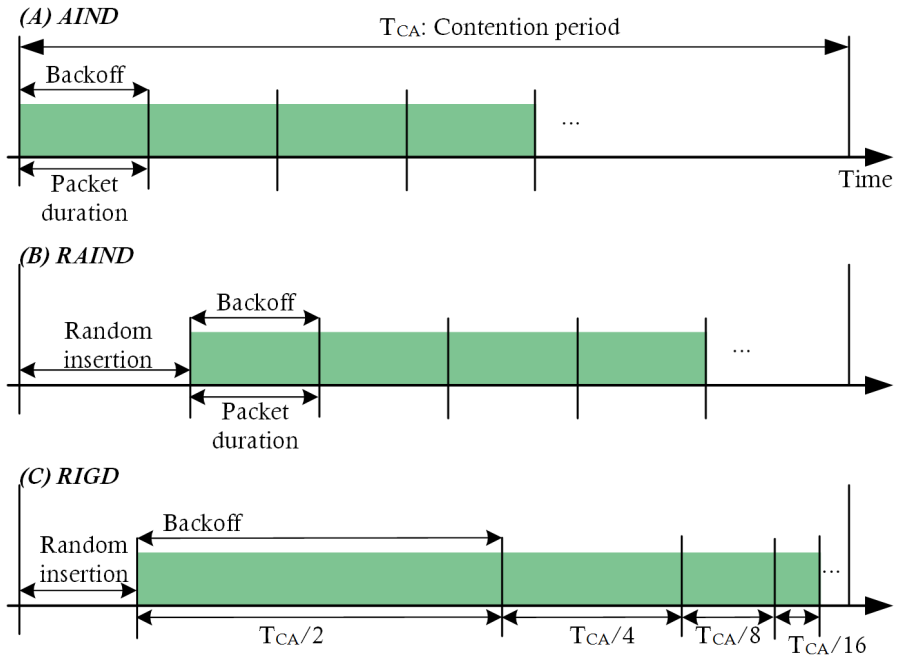

Figure 2.22: DASH7 collision avoidance models.

In AIND mode, a linear slot backoff time is implemented, and the CSMA process is executed at the beginning of the slot. The slot length is fixed and approximately equals the

duration of the transmission. If the transmission fails, the transmitter will wait for a random duration that is equal to a multiple of the slot duration. If the total wait duration exceeds a certain time limit, called contention time, the transmission fails. RAIND applies the same process above for AIND except that a random wait duration is initially implemented before executing the CSMA process. RIGD is similar to RAIND, but the slot length decays by a factor of $(1/(2^{n+1}))$ for each transmission attempt (Ayoub, Samhat, *et al.*, 2018; Vilajosana *et al.*, 2014; Weyn *et al.*, 2015; DASH7 Alliance, 2015; Weyn *et al.*, 2013; Lee *et al.*, 2013; DASH7 Alliance, 2017). As reported by (Lee *et al.*, 2013), simulation results show that AIND algorithm provides the lowest collision avoidance among the previous methods.

2.4.2 Ingenu

In 2013 the Company Ingenu, which was formerly known as On-Ramp Wireless and re-branded in September 2015, announced its first LPWAN system specifications by adapting its previous industrial wireless network to fulfil the modern M2M communication systems. Ingenu is a founder member of the IEEE 802.15.4k task group, which adopts the use of the On-Ramp innovative channel access method called Random Phase Multiple Access (RPMA) protocol. Ingenu employs the RPMA technology with the direct sequence spread spectrum (DSSS) technique, a Viterbi channel coding algorithm, message spreading, and other error correction algorithms to achieve the long-range requirement in the 2.4 GHz frequency band with a minimum Bit Error Rate (BER) (Bembe *et al.*, 2019; Kail *et al.*, 2018; Carlsson *et al.*, 2018; Centenaro *et al.*, 2016; Sanchez-Iborra and Cano, 2016; Myers *et al.*, 2009; Evans-Pughe, 2013).

Ingenu employs the BPSK modulation scheme with a transmission power of 21 dBm (125 mW) and a low receiver sensitivity of -145 dBm to attain its long-range communication. Ingenu claims that each base station provides a line of sight communication of up to 65 km and non-line of sight communication of about 15 km. It also provides a coverage range of 5 km in urban areas and 2 km for underground nodes. Furthermore, it claims that with such a transmission power the battery life can be between 10 to 20 years depending on the number of messages per day (Carlsson *et al.*, 2018; Centenaro *et al.*, 2016; Sanchez-Iborra and Cano, 2016; Myers *et al.*, 2009; Ofcom, 2014; Ingenu, 2015a; Ingenu, 2015b).

Ingenu utilises a message payload of 11 bytes with a data rate of 19 kbps. It also utilises a channel width of 1 MHz and channel spacing of 2 MHz, which provides a total number of 80 channels in the 80 MHz available bandwidth for the 2.4 GHz band, as shown in Figure 2.23. However, Ingenu uses only 8 channels from these available channels to mitigate the

interference with other channels and with the coexistence signals like the WiFi 802.11. Although RPMA technique supports the demodulation of up to 1200 overlapped signals, Ingenu base station utilises 1000 overlapped signals from different nodes on each channel. This provides a total number of up to 8000 devices that can be connected in a star topology with the base station. Moreover, Ingenu supports the tree network topology (Bembe *et al.*, 2019; Ofcom, 2014; Sanchez-Iborra and Cano, 2016; Ingenu, 2015a; Myers *et al.*, 2009; Ingenu, 2015b; Ingenu, 2016a).

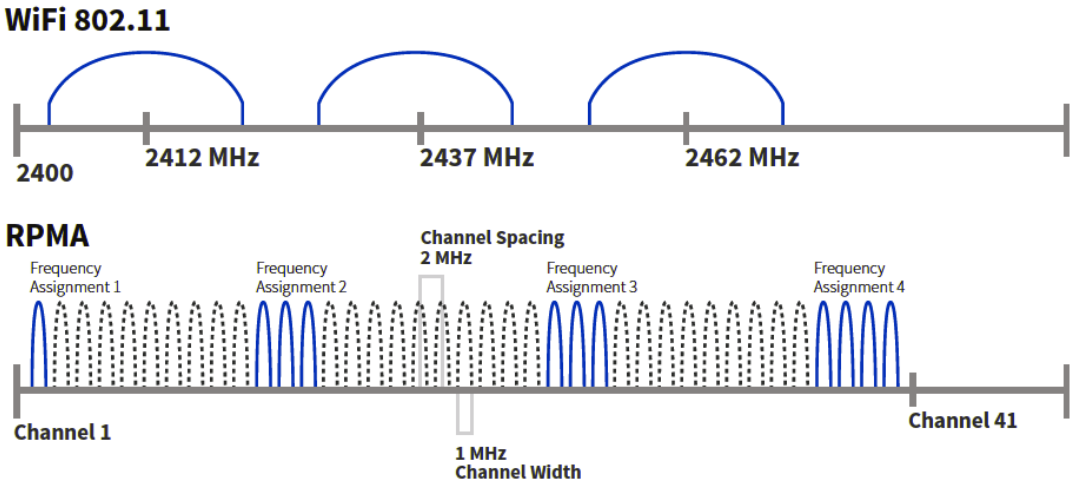

Figure 2.23: RPMA operating channels (Ingenu, 2016a).

The data scheduling process used by Ingenu technology to reduce the probability of collision is a mix between the random time access and a frame synchronisation technique. First, the base station synchronises the start time of the transmission frame with all nodes, then each node will choose a random time delay to start its data transmission. The random time delay plus the frame length should always be less than a time slot that is defined by the base station to listen to the nodes, as shown in Figure 2.24.

To simplify the demodulation process, the base station uses a blind demodulation technique that is based on the hypothesis that all data have been received correctly. The base station then uses the cyclic redundancy check (CRC) technique to indicate any error in the received data. If an error is detected, the message will be neglected, and no acknowledgement will be sent to the end node. Therefore, the end node should send the message again until receiving the acknowledgement. The collision occurs in RPMA system when more than one node chooses the same random time delay to start its transmission.

In such a case the base station cannot demodulate the signals separately (Ingenu, 2015a; Myers *et al.*, 2009; Ingenu, 2015b; Ingenu, 2016b; Ingenu, 2016a).

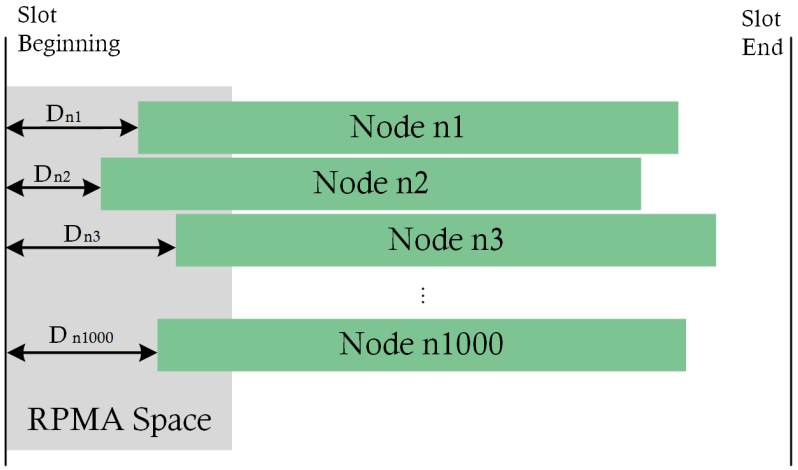

Figure 2.24: RPMA scheduling scheme.

2.4.3 IEEE 802.11ah

IEEE 802.11ah is a long-range wireless communication technology designed by the IEEE 802.11ah task group (called TGah) to fulfil the long range and low power requirements of the M2M systems. In 2010, the IEEE 802.11ah task group was founded to design the new IEEE 802.11ah standard, and in 2013 the task group announced the first version of the IEEE 802.11ah standard. Later in 2017, TGah published the final version of IEEE 802.11ah specifications standard (Bembe *et al.*, 2019; Sun *et al.*, 2017; IEEE Computer Society, 2017; Domazetovic *et al.*, 2016; Khorov *et al.*, 2015; Park, 2015; Adame *et al.*, 2014). IEEE 802.11ah supports the periodic sleeping approach to reduce the power consumption with a maximum communication range of 1 km. In addition, the maximum payload size supported by IEEE 802.11ah is limited to 256 bytes, which is adequate for most M2M applications (Kos *et al.*, 2019; U. and A. V., 2019; Soares and Carvalho, 2019; Bembe *et al.*, 2019; Qiao *et al.*, 2018; Liu *et al.*, 2018; Rao *et al.*, 2018; Kocan *et al.*, 2017; Domazetovic and Kocan, 2017; Khorov *et al.*, 2015; Aust *et al.*, 2015).

IEEE 802.11ah supports a wide range of sub-1 GHz ISM bands, excluding the TV white space spectrum, as shown in Figure 2.25. Moreover, it employs different modulation schemes including BPSK, QPSK, 16-QAM, 64-QAM, and 256-QAM with a channel

bandwidth of 1 MHz, 2 MHz, 4 MHz, 8 MHz, or 16 MHz depending on the used band, the maximum required throughput, and the coverage range. IEEE 802.11ah provides an extensive range of data rates within the range of 150 kbps up to 347 Mbps. Furthermore, IEEE 802.11ah supports a transmission power of 0 – 30 dBm (1 – 1000 mW) with a battery lifetime from months up to several years, especially that terminals are able to sleep for up to 5 years without disassociation from the access point (AP) (U. and A. V., 2019; Kos *et al.*, 2019; Bembe *et al.*, 2019; Liu *et al.*, 2018; Rao *et al.*, 2018; Sun *et al.*, 2017; Domazetovic and Kocan, 2017; Kocan *et al.*, 2017; Tian *et al.*, 2017; Domazetovic *et al.*, 2016; Damayanti *et al.*, 2016; IEEE Computer Society, 2017).

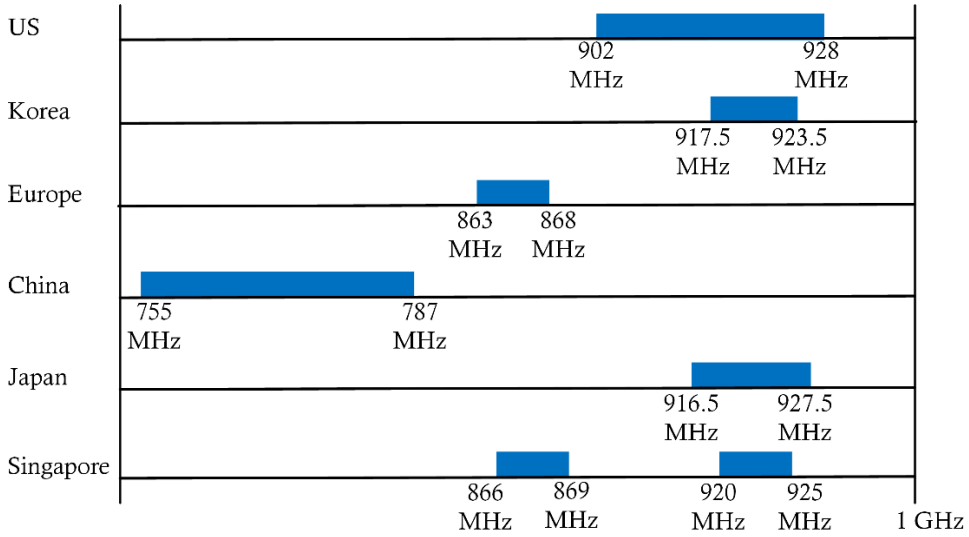

Figure 2.25: ISM bands utilised by the IEEE 802.11ah standard.

IEEE 802.11ah is based on the star and the tree network topologies and was first designed to handle up to 6000 end devices, which are called stations (STAs), then it was extended to supports up to 8191 STAs (U. and A. V., 2019; Chang *et al.*, 2019; Rao *et al.*, 2018; Gopinath and Nithya, 2018; Tian *et al.*, 2017; Damayanti *et al.*, 2016; Park, 2015; Khorov *et al.*, 2015; Aust *et al.*, 2015; Ji *et al.*, 2015; Adame *et al.*, 2014). Stations in the IEEE 802.11ah are divided into three types according to the channel access mechanism and the data transmission scheme illustrated in Figure 2.26 (U. and A. V., 2019; Chang *et al.*, 2019; Soares and Carvalho, 2019; Ali *et al.*, 2019; Gopinath and Nithya, 2018; Bel *et al.*, 2018; Tian *et al.*, 2017; Sun *et al.*, 2017; Khorov *et al.*, 2015; Park, 2015; Adame *et al.*, 2014; Park *et al.*, 2014; Park, 2014; IEEE Computer Society, 2017). These types are:

1. Traffic indication map (TIM) stations, which are intended for high traffic nodes with minimum power consumption by employing a periodic data transmission approach. To send and receive data, TIM stations should first listen to the AP beacons and access the channel within a restricted time window called Restricted Access Window (RAW).
2. Non-TIM stations, which can directly connect to the AP at any time and send data in a periodically restricted access window (PRAW) that defined by the AP.
3. Unscheduled stations, which are designed for applications that need to send data irregularly. These stations can send an immediate channel access request to the AP at any time. The AP then defines a special access window to receive data from these stations, which should be outside both RAW and PRAW windows.

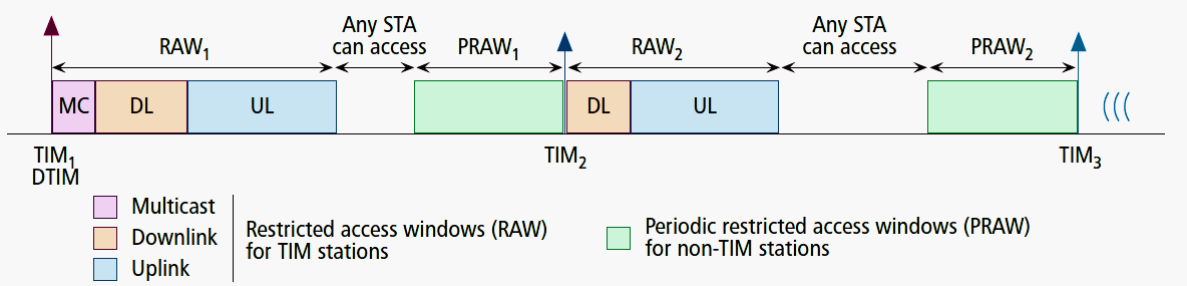

Figure 2.26: IEEE 802.11ah channel access approach (Adame *et al.*, 2014).

Moreover, IEEE 802.11ah employs packet acknowledgements to improve system performance and reduce the probability of lost messages. However, the channel access approach described above provides a high network latency as the number of stations becomes high. Moreover, the probability of collision will be high especially if many stations received the same beacon from the AP and try to access the channel at the same RAW. Also, if many unscheduled stations need to transmit data at the same time, the probability of collision will be high. Therefore, increasing the number of stations is one of the most important factors that significantly affects system reliability and performance (Soares and Carvalho, 2019; Chang *et al.*, 2019; Gopinath and Nithya, 2018; Damayanti *et al.*, 2016; Aust *et al.*, 2015; Khorov *et al.*, 2015; Park, 2015; Park, 2014).

2.4.4 LoRaWAN

In January 2015 LoRa Alliance published the first version of its new M2M communication technology named LoRaWAN, which was formerly designed by Semetch Corporation. LoRa intended to provide long-range communication with low power and low data rate

by utilising the Chirp Spread Spectrum (CSS) technique with the FSK modulation scheme. It supports three channel bandwidths of 125 kHz, 250 kHz, and 500 kHz, and is designed to work in sub-1GHz bands of 430 MHz, 433 MHz, 868 MHz, and 915 MHz. In addition, LoRaWAN supports 3 channels in Europe and 8 channels in the US. It also provides a data rate of 0.3 – 50 kbps with a maximum payload of 250 bytes. Furthermore, LoRaWAN supports an adaptive data rate scheme, in which the terminal node automatically changes its data rate according to the channel conditions. LoRaWAN provides a communication range of 5 km in urban areas and up to 15 km in rural areas with typical transmission power of 14 – 20 dBm (25 – 100 mW) in Europe and up to 27 dBm (500 mW) in the US. Despite this high transmission power, LoRa claims that the battery lifetime of end devices can be in the range of 5 – 10 years based on data scheduling. LoRaWAN utilises different spreading factors (SF) in the range of 7 – 12, where using a higher spreading factor increases the communication range and decreases the transmission throughput. (Mekki *et al.*, 2019; Bembe *et al.*, 2019; Kos *et al.*, 2019; Ayoub, Samhat, *et al.*, 2018; Carlsson *et al.*, 2018; Croce *et al.*, 2018; Dias and Grilo, 2018; Lee and Ke, 2018; Nugraha *et al.*, 2018; Qadir *et al.*, 2018; Fehri *et al.*, 2018; Adelantado *et al.*, 2017; Casals *et al.*, 2017; Lavric and Popa, 2017a; Lavric and Popa, 2017b; LoRa Alliance, 2017; Bor *et al.*, 2016; Centenaro *et al.*, 2016; Nolan *et al.*, 2016; Mehboob *et al.*, 2016; Sanchez-Iborra and Cano, 2016; Semtech, 2017; LoRa Alliance, 2015; Semtech, 2015). Figure 2.27 demonstrates the frame structure and the transceiver physical block diagram for LoRaWAN (Ghanaatian *et al.*, 2019).

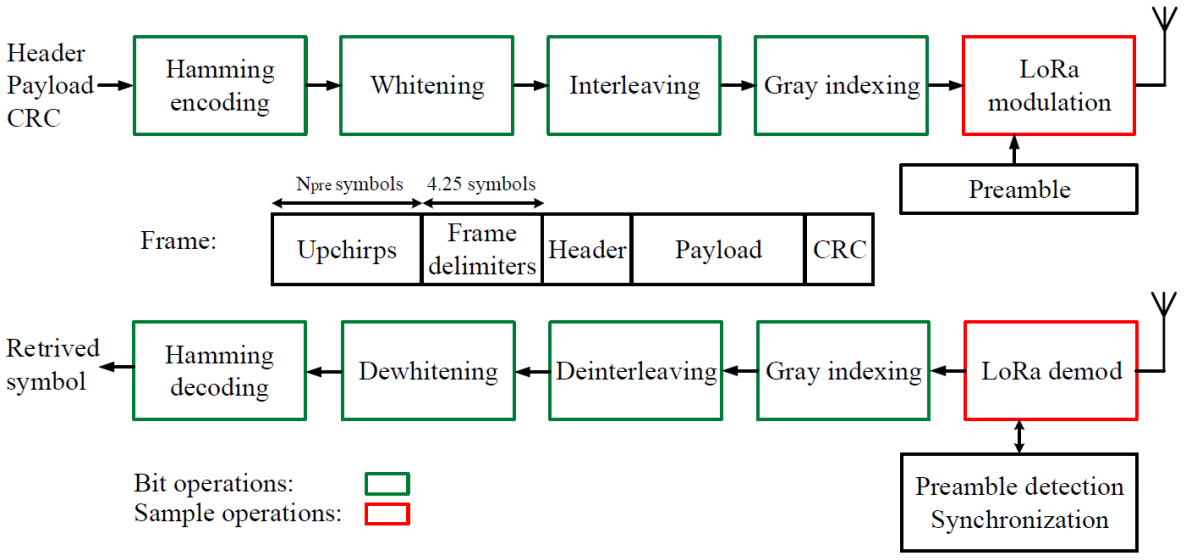

Figure 2.27: LoRaWAN frame structure and PHY block diagram (Ghanaatian *et al.*, 2019).

Figure 2.28 shows the LoRaWAN protocol architecture (Qadir et al., 2018; Casals et al., 2017; Lavric and Popa, 2017b; LoRa Alliance, 2017; LoRa Alliance, 2015). LoRa supports bidirectional communication with an asynchronous uplink scheme. It also supports three types of terminal devices based on LoRaWAN MAC layer classes: Class A, Class B, and Class C (Mekki *et al.*, 2019; Ayoub, Samhat, *et al.*, 2018; Fehri *et al.*, 2018; Carlsson *et al.*, 2018; Qadir *et al.*, 2018; Adelantado *et al.*, 2017; Casals *et al.*, 2017; Lavric and Popa, 2017a; Lavric and Popa, 2017b; LoRa Alliance, 2017; Bor *et al.*, 2016; Centenaro *et al.*, 2016; Nolan *et al.*, 2016; Mehboob *et al.*, 2016; Sanchez-Iborra and Cano, 2016; LoRa Alliance, 2019).

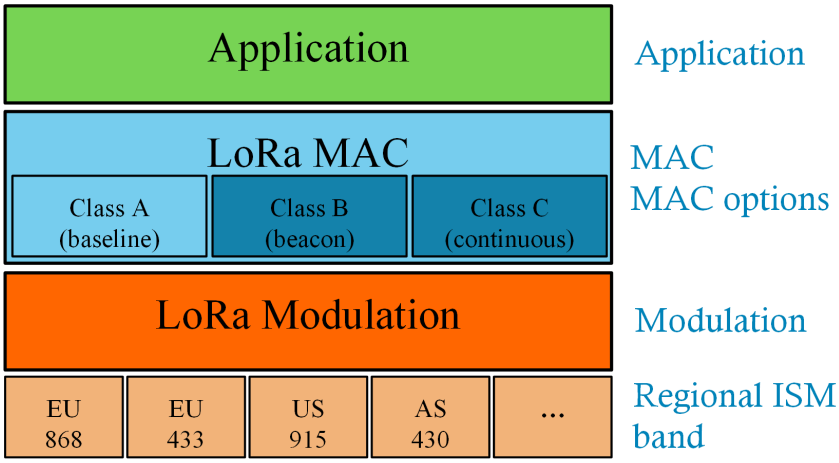

Figure 2.28: LoRaWAN architecture and classes (LoRa Alliance, 2017).

These classes can be summarised as follows:

- **Class A - Lowest power bi-directional end-devices**: Devices in Class A send data according to their needs asynchronously with a random time access scheme based on the ALOHA protocol. Each uplink transmission followed by two short downlink receive windows, as shown in Figure 2.29. Other received data should wait until the next uplink request from the terminal. This operation offers the lowest power consumption for the LoRaWAN since Class A devices can enter long period sleep mode without the need for periodic wakeup.
- **Class B - Bi-directional end-devices with scheduled receive slots**: Class B devices support the random receive windows of Class A. In addition, Class B devices add extra downlink windows at scheduled times, which can be opened after receiving a time

synchronized Beacon from the gateway. This synchronises the terminal downlink communication with the server at certain time slots.

- **Class C - Bi-directional end-devices with maximal receive slots:** Class C offers a continuous receiving window, which only closes in the transmission period. This reduces communication latency and ensures that all downlinks will be received at any time. However, continuous listening significantly increases the power consumption and reduces battery life, where the receiver power consumption is about 50 mW. Therefore, Class C devices are mostly suitable for applications where continuous power is available.

LoRa is based on a star-of-stars network topology with a single hop and a single gateway for each sub-star, as shown in Figure 2.30. Gateways work as a transparent bridge and relay messages between terminal nodes and the LoRa network server. Moreover, devices can communicate with multiple gateways at the same time (Bembe *et al.*, 2019; Dias and Grilo, 2018; Lee and Ke, 2018; Qadir *et al.*, 2018; Adelantado *et al.*, 2017; Casals *et al.*, 2017; Lavric and Popa, 2017b; LoRa Alliance, 2017; Bor *et al.*, 2016; Centenaro *et al.*, 2016; Sanchez-Iborra and Cano, 2016).

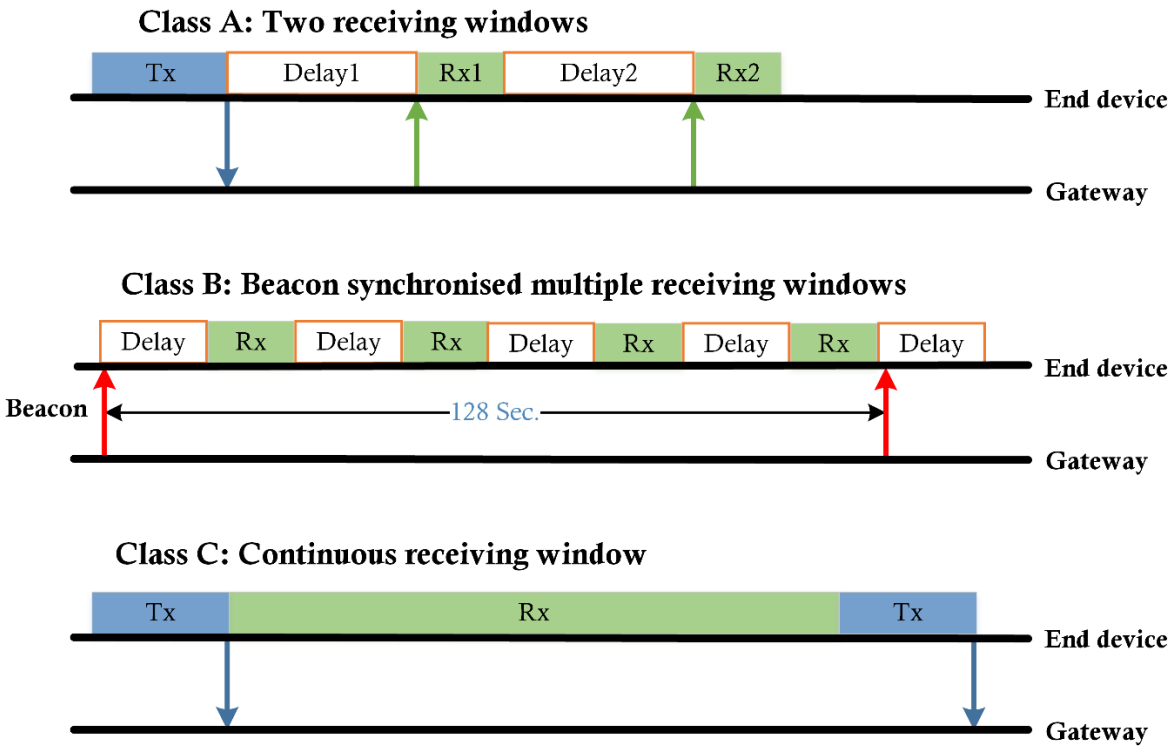

Figure 2.29: LoRaWAN receive slots timing.

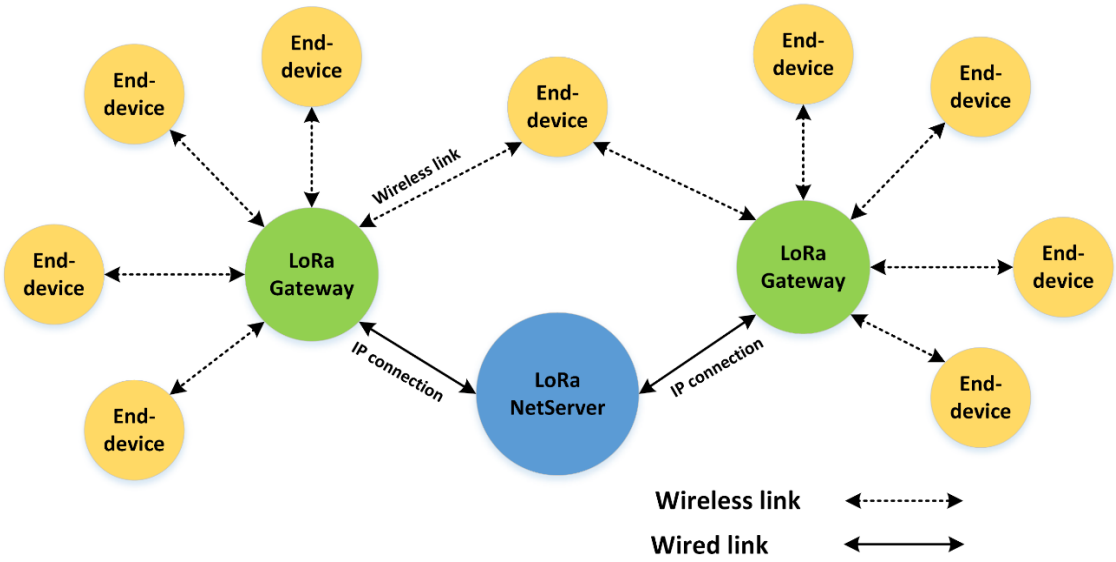

Figure 2.30: LoRaWAN network architecture.

Since LoRaWAN is based on the ALOHA protocol, it depends on low duty cycle transmission and the use of random frequency hopping to mitigate the collision problem. In addition, LoRaWAN employs the message acknowledgement approach to increase system reliability. End devices retransmit the same message if the acknowledgement is not received. This will be continued until either an acknowledgement is received or attempts of 8 retransmissions are reached, after which the message will be dropped. Furthermore, LoRa gateways are designed with the capability of receiving multiple messages on up to 9 channels simultaneously. Moreover, LoRa gateways can decode different messages on the same channel with different spreading factors. This increases the LoRaWAN network capacity (Mekki *et al.*, 2019; Lee and Ke, 2018; Qadir *et al.*, 2018; Fehri *et al.*, 2018; Adelantado *et al.*, 2017; Casals *et al.*, 2017; LoRa Alliance, 2017; Centenaro *et al.*, 2016; Mikhaylov and Petäjäjärvi, 2016; LoRa Alliance, 2015).

In general, LoRaWAN was designed to support several thousands of devices for each network cell. However, using the ALOHA protocol with a limited number of channels (only 3 channels in Europe) provides a high probability of collision. Studies presented by Adelantado *et al.* and Mikhaylov and Petäjäjärvi (Adelantado *et al.*, 2017; Mikhaylov and Petäjäjärvi, 2016) show that the practical range of connected devices may vary from several hundred up to 5000 devices based on the spreading factor and the number of packets per hour.

2.4.5 Sigfox

The company Sigfox was formed in 2008 by Ludovic Le Moan and Christophe Fourtet in Labege, France. Later in 2009, SIGFOX announced its new low-power wide area network (LPWAN) for M2M communication systems by utilising the ultra-narrow band (UNB) technology. Sigfox employs three ISM bands: the 868 MHz band for Europe and the Middle East, the 902 MHz band for North America, and the 923 MHz band for other countries (Bembe *et al.*, 2019; Sigfox, 2019a; Sigfox, 2019b; Kail *et al.*, 2018; Qadir *et al.*, 2018; Adelantado *et al.*, 2017; Centenaro *et al.*, 2016; Mehboob *et al.*, 2016; Cendo´n, 2015).

Sigfox uses the Differential Binary Phase Shift keying (DBPSK) modulation scheme for the upload link with a channel bandwidth of 100 Hz and a low data rate of 100 bps. It also limits the payload with a maximum size of 12 bytes and a total message size of 26 bytes. The maximum message rate of Sigfox is limited to 140 messages per day for each device. On the other hand, Sigfox employs the GFSK modulation scheme with a channel bandwidth of 600 Hz and a bit rate of 600 bps for the downlink. Sigfox limits the number of downlink messages by a maximum rate of 4 messages per day each with a maximum payload of 8 bytes. Sigfox was first designed to utilise 400 UNB channels and in 2017 Sigfox extended the base station bandwidth to support up to 1920 channels (Mekki *et al.*, 2019; Bembe *et al.*, 2019; Lavric *et al.*, 2019; Sigfox, 2019a; Carlsson *et al.*, 2018; Chung *et al.*, 2018; Qadir *et al.*, 2018; Adelantado *et al.*, 2017; Li *et al.*, 2017; Ali *et al.*, 2017; Vejlgaard *et al.*, 2017; Sigfox, 2017a; Sigfox, 2017c; Nolan *et al.*, 2016; Centenaro *et al.*, 2016; Mehboob *et al.*, 2016; Sanchez-Iborra and Cano, 2016; Goursaud and Gorce, 2015; Cendo´n, 2015).

Sigfox is based on the star network topology to cover a wide area with a massive number of devices using a single base station. Sigfox claims that each base station can handle up to one million devices and a communication range of about 3 – 10 km in urban areas. The coverage range is much higher for rural areas and can be in the range of 30 – 50 km. This coverage area can be achieved by Sigfox with a transmission power of 14 dBm (25 mW). With such low power consumption and a low data rate, Sigfox devices can work with a single battery for up to 10 years (Mekki *et al.*, 2019; Bembe *et al.*, 2019; Lavric *et al.*, 2019; Carlsson *et al.*, 2018; Kail *et al.*, 2018; Chung *et al.*, 2018; Qadir *et al.*, 2018; Ali *et al.*, 2017; Sigfox, 2017b; Lauridsen *et al.*, 2017; Vejlgaard *et al.*, 2017; Nolan *et al.*, 2016; Centenaro *et al.*, 2016; Mehboob *et al.*, 2016; Sanchez-Iborra and Cano, 2016; Cendo´n, 2015).

Although Sigfox supports a massive number of connected devices, it utilises the pure ALOHA technique (random time-frequency access) and does not implement the

acknowledgement process or any collision avoidance mechanism. In contrast, to mitigate the collision problem, Sigfox employs the frequency hopping (FH) technique over a large number of ultra-narrow band channels. In addition, Sigfox employs a multiple message copies approach to further mitigate the effect of collisions on the system performance. Each Sigfox device sends three identical copies of each transmitted message on three different randomly selected channels. This increases the probability of successful transmission and improves system reliability (Lavric *et al.*, 2019; Sigfox, 2019a; Adelantado *et al.*, 2017; Li *et al.*, 2017; Sigfox, 2017b; Vejlgaard *et al.*, 2017; Goursaud and Gorce, 2015). Moreover, the low message rate and the small packet size utilised by Sigfox also reduce the effect of collisions on the system performance.

2.4.6 Weightless

Weightless is a LPWAN open standard designed by Weightless Special Interest Group (Weightless-SIG), which was formed in 2011 and based in Cambridge, England. Weightless-SIG promotes the use of TV white space and the sub-GHz spectrum for its new Weightless technology with three different standards: Weightless-W, Weightless-N, and Weightless-P. Each one of these standards was designed with particular characteristics and specifications to fulfil a wide range of applications and markets, as will be explained in the following sections (Webb, 2015; Webb, 2013; Webb, 2012a; Webb, 2012b; Webb, 2012c; Weightless-SIG, 2015b; Weightless-SIG, 2015g).

A. Weightless-W

In 2013, Weightless-SIG published the final release of the Weightless-W standard, which provides extensive features with an average cost in comparison with other LPWAN technologies. It employs the TV white space spectrum with a frequency range of 470 – 790 MHz and a channel bandwidth of 6 or 8 MHz depending on the local regulations. Weightless-W supports different modulation schemes including 16-QAM, QPSK, BPSK, and DBPSK with a wide range of data rates from 1 kbps up to 10 Mbps. The minimum payload supported by Weightless-W is 10 bytes, and the maximum limit is 255 bytes. In addition, Weightless-W is based on the star network topology with a coverage range of up to 5 km in urban areas. Weightless-W terminal nodes can achieve such a communication range with 40 mW (16 dBm) transmission power. Weightless-W supports periodic sleeping so that terminals can work on a single battery from three to five (3 – 5) years depending on the message rate (Bembe *et al.*, 2019; Carlsson *et al.*, 2018; Adelantado *et al.*, 2017; Ali *et al.*, 2017; Sanchez-Iborra and Cano, 2016; Xiong *et al.*, 2015; Goursaud and Gorce, 2015; Webb, 2013; Weightless-SIG, 2015b; Weightless-SIG, 2013; Weightless-SIG, 2015d).

Weightless-W is designed to support up to one million terminals for each base station with a restricted time and frequency synchronisation approach. Moreover, it uses the Time Division Duplex (TDD) technique to divide the data frame between the downlink and the uplink in each transmission. To handle such a vast number of terminal devices, Weightless-W employs Time Division Multiple Access (TDMA) and Frequency Division Multiple Access (FDMA) techniques (Adelantado *et al.*, 2017; Xiong *et al.*, 2015; Webb, 2013; Weightless-SIG, 2013).

For the downlink communication, TDMA is utilised on a single carrier and a single TV channel (6 MHz or 8 MHz) to send commands and synchronisation from the base station to terminal devices. In contrast, Weightless-W employs both TDMA, narrowband FDMA and the frequency hopping technique for uplink communication, as shown in Figure 2.31. It divides each TV channel into 24 narrowband sub-channels and leaves blank spaces between them to reduce the interference between these sub-channels. Furthermore, it utilised only 16 sub-channels to further mitigate the interference problem. To handle the total number of terminals, the base station groups each of 65536 terminals in a single sub-channel using TDMA. Therefore, each terminal should strictly send its data in a certain time slot and on a single sub-channel (Weightless-SIG, 2013).

In addition, Weightless-W employs different techniques like DSSS, message spreading, forward error correction (FEC), cyclic prefixes and postfixes, and a Cyclic Redundancy Check (CRC). All these techniques are implemented to minimise the bit error rate (BER) as much as possible and maintain the synchronisation between the base station and terminals. However, this leads to a complex network structure, high terminal cost, and short battery lifespan, especially with a high message rate. Although this approach does not provide any probability of collisions, there is still a possibility of losing synchronisation between the base station and terminal devices due to (Weightless-SIG, 2013; Webb, 2012a; Webb, 2012c):

- the interference with other terminals on the same sub-channel;
- interference with other sub-channels;
- interference with other adjacent channels that are occupied by high power TV Transmitters.

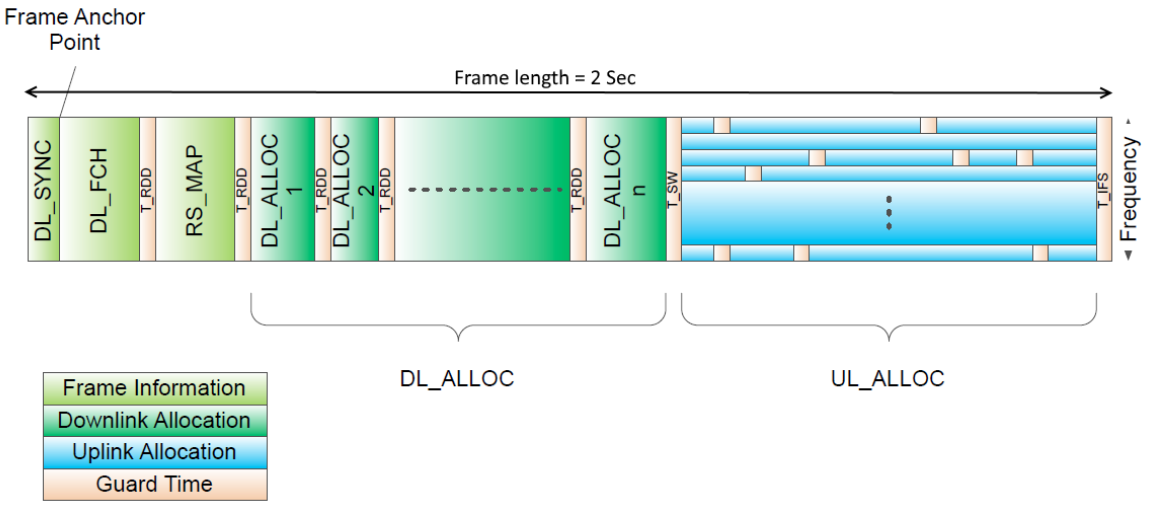

Figure 2.31: Weightless-W frame structure (Weightless-SIG, 2013).

B. Weightless-N

Weightless-N was designed for low cost and long battery life applications with a unidirectional communication scheme. Weightless-SIG announced the final version of the Weightless-N standard in April 2015, which is intended to use the frequency range of 863 – 870 MHz in Europe and the frequency range of 902 – 928 MHz in the USA. It uses the ultra-narrow band (UNB) approach with a channel width of 200 Hz in Europe and 100 Hz in the USA. Weightless-N employs a large number of UNB channels on six different bands as 1200, 1500, 2499, 3000, 9990, and 15000 channels. Weightless-N utilises the DBPSK and provides a low data rate of 100 bps with a maximum message rate of one message per minute. Using a periodic sleeping technique and a low message rate can expand battery life for up to 10 years with a transmission power of 14 dBm (Bembe *et al.*, 2019; Carlsson *et al.*, 2018; Kail *et al.*, 2018; Mehboob *et al.*, 2016; Sanchez-Iborra and Cano, 2016; Weightless-SIG, 2015c).

Weightless-N provides a coverage area of up to 5 km in urban areas with tens of thousands of terminal nodes. To mitigate the collision problem with such a massive number of devices, Weightless-N uses ALOHA protocol and the frequency hopping technique (random time-frequency access) (Bembe *et al.*, 2019; Carlsson *et al.*, 2018; Kail *et al.*, 2018; Goursaud and Gorce, 2015). In addition, each node sends multiple copies of each message to reduce the probability of losing the message due to the collision. The number of message copies can be set in the range of 3 – 8 message copies depending on the application and the

required quality of service (QoS). The frequency hopping sequence used by the Weightless-N is designed to randomise the selected channel on each transmission and ensure that different channels will be selected by different nodes at the same time (Abbas *et al.*, 2017; Weightless-SIG, 2015c).

The Weightless-N channel selection process is divided into two stages. The first stage is by dividing each band into three frequency segments called macro-channels. Each macro-channel contains a number of UNB channels called micro-channels. Before each transmission, each node selects one of these macro-channels using a special randomisation algorithm that is based on the internal timer of this node. The second stage is designed to randomise the selection of micro-channels in each macro-channel based on the internal timer and the ID of the sender node. These two randomisation stages reduce the probability of selecting the same channel by any two different nodes at the same time. Nevertheless, there is a high probability of losing the message due to collisions and other factors that affect communication medium like noise and interference, especially that Weightless-N does not employ any synchronisation or acknowledgement mechanism (Abbas *et al.*, 2017).

C. Weightless-P

In December 2015, Weightless-SIG with the cooperation of M2Comm published the final version of its newest M2M standard named Weightless-P. It is designed to work in all sub-1GHz ISM bands including the frequency bands of 138 MHz, 169 MHz, 433 MHz, 470 MHz, 780 MHz, 868 MHz, 915 MHz and 923 MHz (Weightless-SIG, 2015b; Weightless-SIG, 2015e; Weightless-SIG, 2015f; Weightless-SIG, 2015d; Weightless-SIG, 2015g; Weightless-SIG, 2015a). Weightless-P supports a broad range of data rates for the uplink from 0.625 kbps up to 100 kbps. Weightless-P employs the Gaussian Minimum Shift Keying (GMSK) and the Offset Quadrature Phase Shift Keying (OQPSK) modulation schemes with a typical transmission power of 14 dBm (25 mW). It also provides a coverage range of 2 km in urban areas and battery lifetime of 3 – 8 years (Bembe *et al.*, 2019; Carlsson *et al.*, 2018; Ali *et al.*, 2017; Sanchez-Iborra and Cano, 2016; Goursaud and Gorce, 2015; Weightless-SIG, 2015b; Weightless-SIG, 2015e).

Weightless-P provides fully acknowledged bidirectional communication and employs the TDD technique to divide each frame between the downlink and the uplink with a similar structure to the Weightless-W frame, see Figure 2.31. For the downlink, Weightless-P utilises a single channel with a bandwidth of 100 kHz and TDMA scheme to provide a data rate of 100 kbps. On the other hand, it utilises 8 narrowband sub-channels each with

12.5 kHz bandwidth for the uplink to form a total channel width of 100 kHz. It also employs the TDMA and FDMA for the uplink to handle up to 10000 connected devices simultaneously (Sanchez-Iborra and Cano, 2016; Goursaud and Gorce, 2015; Weightless-SIG, 2015b; Weightless-SIG, 2015e; Weightless-SIG, 2015d; Weightless-SIG, 2015g). Furthermore, to handle such a large number of nodes, Weightless-P supports a long frame duration of up to 16 seconds with a maximum payload of 48 bytes. Each frame is sent in multiple timeslots of 50 ms. However, this provides a high system latency. Weightless-P also uses the frequency hopping technique to reduce the interference problem and improve system robustness (Weightless-SIG, 2015e).

2.4.7 NB-IoT (Narrowband Internet of Things LTE CAT-N)

In 2016, the 3rd Generation Partnership Group (3GPP) announced the first version of the NB-IoT specifications standard which is designed for M2M communication systems. NB-IoT inherits most features of the Long-Term Evolution (LTE) cellular system like operating frequency bands. Unlike LTE, NB-IoT was designed with lower cost, lower power consumption, lower data throughput, and a higher network capacity. NB-IoT supports a transmission power of 23 dBm (200 mW) with battery life of up to 10 years. It also offers a coverage range of 2 km in urban areas and up to 10 km in rural areas (Mekki *et al.*, 2019; Wan *et al.*, 2019; Andres-Maldonado *et al.*, 2019; Martinez *et al.*, 2019; Xu *et al.*, 2018; Ali *et al.*, 2018; ElNashar and El-saidny, 2018; Carlsson *et al.*, 2018; Ayoub, Samhat, *et al.*, 2018; Lauridsen *et al.*, 2017; Vejlgaard *et al.*, 2017; Ali *et al.*, 2017; Shin and Jo, 2017; Ratasuk *et al.*, 2016; Vodafone Group, 2017).

NB-IoT utilises the licenced spectrum band of 700 – 900 MHz with the BPSK and the QPSK modulation schemes. NB-IoT supports three operating modes in this band: stand-alone mode, guard-band mode, and in-band mode, as shown in Figure 2.32. For the stand-alone operation, NB-IoT uses a dedicated carrier inside the Global System for Mobile communication (GSM) spectrum, but it is outside LTE channels, with a bandwidth of 200 kHz. In the guard-band operating mode, NB-IoT utilises the guard bands of the LTE operating spectrum with a bandwidth of 180 kHz. On the other hand, the same LTE channels are employed by the NB-IoT for the in-band operation with a 180 kHz bandwidth (Bembe *et al.*, 2019; Mekki *et al.*, 2019; Wan *et al.*, 2019; Ayoub, Samhat, *et al.*, 2018; Xu *et al.*, 2018; Ali *et al.*, 2018; ElNashar and El-saidny, 2018; Oh and Song, 2018; Ali *et al.*, 2017; Yu *et al.*, 2017; Ratasuk *et al.*, 2016; Vodafone Group, 2017).

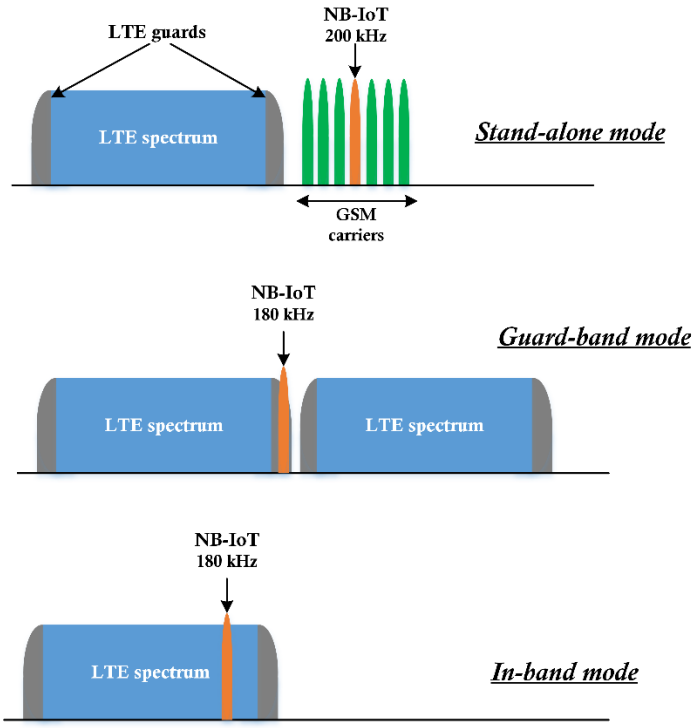

Figure 2.32: NB-IoT operating modes.

NB-IoT employs Orthogonal Frequency-Division Multiple Access (OFDMA) scheme for the downlink communication with 12 subcarriers each of 15 kHz width. For the uplink transmission, NB-IoT uses two channel access schemes: mandatory single-tone Frequency-Division Multiple Access (FDMA), like LTE, and optional multi-tone Single-Carrier Frequency Division Multiple Access (SC-FDMA). Single-tone transmission supports two different channel bandwidths: 15 kHz and 3.75 kHz. The 15 kHz channel bandwidth supports four different numbers of subcarriers: 1, 3, 6, and 12. On the other hand, the multi-tone transmission is based only on the 15 kHz subcarrier spacing. With such specifications, NB-IoT offers a maximum data rate of up to 200 kbps for download communication with a maximum payload size of 85 bytes. In contrast, for upload communication, it provides either up to 144 kbps with the multi-tone transmission or up to 20 kbps with the single-tone transmission with a maximum payload size of 128 bytes. (Bembe *et al.*, 2019; Mekki *et al.*, 2019; Wan *et al.*, 2019; Andres-Maldonado *et al.*, 2019; Bao *et al.*, 2018; Ayoub, Samhat, *et al.*, 2018; Xu and Darwazeh, 2018; Xu *et al.*, 2018; Ali *et al.*, 2018; ElNashar and El-saidny, 2018; Oh and Song, 2018; Chen *et al.*, 2018; Ayoub, Mroue, *et al.*, 2018; Kim *et al.*, 2018; Vejlgaard *et al.*, 2017; Ali *et al.*, 2017; Yu *et al.*, 2017; Andres-Maldonado *et al.*, 2017; Sinha *et al.*, 2017; Lin *et al.*, 2016; Wang *et al.*, 2017; Elsaadany *et al.*, 2017; Persia and Rea, 2016; Dawaliby *et al.*, 2016).

NB-IoT is based on the star network topology and was designed to support up to 50 thousand nodes for each cell, based on low rate end devices (Wan *et al.*, 2019; Xu and Darwazeh, 2018; Xu *et al.*, 2018; Song *et al.*, 2017; Ratasuk *et al.*, 2016; Wang *et al.*, 2017; Biral *et al.*, 2015). To handle such a large number of connected devices, NB-IoT offers two channel access mechanisms for the uplink transmission: Narrowband Physical Uplink Shared Channel (NPUSCH) and Narrowband Physical Random Access Channel (NPRACH). NPUSCH used by terminal nodes to send acknowledgements to the base station to ensure receiving commands and resources allocations. On the other hand, NPRACH is used by connected devices to send its data to the base station (Wan *et al.*, 2019; Andres-Maldonado *et al.*, 2019; Martinez *et al.*, 2019; Harwahyu *et al.*, 2019; Ayoub, Samhat, *et al.*, 2018; Ali *et al.*, 2018; ElNashar and El-saidny, 2018; Yu *et al.*, 2017; Andres-Maldonado *et al.*, 2017; de Andrade *et al.*, 2016). To transmit data, devices need to perform a random request among the available channels (NPRACH) by sending a randomly chosen preamble. The total number of narrowband channels is either 12 in the case of 150 kHz channel width or 48 in the case of 3.75 kHz channel width. The base station can detect the non-collided packets and send random access response messages with a dedicated time offset for each detected preamble. Devices then send data on these dedicated resources (Andres-Maldonado *et al.*, 2019; Harwahyu *et al.*, 2019; Ayoub, Samhat, *et al.*, 2018; ElNashar and El-saidny, 2018; Andres-Maldonado *et al.*, 2017; Lin *et al.*, 2016; Wang *et al.*, 2017).

When two or more nodes select the same channel to send the preamble or select the same channel to send data, due to the same preamble selection, collisions occur. To mitigate the collision effect, NB-IoT utilises the frequency hopping technique with a pseudorandom channel selection sequence to send the preamble and the data on different channels each time. Furthermore, NB-IoT devices use acknowledgements to ensure data reception. In addition, NB-IoT employs another key feature called message repetitions approach to further reduce the effect of collisions and increase the coverage range. If devices do not receive the acknowledgement, they will resend the packet again using the same random channel access technique. The main advantage of the repetitions approach implemented by the NB-IoT is the large number of supported repetitions, where a maximum number of 128 repetitions is permitted. However, although this increases the probability of successful transmission, it significantly increases the network latency (Andres-Maldonado *et al.*, 2019; Martinez *et al.*, 2019; Harwahyu *et al.*, 2019; Ayoub, Samhat, *et al.*, 2018; Chen *et al.*, 2018;

ElNashar and El-saidny, 2018; Yu *et al.*, 2017; Bonnefoi *et al.*, 2018; Alavikia and Ghasemi, 2018; Lin *et al.*, 2016; Wang *et al.*, 2017; Wiriaatmadja and Choi, 2015; Aijaz, 2014).

2.4.8 LTE-M (LTE CAT-M2)

LTE-M, or LTE-MTC (Long-Term Evolution – Machine Type Communication) or LTE CAT-M (category MTC), is a new low power long range communication system based on the legacy LTE cellular system to fulfil M2M and IoT communication requirements. In 2016, the 3GPP announced the first version of the LTE-M specifications in the LTE Release 13 called CAT-M1. CAT-M1 was designed to utilise the same LTE licenced spectrum in the 800 MHz, 1800 MHz, and 2600 MHz bands with a channel bandwidth of 1.4 MHz. It offers 6 narrowband subchannels called Physical Resource Blocks (PRBs) with a special enhanced machine type communication (eMTC) and a new Machine-type Physical Download Control Channel called (MPDCCH) to adopt the low power and low data rate IoT communication in the legacy LTE cellular system. In 2017, a new LTE-M version was published by the 3GPP called CAT-M2 (Release 14). This version supports a new channel bandwidth of 5 MHz with 24 PRBs in addition to the original 1.4 MHz channel (Bembe *et al.*, 2019; Carlsson *et al.*, 2018; ElNashar and El-saidny, 2018; Elsaadany *et al.*, 2018; Hsieh *et al.*, 2018; Benhiba *et al.*, 2018; Dawaliby *et al.*, 2018; El Fawal *et al.*, 2018; Elsaadany *et al.*, 2017; Deshpande and Rajesh, 2017; Dawaliby *et al.*, 2017; Ratasuk *et al.*, 2017; Persia and Rea, 2016; Dawaliby *et al.*, 2016; Lauridsen *et al.*, 2016; Fawal *et al.*, 2017).

CAT-M2 provides a data rate of up to 1 Mbps for both downlink and uplink using the QPSK and the 16-QAM modulation schemes with the OFDMA technique and a payload of up to 1024 bytes. Also, CAT-M2 provides a battery lifetime of 10 years for low data rate devices (with about 200 bytes per day) with power consumption of 20 dBm (100 mW). Moreover, CAT-M2 offers a coverage range of up to 7 km in urban areas and up to 15 km in rural areas with coverage enhancement (CE) technique, where a Maximum Coupling Loss (MCL) of up to 155 dB can be achieved. To attain such an MCL value and this large coverage area, CAT-M2 utilises the message repetitions approach with two coverage enhancement modes: CE Mode A and CE Mode B. For CE Mode A, devices can select a repetition number from the set {1, 2, 4, 8, 16, and 32}. In comparison, for CE Mode B the maximum number of repetitions can be configured up to 2048 repetitions. The repetitions number can be chosen automatically by terminal devices based on the signal power received from the base station (ElNashar and El-saidny, 2018; Elsaadany *et al.*, 2018; Hsieh *et al.*, 2018; GSM Association, 2018; Benhiba *et al.*, 2018; Elsaadany *et al.*, 2017; Dawaliby

et al., 2017; Ratasuk *et al.*, 2017; Dawaliby *et al.*, 2016; Hongli Zhao and Hailin Jiang, 2016; Lauridsen *et al.*, 2016; Fawal *et al.*, 2017; Sierra Wireless, 2017; MathWorks, 2019).

LTE CAT-M2 is designed to support up to 100 thousand devices by utilising the Physical Upload Shared Channel (PUSCH) with the frequency hopping technique and the message repetition approach. To handle such a large number of devices and mitigate the effect of collisions, connected devices send data on randomly selected PRBs and use acknowledgements to ensure message delivery. If a transmission is unacknowledged, the device randomly selected another PRB from the available 24 PRBs and resend the message until the maximum number of allowed repetitions reached based on the CE operating mode. This improves system performance and raises the probability of successful transmission. However, it escalates the power consumption and degrades the network throughput (ElNashar and El-saidny, 2018; Hsieh *et al.*, 2018; Elsaadany *et al.*, 2017; Ratasuk *et al.*, 2017; Lauridsen *et al.*, 2016; Fawal *et al.*, 2017; Biral *et al.*, 2015; MathWorks, 2019).

2.4.9 A comparative summary of long-range M2M technologies

Long-range M2M communication systems are designed to support a broad range of applications especially those that are intended for smart cities and the IoT with a long-range coverage, a massive number of connected devices, minimum power consumption, and minimum complexity. Over the last several years, the long-range M2M technologies have been developed by different companies to fulfil these requirements at low cost (see Figure 2.33).

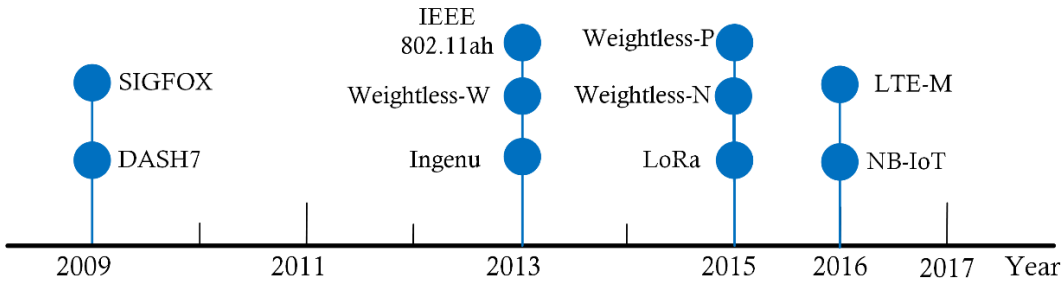

Figure 2.33: Long-range M2M communication technologies timeline.

The maximum number of end nodes for each base station is a vital factor that must be considered for the M2M technologies, especially with the enormous number of devices that will be connected in smart cities and IoT applications. Sigfox and Weightless-W support a tremendous number of devices with up to one million devices for each cell, as shown in Figure 2.34. However, Weightless-W employs TDMA and FDMA techniques

to support this number of devices, while Sigfox depends only on a low message rate approach, the frequency hopping technique, and multiple message copies. Furthermore, Weightless-N and LTE-M CAT-M2 claim to support up to 100000 nodes for each base station while NB-IoT claims to support up to 50000 devices. In contrast, other technologies offer a network scale within a range of several thousands of nodes. Furthermore, to improve system performance and reduce the probability of lost messages with such a massive number of devices, some technologies employ acknowledgements and CSMA techniques. However, this can significantly escalate power consumption and shorten the battery lifetime.

As most end nodes are powered by a single battery, the power consumption is another key factor that affects the selection of the appropriate technology for specific applications. In general, most of the long-range M2M technologies claim a battery lifetime of several years, depending on the data rate and the number of messages per day. However, reducing transmission power might significantly influence the communication range. Sigfox offers the most extended coverage range of 10 km. On the other hand, IEEE 802.11ah offer a range of 1 km but with higher transmission power in comparison with other long-range technologies. Figure 2.35 depicts the maximum indoor cell coverage range in urban areas in km in relation to the maximum transmission power in mW for different long-range M2M technologies.

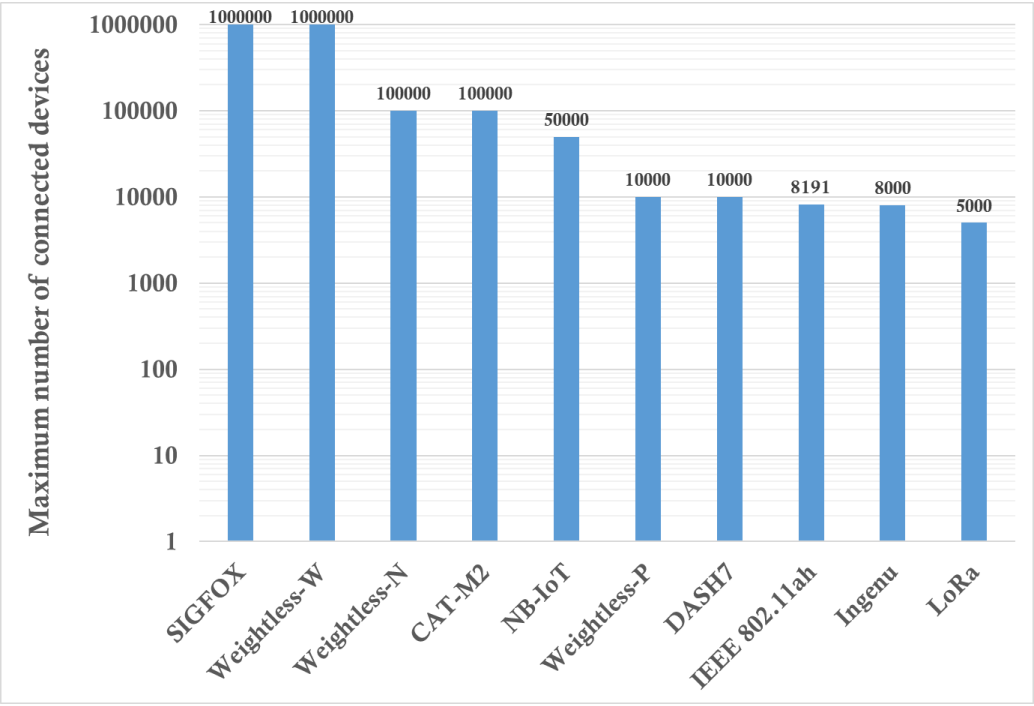

Figure 2.34: The maximum number of connected devices for long-range M2M technologies.

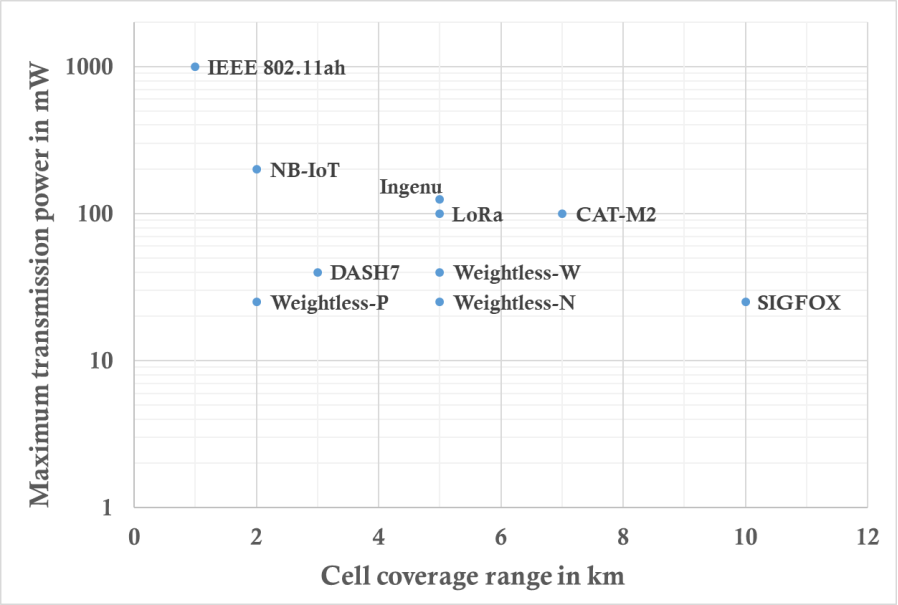

Figure 2.35: Long-range M2M technologies coverage range in km versus the transmission power in mW.

IEEE 802.11ah provides an extensive range of data rates from 150 kbps up to 347 Mbps. Though high throughputs cannot be achieved with long communication range and the data rate is significantly affected by the distance between the node and the AP. Similarly, Weightless-W offers a wide range of throughputs from 1 kbps up to 10 Mbps. On the other hand, Sigfox and Weightless-N provide the lowest data rate among the long-range M2M technologies with a throughput of 100 bps (see Figure 2.36).

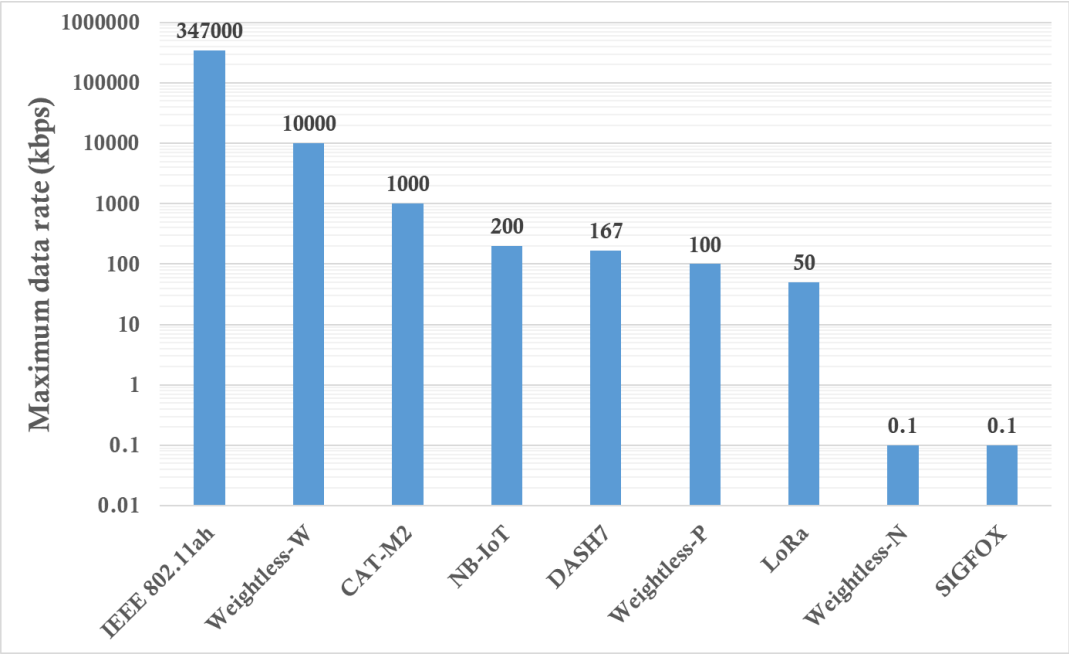

Figure 2.36: The maximum data rate for the long-range M2M technologies.

Figure 2.37 and Table 2.5 show a detailed comparison between long-range M2M communication technologies discussed previously.

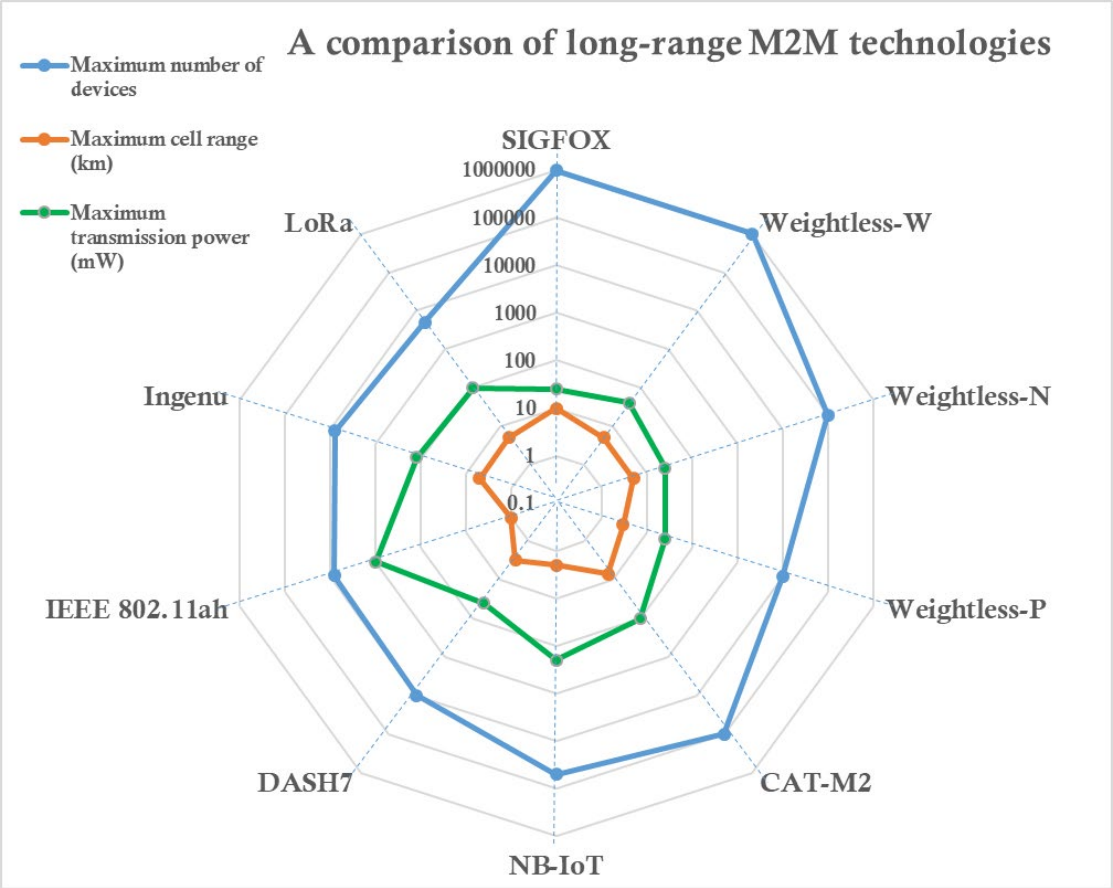

Figure 2.37: A comparison of long-range M2M technologies in terms of the number of connected devices, the coverage range, and the transmission power.

Table 2.5: Summary of the long-range M2M technologies features and characteristics.

Characteristic	DASH7	Ingenu	IEEE 802.11ah	LoRa	SIGFOX	Weightless			NB-IoT	CAT-M2
						W	N	P		
Operating frequency (MHz)	433, 868, 915	2400	755 – 928	430, 433, 868, 915	868, 902, 923	470 – 790	868, 915	138, 169, 433, 470, 780, 868, 915, 923	700 – 900	800, 1800, 2600
Number of channels	15, 8, 4	8	1	8, 3	1920	16	1200, 1500, 2500, 3000, 9999, 15000	1, 8	12, 48	6, 24
Channel bandwidth	108, 216, 432 kHz	1 MHz	1, 2, 4, 8, 16 MHz	125, 250, 500 kHz	100 Hz	6, 8 MHz	100, 200 Hz	100, 12.5 kHz	200, 180 kHz	1.4, 5 MHz
Modulation scheme	GFSK	BPSK	BPSK, QPSK, 16-QAM, 64-QAM, 256-QAM	CSS / FSK	DBPSK	DBPSK, BPSK, QPSK, 16-QAM	DBPSK	GMSK, OQPSK	BPSK, QPSK	QPSK, 16-QAM
Channel access / collision avoidance technique	CSMA/CA with slotted ALOHA	RPMA with random time access	Slotted ALOHA	ALOHA / Slotted ALOHA	ALOHA / FH with 3 message copies	TDMA, FDMA with FH	ALOHA / FH with 3 – 8 message copies	TDMA, FDMA with FH	ALOHA / Slotted ALOHA with FH / 128 repetition	ALOHA / FH / 32, 2048 repetition
Acknowledgement	Yes	Yes	Yes	Yes	No	Yes	No	Yes	Yes	Yes
Network topology	Star, tree, mesh	Star	Star, tree	Star-of-stars	Star	Star	Star	Star	Star	Star
Maximum number of nodes	10000	8000	8191	5000	1000000	1000000	100000	10000	50000	100000
Data rate	9.6, 55.555, 166.667 kbps	19 kbps	150 kbps – 347 Mbps	0.3 – 50 kbps	100 bps	1 kbps – 10 Mbps	100 bps	0.625 – 100 kbps	200, 144, 20 kbps	1 Mbps
Maximum payload (byte)	250	11	256	256	12	255	20	48	128	1024
Coverage range (km)	3	5	1	5	10	5	5	2	2	7
Transmission power (dBm)	0 – 16 (Typical 16)	21	0 – 30	14 – 20 (Typical 14)	14	16	14	14	23	20

2.5 Summary

The new era of smart cities and IoT poses formidable challenges to the current wireless communication systems, including the coverage area, the number of connected devices, the devices power consumption, and the cost of both end devices and the network. In this chapter, the prominent M2M communication technologies are reviewed and a detailed study of their features and characteristics is presented. With respect to the number of connected devices, the data collision problem is highlighted, and an in-depth description of the utilised channel access mechanism and collision avoidance techniques is presented.

In general, short-range M2M communication technologies provide the best solution for home and residential automation applications. On the other hand, long-range M2M technologies offer a wide coverage area with an enormous number of connected devices, which can be placed anywhere, even underground, and connected to a single base station. These technologies might be the most feasible solution for smart cities applications like smart grid, smart meters, traffic monitoring, environment monitoring, and agriculture applications.

All M2M communication technologies should maintain reliable communication over the whole network with minimum cost and power consumption, especially with a large network size. Therefore, most of these technologies do not support complex synchronisation techniques that are used in other power consuming and expensive terminals like mobile devices. On the contrary, they rely on using simple collision avoidance techniques like frequency hopping and random time access based on the ALOHA protocol. Although these techniques do not ensure message delivery, they can significantly reduce the probability of collision and improve system performance. On the other hand, some M2M technologies employ acknowledgements, CSMA/CA, TDMA, FDMA, or message repetitions to enhance system performance and reliability. However, this could affect the network latency, especially with a massive number of nodes, and escalates the power consumption and the devices cost in comparison to other M2M technologies. Figure 2.38 illustrates the channel access and collisions avoidance techniques employed by different M2M technologies.

Despite other factors that might influence M2M systems performance and consistency like channel noise and interference with other coexisting signals, the collisions problem is the vital factor that affects their reliability and restricts applications range.

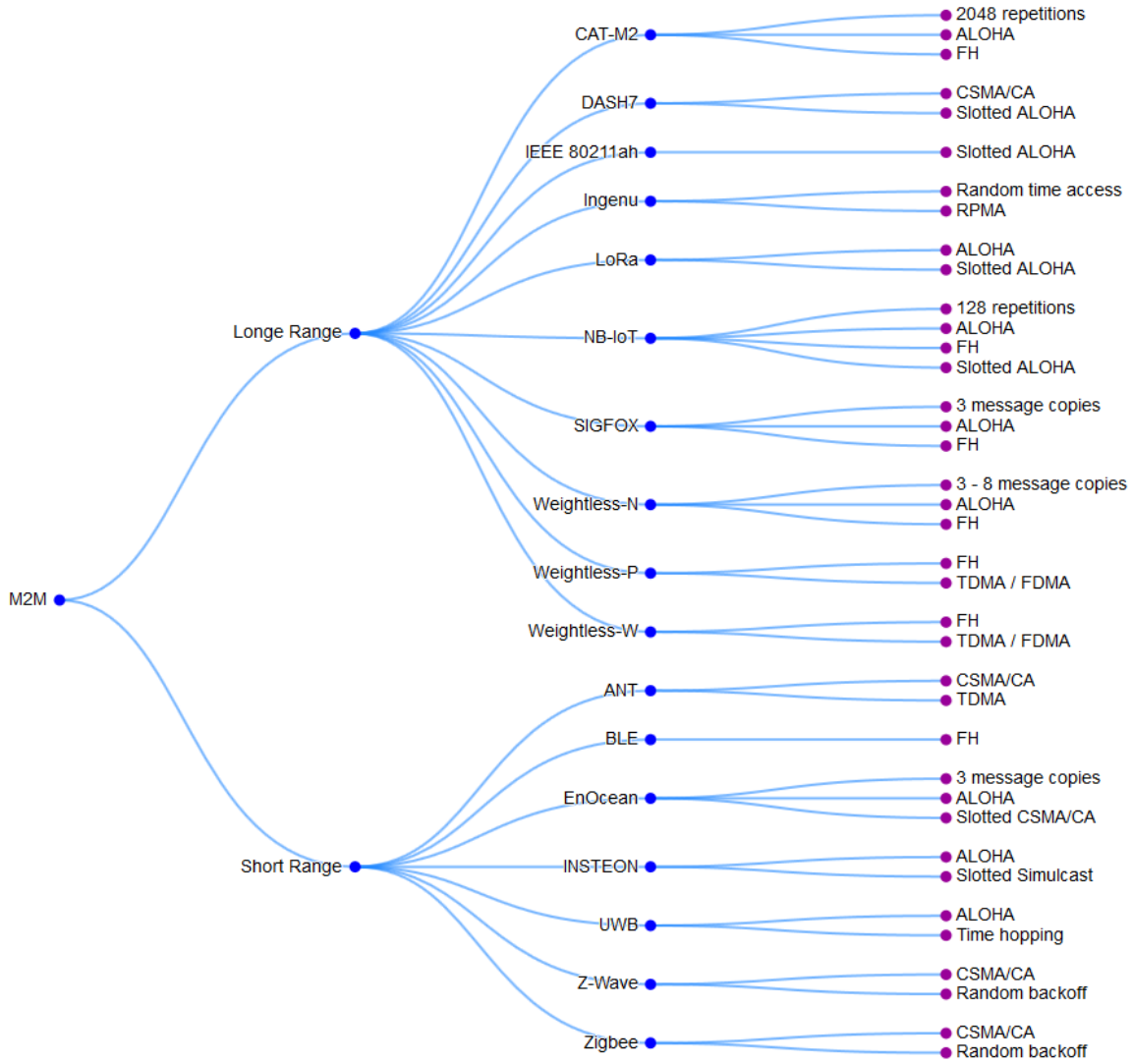

Figure 2.38: Channel access and collisions avoidance techniques utilised by different M2M technologies.

Chapter 3

Development of A Novel Random Channel Selection Technique

3.1 Introduction

The ALOHA like random access technique is widely used in wireless communication systems (Abramson, 2009). LPWAN technologies employ this technique to support low data rate M2M communication with low complexity, cost, and power consumption (Anton-Haro and Dohler, 2015; Anteur *et al.*, 2014; Centenaro *et al.*, 2016; Al-Shammari *et al.*, 2018; Laya *et al.*, 2015). However, with the new era of the IoT and smart cities, billions of devices are predicted to be connected to these systems in the next decade (Al-Shammari *et al.*, 2018; Laya *et al.*, 2015; Webb, 2015; Gomez and Paradells, 2015). With such an enormous number of connected devices that work without synchronisation, acknowledgement, and carrier sensing mechanisms, interference between devices and the packet collision problems have a substantial impact on the system reliability and performance (Li *et al.*, 2017; Centenaro *et al.*, 2017; Vejlgaard *et al.*, 2017; Yu *et al.*, 2017; Lauridsen *et al.*, 2016; Goursaud and Mo, 2016; Do *et al.*, 2014; Biral *et al.*, 2015; Reynders *et al.*, 2016).

Some LPWANs, like Weightless-N and Sigfox, utilise the UNB scheme with a frequency hopping technique to mitigate the collision problem and interference between connected devices. In such systems, the random channel selection algorithm that is used to generate the frequency hopping sequence is the vital factor that affects data collision and system performance. Most M2M standards, as detailed in the second chapter, do not include acknowledgements to confirm message delivery or guarantee of the quality of service. Even if they do, message retransmission will be required in the case of a collision which drains power. It is therefore paramount to design communication protocols that minimise message collisions. Current algorithms do not exhibit uniform distribution over communication channels which leads to an increase in lost messages. Hence, there is a need to develop a new algorithm to improve system reliability (Abbas *et al.*, 2017).

This chapter presents a detailed description of the standard channel selection algorithm used by the Weightless-N technology and the novel randomisation algorithm. The new developed random channel selection algorithm, which is called a Uniform Randomisation Channel Selection Technique (URCST), provides a lower probability of collision in comparison with the standard Weightless-N algorithm. Also, the chapter provides a

comparison of the system performance using the two algorithms in addition to the standard uniform random distribution algorithm, the Mersenne Twister (MT19937), with a variable number of devices, message copies, and payload. In addition, a comparison between the URCST and MT19937 algorithms is presented in this chapter in terms of performance, complexity, and implementation.

3.2 Weightless-N Channel Selection Algorithm

The details of the weightless-N channel selection algorithm have been provided in the previous chapter. However, a brief recapitulation of the main facts is reintroduced here to keep the flow information. Weightless-N utilises the sub-GHz ISM band of 868 MHz in Europe and divides this band into six wide bands, as shown in Table 3.1 (Weightless-SIG, 2015c; Abbas *et al.*, 2017). Each base station will be associated with one of these six wide bands and can detect all transmissions within its range of frequency. On the other hand, terminal devices work on an ultra-narrow frequency band of 200 Hz, called micro-channels. This offers a large number of UNB channels that can be used by any terminal. Furthermore, Weightless-N divides each wideband into three sub-bands called macro-channels, with each containing a number of micro-channels. For example, each macro-channel in the 0.6 MHz band contains 1000 channels.

Table 3.1: Weightless-N frequency bands.

Band No.	Lower band (MHz)	Upper band (MHz)	Bandwidth (MHz)	Number of channels
1	863	864.998	1.998	9990
2	865	868	3	15000
3	868	868.6	0.6	3000
4	868.7	869.2	0.5	2499
5	869.4	869.64	0.24	1200
6	869.7	870	0.3	1500

Weightless-N supports a bit rate of 100 bps and limits the number of messages for each device by a maximum rate of one message per minute. It also supports a payload of up to 20 bytes with a total packet size of 37 bytes. Each message sent from a terminal consists of 7 blocks, as shown in Table 3.2, where FCS represents a Frame-Check Sequence to indicate any error in the message. The base station will check the FCS, and if any error occurs, the message will be neglected. Otherwise, the base station will check the timestamp, which is a count of minutes on the terminal's internal timer. Messages that have the same timestamp are assumed to be copies of the same message.

Table 3.2: The Weightless-N message structure.

Preamble	ID	Data length	Time stamp	payload	MAC	FCS
3 bytes	6 bytes	5 bits	19 bits	0 – 20 bytes	24 bits	16 bits

In addition, Weightless-N utilises the approach of using multiple copies of each message to mitigate the effect of the collision on system performance and increase the probability of successful message delivery. Each terminal sends three identical copies of each message on different macro-channels and micro-channels using the frequency hopping regime, as shown in Figure 3.1. However, according to the Weightless-N standard, the total number of message copies can be increased to 8 for applications requiring a high QoS.

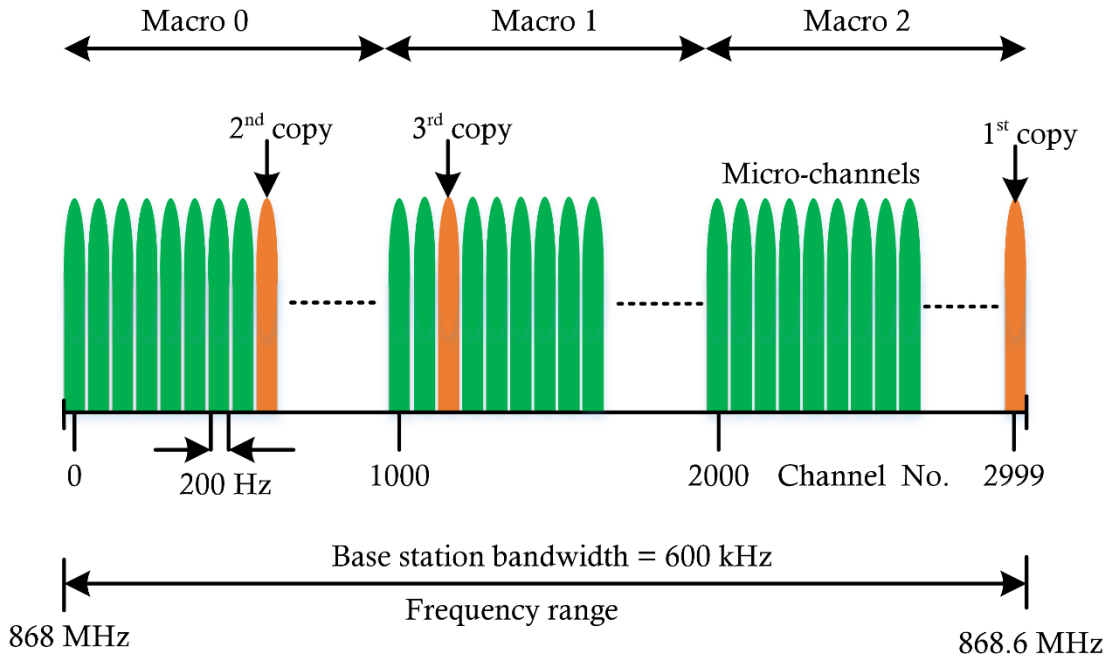

Figure 3.1: Weightless-N channels with three message copies.

The channel selection algorithm used by the Weightless-N is based on the two least significant bytes of both the ID and the internal timer of the terminal counting in seconds. This randomisation scheme is implemented so that any connected device generates a different hopping sequence on each message transmission since the internal timer will be increased at least by 60 seconds on each transmission. Moreover, this reduces the probability of selecting the same hopping sequence by two different devices since each one generates a dissimilar sequence based on its ID.

Assuming that the two least significant bytes of the ID is represented by *0xZZZZ* (in hexadecimal format) and the two least significant bytes of the timer are *0xMMSS*, the Weightless-N standard channel selection algorithm is divided into two stages: macro-channel selection and micro-channel selection (Weightless-SIG, 2015c; Abbas *et al.*, 2017). These stages are explained in the following two sections for three message copies. For message copies that are more than three, the same procedure will be repeated to define the next macro-channels and micro-channels for each message copy.

3.2.1 Tier-1 Macro-Channels Selection

The least significant byte of the device's internal timer *0xSS* is used to define the macro-channel sequence for all message copies in Weightless-N. The first macro-channel M_1, which will be used to send the first message copy, will be selected according to the formula, given by Equation 3.1:

$$M_1 = 0xSS \ mod \ 3 \tag{3.1}$$

M_2 and M_3 which are used to send the second and third message copies will be selected based on the result of the formula given by Equation 3.2:

$$0xSS \ mod \ 2 \tag{3.2}$$

If the result of the second formula equals zero, then the lower remaining macro-channel index will be chosen for the second message copy and the higher macro-channel index will be used to send the third message copy. Conversely, the highest remaining macro-channel index will be used for the second message copy and the lower index for the third message copy if the result of the second formula equals one.

3.2.2 Tier-2 Micro-Channel Selection

After defining the macro-channels sequence, each message copy will be sent on a randomly selected micro-channel inside the corresponding macro-channel as shown in Figure 3.1. The micro-channel selection algorithm is based on the two least significant bytes of both the device ID and its internal timer.

Assuming that *n* represents the number of message copies and the total number of channels in each macro-channel is *NC*, the micro-channels index (mc_j) for each message copy are given by Equations 3.3, 3.4, and 3.5, where $j = 1, 2, \ldots n$.

$$mc_1 = (0xZZZZ \ \ XOR \ \ oxMMSS) \ mod \ NC \quad 3.3$$

$$mc_2 = (0xZZZZ \quad OR \quad oxMMSS) \ mod \ NC \quad 3.4$$

$$mc_3 = (0xZZZZ \ \ AND \ \ oxMMSS) \ mod \ NC \quad 3.5$$

Figure 3.2 shows the hopping sequence generated by the Weightless-N standard algorithm and the packets timing for two different transmissions from the same device on two different times. In addition, message timing shows that there is a time of 0.3 seconds between any two message copies. This time was obtained from the experiments that was done on the Weightless-N development kit shown in Figure 3.3.

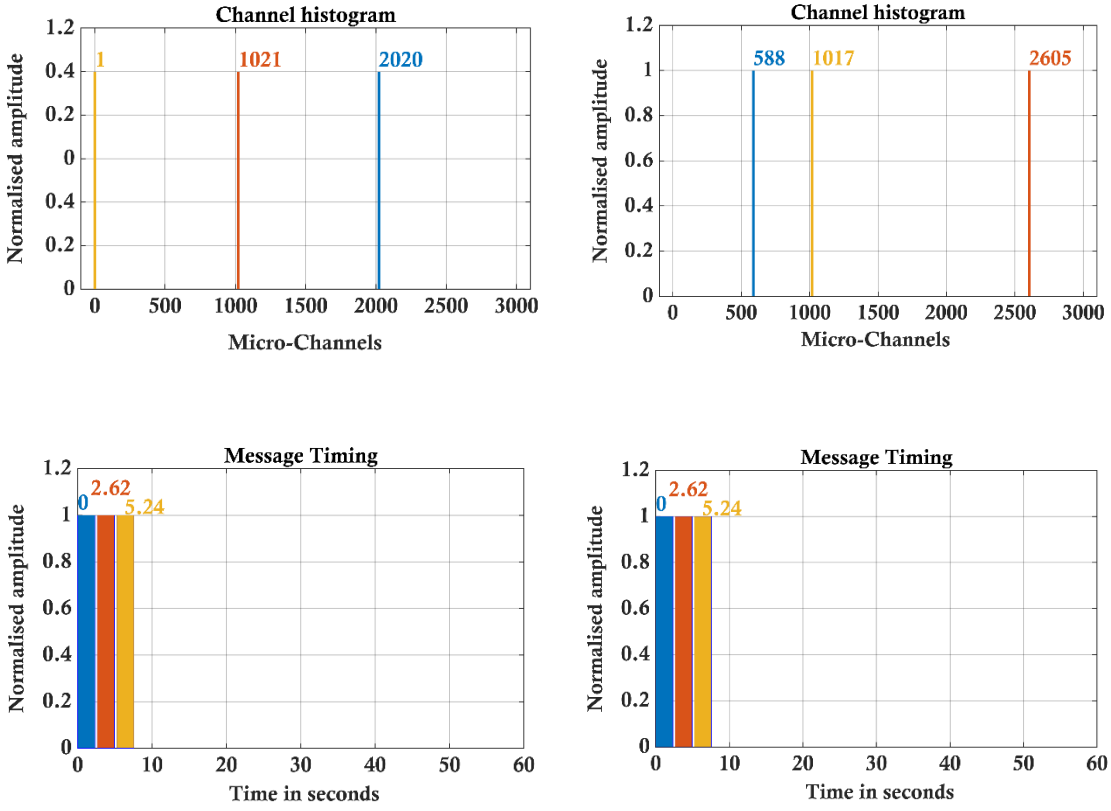

a) Internal timer = 5 sec. b) Internal timer = 605 sec.

Figure 3.2: Weightless-N hopping sequence and messages timing for the same device and different transmissions, where device ID = 17, macro-channels = 3, micro-channels = 3000, *NC* = 1000, *n* = 3 and payload = 12 bytes.

On the other hand, Figure 3.4 presents the hopping sequence of two different devices with different IDs and the same internal timer. The packets timing is the same as the case in Figure 3.2 since the same payload is used.

Figure 3.3: Weightless-N development kit.

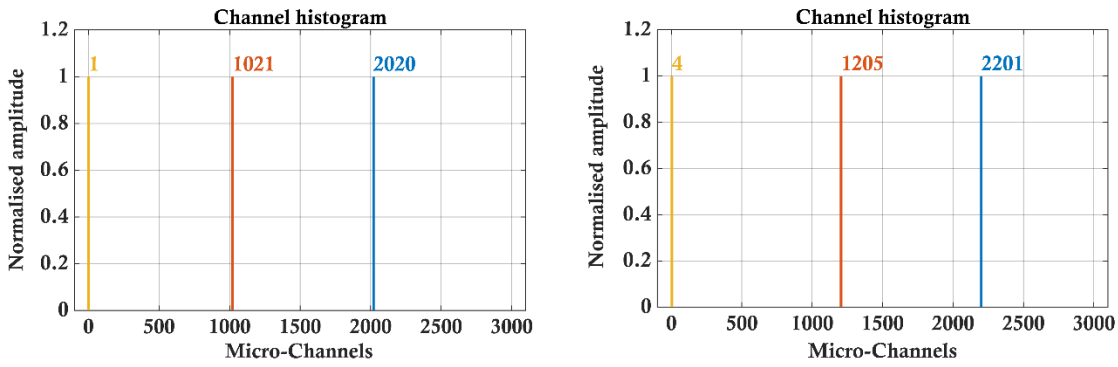

a) Device ID = 17.

b) Device ID = 204.

Figure 3.4: Weightless-N hopping sequence for different devices and the same transmission time, where internal timer = 5, macro-channels = 3, micro-channels = 3000, *NC* = 1000, *n* = 3 and payload = 12 bytes.

According to the Weightless-N standard (Weightless-SIG, 2015c), the same channel selection procedure will be repeated for the next three message copies (4th, 5th, and 6th) and then will be repeated for the 7th and 8th message copies. However, these message copies will be sent on different time slots and have a different probability of collision.

In fact, to obtain a good understanding of the system performance and the collision problem with a massive number of devices, a full channel histogram for all transmissions from all devices is required. This is discussed in more details in the next section 3.2.3.

3.2.3 Weightless-N Channel Distribution

A channel histogram can demonstrate a detailed view of the system performance and the distribution of messages over all channels for different devices and transmission times. An analysis was made to evaluate the standard Weightless-N algorithm with a total number of 8000 devices (k = 8000) and three message copies (n = 3). The analysis employs the 0.6 MHz band with 3000 channels (N = 3000) and shows the total number of sent messages on each micro-channel and the total number of lost messages on these channels. Moreover, the total number of devices were divided into four groups with different characteristics to achieve more realistic results as follows, see Figure 3.5:

- ***Group 1 (G1):*** represents 40% of the total number of devices and each device sends a message periodically every 2 minutes. Each message payload was set to be 8 bytes.
- ***Group 2 (G2):*** represents 20% of the total number of devices and each device sends a message randomly in the period of 1 – 2 minutes. Each message payload was set to be 10 bytes.
- ***Group 3 (G3):*** represents 20% of the total number of devices and each device sends a message periodically every 4 minutes. Each message payload was set to be 12 bytes.
- ***Group 4 (G4):*** represents 20% of the total number of devices and each device sends a message randomly in the period of 2 – 4 minutes. Each message payload was set to be 14 bytes.

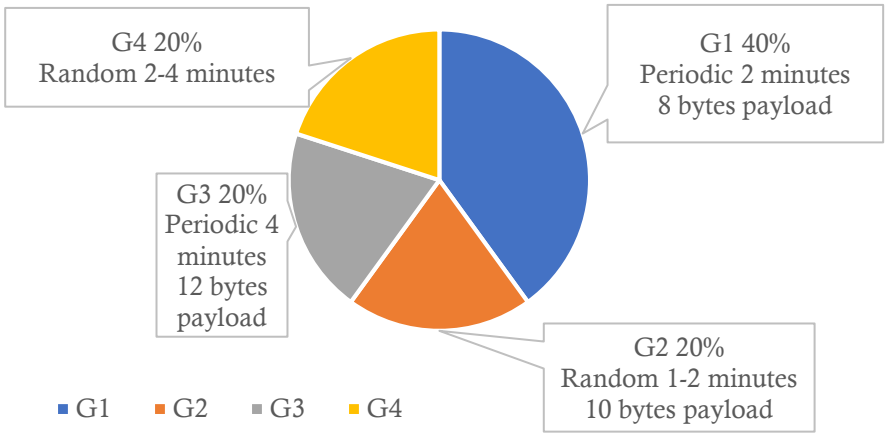

Figure 3.5: Analysis groups' characteristics.

The simulation was carried out for one hour assuming that all devices start working randomly within the first 10 minutes.

Figure 3.6 shows the Macro-channels histogram, which represents the total number of sent messages on each macro-channel from all devices for one hour. It is important to notice from this figure that the three message copies from all devices are equally distributed over the three macro-channels. This signifies that the Weightless-N standard algorithm used to select the macro-channels sequence provides a uniform distribution.

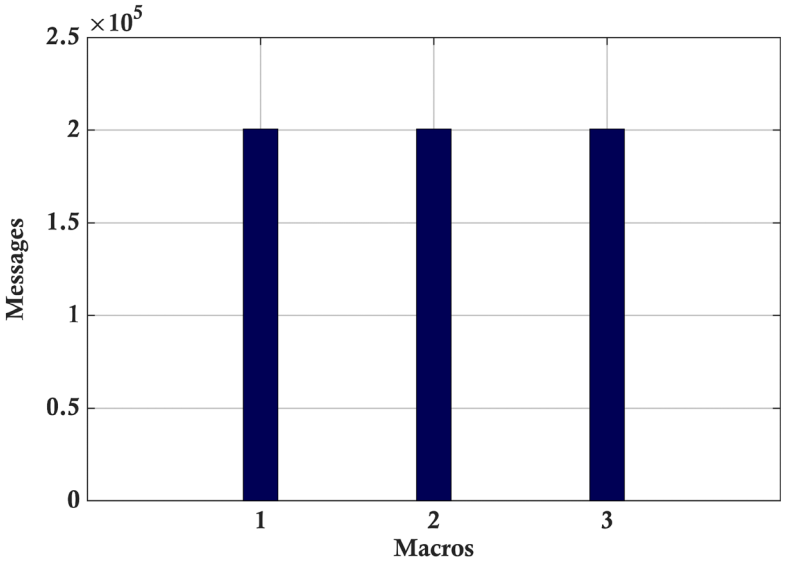

Figure 3.6: Weightless-N macro-channels histogram, where k = 8000, n = 3, the total number of sent messages = 200568.

Figure 3.7(a) presents the total number of sent messages from all devices for one hour on each micro-channel and Figure 3.7(b) shows the total number of lost messages on each channel. It is evident from Figure 3.7(a) that the Weightless-N micro-channels selection algorithm does not provide a uniform distribution over all channels and the channel request is crowded at the first part of each macro-channel. This increases the probability of collisions and leads to a high number of lost messages. In particular, this is due to the fact that Equations 3.4 and 3.5 provide a high probability of selecting the same channels from different terminals at the same time, as illustrated in Figure 3.8. For example, the logical ***AND*** operation of number 1 with all even numbers gives 0 and gives 1 with all odd numbers. Moreover, ANDing many different numbers leads to zero which significantly increases the selection of this channel. This rises the probability of selecting the first few channels in each macro-channel, especially channel number 0. In addition, Figure 3.8(a)

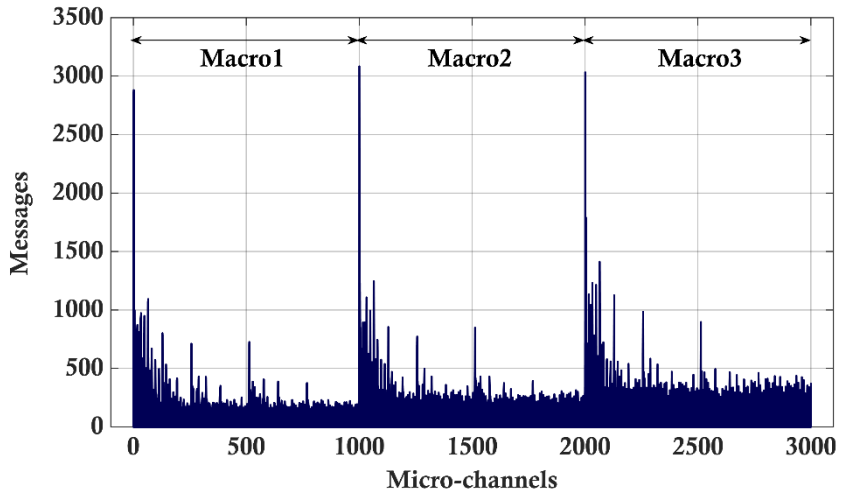

a) Total messages histogram.

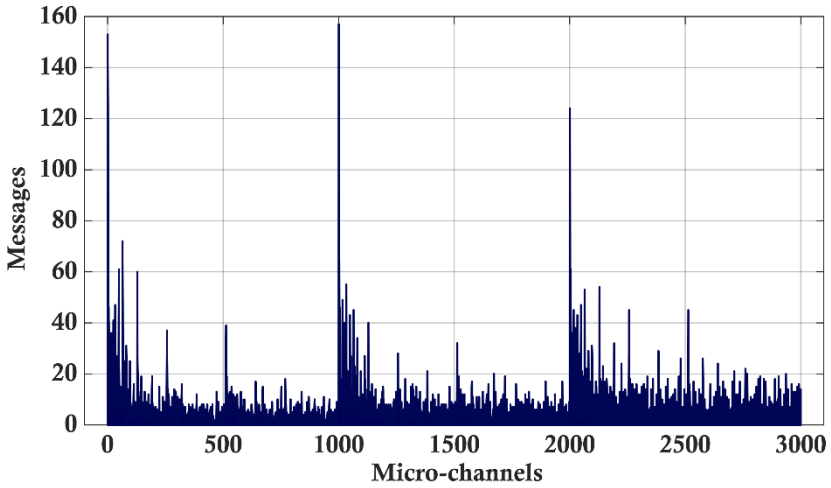

b) Lost messages histogram.

Figure 3.7: Weightless-N micro-channels histogram, where N = 3000, k = 8000, n = 3, The total number of sent messages = 200568, the total number of lost messages = 5427, and the MLR = 2.71 %.

shows that using the ***XOR*** logical operation, which is implemented in Equation 3.3 for the first message copy, provides a more equitable distribution of messages over the whole band. However, the messages' collisions of the first message copy are still affected by the non-uniform distribution of other messages provided by the 2nd and 3rd message copies, as illustrated in Figure 3.8(b). Moreover, Figure 3.9 depicts a 3D view for the sent and lost messages from all devices over all channels. It is apparent from this figure that all devices from all groups with different specifications face the same problem and it is not related to certain groups or characteristics.

Therefore, developing a new channel selection algorithm that can provide a better channel distribution is important to reduce the data collision and improve the system performance.

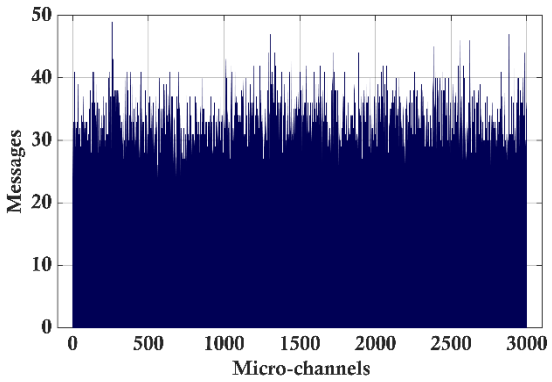

a) 1st message copy total messages histogram.

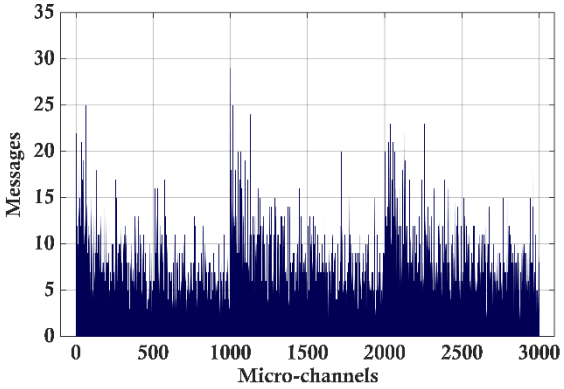

b) 1st message copy total collisions histogram.

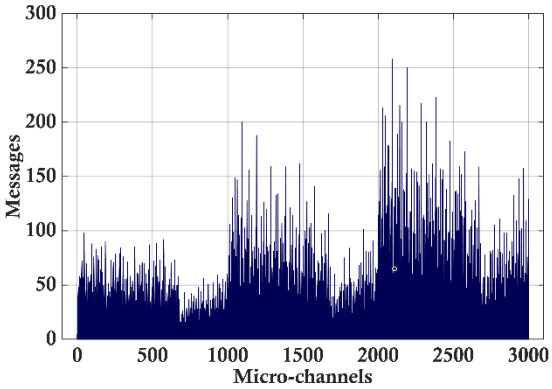

c) 2nd message copy total messages histogram.

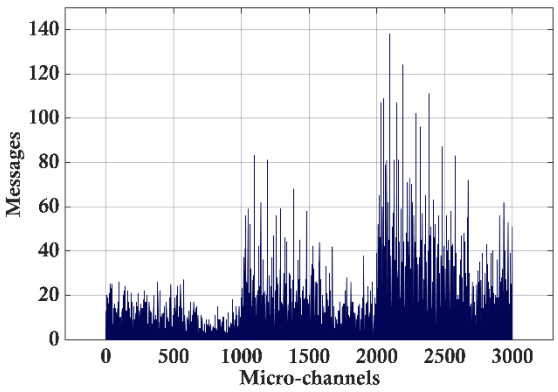

d) 2nd message copy total collisions histogram.

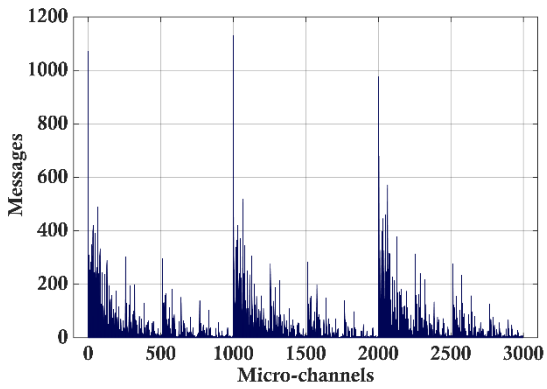

e) 3rd message copy total messages histogram.

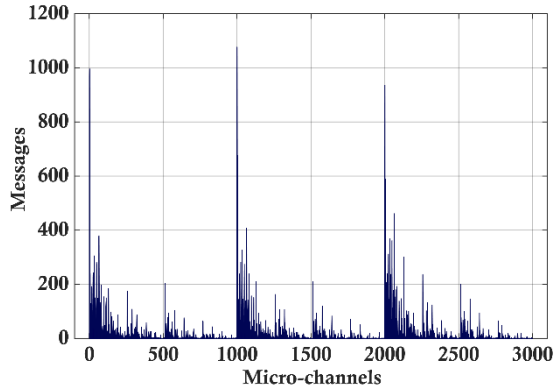

f) 3rd message copy total collisions histogram.

Figure 3.8: Weightless-N individual message copies histogram for G1, where *group* = *G1*, *N* = 3000, *k(G1)* = 3200, *n* = 3, *M* = 3, The total number of sent messages = 87962, the total number of lost messages = 2159.

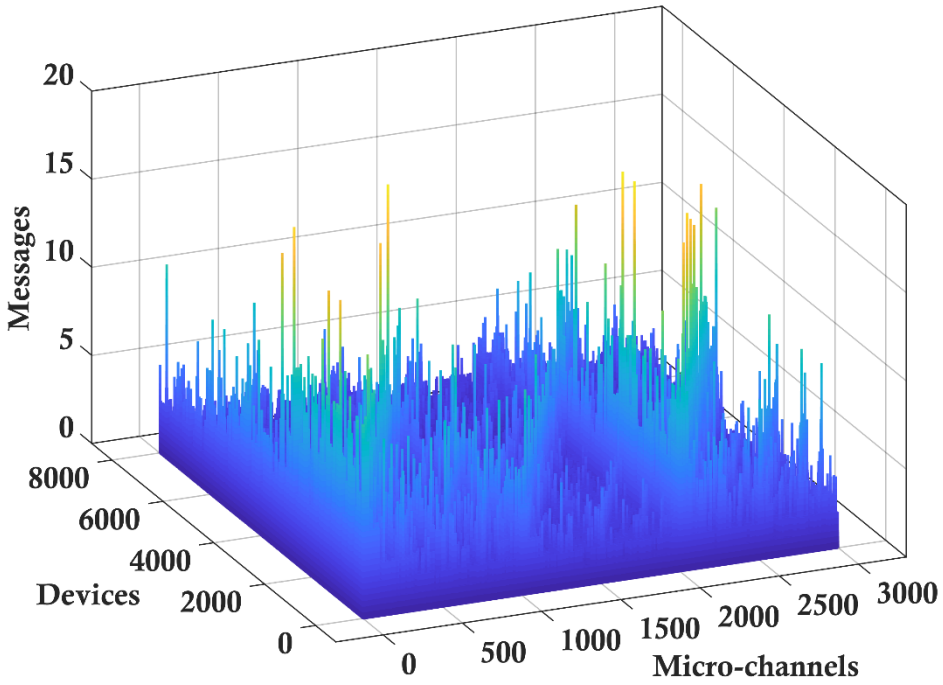

a) Total messages 3D-histogram.

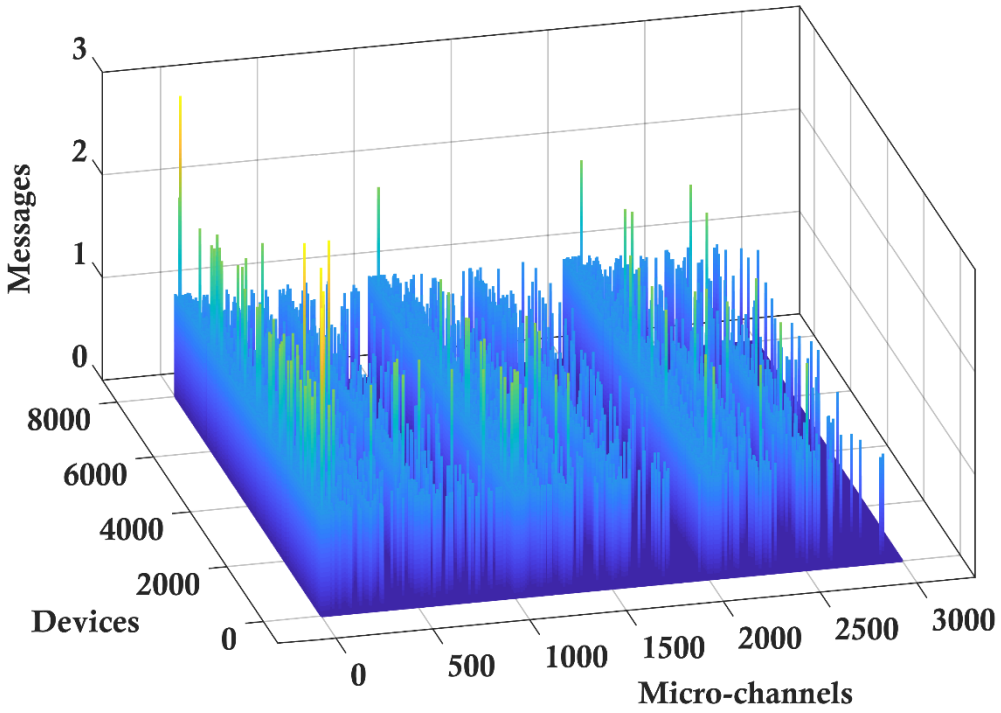

b) Lost messages 3D-histogram.

Figure 3.9: Weightless-N micro-channels 3D histogram, where N = 3000, k = 8000, n = 3, M = 3, The total number of sent messages = 200568, the total number of lost messages = 5427, and the MLR = 2.71 %.

3.3 Uniform Randomisation Channel Selection Technique (URCST)

The aim of developing the new algorithm is to provide better message spreading in the frequency domain for all message copies from different devices and achieve uniform distribution over all channels. Since the macro-channel selection procedure utilised by the Weightless-N standard, which is described in section 3.2.1, offers a uniform distribution for the three macros, the same selection process will be implemented by the new developed algorithm called the Uniform Randomisation Channel Selection Technique (URCST). In addition, the procedure will be repeated for any message copy that is larger than three.

On the other hand, the micro-channel selection procedure utilises a random number generator that is based on a ring shift register of the internal timer of the terminal. For each hop, the micro-channel will be selected by shifting the timer *0xMMSS* to the left by one bit and the most significant bit will be fed to the least significant bit of the register. Then, an ***XOR*** logical operation will be applied to the resulting number of the ring register and the terminal's ID, as shown in Figure 3.10. This reduces the probability of selecting the same channel by different terminals at the same time and provides a better channel distribution in comparison with the standard algorithm for all message copies.

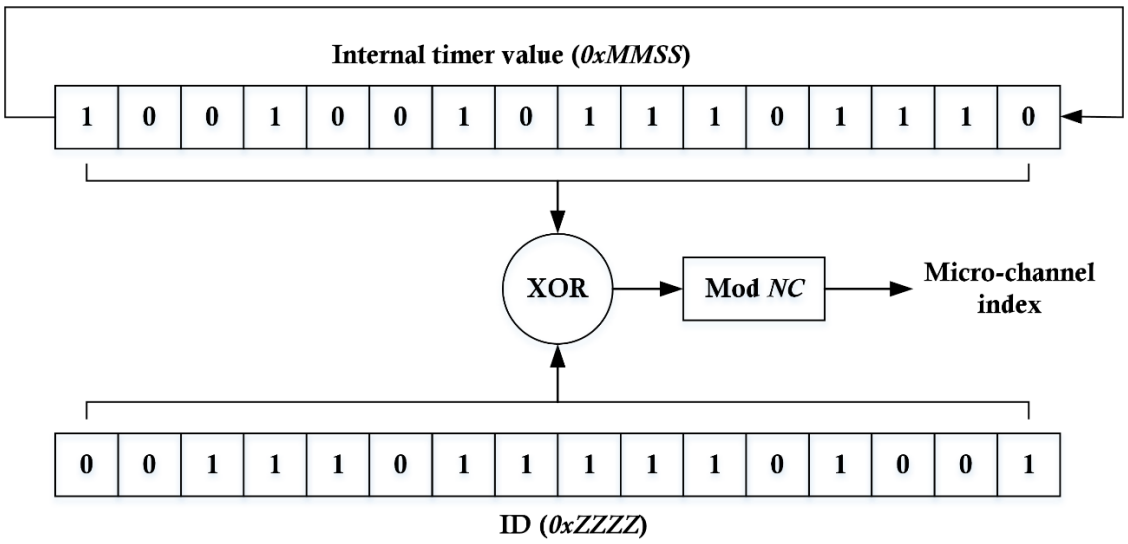

Figure 3.10: URCST micro-channels selection algorithm.

With *n* representing the number of message copies, the micro-channel number for the current hop can be obtained by Equation 3.6.

$$mc_i = \left(0xZZZZ \ \ XOR \ \ (oxMMSS \ll i)\right) mod \ NC \qquad 3.6$$

$$Where \ i = 0,1,2,\dots,n-1$$

Also, Figure 3.11 shows the pseudocode of the URCST algorithm.

URCST Algorithm: Pseudocode of channel selection algorithm

SET ***t*** = Timer, ***id*** = ID, ***n*** = number of message copies, ***M*** = Macros, ***mc*** = Micros, ***NC*** = number of channels

T1 = ***t*** AND 0xFF
M(1) = T1 mod 3
If (T1 mod 2) == 0
    M(2,3) = sort remaining values of 1,2,3 ascendingly
Else
    M(2,3) = sort remaining values of 1,2,3 in a descending order
End

T2 = ***t*** AND 0xFFFF
id = ***id*** AND 0xFFFF

For i = 0 to ***n***-1
    Select Macro from ***M***
    mc(i) = (T2 XOR ***id***) mod ***NC***
    B15 = T2 AND 32768
    B15 = B15 >> 15
    T2 = T2 << i+1
    T2 = T2 OR B15
end

Figure 3.11: Pseudocode of the URCST algorithm.

3.3.1 URCST Channel Distribution

The micro-channels histogram of the URCST algorithm shown in Figure 3.12 clearly demonstrates that this algorithm provides a much better uniform channel distribution among all micro-channels. This significantly reduces the probability of collision and the percentage of lost messages (MLR), which is in this case 1.18% in comparison with 2.71 % for the Weightless-N standard algorithm.

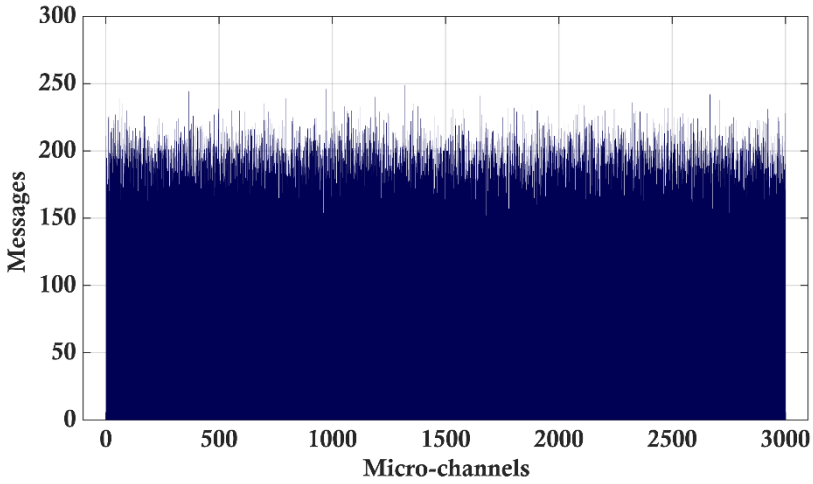

a) Total messages histogram.

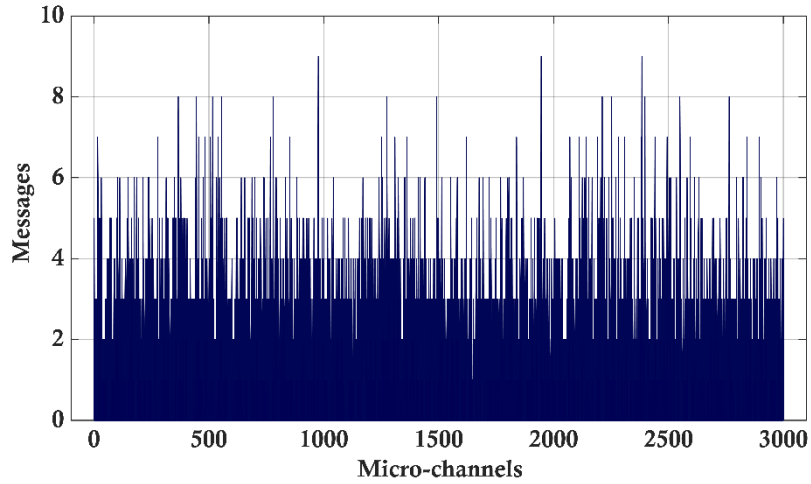

b) Lost messages histogram.

Figure 3.12: URCST micro-channels histogram using three macro-channels, where N = 3000, k = 8000, n = 3, M = 3, The total number of sent messages = 198299, the total number of lost messages = 2347, and the MLR = 1.18 %.

3.3.2 Final URCST Algorithm Without Macro-channels

In general, design and implementation of LPWANs is a trade-off between complexity and performance. Therefore, algorithm complexity is an important factor to be consider in such systems, and reducing complexity leads to the reduction of power consumption and cost.

In this section, a critical improvement on algorithm complexity is presented by eliminating the macro-channels part of the algorithm. From Figure 3.12 it is clear the macro-channel segments do not have any effect on the micro-channels distribution. In fact, since URCST algorithm provides a uniform distribution over all micro-channels in each individual macro-channel, it can be implemented for the whole band as a single segment.

Figure 3.13 shows the channels histogram (will be called channels not micro-channels for the rest of the thesis) for the same system without using the macro-channels. The system still provides similar performance with a uniform distribution over all channels using the micro-channels selection part only.

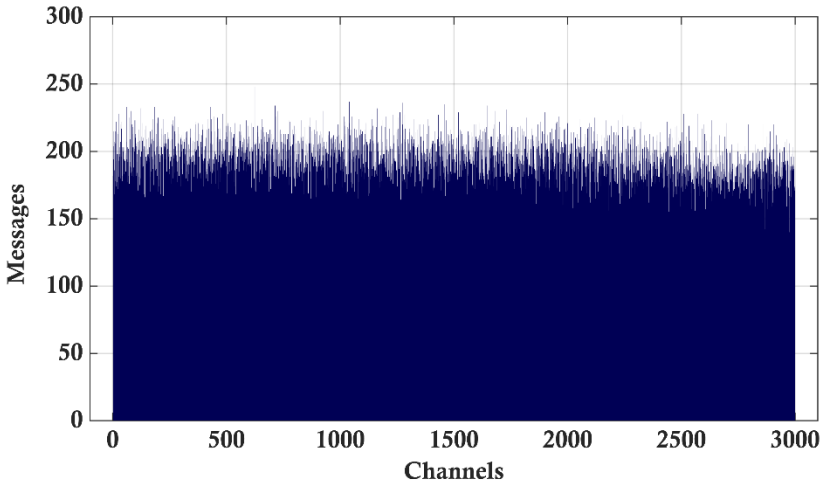

a) Total messages histogram.

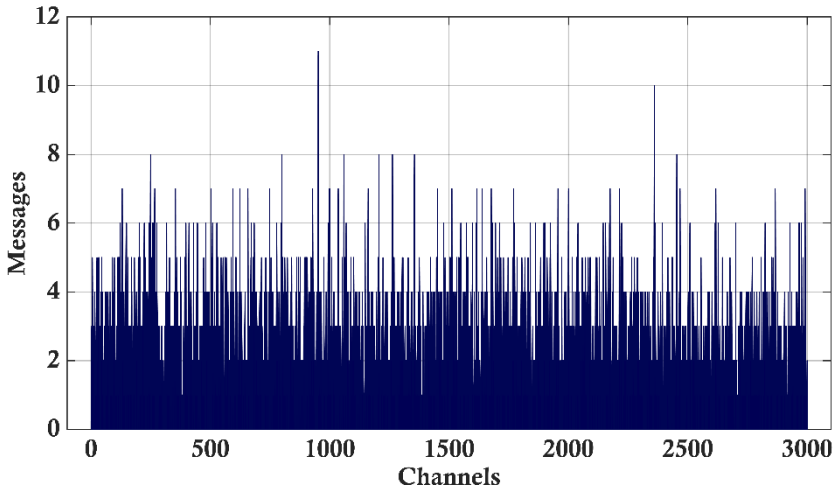

b) Lost messages histogram.

Figure 3.13: URCST channels histogram without macro-channels, where N = 3000, k = 8000, n = 3, The total number of sent messages = 195252, the total number of lost messages = 2158, and the MLR = 1.11 %.

In addition, Figure 3.14 shows a 3D view for the sent and lost messages from all devices over all channels. It is also evident from this figure that the URCST algorithm provides almost a uniform distribution for all devices from all groups despite variable IDs and transmission times.

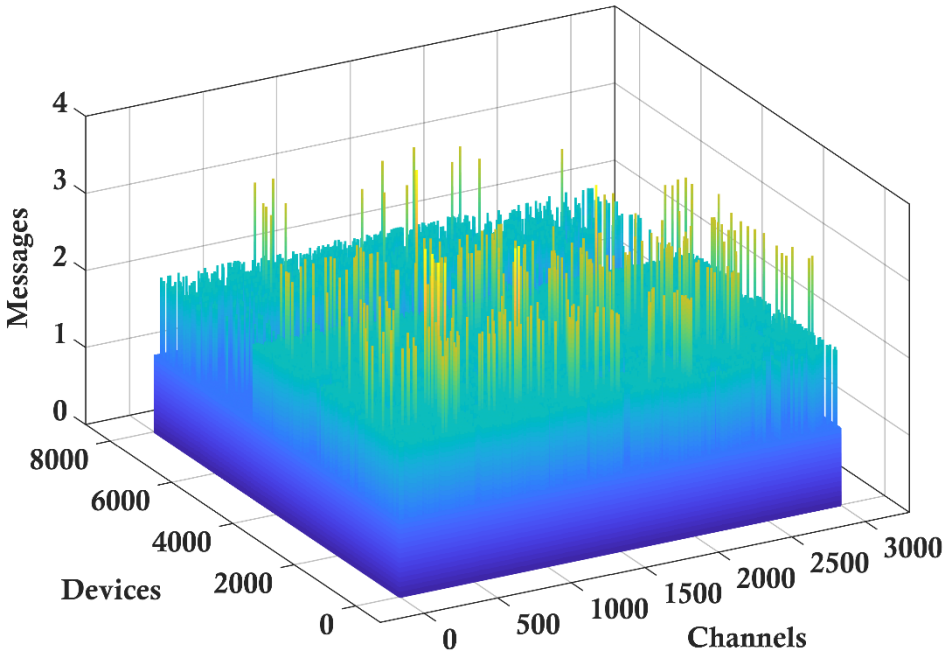

a) Total messages 3D-histogram.

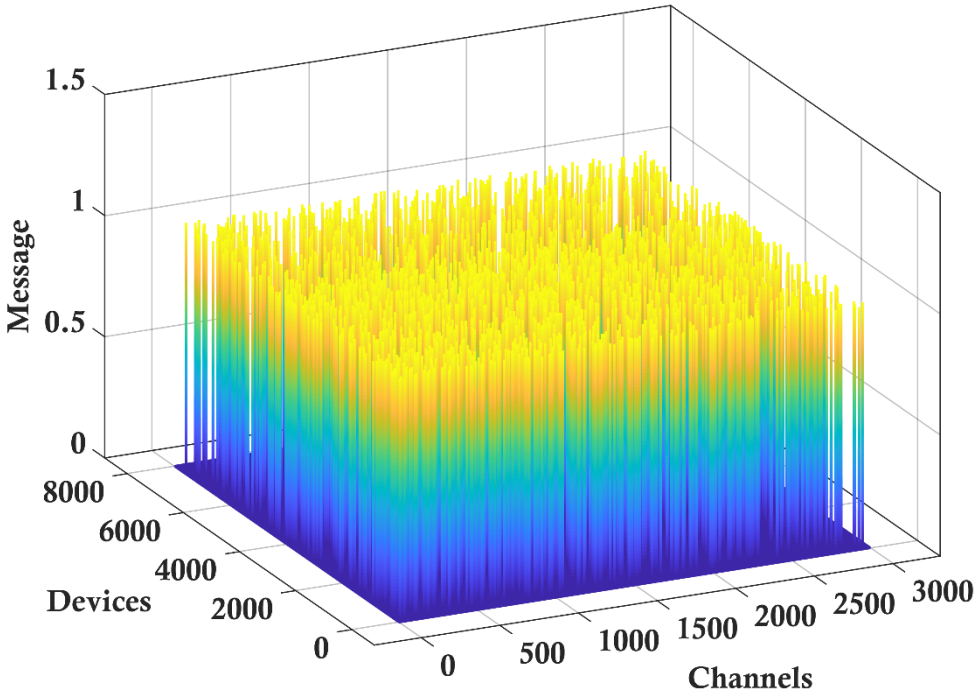

b) Lost messages 3D-histogram.

Figure 3.14: URCST micro-channels 3D histogram, where N = 3000, k = 8000, n = 3, The total number of sent messages = 195252, the total number of lost messages = 2158, and the MLR = 1.11 %.

Another two tests are presented in this section to ensure that the URCST algorithm provides the same performance with and without the macro-channels by implementing the two approaches for a variable number of devices and a variable number of message copies, as depicted in Figure 3.15, and check the system performance. These tests demonstrate that eliminating macro-channels does not affect the algorithm functionality and the system still provides similar performance despite using a variable number of devices and message copies while it reduces the algorithm complexity.

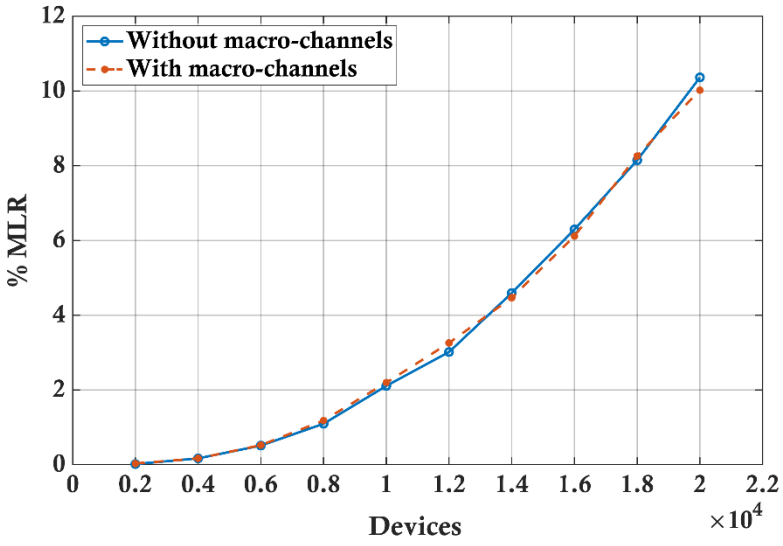

a) MLR versus the number of devices k, where $n = 3$.

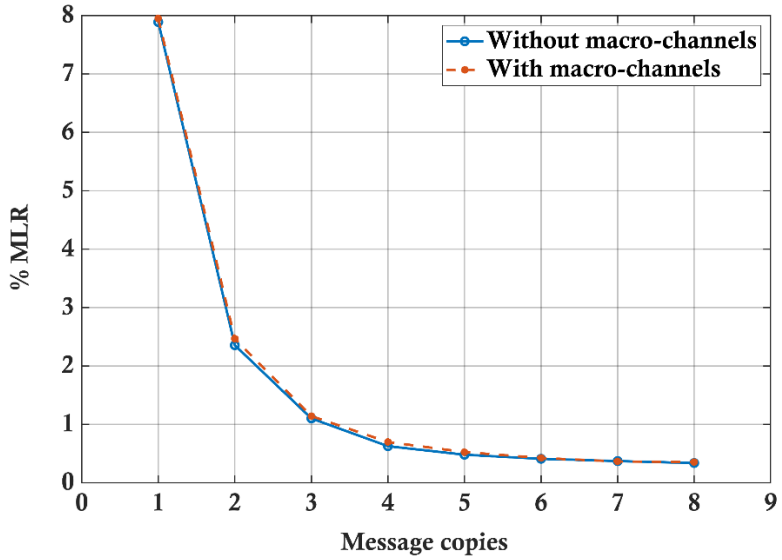

b) MLR versus the number of message copies n, where $k = 8000$.

Figure 3.15: Weightless-N system performance using the URCST algorithm with and without macro-channels, where $N = 3000$.

3.4 Mersenne Twister Algorithm (MT19937)

Mersenne Twister MT19937 algorithm is one of the most prominent pseudorandom number generators that is widely used in high performance computing applications (Tian and Benkrid, 2009; Li *et al.*, 2012). It is well-known for long period generation of $(2^{19937} - 1)$ and its uniform distribution over all generated numbers. MT19937 can generate 623-dimensional equidistributional 32-bit numbers while using a working area of 624 words (Matsumoto and Nishimura, 1998; Echeverría and López-Vallejo, 2013). However, the complexity of MT19937 is very high in comparison with the Weightless-N and URCST algorithms since a high number of iterations and two matrix multiplications are required to generate each random number. The iteration complexity of the MT19937 algorithms can be expressed, according to the Big-O notation, as $O(p^2)$ where p is the degree of the polynomial, which is 19937 in this case (Matsumoto and Nishimura, 1998; Echeverría and López-Vallejo, 2013; Saito and Matsumoto, 2013; Bonato *et al.*, 2013). Figure 3.16 illustrates the MT19937 algorithm structure (Li *et al.*, 2012).

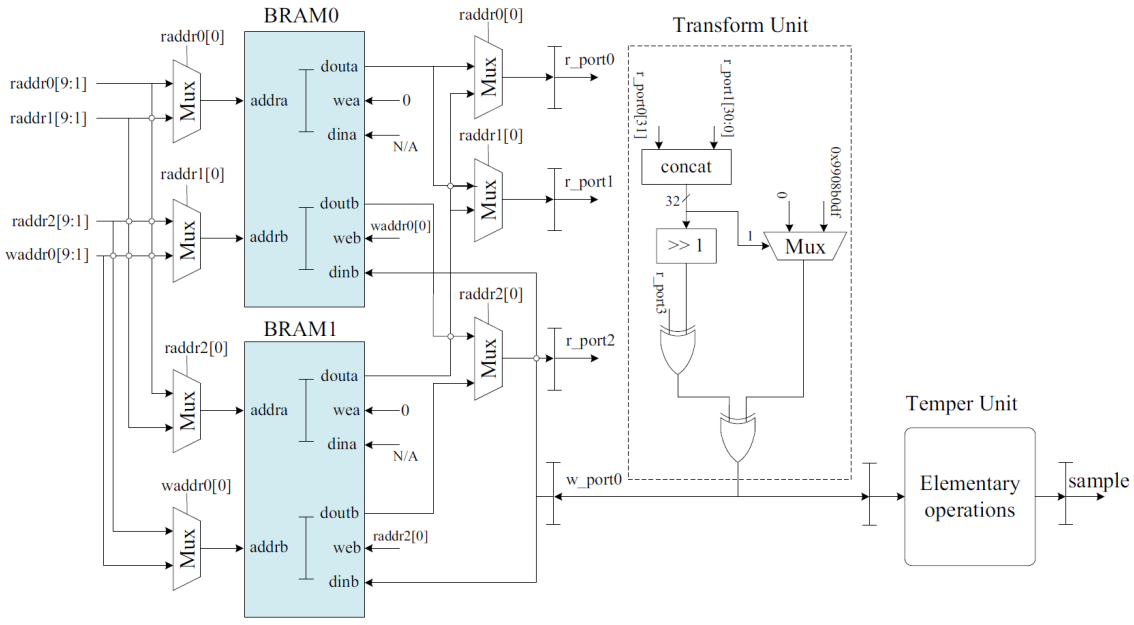

Figure 3.16: Mersenne Twister MT19937 algorithm' architecture (Li *et al.*, 2012).

To evaluate the system performance using the MT19937 algorithm, the same approach used in the URCST algorithm is implemented here by removing the macro-channels and employing the MT19937 for the whole band as a single segment. The results illustrated in Figure 3.17 shows that the resulting channels histograms are similar to the results obtained with the URCST algorithm and the MLR are almost the same in both cases.

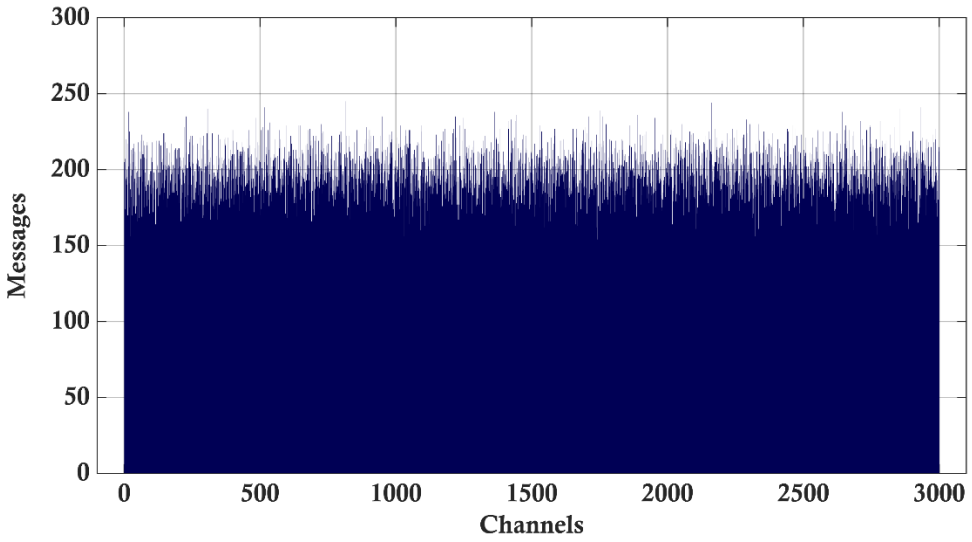

a) Total messages histogram.

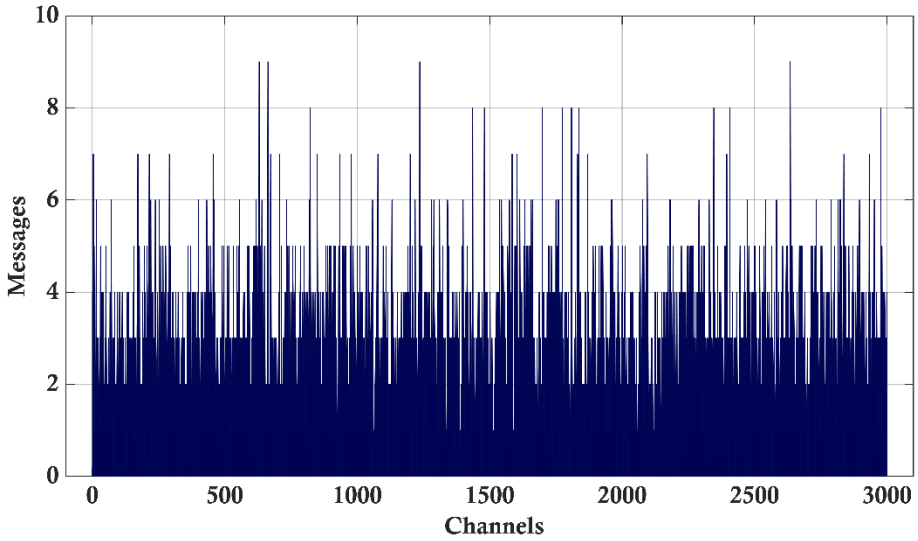

b) Lost messages histogram.

Figure 3.17: MT19937 channels histogram, where N = 3000, k = 8000, n = 3, The total number of sent messages = 198440, the total number of lost messages = 2226, and the MLR = 1.12 %.

It is important to highlight here that the high complexity of the MT19937 rises the cost and power consumption of terminal devices which is not preferred in M2M applications. On the other hand, URCST provides similar performance with much lower cost and power consumption. To have a good understanding of the system performance with different algorithms, the next section presents a detailed evaluation of the system using the three algorithms with several working scenarios.

3.5 System Evaluation and Performance Analysis

In this section, an evaluation of the three aforementioned algorithms is presented based on the four groups scheme employed in section 3.2.3. The evaluation is divided into three working scenarios: a variable number of connected devices, a variable number of message copies, and a variable payload. The system performance is assessed based on the message lost ratio (MLR) for the three algorithms in each analysis. The percentage of the lost messages shown on the graphs represent the total number of the lost messages from all devices for one hour. In addition, the analysis considers all the available range for the message copies (n = 1 – 8) although it is limited to be in the range (3 – 8) by the Weightless-N standard.

3.5.1 Variable Number of Devices

Figure 3.18 shows the MLR for the standard algorithm, the URCST algorithm, and the MT19937 versus a different number of devices. As the number of connected devices increases, the probability of collision rises. The analysis shows that the MLR rises exponentially as the number of devices increases. It also shows that as the number of devices increases the URCST algorithm provides better performance than the Weightless-N standard algorithm and almost the same MLR in comparison with the MT19937 algorithm.

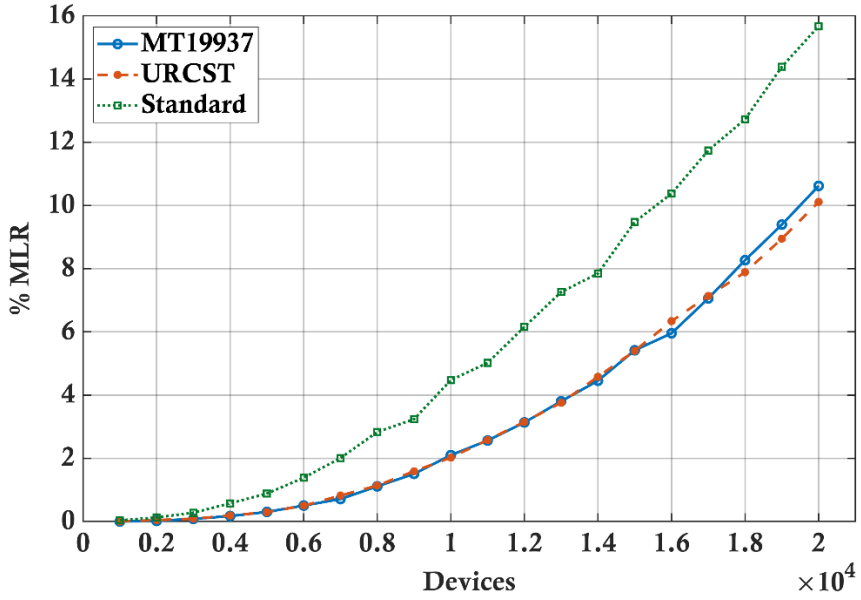

Figure 3.18: MLR versus the number of devices (*k*) using the MT19937, URCST, and standard algorithms, where N = 3000 and n = 3.

3.5.2 Variable Number of Message Copies

Figure 3.19 illustrates the MLR for the three algorithms versus a different number of message copies. Both the URCST algorithm and the MT19937 provide nearly the same percentage of lost messages that declines as the number of message copies increase. On the other hand, the standard algorithm provides the best performance at four message copies. Nevertheless, the percentage of lost messages rises for more than four message copies. It is clear from this analysis that URCST algorithm provides much lower MLR for $n > 4$, which is important for applications that require a high QoS.

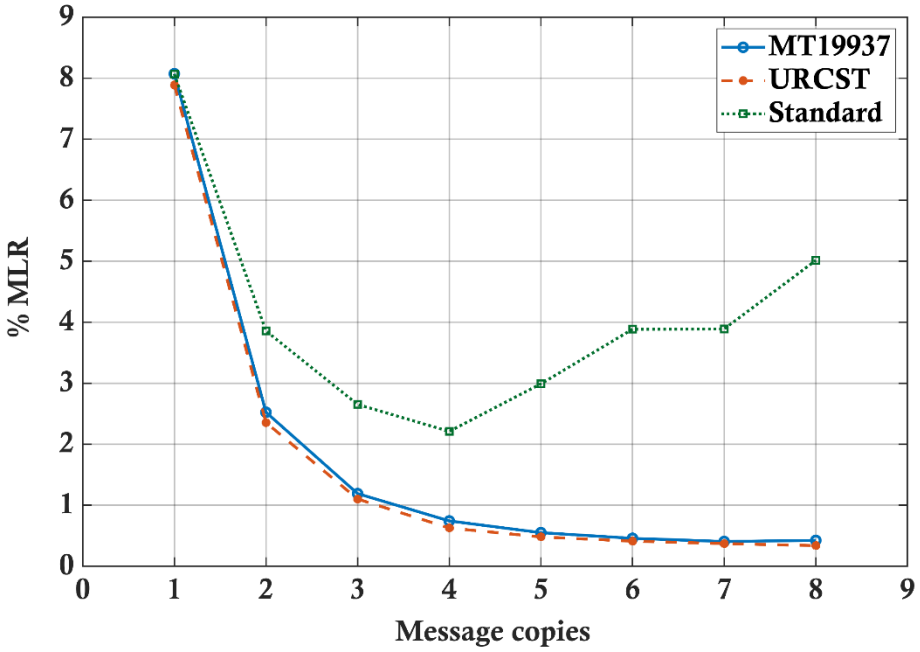

Figure 3.19: MLR versus the number of message copies (*n*) using the MT19937, URCST, and standard algorithms, where $N = 3000$ and $k = 8000$.

3.5.3 Variable Payload

As the payload size in bytes increases, the packet size enlarges, and the probability of collision escalates. Therefore, another test is presented in this section to evaluate the system performance with a variable payload using the three algorithms.

Figure 3.20 demonstrates the MLR versus different payload size for the MT19937, URCST, and the standard algorithms. Again, URCST offers lower MLR than the standard algorithm for the whole range of the used payloads. In addition, it provides similar performance in comparison with the MT19937 algorithm.

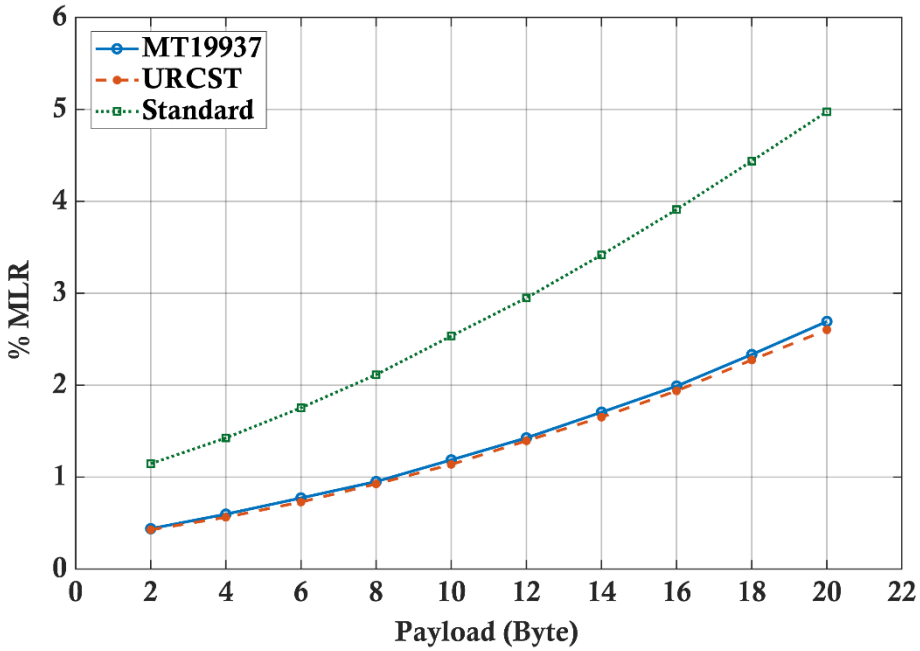

Figure 3.20: MLR versus payload size in bytes using the MT19937, URCST, and standard algorithms, where N = 3000, k = 8000, and n = 3.

3.6 A Comparison Between URCST and MT19937 Algorithms

Although the URCST and the MT19937 algorithms provide almost the same system performance with different working scenarios, using the URCST algorithm has many advantages over the MT19937 algorithm in IoT and M2M systems. Low cost and power consumption are two crucial requirements for feasible LPWANs. High complexity and resources required to implement MT19937 in comparison to URCST can significantly increase both cost and power consumption for terminal devices.

More specifically, URCST can be implemented using a 16-bit microcontroller with a tiny volatile memory (RAM) of about 64 bytes, while MT19937 requires at least 32-bit microcontroller and a RAM of more than 5 kB. These two factors increase the cost of each node, and with millions of devices that are requires to be used in IoT applications the cost of the whole system will be relatively high.

Furthermore, the high iteration complexity of the MT19937 algorithm, which is $O(p^2)$, in comparison with the URCST algorithm, which is only $O(n)$, demands much more power to be executed. This significantly shorten the battery lifespan.

On the other hand, the period of number generation, after which the sequence will be repeated, for the URCST algorithm is too short in comparison with the period of the MT19937. URCST can only generate a sequence of up to 16 numbers while MT19937

period is up to $(2^{19937} - 1)$. However, the maximum period that is required for each transmission is only eight (8), which makes the URCST algorithm more suitable for any M2M application. Table 3.3 summarises the comparison between the URCST algorithm and the MT19937 algorithm.

Table 3.3: A summary of the comparison between URCST and MT19937.

No.	Terms	URCST	MT19937
1	Microcontroller type	Can be implemented using 16-bit microcontrollers or above.	Can be implemented using 32-bit microcontrollers or above.
2	Resources (RAM)	Uses a tiny memory to store a few 16-bit variables (<64 bytes).	Requires a large memory to save matrices (> 5k bytes).
3	Programming complexity	Very easy to implement by microcontrollers, only employs simple logical operations.	Complex to implement by microcontrollers, because of matrices multiplication and other complex operations.
4	Iteration complexity	Low iteration complexity of $O(n)$, which even reduces the time required to calculate the channel index and the power consumption.	High iteration complexity of $O(p^2)$, which affects the calculation time and the power consumption.
5	Period length	Short period length of up to (16).	Very long period of up to $(2^{19937} - 1)$.

3.7 Summary

The data collision problem is one of the most important challenges that faces LPWANs, especially with the massive number of devices that are expected to be connected to these systems with the era of the IoT and smart cities. Therefore, a new channel selection algorithm is proposed in this chapter that can mitigate the collision problem and maintain the low complexity, low power consumption, and low cots requirements for successful LPWANs design and implementation.

The URCST algorithm provides a better system performance and a lower probability of collisions in comparison to the standard Weightless-N algorithm for different working scenarios. Moreover, the URCST algorithm provides better performance as the number of message copies increase while the standard algorithm provides the best performance at four message copies. This might be very useful for applications requiring a high QoS like

security, fire alarms, heart disease monitoring, and Electronic Point of Sale (EPOS) (Ofcom, 2014; Al-Fuqaha *et al.*, 2015).

In addition, the URCST algorithm provides a uniform distribution over all available channels and offers a system performance that is similar to the standard uniform random number generator the MT19937 algorithm. On the other hand, the URCST algorithm can be implemented using simple microcontrollers with much lower hardware resources and much less complexity, computational time, and power consumption in comparison to the MT19937 algorithm.

Chapter 4

Mathematical System Modelling

4.1 Introduction

Most LPWAN technologies focus on reducing the complexity of the terminal devices to achieve the low cost and low power consumption which are essential requirements of modern M2M communication systems. Therefore, the majority of these technologies eliminate the synchronisation process and rely on the ALOHA-based random time-frequency access protocol. For instance, Weightless-N and Sigfox technologies employ the random time-frequency access with the frequency hopping (FH) technique over a wide range of ultra-narrow band channels.

Moreover, Weightless-N and Sigfox utilise the multiple message copies approach to mitigate the effect of the collision on system performance and increase the probability of successful message delivery (Weightless-SIG, 2015c; Abbas *et al.*, 2017; Sigfox, 2019a; Sigfox, 2017b; Sigfox, 2017a; Sigfox, 2017c). This places another challenge to the system modelling and increases the complexity of the collision probability analysis.

Multiple studies have been conducted to try to calculate the packet loss ratio and model the system performance with ALOHA-based random access. However, most of these studies are limited by modelling the probability of collision in one domain, either time or frequency (Li *et al.*, 2017; Goursaud and Mo, 2016; Do *et al.*, 2014). A few other works have been dedicated to the collision modelling in random time-frequency access wireless communication systems based on the duality of the random access in both domains (Anteur *et al.*, 2014; Li *et al.*, 2017; Goursaud and Mo, 2016; Csibi and Gyorfi, 1996; Savaux *et al.*, 2017).

The mathematical model presented in this chapter offers a novel and flexible model for the random time-frequency access with the multiple message copies approach, which is derived by combining the Poisson distribution and the Binomial distribution. The Poisson distribution is implemented to model the packet arrival in the time domain and calculate the probability of successful transmission in the time-frequency plane. The Binomial distribution is applied to find the probability of successful transmission with multiple message copies.

In addition, the chapter presents a review of the existing works on the collision modelling in ALOHA-based LPWANs. It also discusses the collision probability analysis for different

scenarios and offers a detailed description of how the mathematical model is derived for each scenario. Then, the chapter describes the evaluation method that is used to calculate the model accuracy based on the normalised root mean square error (NRMSE) and Nash-Sutcliffe coefficient of efficiency (NSE). The developed model is validated by implementing it on both Weightless-N and Sigfox technologies as a case study and comparing the resulting MLR to the one that obtained from the simulation for all scenarios.

4.2 Time-Frequency Probability Analysis

ALOHA is a long-known medium access protocol (Abramson, 1970; Roberts, 1975), and there is a notable amount of work that evaluates the performance of wireless communication systems that are based on this protocol. However, with the emergence of the IoT and M2M communication technologies, the ALOHA protocol has regained the interest of researchers especially for the performance analysis of LPWANs.

Models of wireless communication systems that employ random access protocol are mainly based on the Poisson distribution (Abramson, 1970; Kaynia and Jindal, 2008; Win *et al.*, 2009; Kaur and Gregory, 2011). This is well suited for the packet arrival in the time domain even for devices that send messages periodically on a fixed timing scheme since all devices start sending messages randomly in real systems. Another study by Do *et al.* (Do *et al.*, 2014) models the probability of collision in the frequency domain for the UNB LPWANs based on the impulse response and the signal-to-interference-plus-noise ratio (SINR).

Nevertheless, modelling transmitted message collisions in one domain, either time or frequency, offers only a limited insight into the LPWANs performance. Therefore, the joint analysis in time and frequency domains is a crucial step to evaluate the real system capacity and reliability with the massive number of connected devices.

In Csibi and Gyorfi's paper (Csibi and Gyorfi, 1996), the probability of collision in random time-frequency access is evaluated assuming pure ALOHA. The Poisson distribution is implemented to model the packet arrival, and the frequency domain effect is combined in the exponential form of the model. The model provided in this work focuses on the channel coding effect on the system performance.

In the paper by Anteur *et al.* (Anteur *et al.*, 2014), the performance of the UNB technique for the LPWANs is studied by modelling the collision problem in the time-frequency plane. In the time domain, the Poisson distribution is employed to model the packet arrival

average while the geometry analysis is utilised to calculate the probability of collision with the frequency drift effect in the frequency domain.

The performance of the UNB technique for the LPWANs is also evaluated by Goursaud and Mo (Goursaud and Mo, 2016) based on the joint analysis of both domains. The Poisson distribution is used to model the packet transmission rate in pure unslotted ALOHA and time-slotted ALOHA. The probability of successful transmission in the time domain is based on the exponential approximation proposed by Abramson (Abramson, 1970). Goursaud and Mo combine the spectral collision in the frequency domain with exponential form in the time domain to calculate the final probability of successful transmission.

Another study by Savaux *et al.* (Savaux *et al.*, 2017) was dedicated to analysing the interference between multiple cells based on the spatial Poisson process in the time domain. The occupancy problem from the probability theory is employed to calculate the probability of collision in the frequency domain and evaluate the system throughput for a variable number of connected devices.

Nonetheless, it remains that the aforementioned studies assume that all devices have the same packet size and transmission time, which stops short from modelling important practical applications with different characteristics. In addition, they lack the multiple message copies approach used by Weightless and Sigfox and evaluate the system performance based on a single message copy.

Li *et al.* (Li *et al.*, 2017) use the stochastic geometry model in the time-frequency domain to evaluate the performance of LPWANs and analyse the probability of collision based on the Card Tossing Game model. Furthermore, the capture effect and, more importantly, the multiple message copies are considered in this work. However, it also lacks the practical system analysis that supports various applications and assumes that all devices have the same packet size and transmission time. Moreover, the model provides a relatively high message loss ratio (MLR) for a single and three message copies even with zero connected devices in the case of Sigfox technology. Therefore, it might not best describe the probability of collision and system performance for UNB LPWANs in terms of the multiple message copies.

The performance of the LoRa, Sigfox, and NB-IoT is also evaluated by Mroue *et al.* (Mroue *et al.*, 2018) based on the probability of collisions for a number of symbols in each packet using the basic probability theory. However, the paper suffers from a lack of clarity in

defining the effect of multiple message copies on the Sigfox performance. Again, the analysis presented in this study assumes that all devices have the same transmission characteristics. It also assumes that all packets are sent within a one-minute time slot utilising only 200 UNB channels. This assumption leads to a very high probability of collisions and shows that Sigfox can only supports up to several hundreds of devices. This does not represent the practical case for Sigfox, where the minimum transmission duration is limited to 10 minutes and the total number of available UNB channels is 1920.

Another study by Vejlgaard *et al.* (Vejlgaard *et al.*, 2017) was dedicated to study the coverage and capacity of Sigfox, LoRa, GPRS, and NB-IoT technologies and provide a comparison among these LPWANs. For GPRS the study utilises the existing Telenor cellular site grid in Northern Denmark while it employs mathematical models for other technologies. The model presented in this paper for Sigfox is based on the exponential approximation proposed by Abramson (Abramson, 1970) and Goursaud and Mo (Goursaud and Mo, 2016) in time-frequency domain. Furthermore, the multiple message copies are considered in this work where the probability of successful transmission is calculated based on the Binomial distribution. However, the paper does not provide validation for the presented model. Moreover, it also lacks the practical system analysis that supports various applications assuming that all devices have the same transmission characteristics and fixed three message copies.

In the work presented by Lavric *et al.* (Lavric *et al.*, 2019), the effect of data collisions on the performance of Sigfox was evaluated by simulation. The analysis conducted in this paper is implemented for two cases: a single message copy and three message copies. Results show that Sigfox offers a high probability of collisions even with several hundreds of nodes. However, the paper lacks the practical system consideration and assumes that all packets are sent within a one-minute time slot. It also suffers from a lack of data validation and rely on simulation results only. Moreover, the paper does not offer any mathematical model for the analysis.

This chapter provides a general mathematical model for the probability of collision in random time-frequency access wireless communication systems with the multiple message copies approach, which is based on the Poisson distribution and the Binomial distribution. The modelling method implemented in this chapter focuses on the intercell interference neglecting any other source of interference and noise. This assumption is used to evaluate the system reliability and emphasise the degradation of performance with the massive

number of connected devices regardless of other factors like noise and coexistence problem.

Unlike previous works, the model and analysis presented in this chapter consider the case of multiple groups of devices that work simultaneously with different transmission characteristics and multiple message copies. This includes an analysis using a variable number of devices, message copies, payload, transmission time, and channels.

4.3 System Model

In the modelling of the probability of collision, the analysis presented in this section considers that k devices are sending messages on N channels to a single base station. Each device sends multiple message copies independently on randomly selected channels. The analysis considers that all devices experience flat channels and all packets are perceived to have a balanced power level at the base station (Goursaud and Mo, 2016; Do *et al.*, 2014; Csibi and Gyorfi, 1996). The analysis is also based on the worst-case scenario of message collision, which calculates the message lost ratio (MLR) by assuming that even a weak overlap between two packets in the time-frequency domain leads to the loss of both. In addition, a uniform channel distribution is utilised in the analysis, considering that all channels have an equally likely probability of selection from all devices (Li *et al.*, 2017; Goursaud and Mo, 2016; Anteur *et al.*, 2014; Savaux *et al.*, 2017; Csibi and Gyorfi, 1996). Consequently, the analysis in the frequency domain can be simplified and modelled independently of the time domain. Therefore, the analysis presented in this chapter is based on the Uniform Randomisation Channel Selection Technique (URCST) described in section 3.3 in Chapter 3.

The model presented in this section is divided into three different scenarios: a single group with periodic or random transmission scheme, multiple groups with various transmission scheme and the same number of message copies, and multiple groups with various transmission scheme and multiple numbers of message copies. This could cover the performance evaluation for LPWANs with the broad applications in the IoT and smart cities. Table 4.1 reports all the used notations in the analysis of these scenarios.

Table 4.1: Table of notations.

Symbol	Description
k	The total number of devices.
N	The total number of channels.
λ	Average packets per channel (the number of total packets per N channels).
τ	Packet duration.
T	Average transmission time.
t_0	The transmission time for periodic transmission.
t_1	The minimum transmission time for on-demand transmission.
t_2	The maximum transmission time for on-demand transmission.
p_r	The packet generation rate for each device.
p_{rk}	The total packet generation rate.
m	The number of message copies.
P_{st}	The probability of successful transmission with a single message copy.
P_s	The final probability of successful transmission with multiple message copies.
P_f	The final probability of lost messages (MLR) with multiple message copies.
G	The number of groups.
i	The groups' number (i = 1, 2, …, G).
j	The index of a specific group.
pgr_j	The packet generation ratio of group j.
p_{rkj}	The packet generation rate for group j.
P_{fj}	The probability of lost messages for group j.
P_{sj}	The probability of successful transmission with multiple message copies of group j.
L	The total number of data points for the goodness of fit calculations.
yo	Observed data from simulation.
yo_{max}	The maximum value in observed data.
yo_{min}	The minimum value in observed data.
yo_{mean}	The mean of observed data.
yp	The predicted data from the model.
PL	The message payload.

4.3.1 Single Group Scenario

In the single group scenario, all devices have identical characteristics, where the same number of message copies, transmission time, and packet size are used. Regarding transmission time, the analysis considers two different transmission schemes: periodic transmission on constant time intervals and on-demand (random) transmission between two-time intervals.

Modelling of the system needs to be divided into two steps: the time-frequency analysis and the multiple message copies analysis. The collision in the time domain can be calculated based on the Poisson distribution given by

$$P(x) = \frac{\lambda^x}{x!} e^{-\lambda} \tag{4.1}$$

Where λ is the average packets per channel, which represent the total number of packets accessing N channels at any time. The probability of successful transmissions can be calculated by setting $x = 0$ as (Goursaud and Mo, 2016; Abramson, 1970; Martolos and Anděl, 2013; Matlab, 2018):

$$P(x = 0) = e^{-\lambda} \tag{4.2}$$

Assuming that the packet duration is τ in seconds and each device transmits m packets for each message on the average transmission time of T seconds, the packet generation rate for each device can be calculated as follows:

$$p_r = m\frac{\tau}{T} \tag{4.3}$$

Where m denotes the number of message copies. Then, the total packet generation rate p_{rk} for all k devices is given by

$$p_{rk} = mk\frac{\tau}{T} \tag{4.4}$$

By neglecting the capture effect and assuming that the overlap between any two packets causes the loss of both packets, the time interval of collision will be 2τ (Abramson, 1970; Roberts, 1975; Goursaud and Mo, 2016). Since all packets during this period are uniformly distributed over the N channels, λ is calculated as follows:

$$\lambda = \frac{2p_{rk}}{N} = \frac{2mk}{N} \times \frac{\tau}{T} \tag{4.5}$$

Then, the probability of successful transmission in the time-frequency domain for a single message copy is given by

$$P_{st} = e^{-\lambda} = e^{\frac{-2mk\tau}{NT}} \tag{4.6}$$

Since each message copy is independent of other copies and is sent on a randomly selected channel, the multiple message copies approach can be solved using the Binomial distribution. Furthermore, as the successful transmission can be achieved with at least one successful transmission for any message copy, the final probability of successful transmission can be obtained from the cumulative distribution function (CDF) of the Binomial distribution. Therefore, the final system successful transmission probability P_s is given by

$$P_s = \sum_{l=1}^{m} \binom{m}{l} (P_{st})^l (1 - P_{st})^{(m-l)} \tag{4.7}$$

Then, the final probability of lost messages, which represent the MLR, is given by

$$P_f = 1 - P_s = 1 - \sum_{l=1}^{m} \binom{m}{l} (P_{st})^l (1 - P_{st})^{(m-l)} \tag{4.8}$$

The average transmission time T can be calculated based on the transmission scheme, where devices either send packets periodically, on specific time intervals t_0, or on-demand, randomly between two-time limits t_1 and t_2. Therefore, T can be obtained as follows:

$$T = t_0 \qquad for\ periodic\ transmission \tag{4.9}$$

$$T = \frac{t_1 + t_2}{2} \qquad for\ random\ transmission \tag{4.10}$$

In addition, the packet duration τ is directly related to the message payload and can be calculated as follows (Botter *et al.*, 2012):

$$\tau = \frac{packet\ size(bits)}{data\ transmission\ rate(bps)} \tag{4.11}$$

4.3.2 Multiple Group Scenario with the Same Number of Message Copies

In practical systems, devices that work together have different transmission characteristics, where various transmission times and packet sizes are used according to the intended applications. However, the same number of message copies might be used for all the connected devices due to the power consumption, application requirements, or technical specifications. For example, Sigfox employs only three message copies for all devices. In such a case, the packet generation rate is calculated as the summation of the packet generation rate for each group of similar devices.

By assuming that there are *G* groups and devices in each group have the same packet duration and transmission time, the total packet generation rate p_{rk} and the average packets per channel λ are calculated as follows:

$$p_{rk} = m \times \sum_{i=1}^{G} k_i \frac{\tau_i}{T_i} \tag{4.12}$$

$$\lambda = \frac{2p_{rk}}{N} = \frac{2m}{N} \times \sum_{i=1}^{G} k_i \frac{\tau_i}{T_i} \tag{4.13}$$

Where k_i , τ_i , and T_i denote the number of devices, the packet duration, and the transmission time for each group respectively. Then, Equations 4.6 and 4.8 can be used to calculate the final probability of lost messages P_f as follows:

$$P_{st} = e^{-\lambda} = e^{\frac{-2m}{N} \times \sum_{i=1}^{G} k_i \frac{\tau_i}{T_i}} \tag{4.14}$$

$$P_f = 1 - \sum_{l=1}^{m} \binom{m}{l} (P_{st})^l (1 - P_{st})^{(m-l)} \tag{4.15}$$

4.3.3 Multiple Group Scenario with Various Numbers of Message Copies

With the broad range of IoT applications, designers may choose a variable number of message copies for each node based on the application requirements and the desired quality of service. The Binomial distribution (Equations 4.7 and 4.8) cannot be implemented directly to calculate the probability of successful transmission since *m* is not the same for

all devices. In such a case, devices will be divided into groups according to the number of message copies despite other characteristics. The analysis is based on finding the MLR for each group and then combining results to obtain the final probability of lost messages.

The total packet generation rate for all devices p_{rk} and the average packets per channel λ are given by

$$p_{rk} = \sum_{i=1}^{G} m_i k_i \frac{\tau_i}{T_i} \quad 4.16$$

$$\lambda = \frac{2p_{rk}}{N} = \frac{2}{N} \times \sum_{i=1}^{G} m_i k_i \frac{\tau_i}{T_i} \quad 4.17$$

Where m_i denotes the number of message copies for each group.

The total probability of successful transmission with a single message copy P_{st} is given by

$$P_{st} = e^{-\lambda} = e^{\frac{-2}{N} \times \sum_{i=1}^{G} m_i k_i \frac{\tau_i}{T_i}} \quad 4.18$$

The probability of successful transmission for each group P_{sj} is calculated based on the number of message copies for the group m_j as:

$$P_{sj} = \sum_{l=1}^{m_j} \binom{m_j}{l} (P_{st})^l (1 - P_{st})^{(m_j - l)} \quad 4.19$$

Where *j* represents the index of the intended group.

The probability of lost messages generated by individual groups P_{fj} is calculated by multiplying the MLR of each group by the group's packet generation ration pgr_j as:

$$P_{fj} = (1 - P_{sj}) \times pgr_j \quad 4.20$$

The packet generation ratio for individual groups pgr_j can be calculated from the ratio of the packet generation rate of each group p_{rkj} to the total packet generation rate of all groups p_{rk} as:

$$pgr_j = \frac{p_{rkj}}{p_{rk}} = \frac{m_j k_j \frac{\tau_j}{T_j}}{\sum_{i=1}^{G} m_i k_i \frac{\tau_i}{T_i}} \quad 4.21$$

Now, the final probability of lost messages is calculated by the summation of P_{fj} over all groups as:

$$P_f = \sum_{j=1}^{G} P_{fj} \quad 4.22$$

4.4 Evaluation of the Model

The Normalised Root Mean Square Error (NRMSE) and the Nash-Sutcliffe coefficient of efficiency (NSE) are two well-known statistical methods used to measure the goodness of fit of mathematical models (Nash and Sutcliffe, 1970; Legates and McCabe Jr., 2005; Gupta and Kling, 2011; Faridnasr *et al.*, 2016). These performance metrics are used in this chapter to evaluate the model accuracy using the predicted data from the mathematical model and the observed data from the simulation. Simulation of both Weightless-N and Sigfox technologies were implemented in MATLAB software based on the Uniform Randomisation Channel Selection Technique (URCST) to achieve the uniform distribution over all channels.

NRMSE and NSE are calculated in the following equations:

$$NRMSE = \frac{\sqrt{\frac{\sum_{i=1}^{L}(yo_i - yp_i)^2}{L}}}{yo_{max} - yo_{min}} \quad 4.23$$

$$NSE = 1 - \frac{\sum_{i=1}^{L}(yo_i - yp_i)^2}{\sum_{i=1}^{L}(yo_i - y_{mean})^2} \quad 4.24$$

NRMSE varies on the range [0,1] where smaller values indicate a better agreement between the observed and the predicted data. On the other hand, NSE has a value in the range $[-\infty, 1]$ where a value of 1.0 refers to the best agreement.

4.5 Validation of the Model

The model validation is based on calculating NRMSE and NSE for the predicted data from the model in comparison with the observed data that obtained from the simulation. The model is implemented to calculate the message lost ratio (MLR) in Weightless-N and Sigfox technologies with different scenarios including a variable number of devices, message copies, payloads, transmission time, and the number of channels in the Weightless-N case. Both technologies utilise the sub-GHz ISM band of 868 MHz in Europe and employ the UNB technique without synchronisation, acknowledgement, and any carrier sensing mechanism.

The single group scenario is implemented only in the Weightless-N case with a variable number of connected devices to evaluate the model accuracy in this special case, where all devices have the same transmission characteristics and the number of message copies. Other analyses consider the general case of multiple groups. In the case of multiple group scenario, the analysis employs the same assumption used in section 3.2.3 in Chapter 3 by implementing four groups of devices that are connected to the same base station with different transmission characteristics, which are denoted by *G1*, *G2*, *G3*, and *G4*. *G1* represents 40% of the total number of connected devices while each of the other groups represents 20%.

4.5.1 Weightless-N Technology

Weightless-N employs UNB channels each with 200 Hz bandwidth and a bit rate of 100 bps. It also supports a payload of up to 20 bytes with a total packet size of 37 bytes ($\tau = 1.44s - 2.96s$), and message copies in the rage from three to eight. However, the analysis includes all the possible range starting from one message copy. Weightless-N limits the number of messages for each device by a maximum rate of one message per minute ($T \geq 60\ sec$). In addition, Weightless-N utilises six frequency bands with six different numbers of channels: 1200, 1500, 2499, 3000, 9990, and 15000 (Weightless-SIG, 2015c; Abbas *et al.*, 2017).

The analysis presented in this section is based on using 1200 channels, except for the case of multiple numbers of channels. Also, the characteristics of each group of devices are in

general as shown in Table 4.2. Also, the payload and transmission time will be variable for the variable *PL* and the variable T analysis presented in sections 4.5.2.2 and 4.5.2.3 respectively.

Table 4.2: Weightless-N group general characteristics.

Group name	Percentage of total devices (%)	Transmission scheme	Transmission time (minutes)	Payload (Byte)
G1	40	Periodic	$t_0 = 2$	8
G2	20	Random	$t_1 = 1$ and $t_2 = 2$	10
G3	20	Periodic	$t_0 = 4$	12
G4	20	Random	$t_1 = 2$ and $t_2 = 4$	14

4.5.1.1 Variable Number of Devices

The analysis presented in this section illustrates the model validation in the case of Weightless-N with a variable number of devices based on two scenarios: single group and multiple groups. The analysis also evaluates the model accuracy with a single message copy and three message copies. These different analyses are presented to ensure that the mathematical model can accurately describe the system performance for all working scenarios, as presented in the next sections.

A. The Single Group Scenario

For the single group scenario, all devices have the same transmission characteristics and the number of message copies. *G1* characteristics shown in Table 4.2 are utilised for the periodic transmission analysis while all devices are set to *G2* for the random transmission analysis.

Figure 4.1(a) shows the simulated and modelled MLR versus the number of connected devices with a single message copy ($m = 1$) for the periodic transmission case with $t_0 = 2$ minutes and $PL = 8$ bytes. The model provides very close results to the data obtained from the simulation with NRMSE $= 0.021$ and NSE $= 0.996$. On the other hand, Figure 4.1(b) shows the MLR versus the number of connected devices with a single message copy ($m = 1$) for the random transmission scheme with $t_1 = 1$ minutes, $t_2 = 2$ minutes, and $PL = 10$ bytes. The model also provides very close results to the data obtained from the simulation with NRMSE $= 0.029$ and NSE $= 0.991$.

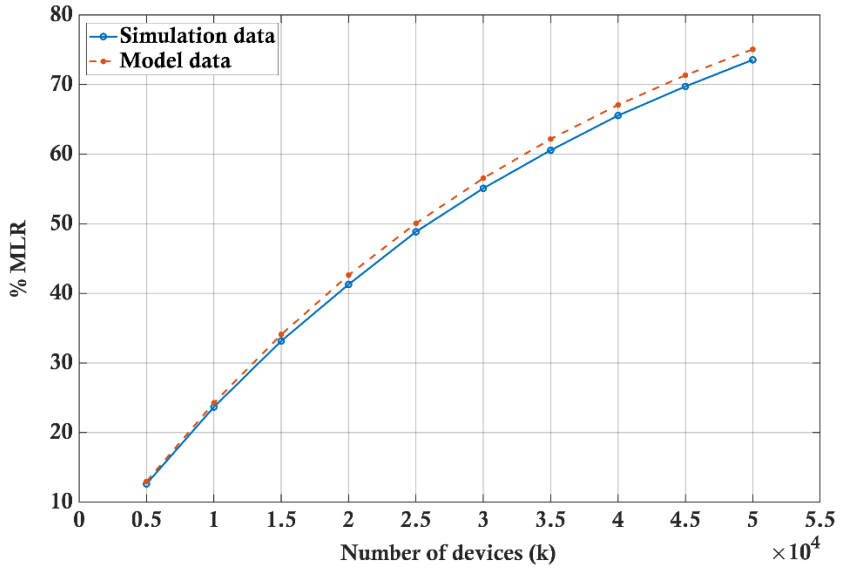

a) A single group with a periodic transmission, where $t_0 = 2$ min and $PL = 8$ bytes. NRMSE = 0.021 and NSE = 0.996.

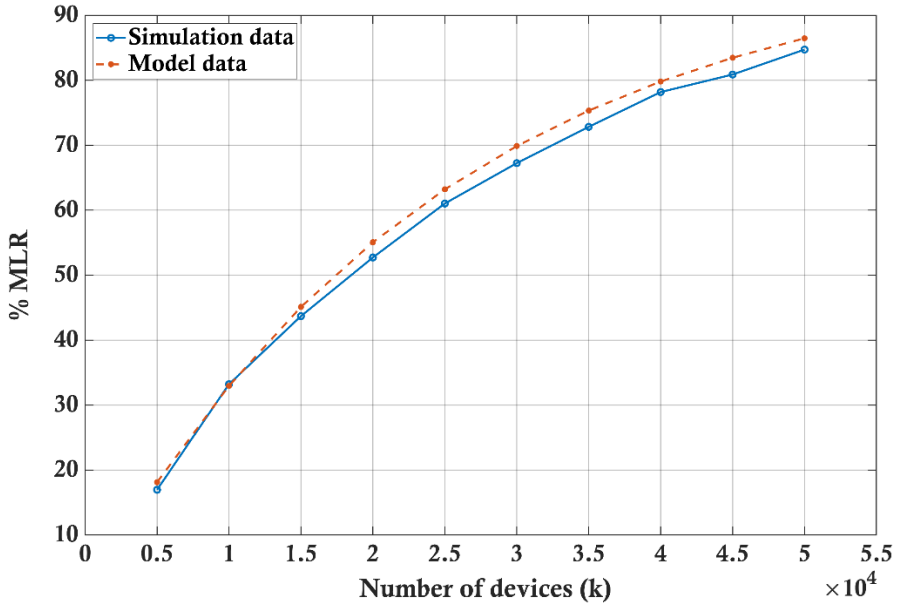

b) A single group with a random transmission, where $t_1 = 1$ min, $t_2 = 2$ min, and $PL = 10$ bytes. NRMSE = 0.029 and NSE = 0.991.

Figure 4.1: The simulated and modelled MLR with a varying number of connected devices k for Weightless-N with a single group and a single message copy, where $N = 1200$ and $m = 1$.

Figure 4.2(a) and (b) depict the MLR versus the number of connected devices with three message copies ($m = 3$) for the periodic and the random transmission schemes respectively. The model provides very close results to the data obtained from the simulation for both cases as shown in Figure 4.2(a) and (b). It is clear from Figure 4.1 and Figure 4.2 that as the number of devices increases the model accuracy slightly decreases.

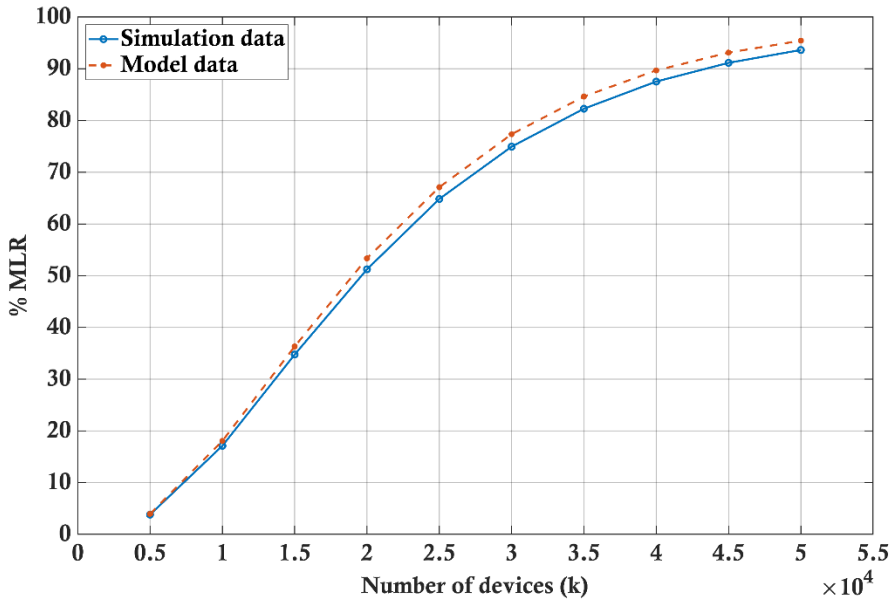

a) A single group with a periodic transmission, where $t_0 = 2$ min and $PL = 8$ bytes. NRMSE = 0.021 and NSE = 0.996.

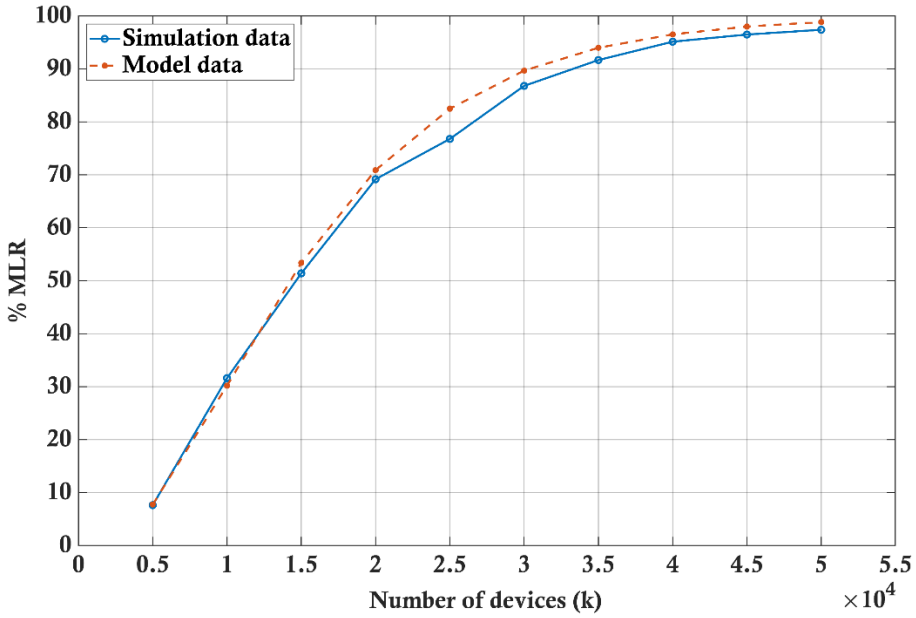

b) A single group with a random transmission, where $t_1 = 1$ min, $t_2 = 2$ min, and $PL = 10$ bytes. NRMSE = 0.028 and NSE = 0.993.

Figure 4.2: The simulated and modelled MLR with a varying number of connected devices *k* for Weightless-N with a single group and three message copies, where $N = 1200$ and $m = 3$.

B. The Multiple Group Scenario

Figure 4.3 shows the simulated and modelled MLR versus the number of connected devices for the multiple group scenario with a single message copy and three message copies. In this analysis, all devices have the same number of message copies. It is apparent

that the model provides a precise evaluation of the system performance with multiple groups that implement different transmission characteristics. Again, it also shows that the model accuracy decreases as the number of devices increases.

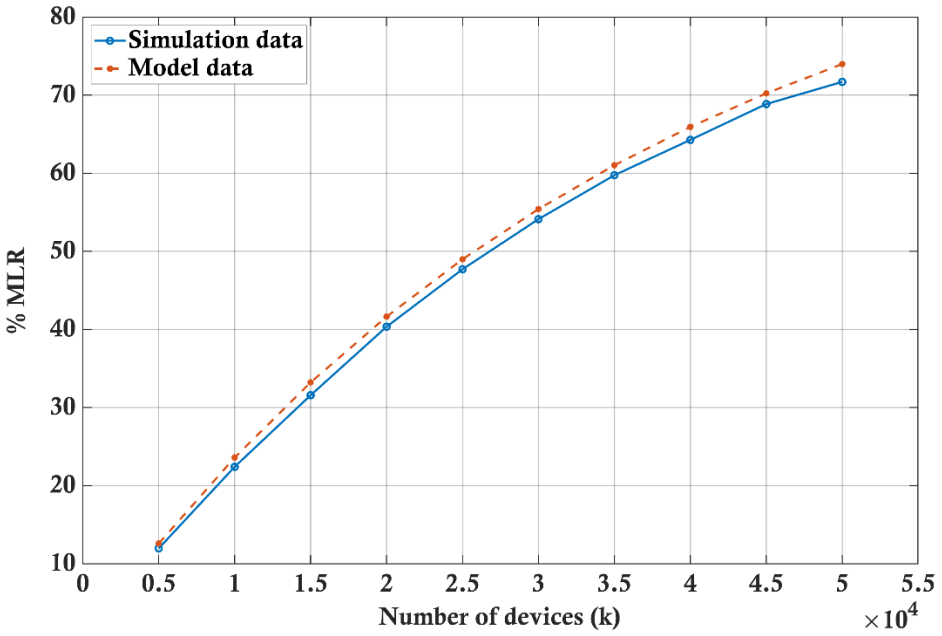

a) Multiple groups with a single message copy (m = 1).
NRMSE = 0.021 and NSE = 0.996.

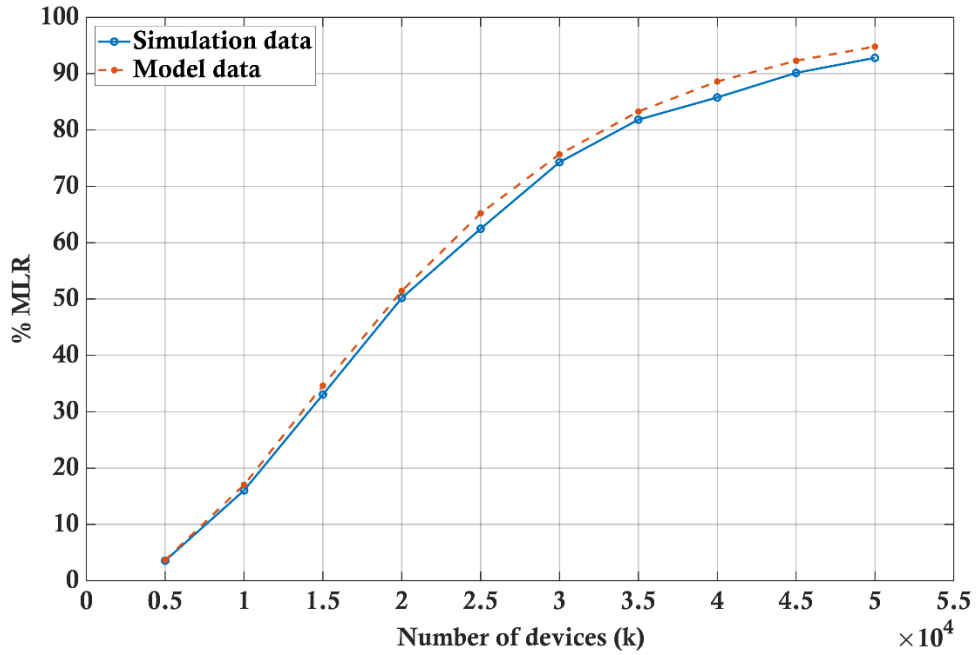

b) Multiple groups with three message copies (m = 3).
NRMSE = 0.020 and NSE = 0.996.

Figure 4.3: The simulated and modelled MLR with a varying number of connected devices k for Weightless-N with multiple groups and the same number of message copies, where All groups have the same number of message copies in each analysis with N = 1200.

Figure 4.4 demonstrates the MLR versus the number of connected devices for the multiple group scenario with various numbers of message copies, where each group employ a different number of message copies. It is evidence from this figure that the model still provides very close results in comparison to the simulation data for both individual groups and the final probability of lost messages.

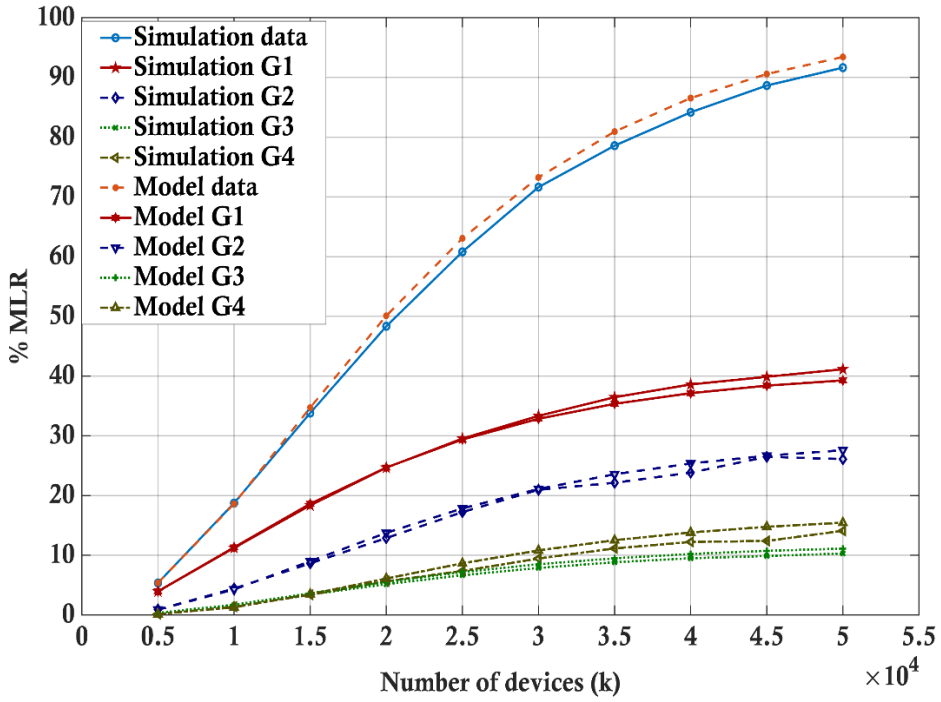

Figure 4.4: The simulated and modelled MLR with a varying number of connected devices *k* for Weightless-N with multiple groups and multiple numbers of message copies, where *N* = 1200, *G1: m* = 2, *G2: m* = 3, *G3: m* = 3, and *G4: m* = 4. NRMSE = 0.020 and NSE = 0.996.

4.5.1.2 Variable Number of Message Copies

Figure 4.5 illustrates the effect of using multiple message copies on the Weightless-N system performance using multiple groups, where all the groups have the same number of message copies in each analysis. Figure 4.5(a) shows the simulation and model data of the MLR for individual groups and the final MLR of the system in the case of using 4000 devices. Figure 4.5(b) shows the simulated and modelled final MLR versus the number of message copies for different numbers of devices. Similarly, analysis depicts that the presented model can precisely describe the system performance with the multiple message copies approach and provides very close results in comparison to the simulation data over the whole range of the applicable number of message copies.

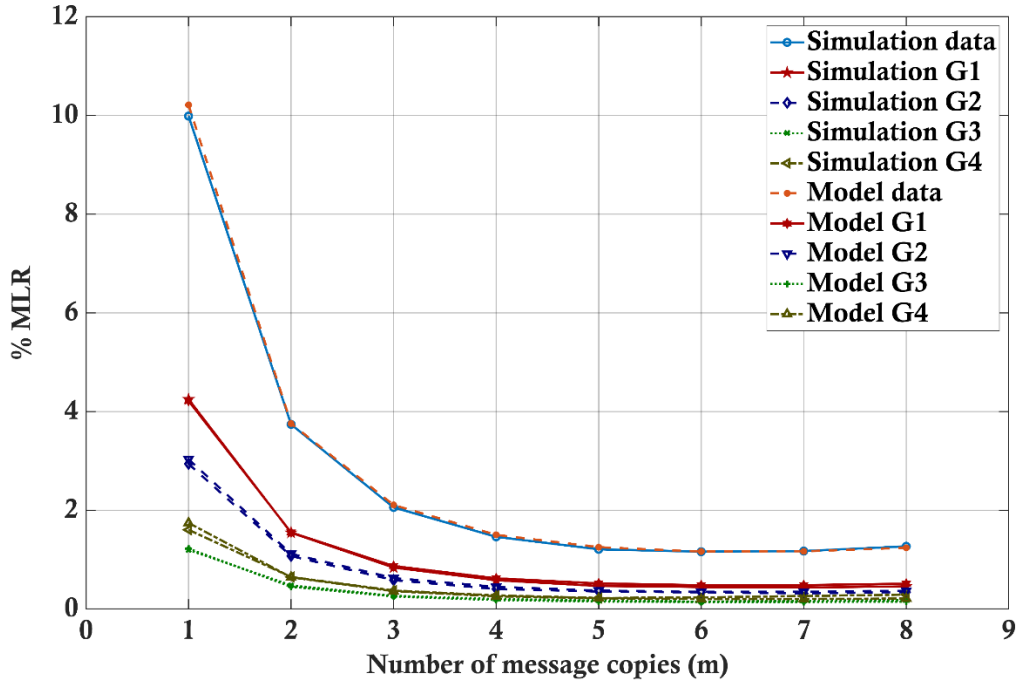

a) Multiple groups with k = 4000.
NRMSE = 0.010 and NSE = 0.999.

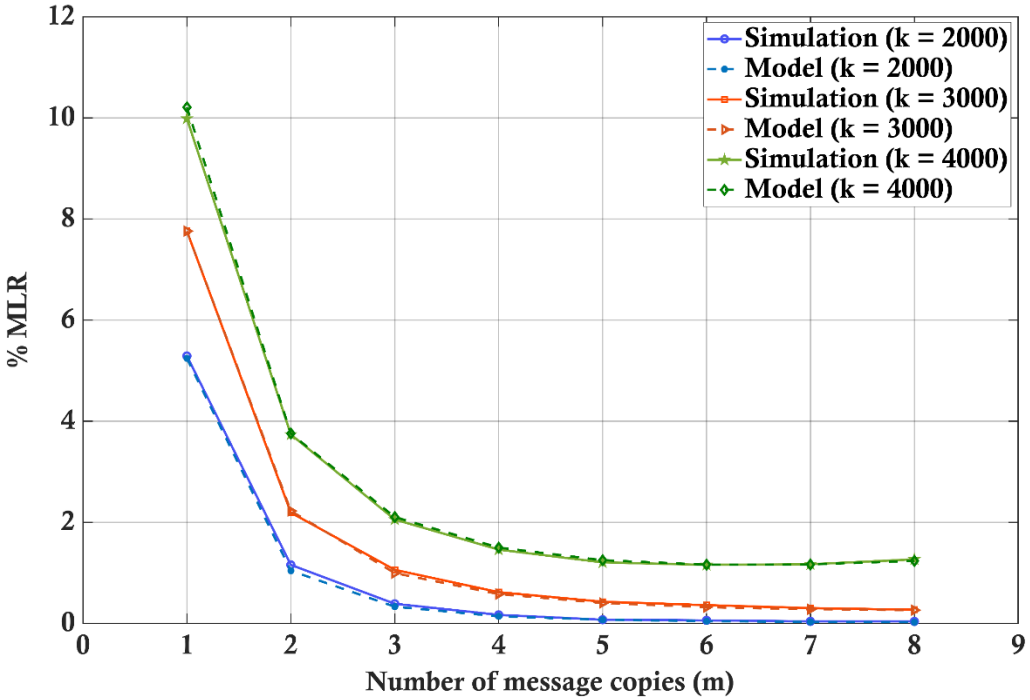

b) Multiple groups with different numbers of devices.
2000 devices: NRMSE = 0.010 and NSE = 0.999
3000 devices: NRMSE = 0.005 and NSE = 1
4000 devices: NRMSE = 0.010 and NSE = 0.999

Figure 4.5: The simulation and model MLR with a varying number of message copies *m* for Weightless-N with multiple groups, where All groups have the same number of message copies in each analysis with *N* = 1200.

4.5.1.3 Variable Payload

Figure 4.6 depicts the effect of using a variable payload on the final probability of lost messages for Weightless-N. It shows the simulated and modelled MLR versus the payload in bytes, and thus the packet duration τ, for both single and three message copies. It is apparent from Figure 4.6 that the model provides close results to the simulation data for the whole range of used payload with different numbers of message copies.

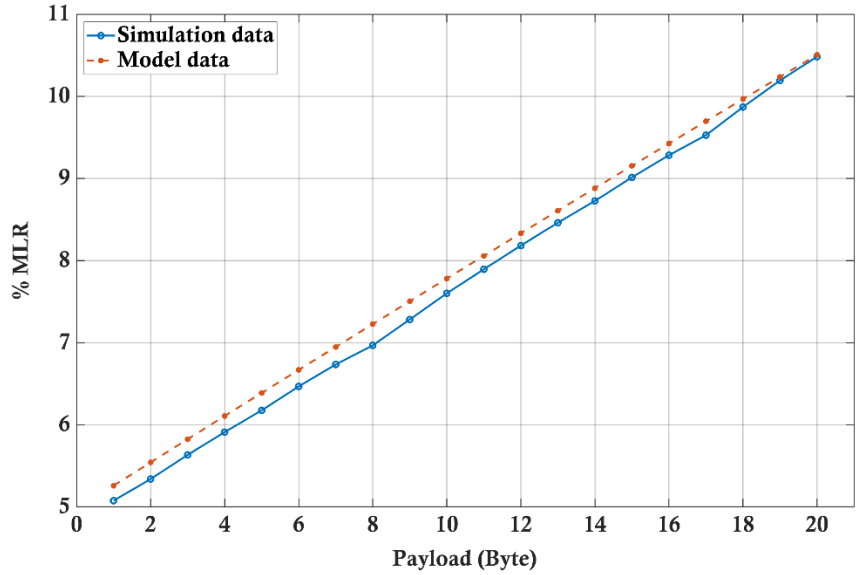

a) Multiple groups with k = 3000 and m = 1.
NRMSE = 0.032 and NSE = 0.989.

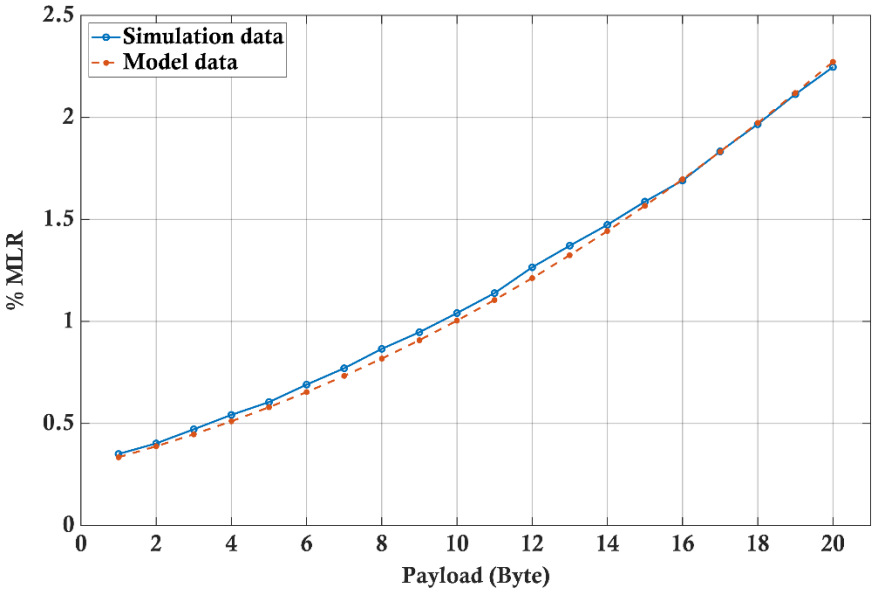

b) Multiple groups with k = 3000 and m = 3.
NRMSE = 0.016 and NSE = 0.997

Figure 4.6: The simulation and model MLR with a varying payload *PL* for Weightless-N with multiple groups, where All groups have the same number of message copies in each analysis with N = 1200 and k = 3000.

4.5.1.4 Variable Transmission Time

The analysis presented in this section is based on the single group scenario to evaluate the model accuracy with variable transmission time. All groups have the same characteristics as a periodic transmission scheme. Figure 4.7 shows the probability of lost messages for the Weightless-N technology using different transmission time and three message copies and demonstrates the simulated and modelled MLR versus a variable number of connected devices. It is evident from Figure 4.7 that the model offers close results in comparison to the simulation data for variable transmission time. It also depicts that as the transmission time increases the model accuracy slightly decreases.

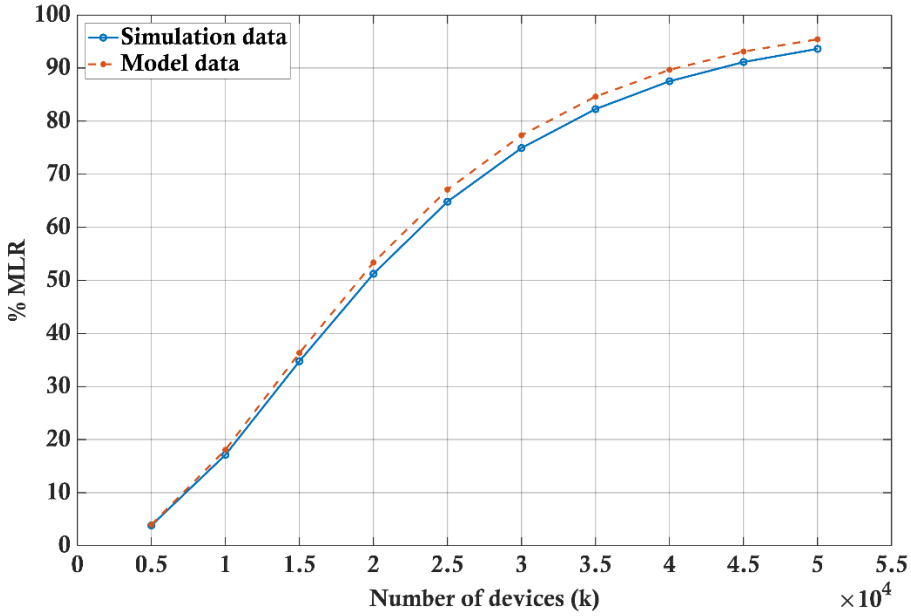

a) T = 2 min, NRMSE = 0.021 and NSE = 0.996.

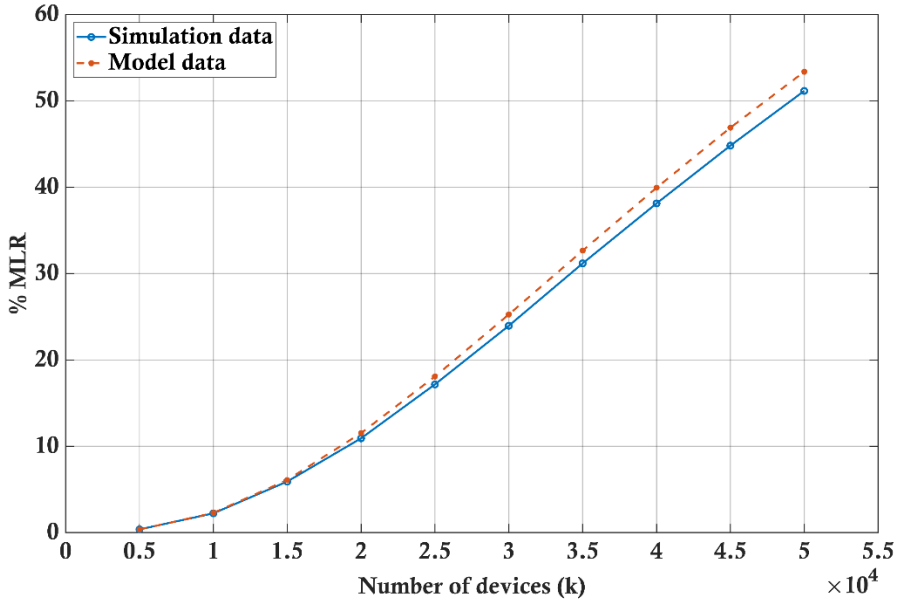

b) T = 5 min, NRMSE = 0.026 and NSE = 0.994.

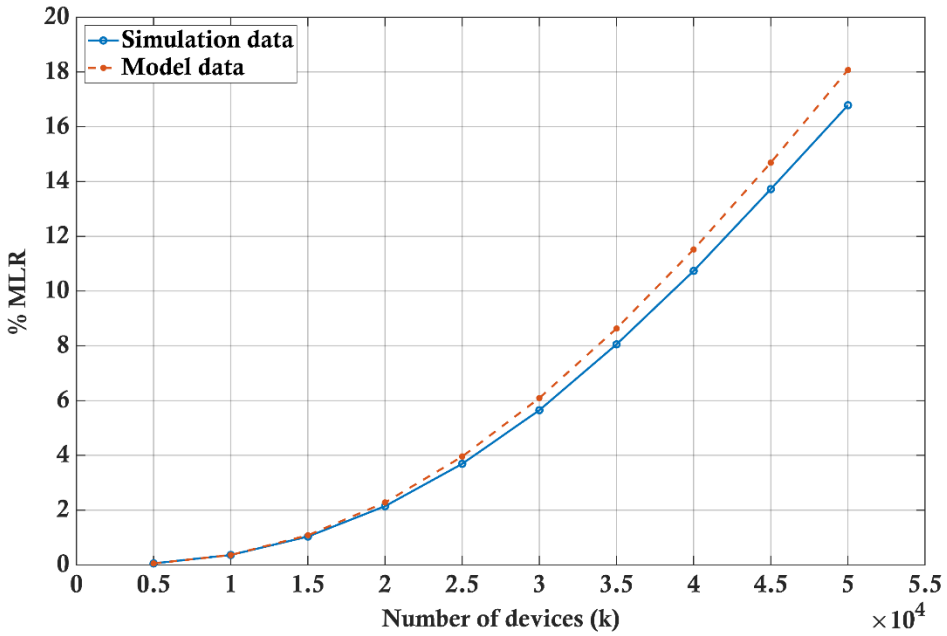

c) T = 10 min, NRMSE = 0.037 and NSE = 0.988.

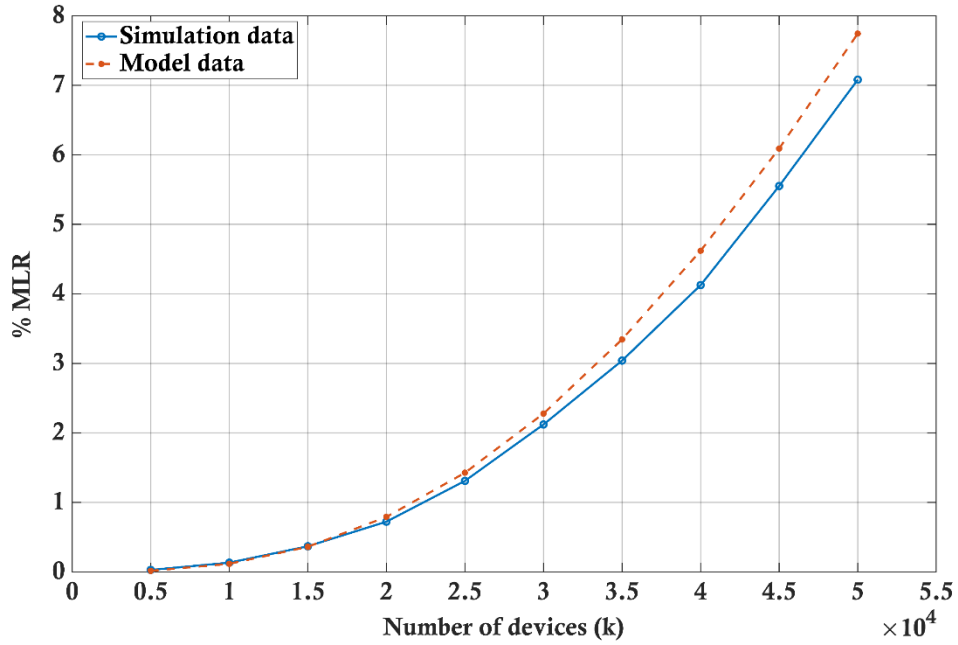

d) T = 15 min, NRMSE = 0.047 and NSE = 0.980.

Figure 4.7: The simulated and modelled MLR with a varying number of connected devices *k* for Weightless-N with a single group and a single message copy, where *N* = 1200 and *m* = 1.

4.5.1.5 Variable Number of Channels

In this analysis, the multiple group scenario is implemented to evaluate the model accuracy using all utilised frequency bands by Weightless-N with different numbers of ultra-narrow band channels. Figure 4.8 shows the simulated and modelled final probability of lost messages with a varying number of connected devices employing different numbers of

channels. The analysis is also based on using three message copies (m = 3) for all groups. In the case of 1200 channels, NSE is 0.996 and in the case of using 1500 channels NSE is 0.997. Also, in the case of 2499 channels, NSE is 0.996 and in the case of using 3000 channels NSE is also 0.996. Also, NSE is 0.995 in the case of utilising 9990 channels and NSE is 0.999 when 15000 channels are used. Again, Figure 4.8 depicts that the model provides a precise description of the Weightless-N system performance in comparison to the simulation data for all the six bands.

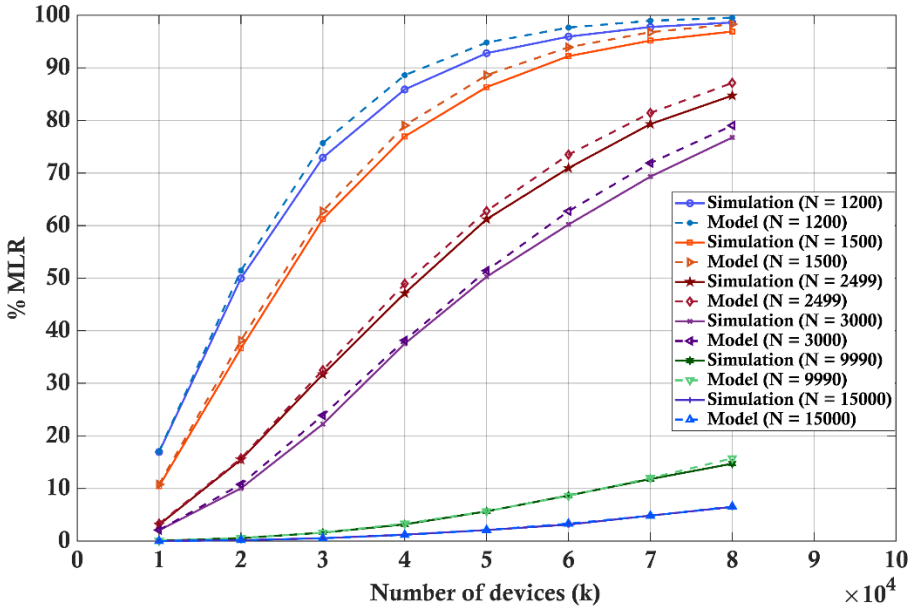

Figure 4.8: The simulated and modelled MLR with a varying number of connected devices *k* for Weightless-N with multiple groups and multiple numbers of channels, where *m* = 3.

4.5.2 Sigfox Technology

Sigfox utilises a total bandwidth of 192 kHz in the 868 band in Europe with 1920 UNB channels each with a bandwidth of 100 Hz and a bit rate of 100 bps. Sigfox also supports a payload of up to 12 bytes with a total packet size of 26 bytes ($\tau = 1.2s - 2.086s$). Moreover, Sigfox employs the multiple message copies approach with three message copies for each transmission. In addition, Sigfox limits the minimum transmission time by approximately a message every 10 minutes, where the maximum number of messages for each device is limited by a rate of 140 message per day (Sigfox, 2019a; Vejlgaard *et al.*, 2017; Nolan *et al.*, 2016; Sigfox, 2017b; Sigfox, 2017c; Sigfox, 2017a; Ofcom, 2014; Burns *et al.*, 2015).

The analysis presented in this section considers only the case of three message copies to evaluate the model accuracy. In the variable number of devices case, both the single group

and multiple groups are implemented while in the variable payload scenario only the single group is considered.

4.5.2.1 Variable Number of Devices

Figure 4.9(a) demonstrates the simulated and modelled MLR for the Sigfox technology with a varying number of connected devices and three message copies ($m = 3$). In this analysis, a single group scenario is implemented using a periodic transmission with $t_0 =$ 10 minutes and $PL = 12$ bytes.

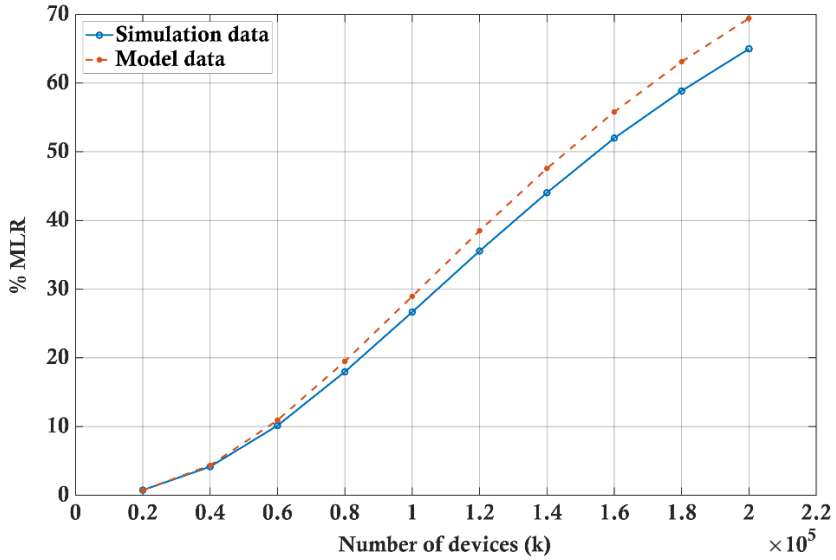

a) A single group with a periodic transmission, where $t_0 = 10$ min and $PL = 12$ bytes. NRMSE = 0.044 and NSE = 0.983.

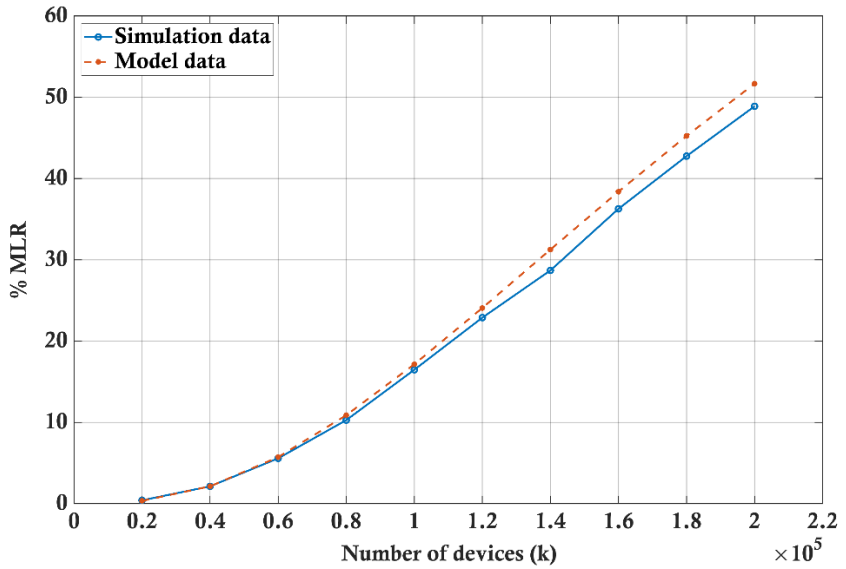

b) Multiple groups. NRMSE = 0.034 and NSE = 0.990

Figure 4.9: The simulated and modelled MLR with a varying number of connected devices *k* for Sigfox with a single group and multiple groups, where all groups have the same number of message copies in each analysis with *m* = 3.

Figure 4.9(b) shows the simulated and modelled MLR versus the number of connected devices with a multiple group scenario. All groups employ three message copies with different transmission characteristics, as shown in Table 4.3.

Table 4.3: Sigfox group general characteristics.

Group name	Percentage of total devices (%)	Transmission scheme	Transmission time (minutes)	Payload (Byte)
G1	40	Periodic	$t_0 = 10$	12
G2	20	Random	$t_1 = 10$ and $t_2 = 15$	10
G3	20	Periodic	$t_0 = 15$	8
G4	20	Random	$t_1 = 15$ and $t_2 = 20$	6

Like the case of Weightless-N technology, the analysis presented in this section shows that the mathematical model offers an accurate description for the collision problem in the Sigfox technology and provides close results to the simulation data using different scenarios and multiple message copies.

The analysis also depicts that the model accuracy is related to the number of connected devices k. As the number of devices increases the model accuracy declines and the difference between the simulation data and model data increases. However, it still provides a reasonable accuracy to describe the system performance with different transmission characteristics.

4.5.2.2 Variable Payload

Figure 4.10 illustrates the simulated and modelled probability of lost messages for the Sigfox technology with a varying payload size in bytes for different numbers of connected devices. The analysis was implemented using the single group scenario with three message copies and a periodic transmission of ($t_0 = 10$ minutes). In the case of using 50000 devices, NRMSE is 0.06 and NSE is 0.97 while in the case of using 100000 devices, NRMSE increases to 0.102 and NSE decreases to 0.911. Moreover, when 150000 devices are connected, NRMSE increases to 0.117 and NSE drops to 0.883. It is apparent from Figure 4.10 that the model provides close results to the simulation data for the whole range of used payload. Again, it is apparent from Figure 4.10 that the model accuracy is mainly dependent on the number of connected devices and as the number of devices increases the model accuracy decreases.

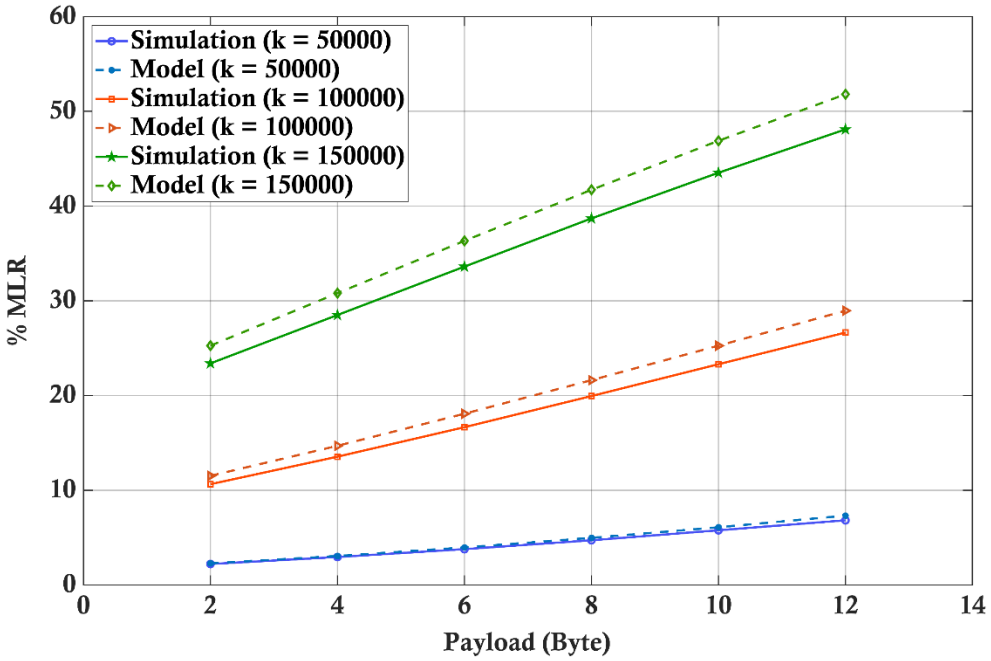

Figure 4.10: The simulated and modelled MLR with a varying payload *PL* for Sigfox with multiple numbers of devices, where $m = 3$ and $t_0 = 10$.

4.6 Model Accuracy

Using the model to evaluate the performance of two LPWAN technologies shows that it provides close results to the simulation data with high goodness of fit and minimum error metrics. On the other hand, the model accuracy varies according to the system characteristics, and it is mainly dependant on the transmission time and the number of connected devices. However, results depict that the model can still provide a precise evaluation for the practical LPWANs performance.

Figure 4.11 demonstrates the effects of transmission time T and the number of connected devices k on the model accuracy based on the Nash-Sutcliffe coefficient of efficiency (NSE). It is apparent from this figure that as T and k increase, the model accuracy decreases and the NSE gradually declines. However, it is evident from Figure 4.11 that the model still offers an acceptable range of error and can reasonably describe the LPWANs performance even with a massive number of devices and a wide range of transmission time. Furthermore, the model provides an accurate predicted data for the practical range of devices and transmission time where the probability of lost messages is within the range of ten per cent (10%).

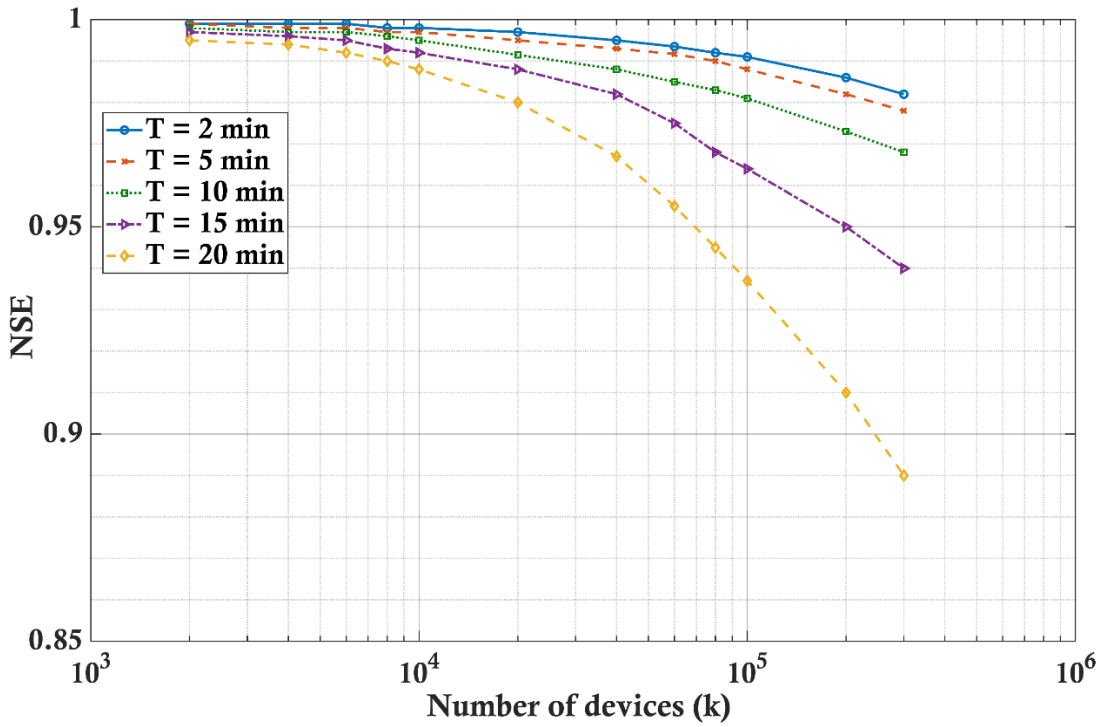

Figure 4.11: NSE versus the number of devices *k* for Weightless-N with a single group and various periodic transmission time, where N = 1200 and m = 3.

4.7 Summary

The mathematical model approach presented in this chapter proposes a novel and general model for the random time-frequency access utilised by LPWANs in terms of the probability of lost messages. It is also flexible and easy to implement for different systems and various working scenarios. The modelling is based on the Poisson distribution to model the time-frequency access and the Binomial distribution to calculate the final probability of lost messages with the multiple message copies approach. Results show that the model provides an excellent fit to the simulation data for different working scenarios. It also offers an advantageous understanding of LPAWNs performance with different applications and various transmission characteristics. In addition, the chapter presents a systematic analysis of practical applications focussing on various groups of devices that are connected to the same base station and employ different transmission times, payloads, and numbers of message copies.

Chapter 5

Evaluation of LPWANs Performance Using the URCST Algorithm

5.1 Introduction

With the broad range of applications used in the IoT and smart cities and the enormous number of devices that are expected to be connected to each base station, a comprehensive analysis in terms of packet collision is required to evaluate the performance of LPWA technologies that utilise the random time-frequency access protocol. Such analysis is a crucial step to be considered in the early stage of any wireless system design to ensure its reliability. However, due to the high cost and complexity of conducting such evaluation in real systems, especially with a massive number of connected devices, it is reasonable to perform the analysis by utilising simulation tools and mathematical modelling.

Having illustrated the new channel selection algorithm (URCST) and the modelling approach used to model the probability of lost messages in the two previous chapters, the performance of the LPWANs is evaluated by presenting analysis results of two candidate LPWA technologies, namely Weightless-N and Sigfox. The evaluation described in this chapter is based on analysing the system performance with respect to the power consumption and the message lost ratio (MLR) using the URCST algorithm with various working scenarios.

This chapter provides a systematic and thorough analysis of the LPWANs performance in terms of the MLR versus other system transmission parameters including the number of connected devices, the number of message copies, the payload in bytes, the transmission time, and the number of channels. Simulations of Weightless-N and Sigfox LPWAN technologies offer some important insights into the LPWANs performance. For example, increasing the number of message copies reduces the MLR but only up to a certain number of connected devices. After which, the redundancy in packet transmission is no longer beneficial.

The analysis presented in this chapter was conducted by utilising the MATLAB software to develop three simulation testbeds to evaluate the performance of the two nominated technologies, as presented in section 5.2. Other sections are organised as follows: section 5.3 presents the performance evaluation of the Weightless-N technology with a variable number of devices, message copies, payload, transmission time, and channels. In section

5.4, the performance of the Sigfox technology is evaluated using a variable number of devices, message copies, payload, and transmission time. Section 5.5 illustrates the power consumption in terminal devices for both technologies with the multiple message copies approach. In section 5.6, the performance of the two technologies is evaluated with a particular case of smart meters and a study of the optimum number of message copies for this application is presented. Finally, section 5.7 provides a summary of the LPWANs performance evaluation.

5.2 Simulation Testbeds

Studying and analysing the effect of packet collision on wireless communication in real systems is immensely complex since it is not only dependent on the number of connected devices, but it is also related to several other system characteristics like packet size and transmission time. Due to the high cost of connecting a massive number of devices and the high complexity of such systems, it is vital to use simulators to study and evaluate the effect of collisions on the system performance and reliability.

This section presents a general description of the simulation testbeds that were developed by the author during the research period and used to simulate the effect of the packet collision on the LPWANs performance utilising the Weightless-N and Sigfox technologies as a case study. Three different simulators were developed to imitate all parameters affecting the packet collision, namely URCST channel histogram simulator, URCST collision simulator, and URCST system modelling simulator. These simulators provide a comprehensive analysis environment for the packet collision problem in LPWANs and facilitate the study of the effect of other system's parameters on the probability of collision. Each simulator supports four groups of devices and offers the capability of changing different transmission characteristics for each group individually including the number of connected devices, the number of message copies, the number of macro-channels, the payload size, and the transmission scheme and time. Simulators also offer the functionality of using different channel selection algorithms and various bandwidths. They also facilitate saving a simulation result in different file formats like the MATLAB file format, Microsoft office, and various image formats.

5.2.1 URCST Channel Histogram Simulator

This simulator provides a detailed view of the channel histogram, including both macro-channels and micro-channels, in terms of the total number of transmissions, the total

number of collisions, and the total number of lost messages on each channel. It consists of five tabs each with different functionality, as shown in Figure 5.1.

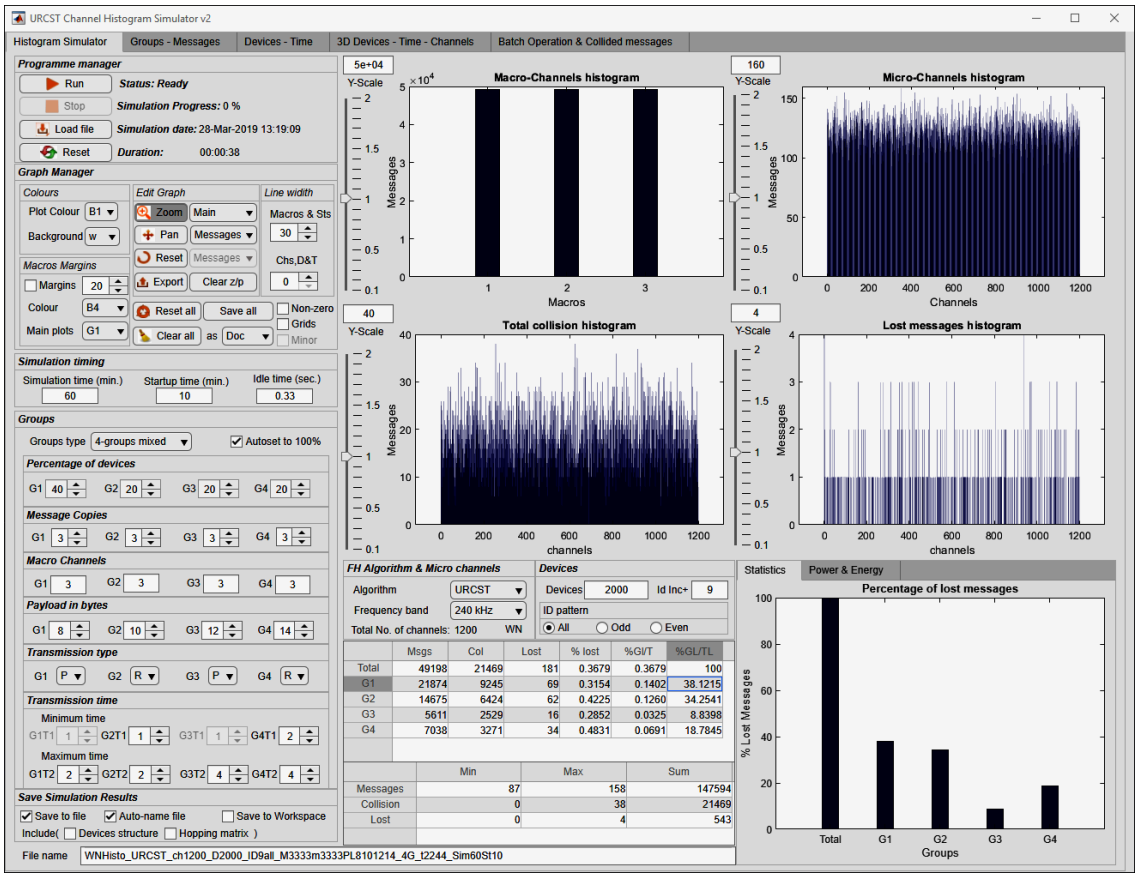

Figure 5.1: An example of the URCST Channel histogram simulator 1st tab (Histogram Simulator).

The first tab represents the main graphical user interface (GUI), which can be used to run the simulation and set all transmission parameters, as shown in Figure 5.1. It also offers a statistical overview for individual groups in addition to the average energy and power consumption of devices in each group. Moreover, analysis can be implemented as a single group or multiple groups.

Figure 5.2 illustrates an example of the second tab which provides the channel histogram of each group separately. In addition, it depicts the histogram of each discrete message copy for each group. This offers a detailed understanding of the collision problem in each group with specific transmission characteristics and offers fresh insights into the system behaviour with different application and the interference between these applications.

The third tap depicts the histogram of the total number of transmissions, the total number of collisions, and the number of lost messages on each channel versus both devices and running time, as demonstrated in Figure 5.3. This is useful to understand the uniformity of the message distribution over all channels for different devices and working periods.

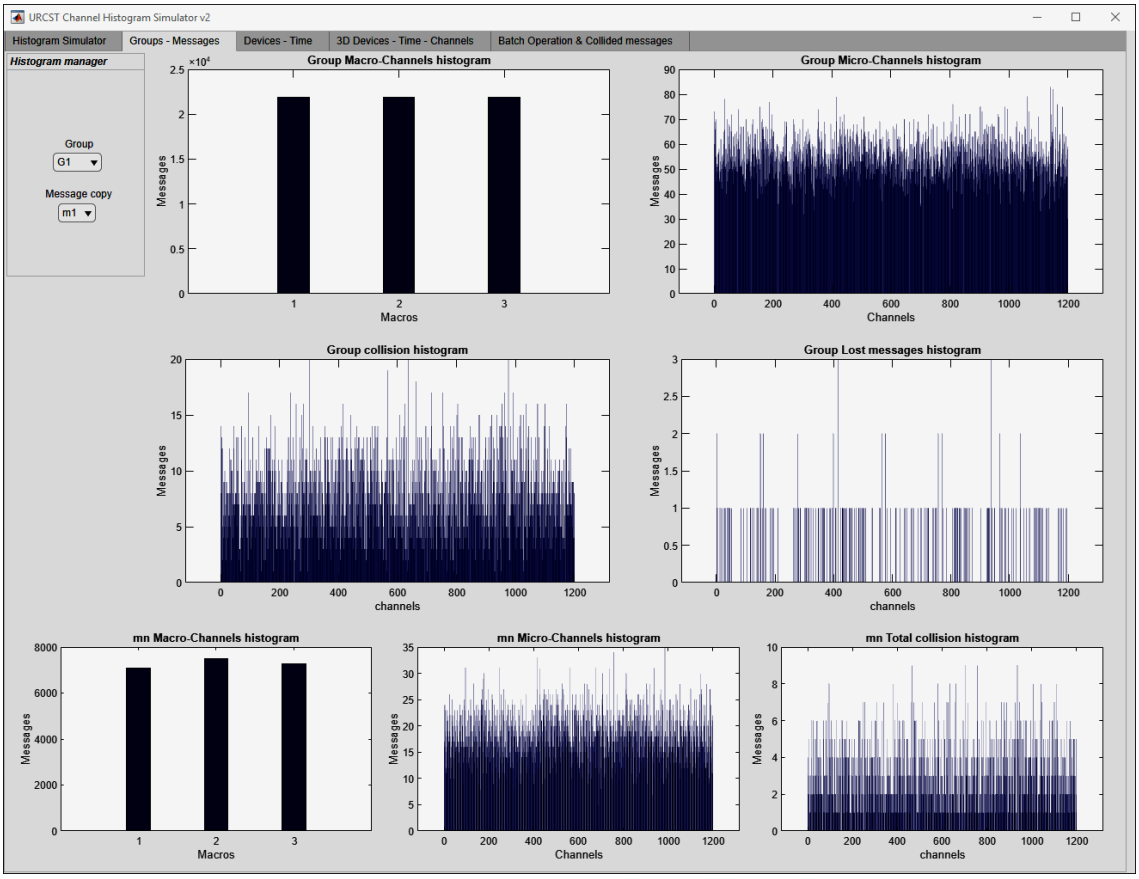

Figure 5.2: An example of the channel histogram simulator 2nd tab (Groups-Messages).

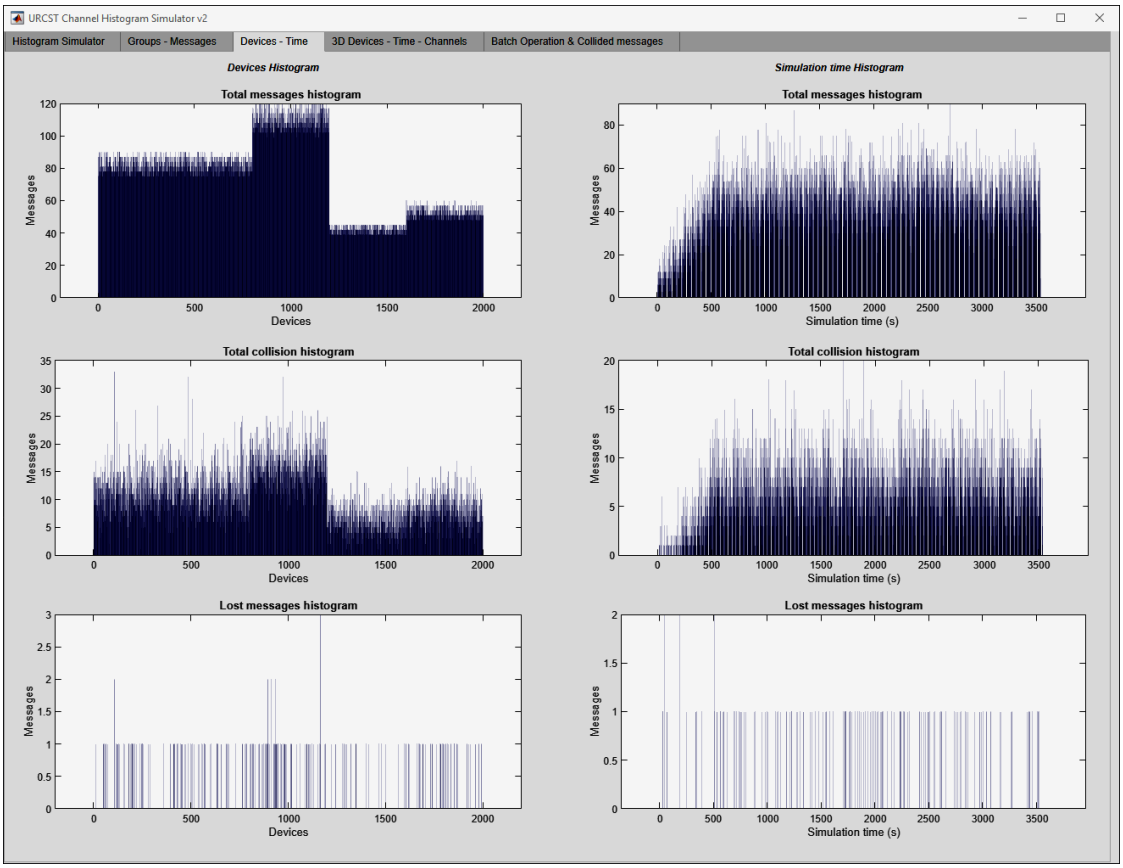

Figure 5.3: An example of the channel histogram simulator 3rd tab (Devices-Time).

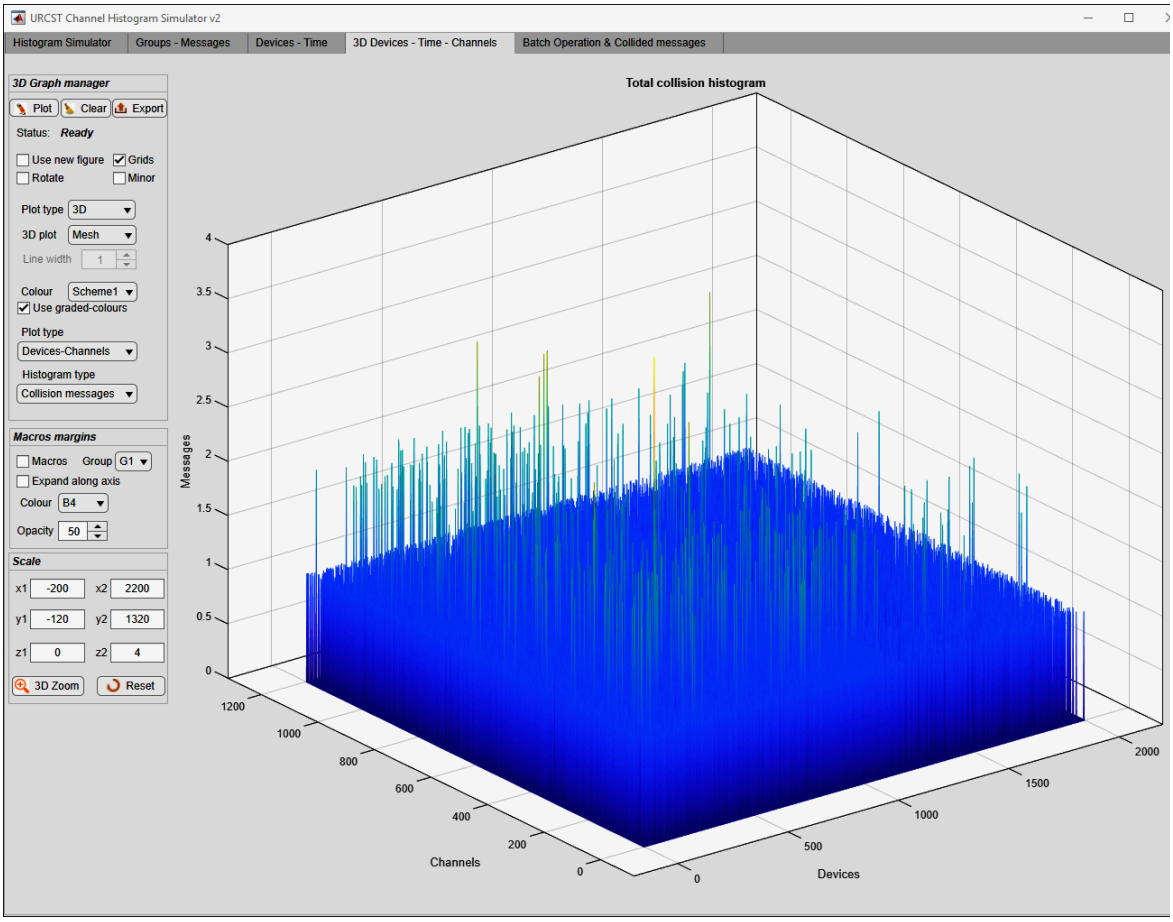

Figure 5.4: Channel histogram simulator 4th tab example (3D Devices-Time-Channels).

Figure 5.4 shows an example of the fourth tab which illustrates the 3D histogram graph for both devices and time. This offers a clear view of the distribution of transmissions, collisions, and lost messages over the whole bandwidth with different groups of devices and various transmission characteristics.

The fifth tab of the channel histogram simulator facilitates the understanding of collisions for individual packets, as shown in Figure 5.5. In this tab, each packet collision is illustrated in detail in both time and frequency domains. The simulator demonstrates the start and end time of each collided packet and shows the channel where the collision appears. Furthermore, it shows other packet information like the devices ID and the message copy number on which the collision happened. All packets' power is normalised and assumed with a unity amplitude.

This tab also offers another useful functionality by facilitating a batch simulation process. Using this function, several analyses can be conducted sequentially by providing a list of analysis information in a special text box.

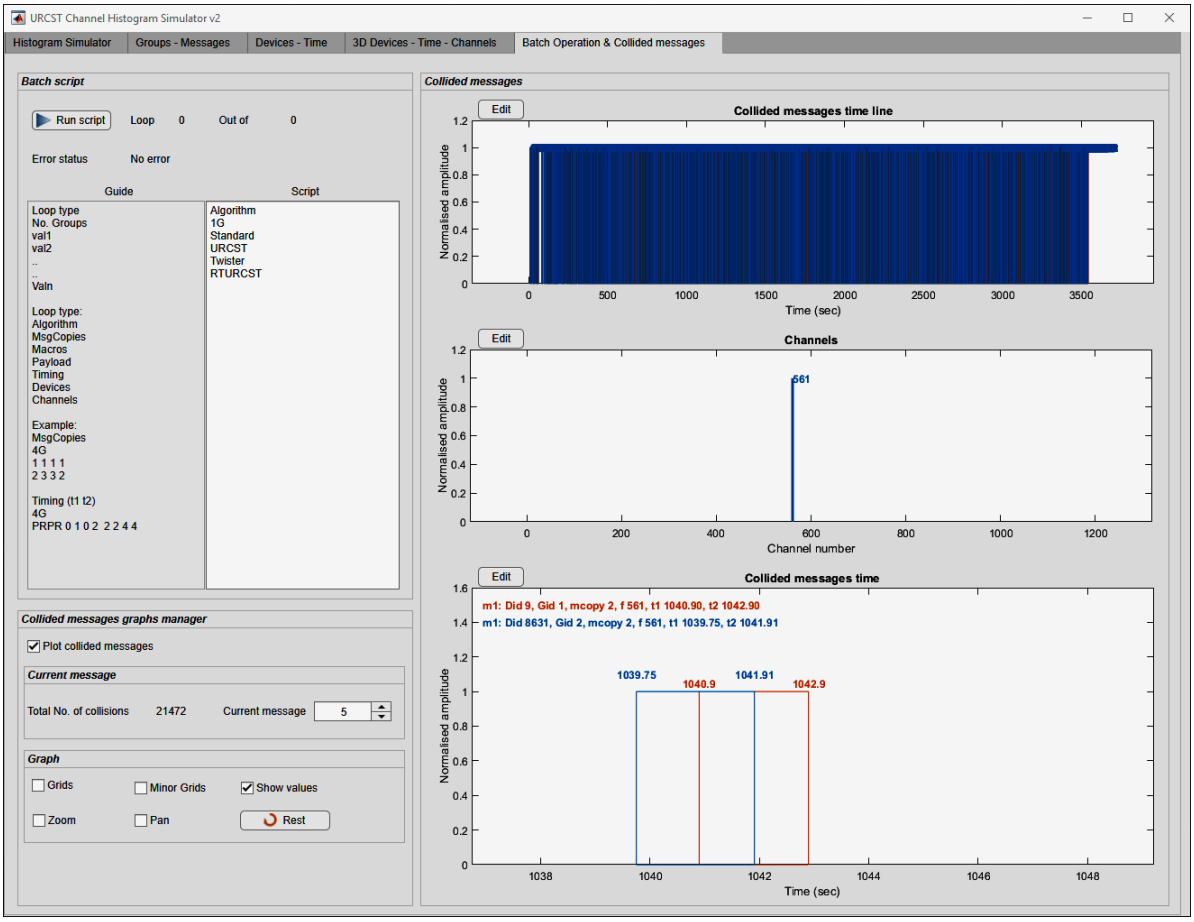

Figure 5.5: An example of the channel histogram simulator 5th tab (Batch Operation & Collided Messages).

5.2.2 URCST Collision Simulator

The URCST collision simulator provides an extensive testbed for random time-frequency access LPWANs in terms of the collision problem and the probability of lost messages. It offers a wide range of analysis methods that can be utilised to evaluate system performance using various transmission characteristics and working scenarios. The analysis provided by this simulator is based on finding the MLR with respect to varying other parameters including the number of connected devices, the number of message copies, the number of macros, the payload size, the transmission time, and the percentage of devices in each group. It also facilitates the use of different channel selection algorithms, bandwidths, devices IDs, and idle time. In addition, it offers the capability of analysing the system as either a single group or multiple groups. In multiple group scenario, all variable parameters can be set to a single group, individual groups, or all groups. Furthermore, the parallel processing toolbox of MATLAB was utilised to improve simulator capabilities and shorten the simulation time.

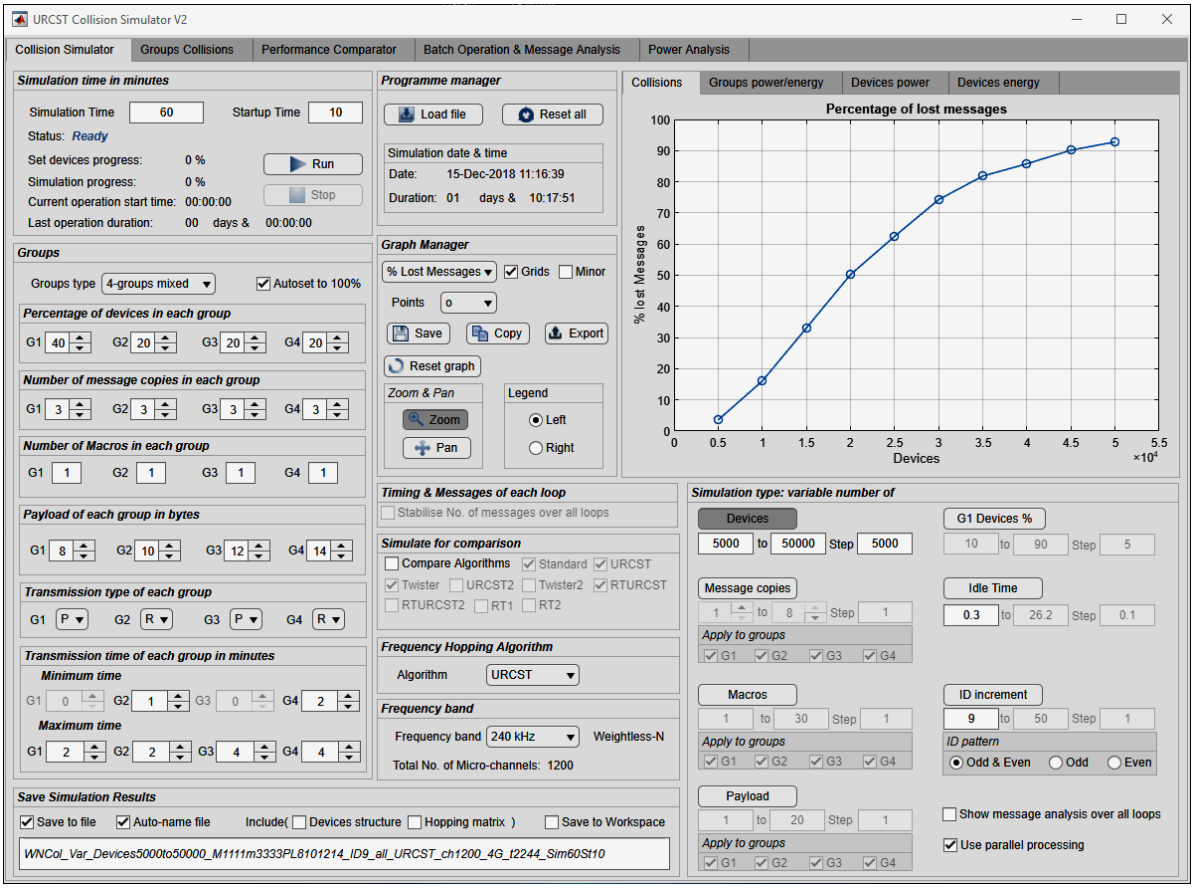

Figure 5.6: An example of the collision simulator 1st tab (Collision Simulator).

This simulator consists of five tabs each with different functionality, as shown in Figure 5.6. The first tab represents the main GUI, which can be used to set all transmission characteristics and depicts the MLR versus other variable parameters. It offers various types of simulations including the number of devices, the number of message copies, and the payload with full control over all analysis boundaries. Furthermore, multiple algorithms can be simulated simultaneously, provided that all other parameters are the same during the analysis, which provides a more reliable comparison. Moreover, the graph window can be set to illustrate the total number of messages, collisions, and lost messages. In addition, this tab provides detailed information about the average energy and power consumption of devices in each group.

This tab also facilitates the capability of implementing analysis on different working scenarios. For example, in the case of the multiple group scenario, the variable parameter can be applied either for all groups at the same time or for a part of the groups. This offers high flexibility to cover different applications and study the interference between these applications.

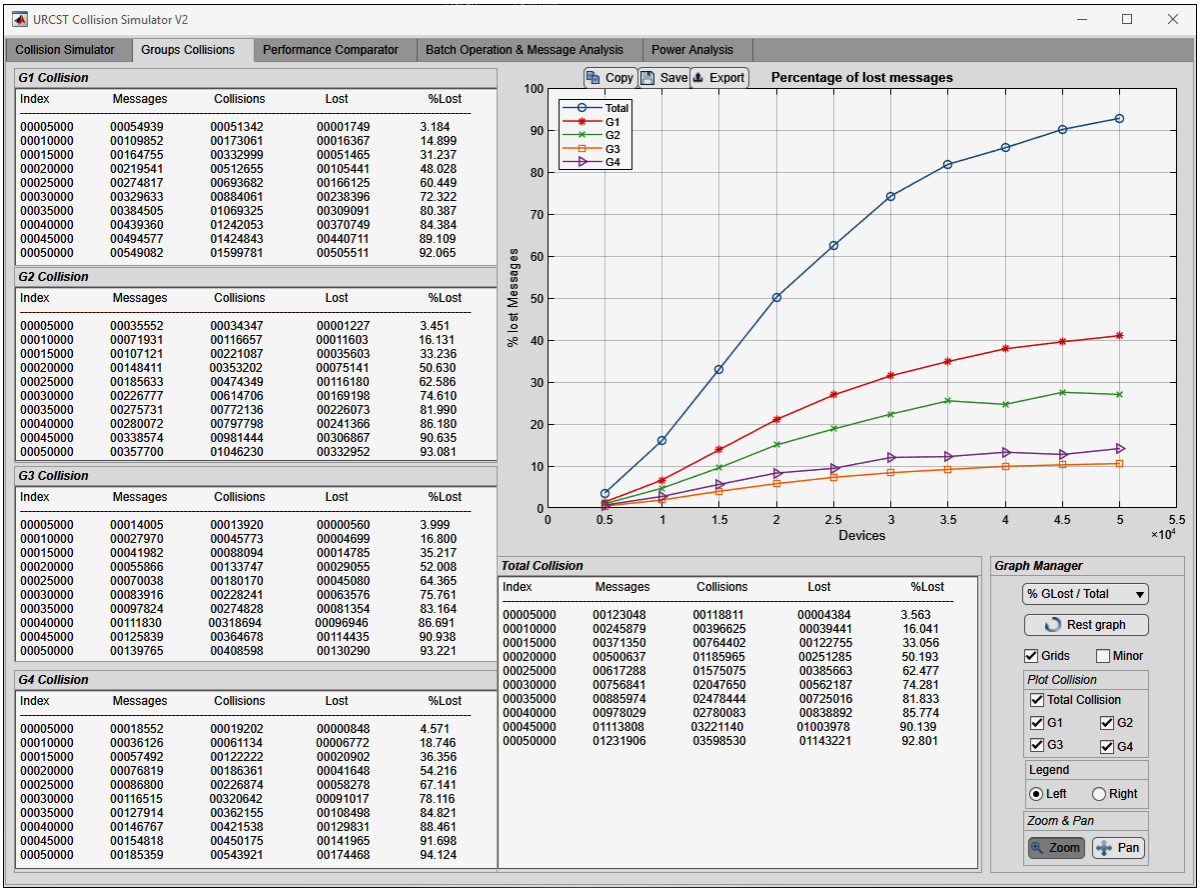

Figure 5.7: An example of the collision simulator 2nd tab (Groups Collisions).

Figure 5.7 shows the second tab which demonstrates the final MLR versus other parameters for the whole system and the MLR for individual groups. In addition, this tab offers detailed tabular values for each group, including the total number of messages, the total number of collisions, the total number of lost messages, and the MLR.

The third tab facilitates the comparison of system performance with different scenarios and various transmission parameters, as shown in Figure 5.8. It offers the capability of loading multiple analysis at the same time with full details of each analysis. It also provides a full control over the resultant graph by adding, deleting, hiding, and showing different analyses and the feature of managing the graph's theme.

The fourth tab of this simulator offers full details of all packets from all devices, as shown in Figure 5.9. All message copies of each message can be demonstrated on time and frequency domains based on the device ID and the transmission index. This facilitates a good understanding of the packet distribution over both domains. In addition, this tab offers the capability of the batch simulation, which can be used to conduct multiple simulations sequentially by providing a list of the required analysis in a special text box.

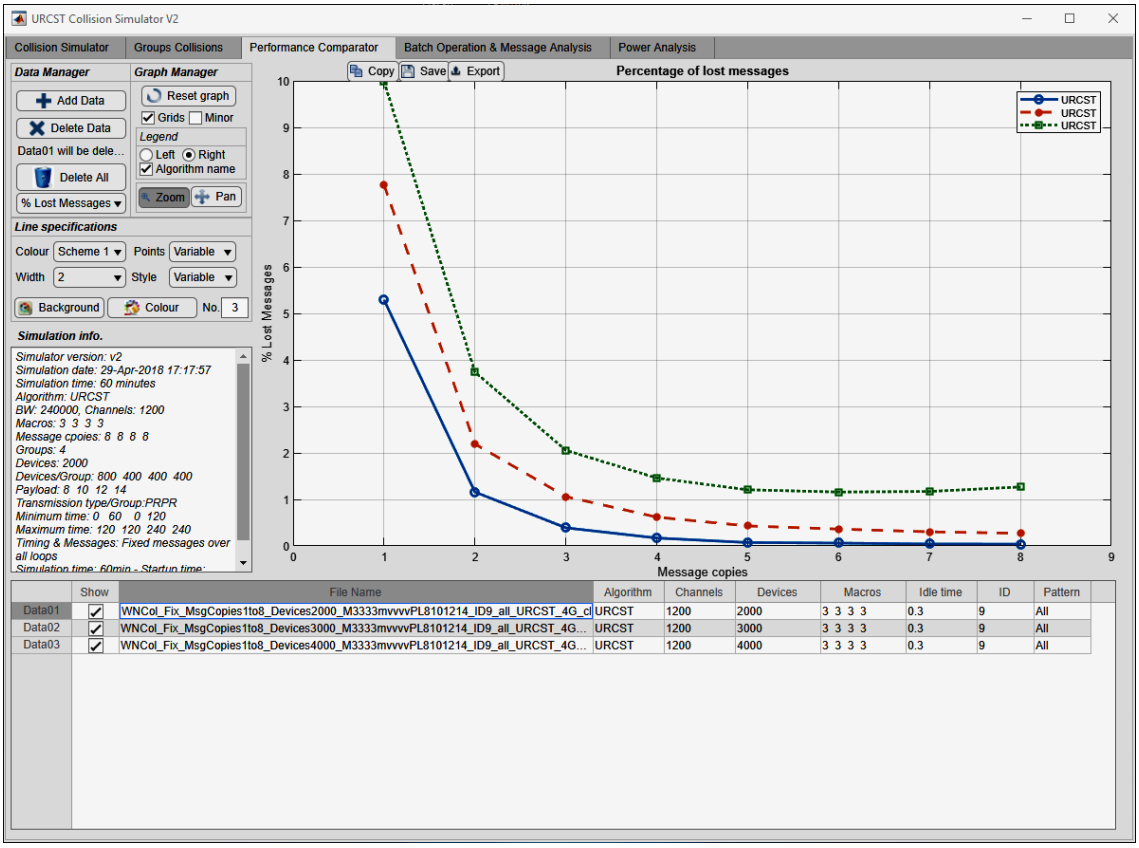

Figure 5.8: Collision simulator 3rd tab example (Performance Comparator).

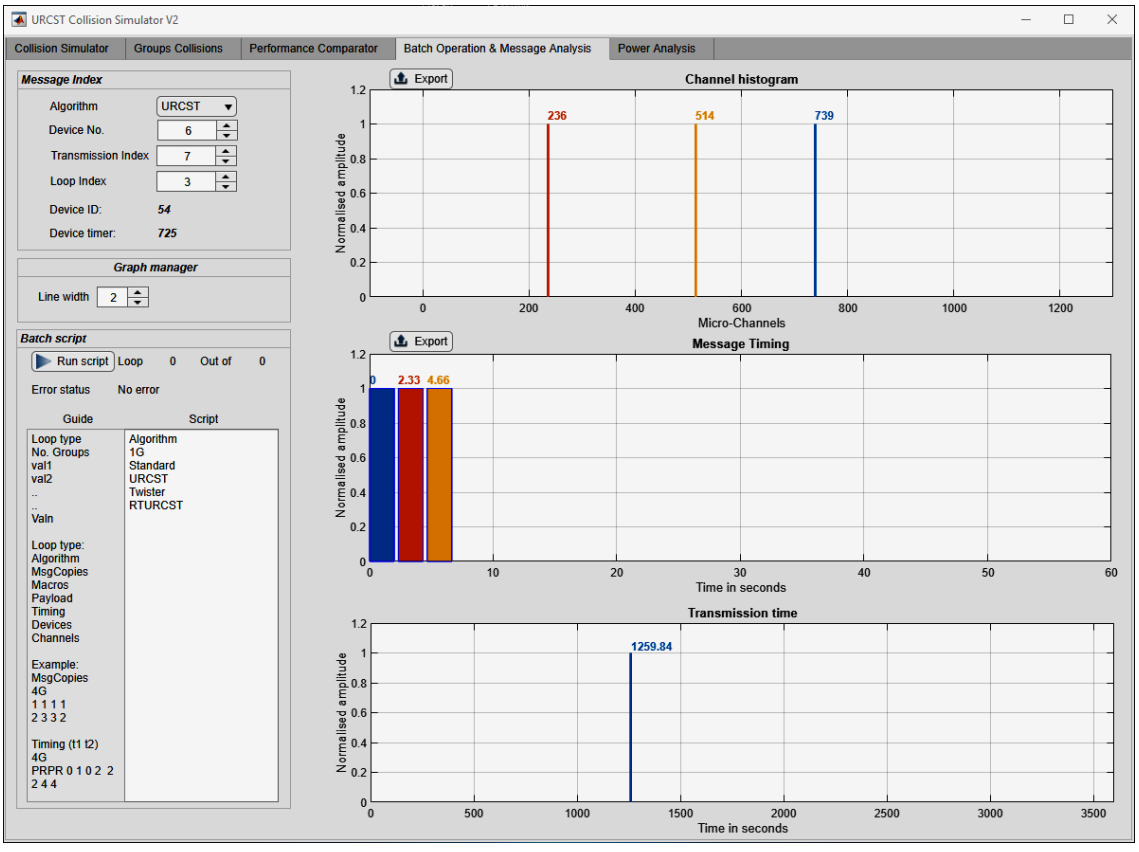

Figure 5.9: Collision simulator 4th tab example (Batch Operation & Message Analysis).

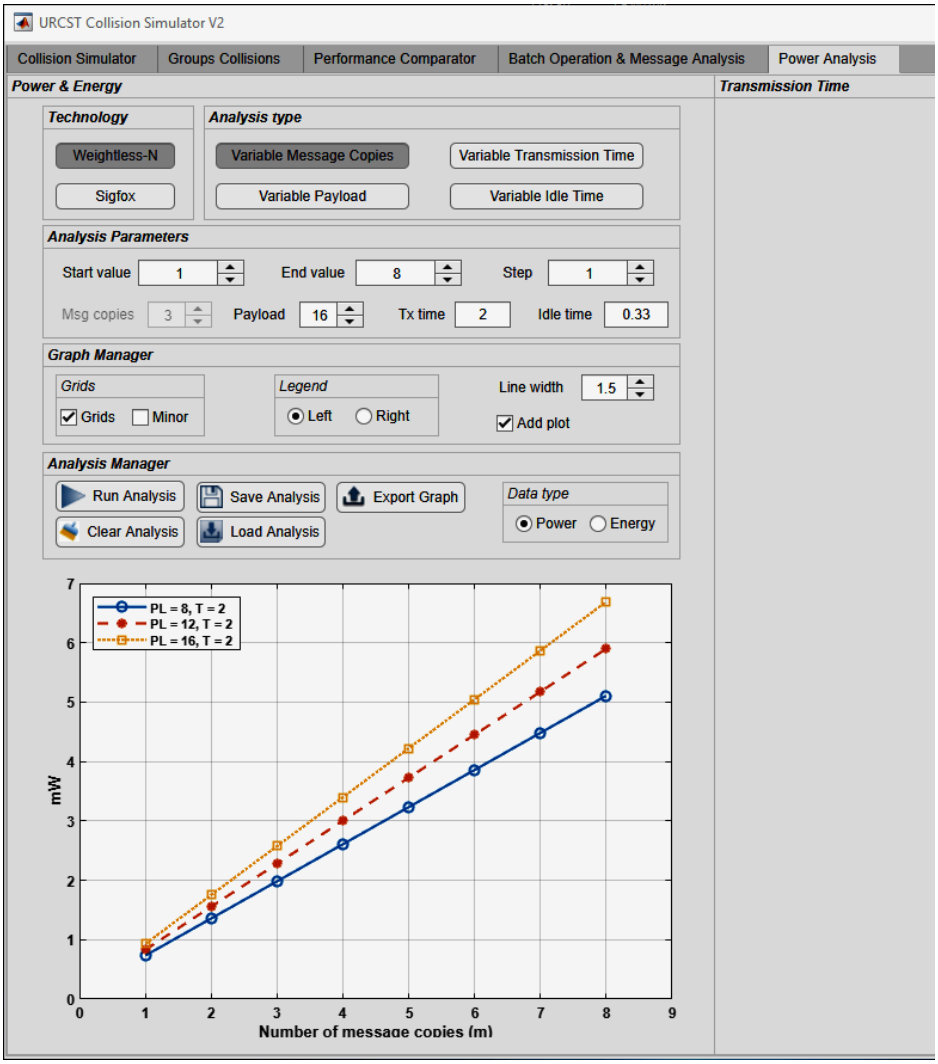

Figure 5.10: An example of the collision simulator 5th tab (Power Analysis).

Figure 5.10 shows the fifth tab which illustrates the analysis and calculations of the consumed energy and power by terminal devices when other transmission characteristics are varied. Analysis includes a variable number of message copies, payload, transmission time, and idle time for both technologies.

5.2.3 URCST System Modelling Simulator

This simulator was developed to evaluate the performance of LPWANs in terms of the MLR based on the mathematical model presented in Chapter 4. It consists of a comprehensive GUI that facilitate the implementation of different scenarios with various transmission characteristics, as illustrated in Figure 5.11. It also offers the capability of importing analysis conducted in the collision simulator described in section 5.2.2 and calculating the goodness of fit in comparison with the mathematical model results. Furthermore, it can be used to import multiple analysis and compare them together at the same time and provide a detailed description of the parameters used in each analysis.

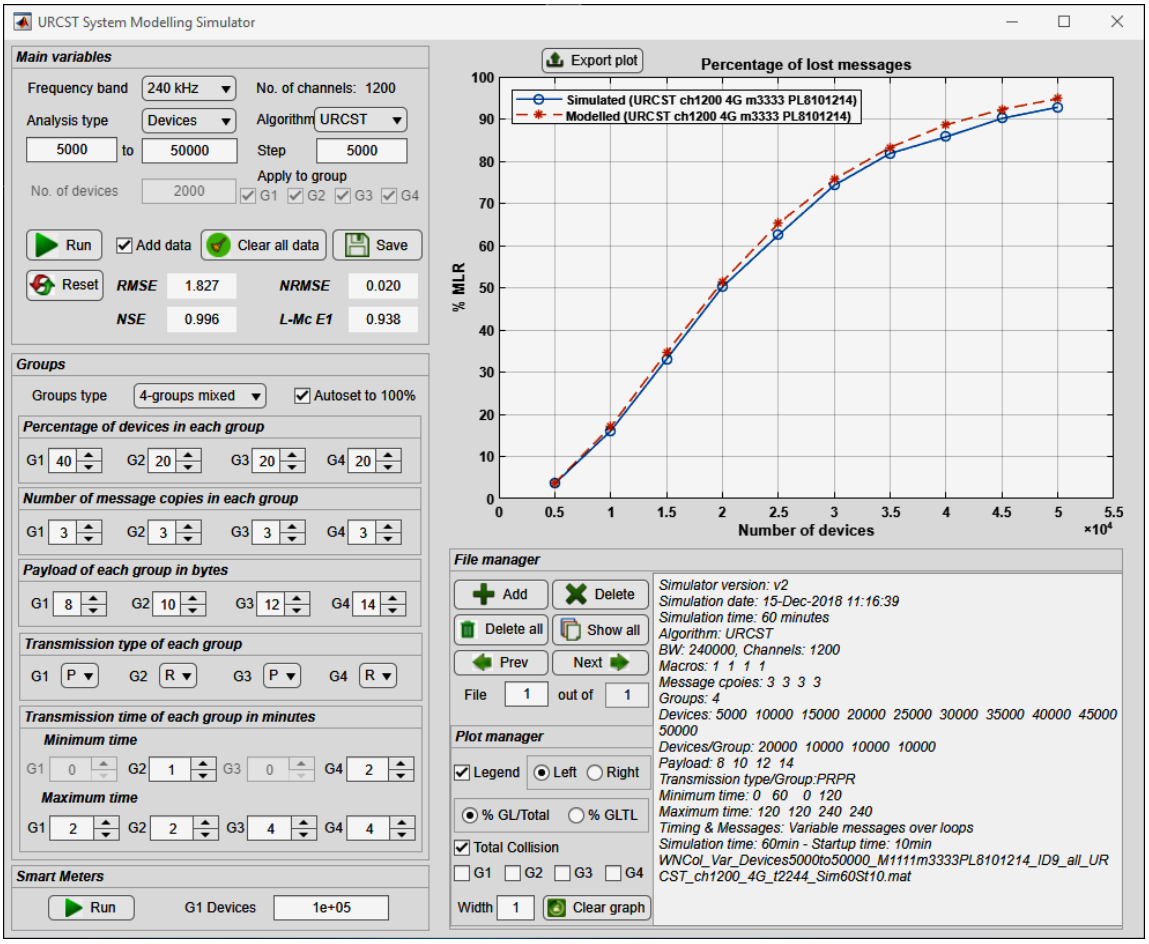

Figure 5.11: URCST system modelling simulator example.

Having proved in the previous chapter that the mathematical model offers a precise description of the LPAWNs performance in terms of the MLR, this simulator will be used in next sections to evaluate the performance of the two candidate LPWA technologies: Weightless-N and Sigfox.

5.3 Weightless-N Technology

Weightless-N employs the random time-frequency access protocol with six different numbers of UNB channels (see section 3.2 in Chapter 3 and section 4.5.1 in Chapter 4). The analysis presented in this section is based on the 1200 channels band, except for the case of multiple channel analysis. Various scenarios and transmission characteristics are implemented in this section to evaluate the performance of Weightless-N including a variable number of devices, a variable number of message copies, a variable payload, variable transmission time, and a variable number of channels. In some analysis, where a single group scenario is utilised, all connected devices have the same characteristics. Cases where devices exhibit different transmission characteristics, the total number of devices is divided into four groups to attain more realistic results. These groups are denoted by *G1*,

G2, *G3*, and *G4*, where *G1* represents 40 per cent of the total number of connected devices while each of the other groups represents 20 per cent. All notations used in this section are denoted in Table 5.1.

Table 5.1: Table of notations.

Symbol	Description
k	The total number of devices.
N	The total number of channels.
T	Average transmission time.
t_0	Transmission time for periodic transmission.
t_1	Minimum transmission time for random transmission.
t_2	Maximum transmission time for random transmission.
m	The number of message copies.
G1, G2, G3, and G4	Group's number.
PL	The message payload.

5.3.1 Variable Number of Devices

Figure 5.12 illustrates the effect of increasing the number of devices on system performance for three different scenarios: a single group with periodic data transmission, a single group with random data transmission, and multiple groups with various transmission schemes. In addition, three different numbers of message copies are utilised by each analysis to assess the effect of the multiple message copies method on the collisions with a variable number of devices. It is noticeable that using two or three message copies instead of one can significantly reduce the MLR, provided that the number of devices is fewer than a certain limit. For instance, Figure 5.12(a) shows the MLR versus the number of connected devices for a single group scenario with periodic transmission of four minutes. It depicts that using two message copies can significantly reduce the MLR, provided that the number of devices is fewer than 34000 devices. Similarly, using three message copies improves system performance in comparison with two message copies when the number of devices is fewer than 20000 devices. Exceeding this threshold increases the MLR and deteriorates the system performance. Moreover, using three message copies shows a higher MLR than using a single message copy with devices more than 27000 devices.

In Figure 5.12(b) a single group scenario is implemented where all devices send messages randomly between one and four minutes. Similarly, this figure shows that using multiple message copies can be beneficial when devices are less than certain thresholds.

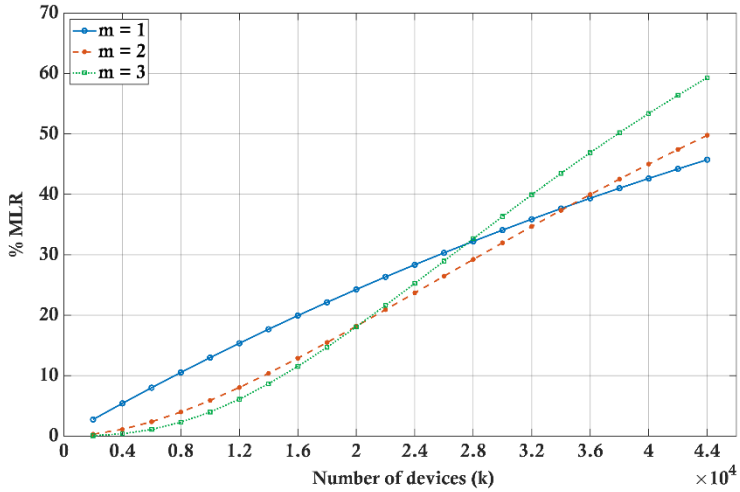

a) A single group with a periodic transmission, where $t_0 = 4$ min, $PL = 8$ bytes.

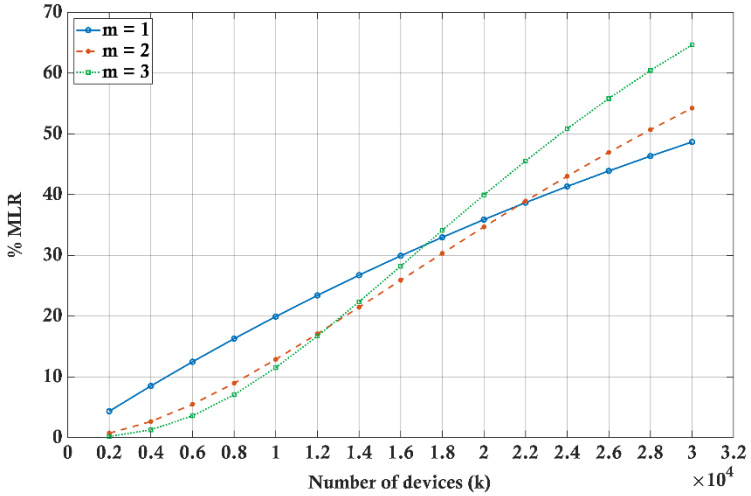

b) A single group with a random transmission, where $t_1 = 1$ min, $t_2 = 4$ min, $PL = 8$ bytes.

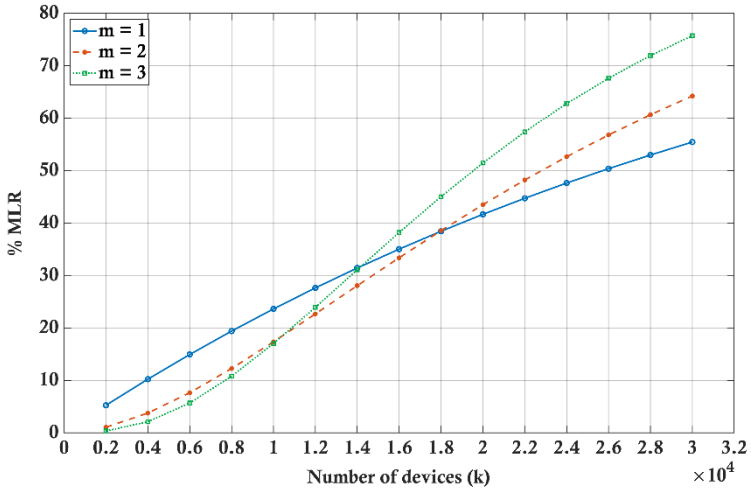

c) Multiple groups with:
G1: $t_0 = 2$ min, $PL = 8$ bytes; *G2*: $t_1 = 1$ min, $t_2 = 2$ min, $PL = 10$ bytes;
G3: $t_0 = 4$ min, $PL = 12$ bytes; *G4*: $t_1 = 2$ min, $t_2 = 4$ min, $PL = 14$ bytes.

Figure 5.12: The MLR with a varying number of connected devices *k* for Weightless-N with three different numbers of message copies, where *m* = 1, 2, 3.

Figure 5.12(c) illustrates the probability of lost messages versus the number of connected devices with the multiple group scenario where various transmission characteristics are used. Again, the analysis shows that using multiple message copies should be employed when the number of devices is fewer than specific limits. Otherwise it can have disadvantageous effects on system performance.

The results show that for a specific transmission time and packet size the maximum number of devices that can be connected to the system is related to the number of message copies and vice versa. Furthermore, increasing the number of message copies decreases the upper limit of connected devices that have a low MLR. This provides an important insight into the performance of LPWANs with the multiple message copies approach. Increasing the number of message copies could dramatically increase the collision and degrade system performance and reliability.

Figure 5.13(a) illustrates the consequences of increasing the number of message copies on the system performance using all the applicable range utilised by Weightless-N with the multiple group scenario. It is apparent from this figure that the upper limit of the connected devices, which can provide a lower MLR, declines as the number of message copies increases. For instance, using two message copies provides a higher MLR than using a single message copy if the connected devices are larger than 18000 devices while using three message copies poses a higher MLR than two message copies if devices exceed 10000 devices. Likewise, using four message copies worsens the system performance in comparison with three message copies when devices are more 8000 devices. Moreover, it is evident from Figure 5.13(a) that using multiple message copies can provide a higher MLR in comparison with a single message copy, provided that the number of devices is higher than a certain limit. As the number of message copies increases, this limit declines. For example, while this limit is 18000 devices for the two message copies, it becomes 14000 devices with three message copies and decreases to 12000 devices when using four message copies, and so on. Using eight message copies drops this limit down to less than 8000 devices with the group combination employed in this analysis.

Figure 5.13(b) focuses on the first part of the analysis where the higher number of message copies does not provide a higher MLR in comparison with the lower number of message copies. Using two message copies significantly reduces the MLR in comparison with a single message copy and using three message copies considerably declines the MLR in comparison with using two message copies.

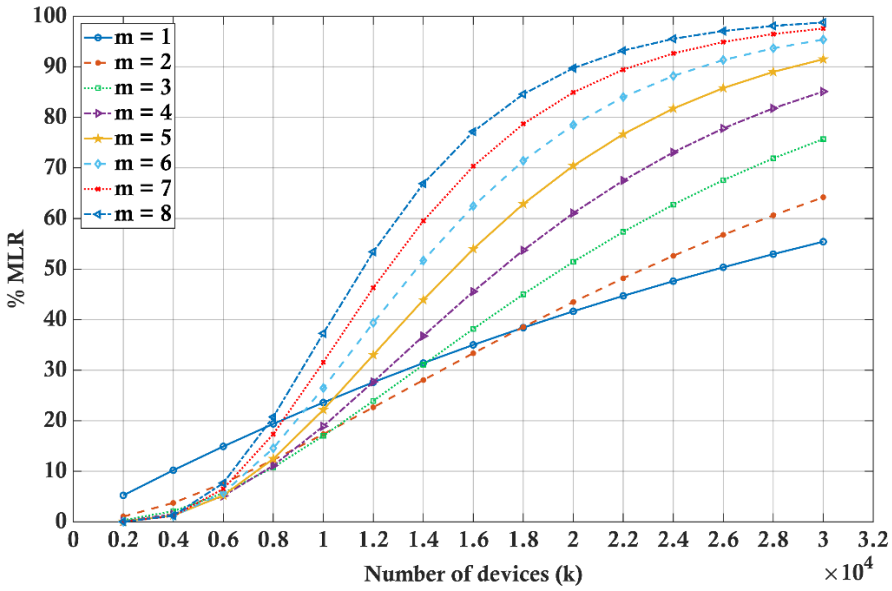

a) MLR versus k with a full range.

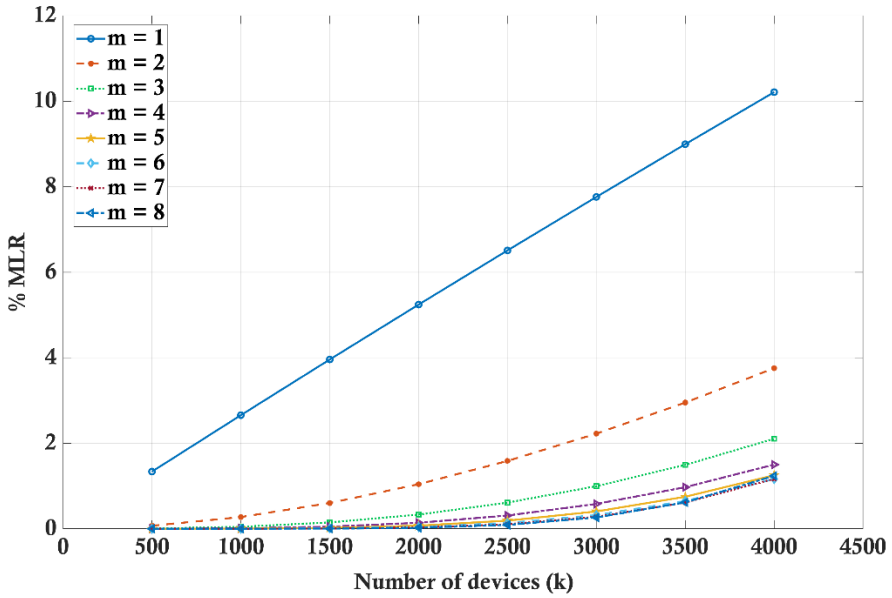

b) MLR versus k with a specific range.

Figure 5.13: The MLR with a varying number of connected devices k for Weightless-N with different numbers of message copies, where multiple groups are utilised with *G1*: t_0 = 2 min, *PL* = 8 bytes; *G2*: t_1 = 1 min, t_2 = 2 min, *PL* = 10 bytes; *G3*: t_0 = 4 min, *PL* = 12 bytes; *G4*: t_1 = 2 min, t_2 = 4 min, *PL* = 14 bytes; m = 1, 2, 3, …, 8.

It is clear from Figure 5.13(b) that using five and six message copies slightly improves system performance while employing seven or eight message copies has no effect on the MLR in comparison with six message copies. This offers another important insight into the performance of LPWANs that employ the multiple message copies approach, where increasing the number of message copies is not necessarily beneficial even with a limited number of connected devices.

5.3.2 Variable Number of Message Copies

In this section, the effect of using a variable number of message copies on the system performance is presented with specific numbers of connected devices. Figure 5.14 depicts the probability of lost messages versus the number of message copies for different numbers of connected devices. The analysis is based on the multiple group scenario where all devices from all groups have the same number of message copies with various transmission characteristics. It is apparent from Figure 5.14 that sending redundant messages increases the likelihood of their receipt when 3000 devices are connected. However, the system exhibits almost a flat MLR for (m = 5 to 7) for the case of 4500 devices and the MLR starts to rise for (m = 8). In such a case, using more than five message copies wastes valuable battery power without tangible improvement in the system performance. Moreover, with 6000 connected nodes, the system offers the best performance using four message copies. Increasing the number of message copies after this point drops the system performance and increases the MLR. On the other hand, when the connected devices are 7500 devices, the optimum number of message copies becomes three. This confirms that the relationship between the number of message copies and the message lost ratio is not independent of the number of connected nodes. Therefore, sending redundant messages will not necessarily guarantee a successful reception when the number of nodes gets bigger.

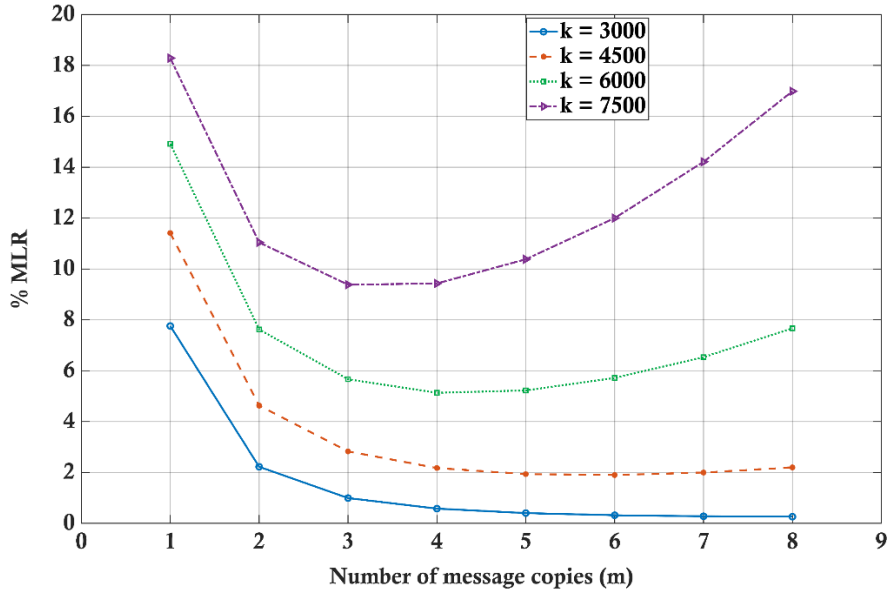

Figure 5.14: The MLR with a varying number of message copies m for Weightless-N with different numbers of devices, where multiple groups are utilised with *G1*: t_0 = 2 min, PL = 8 bytes; *G2*: t_1 = 1 min, t_2 = 2 min, PL = 10 bytes; *G3*: t_0 = 4 min, PL = 12 bytes; *G4*: t_1 = 2 min, t_2 = 4 min, PL = 14 bytes; k = 3000, 4500, 6000, and 7500.

Figure 5.15(a) and (b) show the effect of using a distinct number of message copies for different groups of devices with a total number of 4500 devices. In this particular scenario, some groups have a variable number of message copies while others use a constant number. As seen in Figure 5.15, increasing the number of message copies improves the overall system performance, stipulated that the number of message copies is less than a certain threshold.

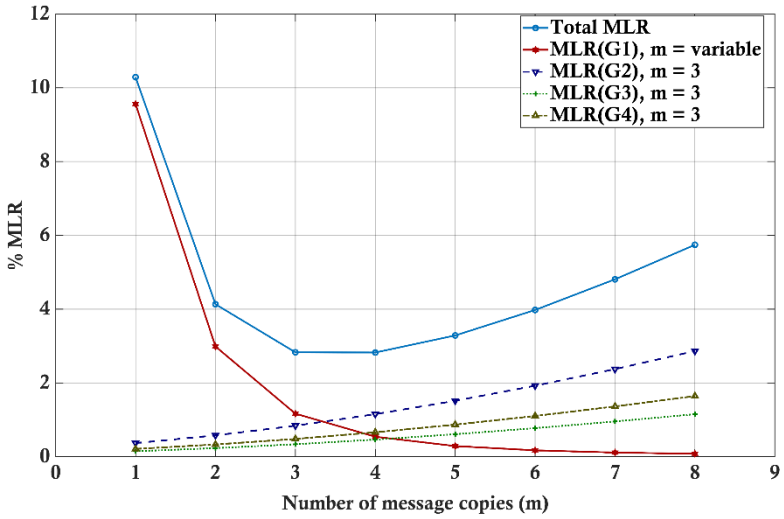

a) *G1*: variable message copies,
G2, G3, and *G4*: m = 3.

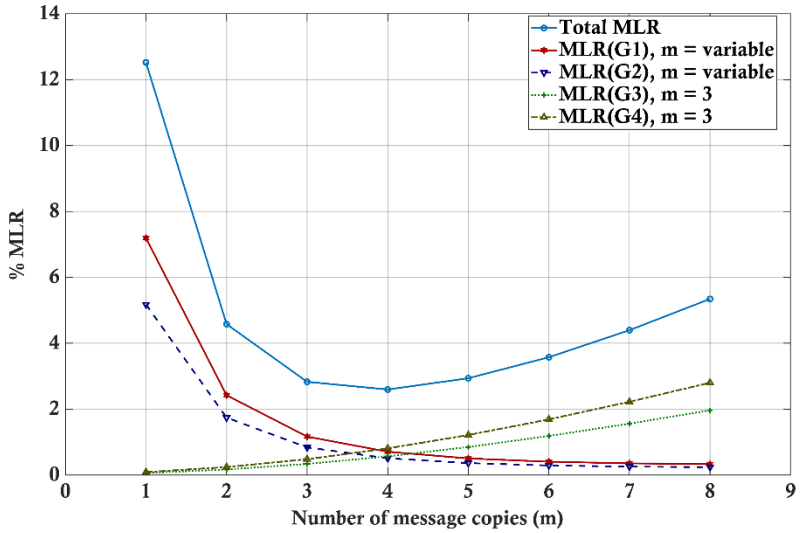

b) *G1* and *G2*: variable message copies,
G3 and *G4*: m = 3.

Figure 5.15: The MLR with a varying number of message copies m for Weightless-N with various groups of devices that employ different numbers of message copies, where multiple groups are utilised with *G1*: t_0 = 2 min, *PL* = 8 bytes; *G2*: t_1 = 1 min, t_2 = 2 min, *PL* = 10 bytes; *G3*: t_0 = 4 min, *PL* = 12 bytes; *G4*: t_1 = 2 min, t_2 = 4 min, *PL* = 14 bytes; k = 4500.

Increasing the number of message copies in a part of the groups decreases the MLR for these specific groups as expected. On the other hand, the probability of message collision of the other groups, which use a constant number of message copies rises. Consequently, the overall system performance changes depending on how crowded the channel is. From Figure 5.15, the final probability of lost messages increases after a specific number of message copies which depends on all groups' characteristics. This point represents the optimum number of message copies that can provide the best performance for the current system. For instance, Figure 5.15(a) shows that the optimum number of copies that should be used for *G1* is three. In contrast, Figure 5.15(b) depicts that using four message copies for both *G1* and *G2* offers the minimum MLR and the best system performance in this specific case.

This draws attention to another important feature of the system design and implementation. In the case of various applications that involve different numbers of message copies, selecting an optimum number of message copies for each application is a key factor that should be considered in the design phase in order to reduce the power consumption while retaining a good quality of service. In general, selecting the number of message copies for some applications is a trade-off between the required QoS and the impact on other devices that are connected to the same base station.

5.3.3 Variable Payload

Figure 5.16(a) shows the probability of lost messages versus the payload in bytes for different numbers of message copies and a total number of 3000 devices employing the multiple group scenario. All devices in all groups have the same payload on each analysis. It is reasonable to assume that the larger the packet size, the higher the probability of collision. However, employing the multiple message copies approach significantly improves system performance and reduces the MLR for up to five message copies in this case. Using more than five message copies is not beneficial since the system exhibit almost the same performance from five up to eight message copies.

On the other hand, when 6000 devices are connected, system performance considerably improved with up to three message copies, as demonstrated in Figure 5.16(b). Using four message copies slightly enhances the system performance, provided that the payload is less than 16 bytes. Similarly, using five message copies enhances system performance to some extent in comparison with four message copies when the payload is below 8 bytes. Exceeding these limits increases the MLR and degrades the system performance.

Moreover, using five message copies shows a higher MLR than using two message copy with payloads more than 18 bytes. More importantly, with eight message copies, the system poses a higher MLR in comparison with using four message copies when the payload is larger than three bytes. Furthermore, it presents a higher MLR in comparison with even a single message copy if the payload is 18 bytes or more.

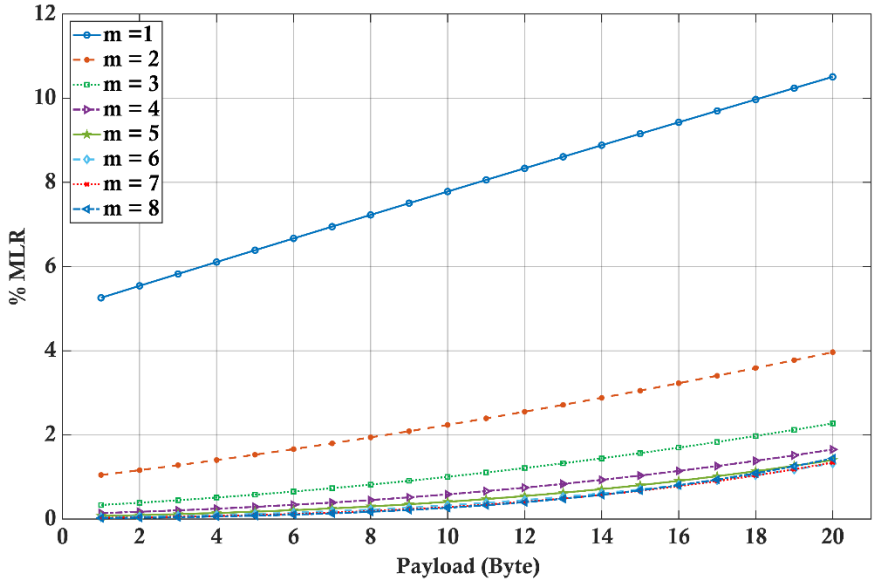

a) k = 3000 devices.

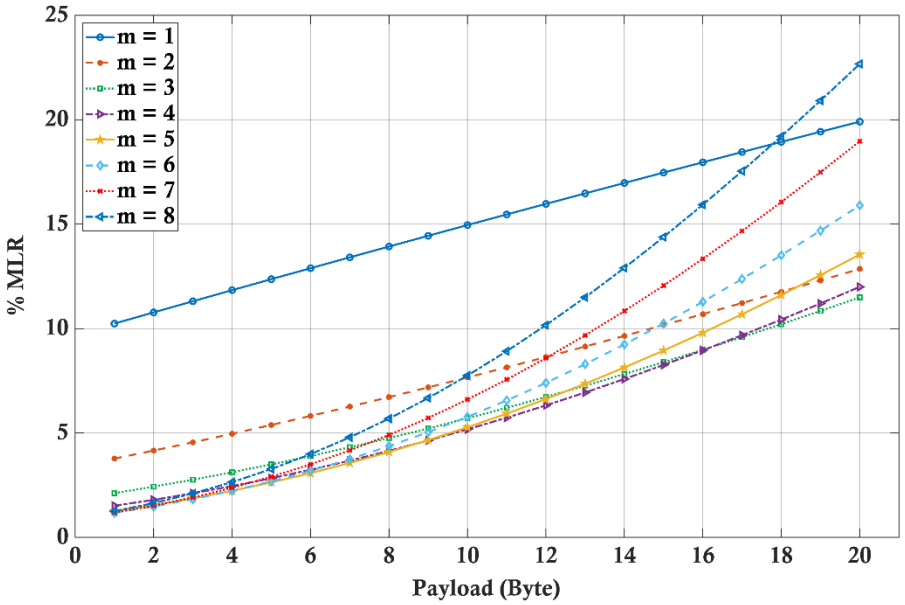

b) k = 6000 devices.

Figure 5.16: The MLR as a function of the payload in bytes for Weightless-N with different numbers of message copies, where multiple groups are utilised with *G1*: t_0 = 2 min; *G2*: t_1 = 1 min, t_2 = 2 min; *G3*: t_0 = 4 min; *G4*: t_1 = 2 min, t_2 = 4 min; m = 1, 2, 3, …, 8.

It is evident from Figure 5.16(b) that the MLR increases as message copies are incremented with respect to the packet size if the number of connected devices exceeds a certain limit. Consequently, using a higher number of message copies might provide a higher MLR in comparison with the lower number of message copies for specific payloads as in the case of using more than three message copies.

Figure 5.17 depicts the effect of using different payloads on the system performance with a variable number of message copies using multiple group scenario with 4500 connected devices, where all groups have the same payload. It is clear from Figure 5.17 that the larger the payload, the higher the probability of obtaining higher MLR as the number of message copies increases. For example, using a payload of four bytes shows that the system performance improves as the number of message copies increases while the system offers almost a flat MLR for (m = 6 to 8) for the case of a payload of eight bytes. In comparison, the system presents the lowest MLR at five message copies when the payload is 12 bytes, and the MLR starts to rise where m is larger than five. In contrast, using four message copies represents the optimum value that should be used in this system for a payload of 16 to 20 bytes. Again, this emphasises the importance of the selection of groups' specifications in relation to the number of message copies and connected devices.

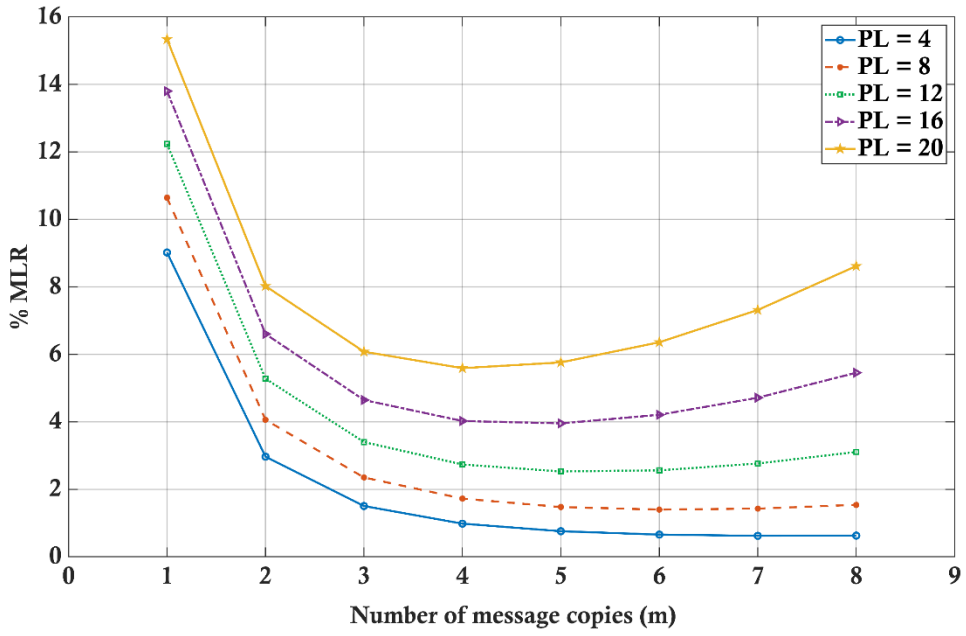

Figure 5.17: The MLR with a varying number of message copies m for Weightless-N with different payloads PL in bytes, where multiple groups are utilised with $G1$: t_0 = 2 min; $G2$: t_1 = 1 min, t_2 = 2 min; $G3$: t_0 = 4 min; $G4$: t_1 = 2 min, t_2 = 4 min; k = 4500 and PL = 4, 8, 12, 16, and 20 bytes.

5.3.4 Variable Transmission Time

This section presents the effect of transmission time (T) on the probability of collision and system performance. All simulations are based on a single group scenario where all devices have the same transmission time and other transmission characteristics. Figure 5.18 demonstrates the MLR versus the number of connected devices with different values of transmission time using three message copies and a payload of eight bytes. It is reasonable to assume that the larger the transmission time, the lower the probability of collision. However, it is apparent from Figure 5.18 that the transmission time has a substantial impact on the system performance in terms of collisions. As the transmission time declines, the MLR starts dramatically increasing versus the number of connected devices. For instance, with a transmission time of (T = 4 minutes), the MLR slightly escalates in comparison with (T = 5 minutes). In contrast, with (T = 1 minute), the system exhibits an extreme increment in the MLR compared to using transmission time of two minutes.

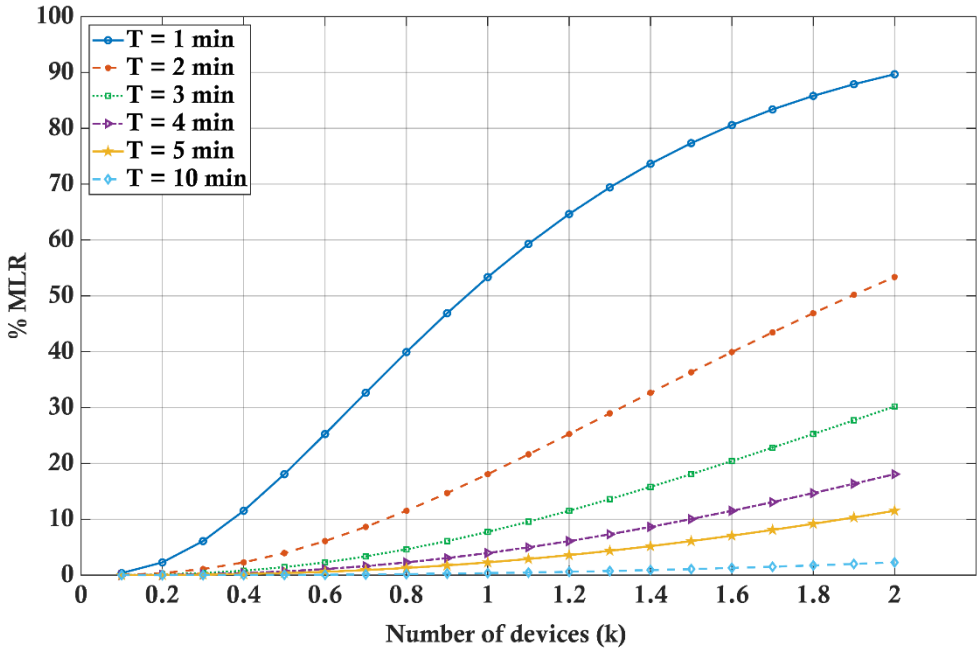

Figure 5.18: The MLR with a varying number of devices *k* for Weightless-N with different transmission time *T*, where a single group is utilised with a periodic transmission and *m* = 3, *PL* = 8 bytes, and *T* = 1, 2, 3, 4, 5, and 10 minutes.

Figure 5.19 depicts the effect of using variable transmission time on the system performance and the MLR using different payloads and 12000 devices. It is clear from this figure that using a short transmission time has a significant effect on system performance.

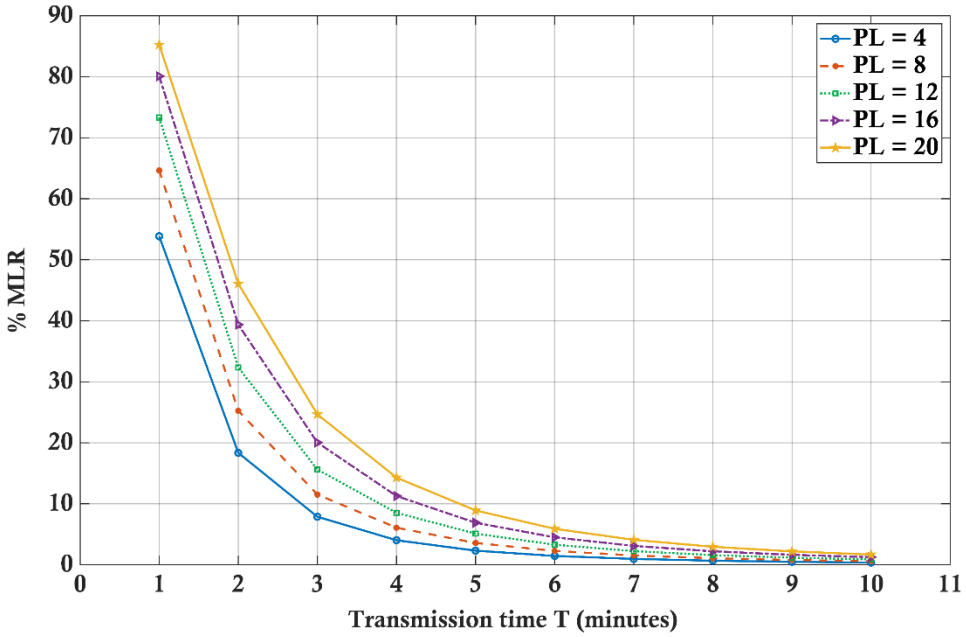

Figure 5.19: The MLR with varying transmission time *T* for Weightless-N with different payloads in bytes, where a single group is utilised with a periodic transmission and *m* = 3, *k* = 12000, *PL* = 4, 8, 12, 16, and 20 bytes.

It is also evident from Figure 5.19 that the MLR increases as the payload is incremented with respect to the transmission time. As the payload increases, the increment in the MLR is enlarged with different transmission times.

Figure 5.20 illustrates the effect of using a variable number of message copies on the MLR with different values of transmission time. The figure shows the MLR versus the number of message copies using different values of transmission times with 6000 devices and a payload of 16 bytes.

By increasing the transmission time of five minutes and above, the probability of collision generally drops with multiple message copies sent. However, as the transmission time dropped to four minutes (T = 4 min), the system offers a flat MLR for (m = 6 to 8). On the other hand, as for a short transmission time of three minutes, the MLR starts to rise for six message copies or above. In this case, the system provides the best performance with five message copies. Likewise, the system offers the lowest MLR at three message copies when the transmission time is reduced to two minutes (T = 2 min). Using a higher number of message copies significantly increases the MLR as shown in Figure 5.20. It is also important to highlight that these optimum points are related to other system parameters like the payload and the number of connected devices.

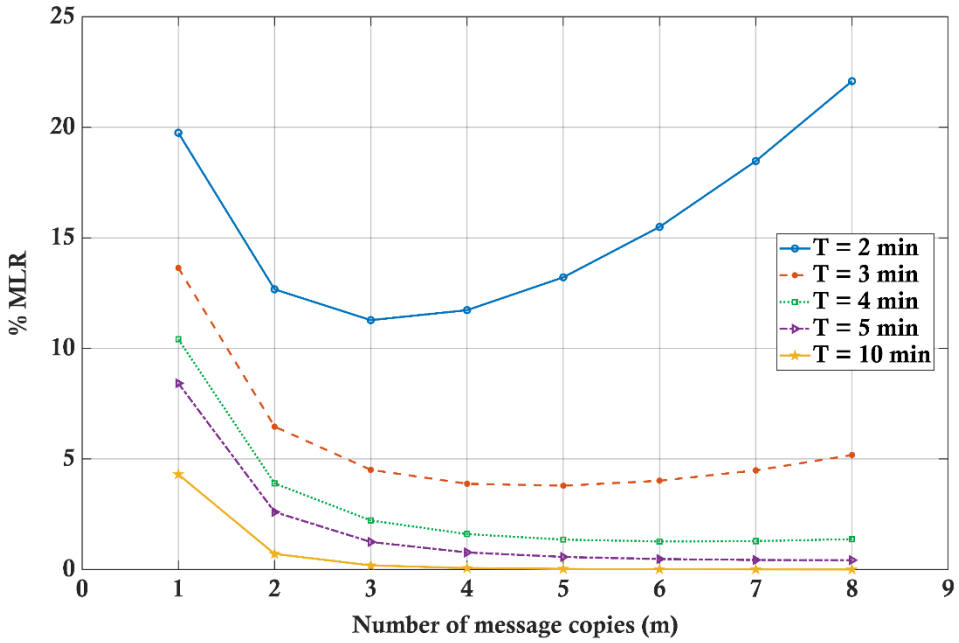

Figure 5.20: The MLR with a varying number of message copies *m* for Weightless-N with variable transmission time, where a single group is utilise with a periodic transmission and *k* = 6000, *PL* = 16 bytes, and *T* = 2, 3, 4, 5, and 10 minutes.

5.3.5 Variable Number of Channels

It is sensible that increasing the total number of utilised channels reduces the probability of collision and improves system performance. This depends on the base station bandwidth and the bandwidth used by the UNB channel to send data from terminal devices. Weightless-N utilises six different bands with 1200, 1500, 2499, 3000, 9990, and 15000 channels.

Figure 5.21 shows the MLR versus the number of connected devices for all the available bands using three message copies (m = 3). The multiple group scenario is implemented in this section to evaluate the system performance where devices utilise various transmission characteristics with the same number of channels on each analysis. It is evident from Figure 5.21 that changing the employed band has a significant impact on the system performance with respect to the number of connected devices. For example, using bands with (N = 9990) or (N = 15000) channels significantly reduces the MLR in comparison with the two bands of (N = 1200) and (N = 1500) channels. This emphasises the importance of the selection of the appropriate band in relation to the number of connected devices and the intended QoS for different applications. Using some bands might not be the best option for some applications such as smart meters, where a considerably high number of devices are required to be connected to each base station.

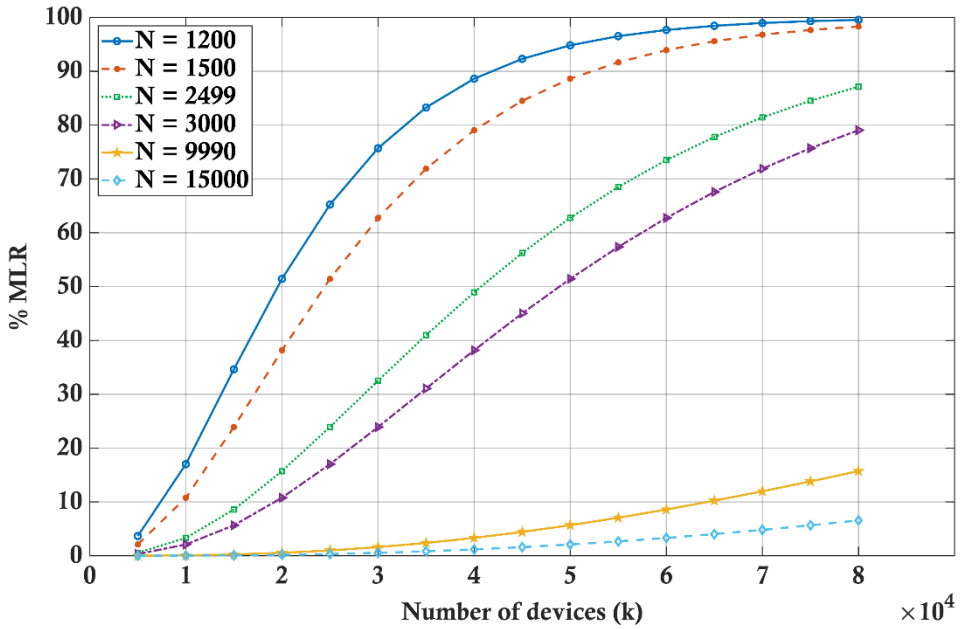

Figure 5.21: The MLR with a varying number of devices *k* for Weightless-N with different numbers of channels, where multiple groups are utilised with *G1*: t_0 = 2 min, *PL* = 8 bytes; *G2*: t_1 = 1 min, t_2 = 2 min, *PL* = 10 bytes; *G3*: t_0 = 4 min, *PL* = 12 bytes; *G4*: t_1 = 2 min, t_2 = 4 min, *PL* = 14 bytes; *m* = 3 and *N* = 1200, 1500, 2499, 3000, 9990, and 15000 channels.

5.4 Sigfox Technology

Sigfox utilises 1920 UNB channels each with 100 Hz bandwidth and supports a payload of up to 12 bytes with a bit rate of 100 bps (see section 4.5.3 in Chapter 4). It also employs the multiple message copies approach with three message copies. In addition, Sigfox limits the number of messages for each device by a maximum rate of 140 messages per day, or approximately a message every 10 minutes.

Various scenarios and transmission characteristics are implemented in this section to evaluate the performance of Sigfox including a variable number of devices, a variable number of message copies, a variable payload, and variable transmission time. Although Sigfox restricts the number of message copies to three, the analysis presented in this section considers a single, two, and three message copies to evaluate the effect of using multiple message copies on the system performance. In the case of multiple groups, the analysis is based on the four groups scenario that is implemented with the Weightless-N technology in section 5.3. All notations used in this section are denoted in Table 5.1.

5.4.1 Variable Number of Devices

This section presents the effect of increasing the number of connected devices on the Sigfox system performance and evaluate the impact of using multiple message copies on the MLR. Figure 5.22 shows the MLR versus the number of connected devices for the Sigfox technology with three scenarios: a single group with a periodic transmission, a single group with a random transmission, and multiple groups with various transmission characteristics. Also, to assess the consequences of using the multiple message copies method on the system performance, three different numbers of message copies are utilised where (m = 1, m = 2, and m = 3). Given that the number of devices is fewer than a certain threshold, using two or three message copies significantly reduces the MLR in comparison with the use of a single message copy

Figure 5.22(a) illustrates the MLR versus the number of connected devices for a single group scenario with periodic transmission of ten minutes (T = 10 min) and a payload of eight bytes. It is apparent from this figure that using two message copies can considerably decrease the MLR, provided that the number of devices is fewer than 160000 devices. Likewise, using three message copies improves system performance in comparison with two message copies when the number of devices is fewer than 90000 devices. Exceeding this threshold increases the MLR and worsens the system performance. Moreover, when the connected devices are more than 125000 devices, the system offers a higher MLR with three message copies in comparison with a single message copy.

Similarly, when a single group scenario is applied with random transmission, where all devices send messages between 10 and 20 minutes, using multiple message copies is advantageous to the system performance if the connected devices are less than certain thresholds. As demonstrated in Figure 5.22(b), the system offers a higher MLR with two message copies than a single message copy when the devices are larger than 235000 devices. Also, using three message copies provides a higher MLR in comparison with two message copies if the connected devices exceed 140000 devices.

Comparably, Figure 5.22(c) illustrates the probability of lost messages versus the number of connected devices with multiple groups. It depicts that using multiple message copies should be employed when the number of devices is fewer than specific limits. Exceeding these limits considerably raises the MLR.

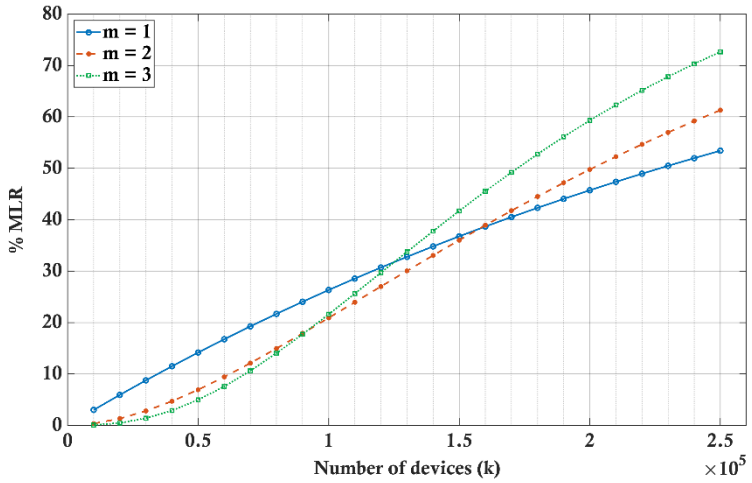

a) A single group with a periodic transmission, where $t_0 = 10$ min, $PL = 8$ bytes.

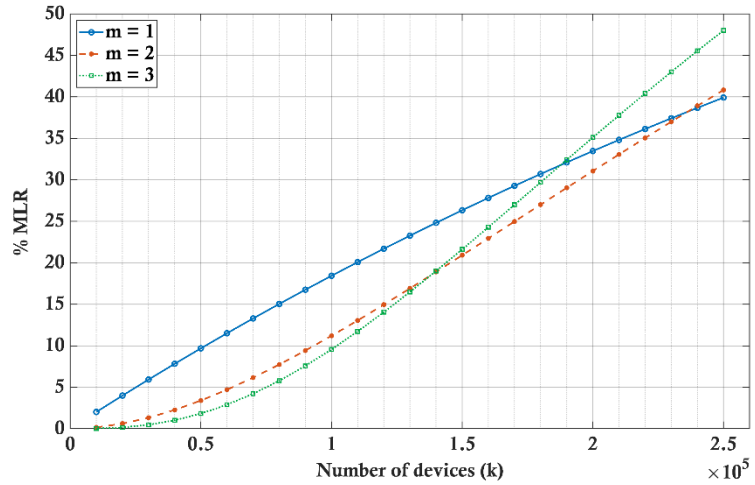

b) A single group with a random transmission, where $t_1 = 10$ min, $t_2 = 20$ min, $PL = 8$ bytes.

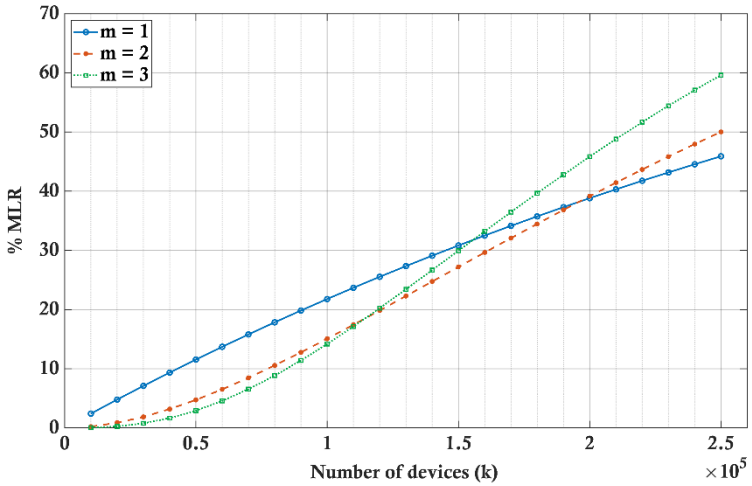

c) Multiple groups with:
G1: $t_0 = 10$ min, $PL = 6$ bytes; *G2*: $t_1 = 10$ min, $t_2 = 15$ min, $PL = 8$ bytes;
G3: $t_0 = 15$ min, $PL = 10$ bytes; *G4*: $t_1 = 15$ min, $t_2 = 20$ min, $PL = 12$ bytes.

Figure 5.22: The MLR with a varying number of connected devices *k* for Sigfox with three different numbers of message copies, where *m* = 1, 2, 3.

5.4.2 Variable Number of Message Copies

Figure 5.23 illustrates the effect of using a variable number of message copies on the probability of lost messages using different numbers of connected devices. The analysis presented in the section is based on the single group scenario where all devices have the same number of message copies and the same transmission characteristics. The minimum transmission time is employed in this analysis with (T = 10 minutes) and a payload of 12 bytes. It is evident from Figure 5.23 that sending redundant messages increases the probability of their receipt when 60000 devices are connected. On the other hand, the system provides almost a flat MLR with two and three message copies for the case of 80000 devices. In comparison, with 100000 connected devices, the system offers the lowest MLR using two message copies. Increasing the number of message copies after this point drops the system performance and increases the MLR. More importantly, if the connected devices are 1400000 devices or more, the system exhibits the minimum MLR with a single message copy. In such a case, using multiple message copies is not beneficial for the system. This confirms that sending redundant messages will not necessarily guarantee a successful reception when the number of nodes is high.

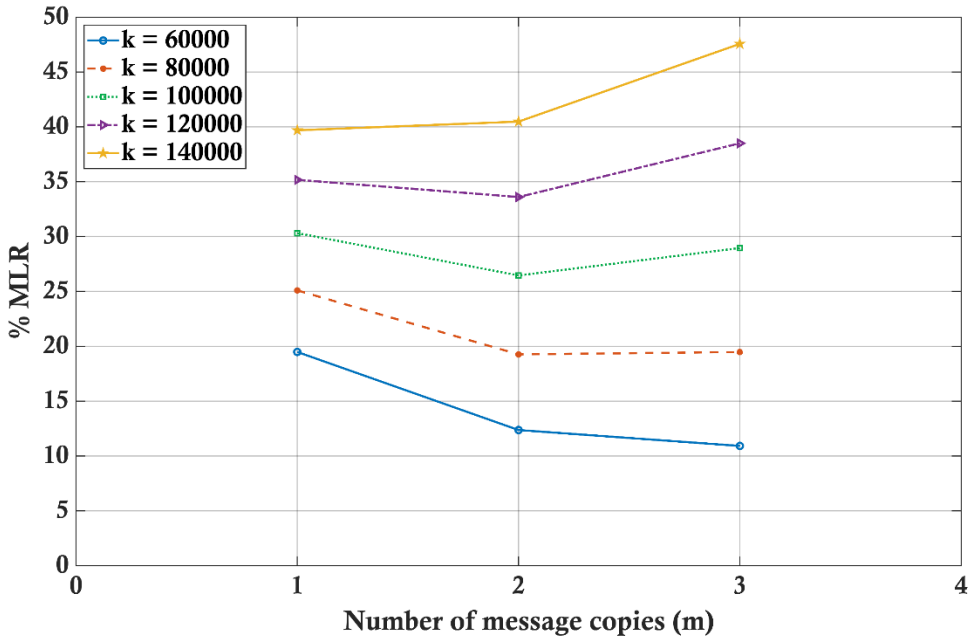

Figure 5.23: The MLR with a varying number of message copies *m* for Sigfox with different numbers of devices, where a single group is utilised with a periodic transmission and T = 10 minutes, PL = 12 bytes, and k = 60000, 80000, 100000, and 120000.

5.4.3 Variable Payload

This section focuses on the effect of using a variable payload on the Sigfox system performance and evaluate the advantage of employing the multiple message copies method. Figure 5.24 shows the probability of lost messages versus the payload in bytes for different numbers of message copies using different numbers of connected devices. The analysis is based on the single group scenario with (T = 10 minutes). Figure 5.24(a) demonstrates the MLR versus the payload in bytes with 60000 devices and three different message copies (m = 1, 2, and 3). It makes sense that increasing the packet size increases the probability of collision. However, employing the multiple message copies approach significantly improves system performance and reduces the MLR for both two and three message copies in this case.

When the connected devices are increased to 100000, the system offers a lower MLR using three message copies in comparison with two message copies only if the payload is less than six bytes, as illustrated in Figure 5.24(b). Moreover, Figure 5.24(b) depicts that as the number of message copies increases, the rate of the MLR is projected to rise sharply with respect to the payload size.

On the other hand, when 120000 devices are connected, system performance is moderately improved with two message copies in comparison to a single message copy, provided that the payload is less than 11 bytes, as shown in Figure 5.24(c). Furthermore, employing three message copies does not improve the system performance in comparison with two message copies even with a payload of one byte. Using a payload of three bytes or more deteriorates the system performance and provides a higher MLR than using two message copies. Moreover, when three message copies are employed, the rate of the MLR escalates, and the system offers a higher MLR than using a single message copy with a payload larger than five bytes. Again, this emphasises the awareness of the selection of the groups' specifications and characteristics limitations.

These results further support the fact that utilising the multiple message copies approach does not necessarily have a beneficial effect on the probability of lost messages and can have an adverse impact on the system performance depending on other transmission characteristics. As these characteristics change, using the redundancy of sent messages can have a contrary impact on the system performance and increases the MLR.

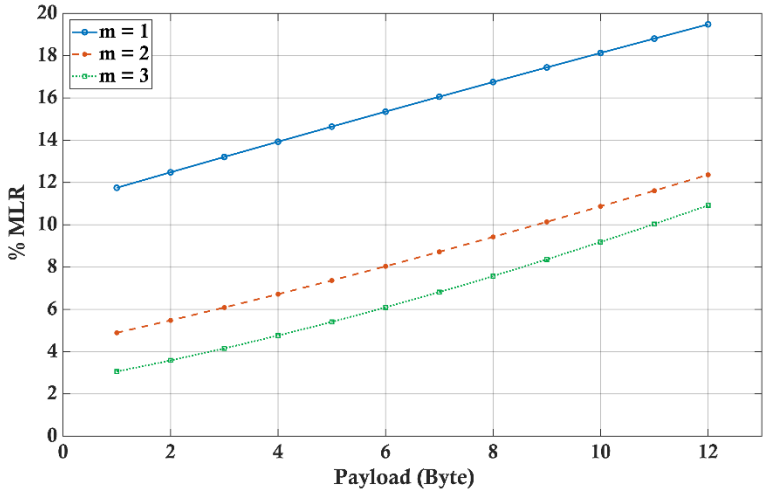

a) k = 60000 devices.

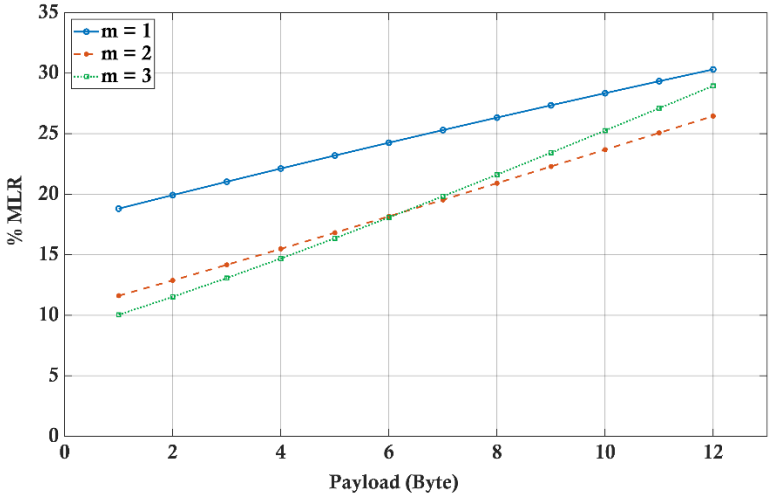

b) k = 100000 devices.

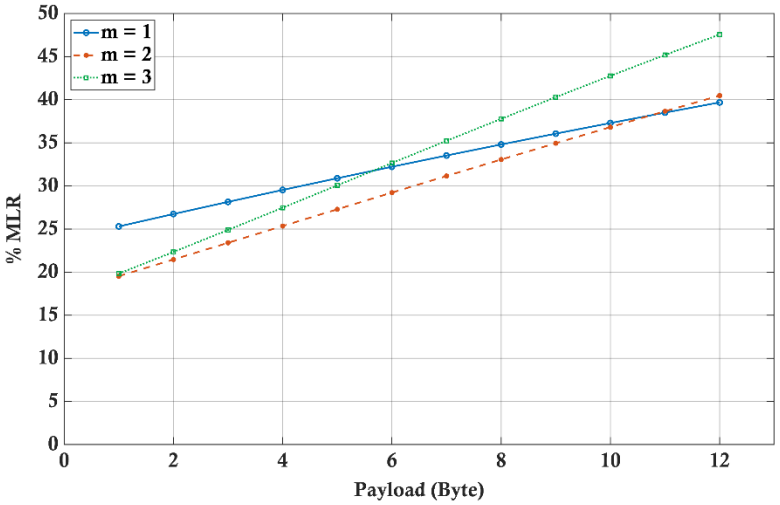

c) k = 120000 devices.

Figure 5.24: The MLR as a function of the payload in bytes for Sigfox with different numbers of message copies, where m = 1, 2, 3.

5.4.4 Variable Transmission Time

Figure 5.25 illustrates the effect of transmission time (T) on the Sigfox system performance. It shows the MLR versus the number of connected devices with different values of transmission time. The analysis presented in this figure is based on the single group scenario where all devices have the same transmission time with three message copies and a payload of eight bytes. It is reasonable that decreasing the transmission time escalates the probability of collision. However, it is evident from Figure 5.25 that as the transmission time declines, the rate of the MLR considerably raises with respect to the number of connected devices. For example, the system offers a moderately higher MLR when using transmission time of 30 minutes in comparison with a transmission time of 25 minutes. On the other hand, the system offers a significant increase in the MLR when (T = 10 minutes) in comparison with (T = 15 minutes).

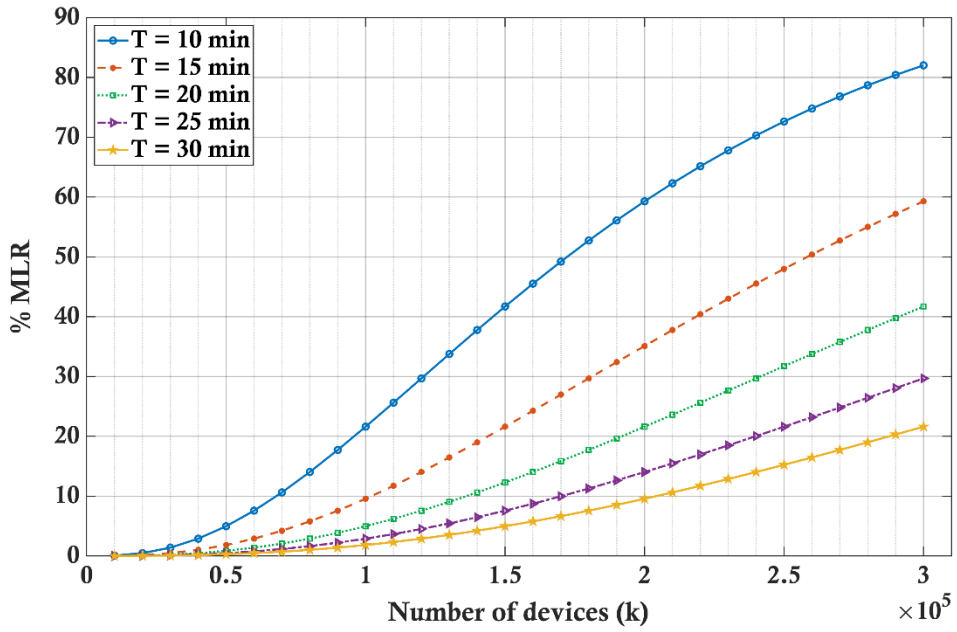

Figure 5.25: The MLR with a varying number of devices k for Sigfox with different transmission time T, where a single group is utilised with a periodic transmission and m = 3, PL = 8 bytes, and T = 10, 15, 20, 25, and 30 minutes.

Figure 5.26 demonstrates the effect of using different numbers of message copies on the MLR with a varying value of transmission time. The figure depicts the MLR versus transmission time (T) in minutes using different values of message copies. The number of connected devices used in this analysis is (k = 200000) devices, and all devices utilise a payload of (PL = 8 bytes).

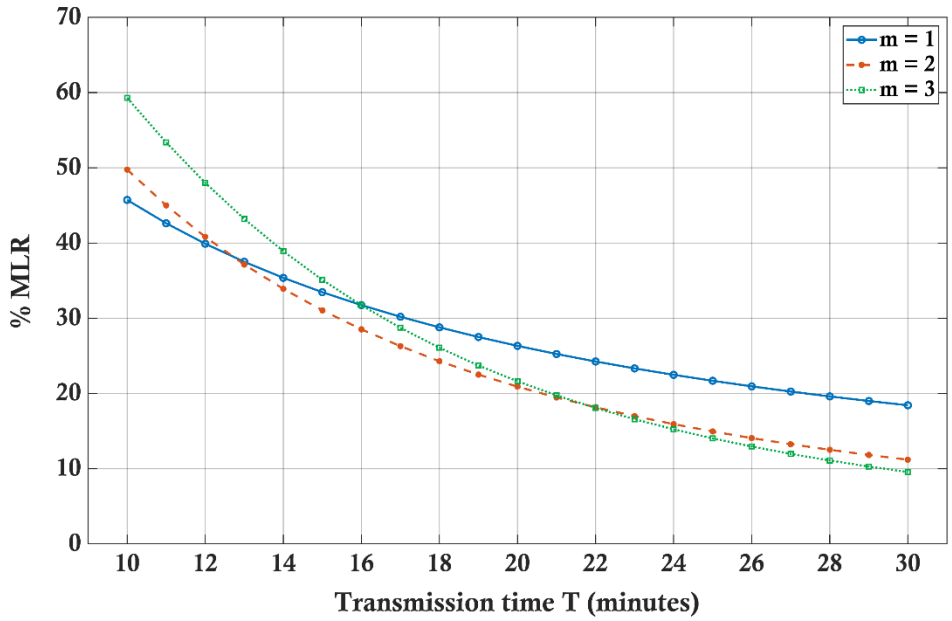

Figure 5.26: The MLR with variable transmission time T for Sigfox with different numbers of message copies, where a single group is utilised with a periodic transmission and k = 200000, PL = 8 bytes, and m = 1, 2, and 3.

Again, it is apparent from Figure 5.26 that as the number of message copies increases, the degree of the change of the MLR substantially increases. Therefore, using multiple message copies can have an adverse effect on the system performance when the transmission time is below certain limits. For example, using two message copies improves the system performance only if the transmission time is larger than 13 minutes. Reducing the transmission time below this threshold increases the MLR in comparison with the provided MLR in the case of a single message copy. This is also evident in the case of using three message copies, where the system exhibits a higher MLR than the case with two message copies, provided that the transmission time is less than 22 minutes. Moreover, when three message copies are implemented, the system provides the same MLR in comparison to a single message copy if the transmission time is decremented to 16 minutes. Using transmission time that is less than this limit has a substantial impact on the system performance and significantly increases the MLR.

These analysis cases confirm that the relationship between the number of message copies and the MLR is not independent of other system parameters and emphasise the importance of the tuning of these parameters to obtain the optimum performance. Furthermore, sending multiple message copies wastes valuable battery power, which significantly shortens the battery lifetime. If there is no tangible improvement in the system

performance, it is essential to avoid sending these redundant messages and preserve battery power. Next section studies the effect of different system characteristics on the power consumption including the impact of sending multiple message copies.

5.5 Power Consumption

Reducing power consumption is one of the crucial requirements for any M2M communication system and IoT device since most connected nodes rely on battery supply. Therefore, LPWA technologies were designed with maximum battery life in mind, presuming that devices can last several years while working on a single coin-cell battery. To achieve the low power consumption and prolong battery lifetime, the design of LPWA technologies is aimed at minimising the radio activity and allowing devices to reside in low power sleep mode most of the operating time and wake up at regular short intervals. However, selecting the optimum transmission power is related to other system characteristics like the modulation scheme and the coverage area (Al-Kaseem and Al-Raweshidy, 2016a; Al-Kaseem and Al-Raweshidy, 2016b; Baker *et al.*, 2017; Mekki *et al.*, 2019; Ali *et al.*, 2016; Xiong *et al.*, 2015; Bel *et al.*, 2018; Jha *et al.*, 2013; Botter *et al.*, 2012; Sethi and Sarangi, 2017; Zhu *et al.*, 2015; International Telecommunication Union, 2012).

In general, the power consumption of LPWANs devices is based on three power states: active mode, idle mode, and sleep mode. Active mode represents the device's transmitting mode where messages are transmitted to the base station. Idle mode denotes the state of the device before each transmission, where the device is activated to read data, select the transmission channel, and set the transmitter for the next hop. Finally, sleep mode indicates the case when the device enters the deep sleep state with minimum power consumption (Al-Kaseem and Al-Raweshidy, 2016a; Al-Kaseem and Al-Raweshidy, 2016b; Bel *et al.*, 2018; Botter *et al.*, 2012). Figure 5.27 illustrates the power consumption diagram for the LPWANs devices with three message copies including all the three working modes. From Figure 5.27, the total power consumption is calculated as follows:

$$P_{total} = m * (P_{active} * \frac{\tau}{T}) + m * (P_{idle} * \frac{T_{idle}}{T}) + (P_{sleep} * \frac{T_{sleep}}{T}) \quad 5.1$$

Where *m* is the number of message copies and time is in seconds. Note that the active time is equal to the packet duration τ. Also P_{active} is the summation of idle state power P_{idle} and the transmission power P_{tx} that is required by the transmitter for data transmission. Therefore, P_{total} can be given by the following equations:

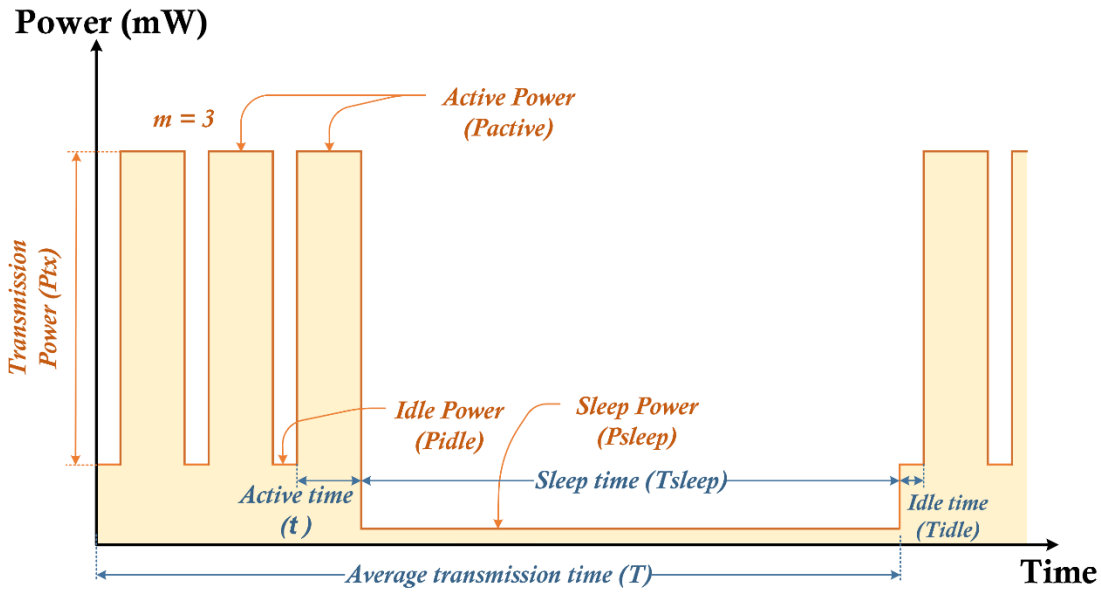

Figure 5.27: Device's power diagram with three message copies.

$$P_{total} = \frac{1}{T}\{m\tau(P_{tx} + P_{idle}) + m(P_{idle}T_{idle}) + (P_{sleep}T_{sleep})\} \quad 5.2$$

$$P_{total} = \frac{1}{T}\{mP_{tx}\tau + mP_{idle}(\tau + T_{idle}) + P_{sleep}T_{sleep}\} \quad 5.3$$

It is reasonable to assume that P_{idle} and P_{sleep} are the same for different technologies since the transmission power P_{tx} is the dominant power and the one that is mostly changes among different technologies. Therefore, P_{idle} and P_{sleep} calculations for both technologies are based on the experiments that were implemented on the Weightless-N development kit.

In general, the P_{tx} is calculated based on the transmission power specified by each technology. For instance, both Weightless-N and Sigfox utilise transmission power of 14 dBm in Europe (Weightless-SIG, 2015c; Raza *et al.*, 2017; Nolan *et al.*, 2016; Burns *et al.*, 2015; Ofcom, 2014). Then, the transmission power is given by:

$$P_{tx}(mW) = 10^{\frac{P_{tx}(dBm)}{10}} = 10^{1.4} = 25\ mW \quad 5.4$$

More precisely, the power consumption during transmission time is slightly higher than the designated transmission power due to the electric current required by other electronic

components on the board, like the transmitter circuit and the serial connection between the microcontroller and the transmitter. Therefore, the Weightless-N development kit was used to calculate the exact value of the power consumption for all working modes including the transmission power, as shown in Figure 5.28.

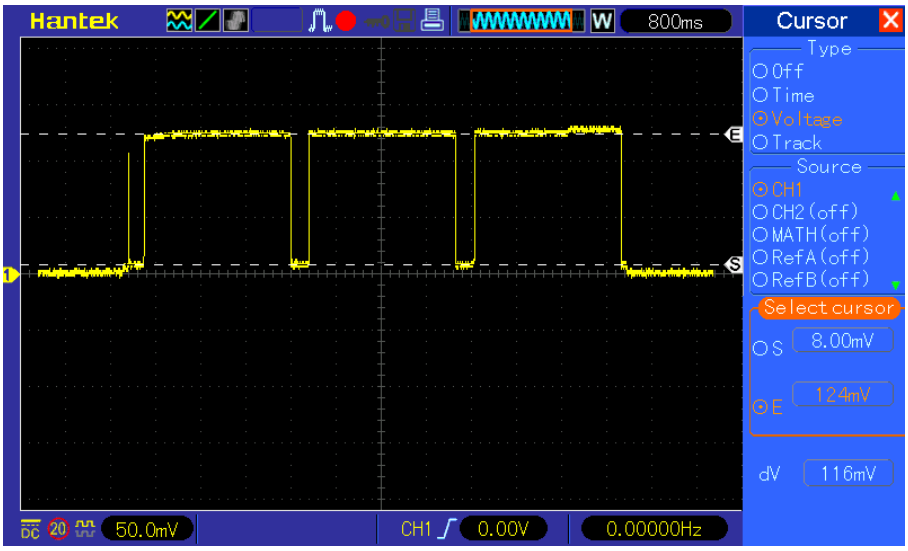

Figure 5.28: Weightless-N development kit input current with three message copies, where I_{tx} = $11.6\ mA$ and $I_{idle} = 0.8\ mA$

Figure 5.28 illustrates the experimental measurements of the input current to the Weightless-N development kit using a current-to-voltage converter with an internal resistance of 10 ohms. As a result, the current is given as follows:

$$I = \frac{V}{10} \tag{5.5}$$

It is clear from Figure 5.28 that the current needed for data transmission is (11.6 mA) while the idle state current I_{idle} is equal to (0.8 mA). In addition, experiment results showed that the sleep state current I_{sleep} is equal to (0.035 mA). Assuming that the power source is a coin cell battery with a constant voltage of (3 volts) for all modes, the transmission power P_{tx} can be calculated as follows:

$$P_{tx} = V * I_{tx} = 3v * 11.6mA = 34.8\ mW \tag{5.6}$$

Similarly, the power consumption during the idle mode is given by:

$$P_{idle} = V * I_{idle} = 3v * 0.8mA = 2.4\ mW \quad 5.7$$

Likewise, the power consumption during the sleep state mode is calculated as follows:

$$P_{sleep} = V * I_{sleep} = 3v * 0.035mA = 0.11\ mW \quad 5.8$$

Now, from Equation 5.3, the total power consumption of each device can be calculated in milliwatts as:

$$P_{total} = \frac{1}{T}\{34.8m\tau + 2.4m(\tau + T_{idle}) + 0.11T_{sleep}\}\ mW \quad 5.9$$

Since the idle time is given by (0.33 sec.), as shown in Figure 5.29, Equation 5.9 can be rewritten as:

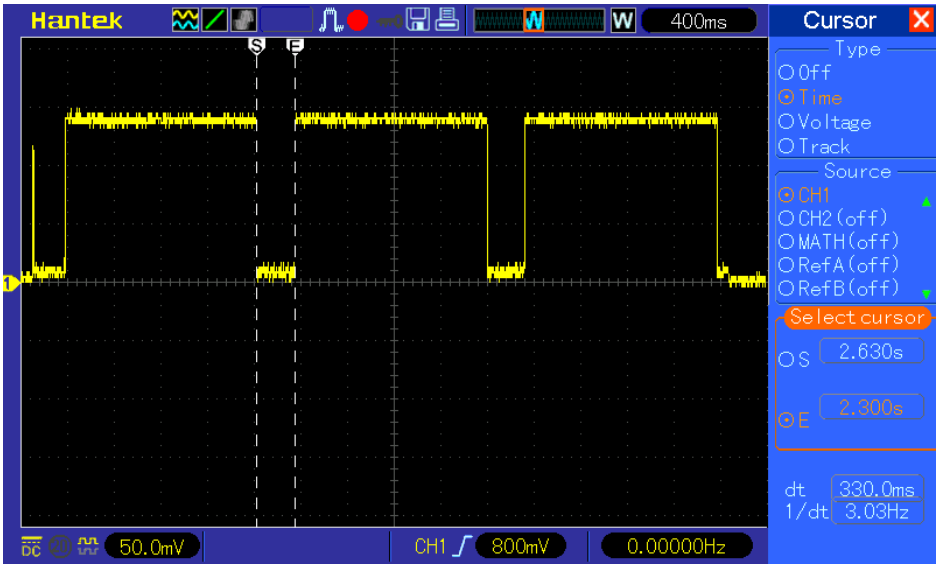

Figure 5.29: Weightless-N development kit input current timing with three message copies, where $T_{idle} = 0.33\ sec$

$$P_{total} = \frac{1}{T}\{34.8m\tau + 2.4m(\tau + 0.33) + 0.11T_{sleep}\}\ mW \quad 5.10$$

$$P_{total} = \frac{1}{T}\{37.2m\tau + 0.11T_{sleep} + 0.79m\}\ mW \quad 5.11$$

In addition, sleeping time T_{sleep} can be expressed in terms of τ and T as follows:

$$T_{sleep} = T - m(\tau + T_{idle}) = T - m(\tau + 0.33) \quad 5.12$$

Then, Equation 5.11 becomes:

$$P_{total} = \frac{1}{T}\{37.2m\tau + 0.11(T - m(\tau + 0.33)) + 0.79m\}\ mW \quad 5.13$$

Finally, the total power consumption for each device connected to either Weightless-N or Sigfox network is given by the following equation:

$$P_{total} = \frac{1}{T}(37.09m\tau + 0.11T + 0.75m)\ mW \quad 5.14$$

It is apparent from Equation 5.14 that the total power consumption is inversely proportional to the average transmission time T and is directly proportional to the number of message copies m and the packet duration τ. τ is directly related to the payload and can be calculated as follows (Botter *et al.*, 2012):

$$\tau = \frac{\text{packet size}(bits)}{data\ transmission\ rate(bps)} \quad 5.15$$

Packet size represents the message payload in addition to other message information like the device's identification number (ID), the timestamp, the MAC address, and the Frame-Check Sequence (FCS). These additional information bytes are defined by 17 bytes (136 bits) for Weightless-N and by 14 bytes (112 bits) for Sigfox. As both technologies utilise a data transmission rate of 100 bps, the packet duration τ is presented in the following equations for each technology respectively based on the payload size *PL* in bytes:

$$\tau = \frac{136 + (8 * PL)}{100} \quad sec \qquad for\ Weightless - N \quad 5.16$$

$$\tau = \frac{112 + (8 * PL)}{100} \quad sec \qquad for\ Sigfox \qquad 5.17$$

Since both technologies utilise the same transmission power of 14 dBm and the same data transmission rate, it is clear from Equations 5.16 and 5.17 that Sigfox offers lower power consumption than Weightless-N if the same number of message copies, payload, and the average transmission time are used. The next sections study the effects of various system characteristics on the total power consumption using the two nominated LPWA technologies, Weightless-N and Sigfox. The analysis presented in the following sections is based on a single group scenario with a periodic transmission scheme.

5.5.1 Weightless-N Technology

Figure 5.30 illustrates the Weightless-N devices power consumption versus a variable number of message copies using different values of transmission time *T*. It is clear from this figure that the power consumption linearly increases with respect to the number of message copies. It is also evident from Figure 5.30 that as the transmission time decreases the rate of the power consumption increment escalates with respect to the number of message copies. As discussed in section 5.3.2, if there is no tangible improvement in system performance with a high number of message copies, reducing message copies is essential to reduce the power consumption and preserve battery power.

Figure 5.31 shows the Weightless-N devices power consumption versus a variable payload size *PL* using different numbers of message copies *m*. It is rational that the higher the payload, the higher the power consumption. It is apparent from Figure 5.31 that the power consumption linearly rises as the payload increases. It is also clear that increasing the payload has less effect on power consumption in comparison with the impact of increasing the number of message copies. However, it is vital for system designers to utilise the optimum number of message copies and the minimum payload, which can provide the necessary data for each application, not only to minimise the collision, but also to maintain valuable battery power.

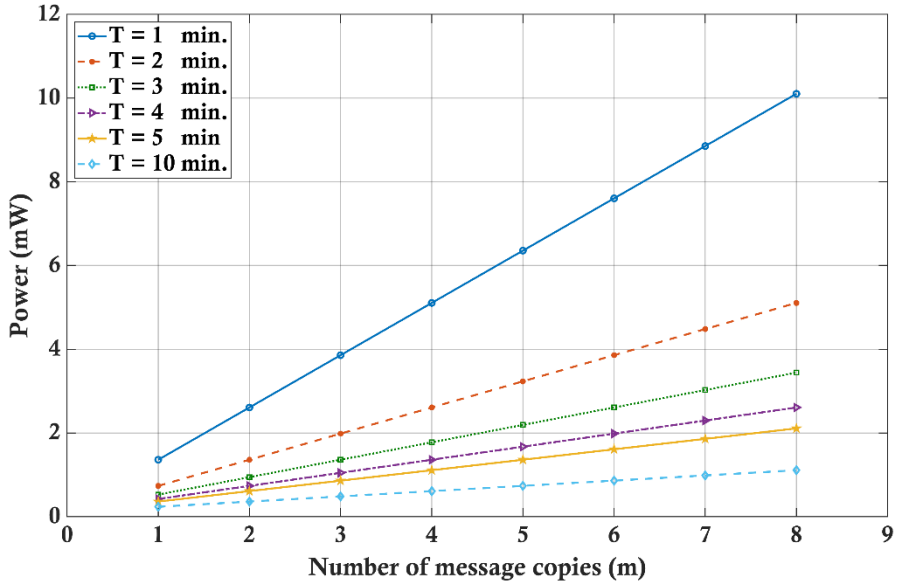

Figure 5.30: Weightless-N power consumption with a varying number of message copies *m* using different values of transmission time *T*, where *PL* = 8 bytes and *T* = 1, 2, 3, 4, 5, and 10 minutes.

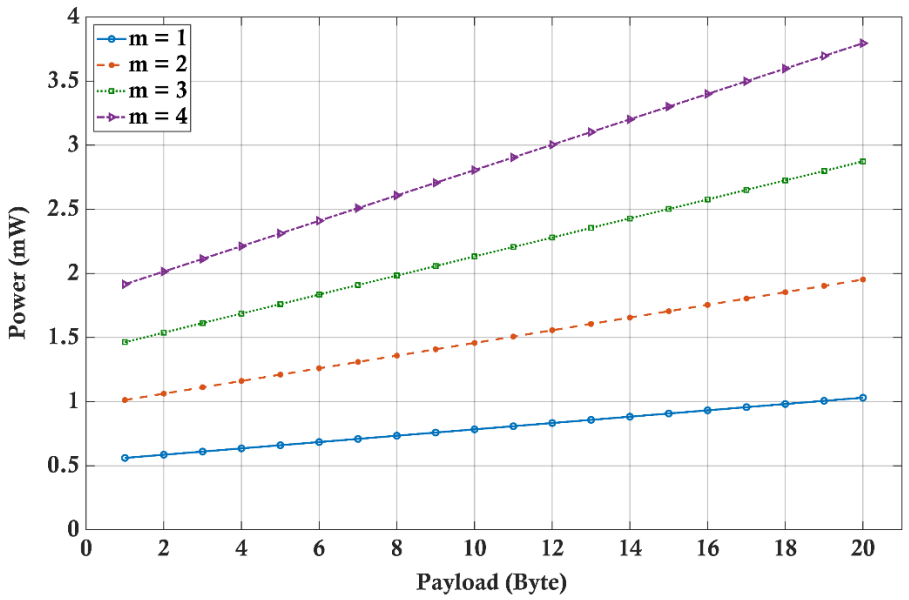

Figure 5.31: Weightless-N power consumption with a varying payload *PL* using different numbers of message copies *m*, where *T* = 2 minutes and *m* = 1, 2, 3, and 4.

Figure 5.32 depicts the effect of the average transmission time on the power consumption in Weightless-N using different numbers of message copies. It is clear from Figure 5.32 that the power consumption dramatically increases as the transmission time decreases. Moreover, as the number of message copies increases, the rate of change in the power consumption enlarges with respect to the transmission time.

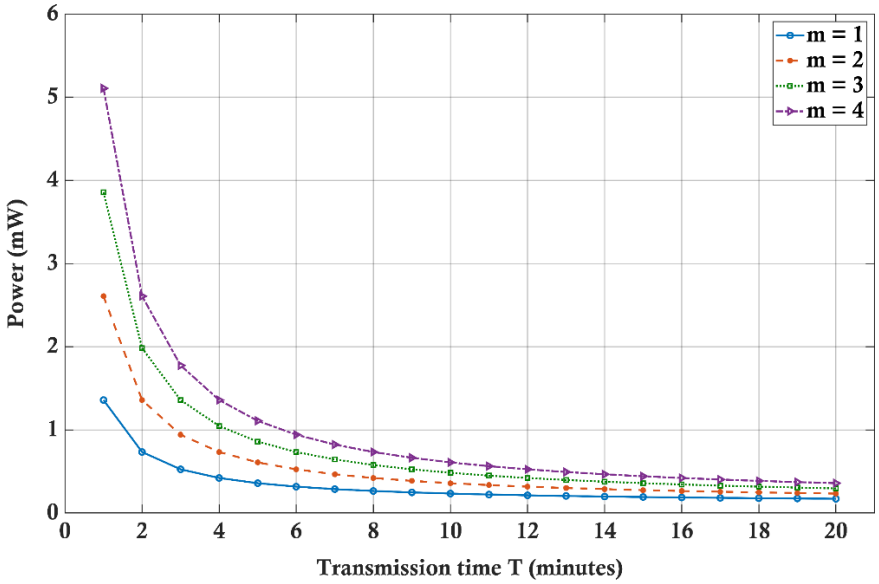

Figure 5.32: Weightless-N power consumption with varying transmission time *T* using different numbers of message copies *m*, where *PL* = 8 bytes and *m* = 1, 2, 3, and 4.

5.5.2 Sigfox Technology

Figure 5.33 shows the Sigfox devices power consumption with a varying number of message copies using different values of transmission time *T*. As the number of message copies increases, the power consumption linearly escalates. Furthermore, the rate of change in the power consumption increases with respect to the number of message copies as the transmission time *T* decreases. Again, if there is no noticeable improvement in system performance with a high number of message copies, reducing message copies is essential to preserve valuable battery power.

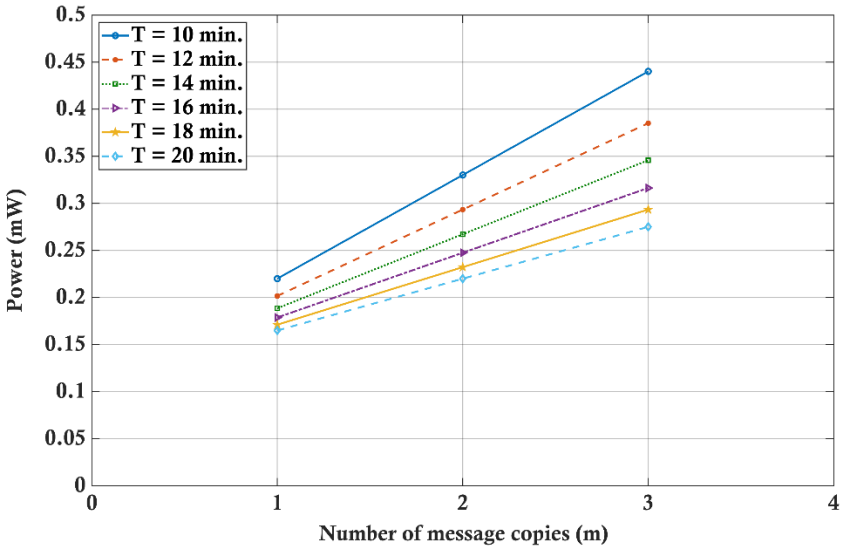

Figure 5.33: Sigfox power consumption with a varying number of message copies *m* using different values of transmission time *T*, where *PL* = 8 bytes and *T* = 10, 12, 14, 16, 18, and 20 minutes.

Figure 5.34 demonstrates the power consumption versus a variable payload size *PL* using different numbers of message copies *m*. Similarly, it is apparent from Figure 5.34 that the power consumption is linearly related to the payload and correspondingly to the packet duration τ.

Figure 5.35 illustrates the power consumption of Sigfox devices with varying transmission time *T* using different numbers of message copies *m*. It is clear from Figure 5.35 that the power consumption increases as the transmission time decreases. Furthermore, it is evident from Figure 5.35 that the higher the number of message copies, the larger the rate of change in power consumption.

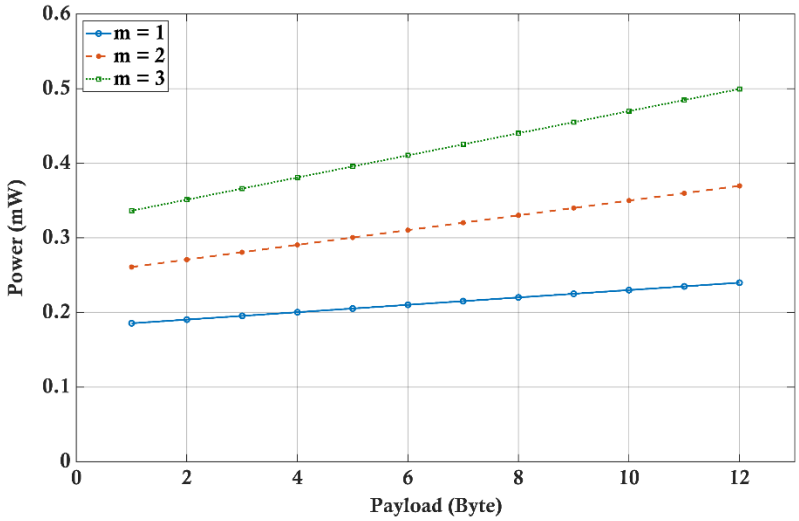

Figure 5.34: Sigfox power consumption with a varying payload *PL* using different numbers of message copies *m*, where *T* = 10 minutes and *m* = 1, 2, and 3.

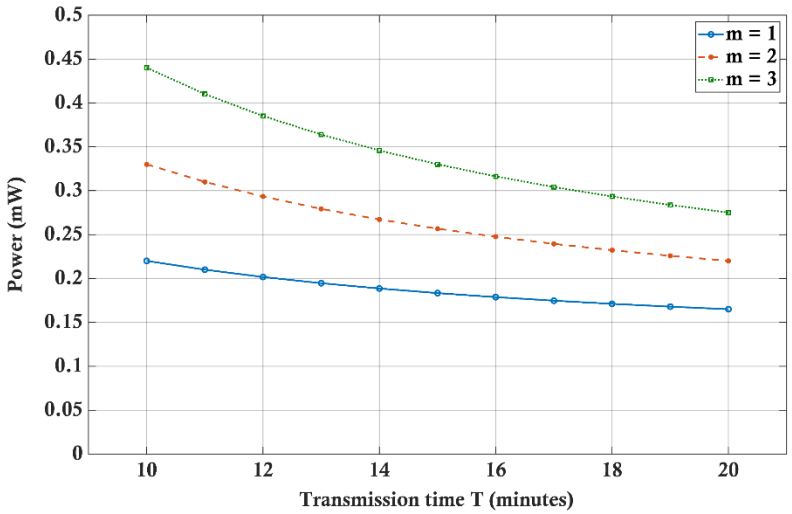

Figure 5.35: Sigfox power consumption with varying transmission time *T* using different numbers of message copies *m*, where *PL* = 8 bytes and *m* = 1, 2, and 3.

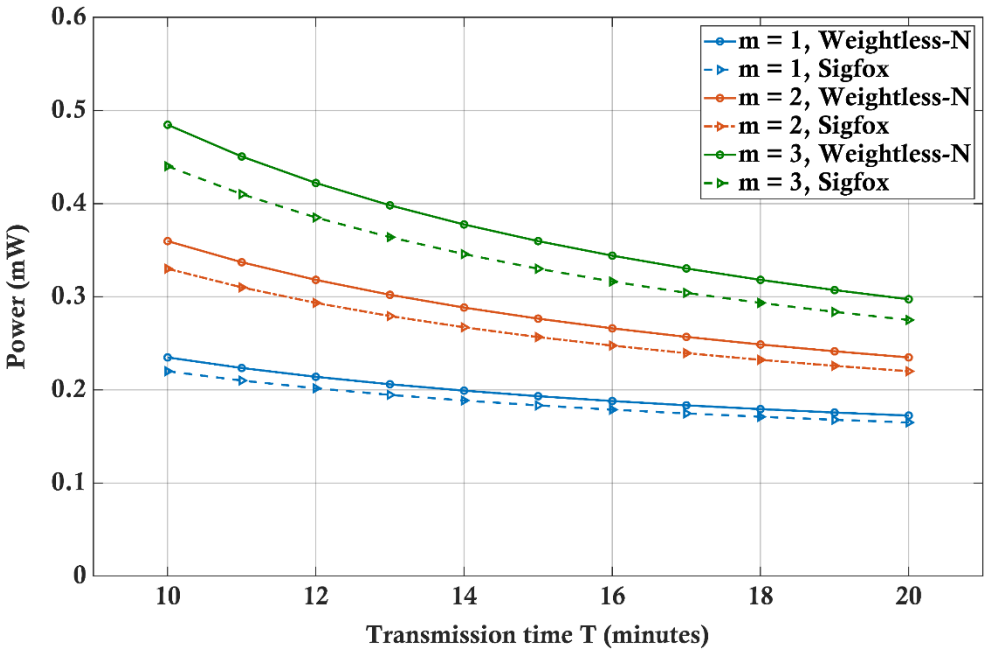

Figure 5.36: Power consumption for Weightless-N and Sigfox with variable transmission time *T* using different numbers of message copies *m*, where *PL* = 8 bytes and *m* = 1, 2, and 3.

Figure 5.36 shows a comparison between Weightless-N and Sigfox in terms of the power consumption with a variable value of the transmission time *T* using different numbers of message copies. It is fair to say that Sigfox technology offers a lower power consumption than Weightless-N as it utilises a shorter packet duration with the same payload. In addition, it is noticeable from Figure 5.36 that as the number of message copies increases the difference in power consumption between Weightless-N and Sigfox increases.

The next section provides a detailed comparison between the two technologies in terms of the message lost ratio (MLR) and the power consumption with the case of the smart meters.

5.6 Evaluation of System Performance with the Smart Meters Application

This section employs the smart meters application as a case study for the LPWANs performance and power consumption using both Weightless and Sigfox technologies. Based on the transmission characteristics of smart meters, this section offers a thorough analysis to choose the optimum number of message copies that can offer an adequate message lost ratio with the minimum power consumption for this application. It is evident from previous sections that optimising the number of message copies is a key factor for reliable LPWANs especially with such a vital application that comprises an immense number of connected devices.

Smart meters are the most essential component in the smart grid and play a fundamental role in smart cities and the IoT. Smart meters are widely utilised around the globe and with the current widespread popularity of smart meters, they represent one of the major parts of IoT devices (Wan *et al.*, 2019; O'Dwyer *et al.*, 2019; Jia *et al.*, 2019; Andreadou *et al.*, 2018; Wang *et al.*, 2018; Sun *et al.*, 2016; Lloret *et al.*, 2016; Nielsen *et al.*, 2015). Millions of devices have been already employed around the world, and millions of devices are planned to be connected in the next few years (Wang *et al.*, 2018; Sun *et al.*, 2016; Barai *et al.*, 2015; Aiello and Pagani, 2014; Wenpeng Luan *et al.*, 2013). By the end of 2018, more than 12 million smart meters were installed in the UK, and 50 million smart meters are planned to be installed across Great Britain by the end of 2020 (Sun *et al.*, 2016; Department for Business Energy and Industrial Strategy, 2018).

Smart meters are powerful devices that can offer valuable information to the utility, helping suppliers to manage the billing system and electricity, gas, and water consumption. Even though a few annual readings can be adequate for the billing system, advanced metering infrastructure (AMI) was designed to provide more frequent information to the utility companies. Such statistical information is beneficial to understanding the individual region's consumption scheme and to improve supply network reliability and efficiency. It also provides important insights into consumers' spending habits and lifestyle (Wan *et al.*, 2019; Andreadou *et al.*, 2018; Sun *et al.*, 2016; Lloret *et al.*, 2016; Barai *et al.*, 2015; Budka *et al.*, 2014).

In general, smart meters employ the periodic transmission scheme with the shortest possible active time and very long sleeping time to minimise the power consumption, where a battery lifetime of 10 to 20 years is expected (Wan *et al.*, 2019). However, there is a wide diversity in the literature regarding the smart meters specifications and the transmission characteristics utilised by them. In particular, various message sizes and average transmission times are exemplified by different research. Moreover, some meters employ data aggregation and send multiple readings in each message to further increase sleeping time and reduce data volume (Wan *et al.*, 2019; Andreadou *et al.*, 2018; Wang *et al.*, 2018; Nielsen *et al.*, 2015; Barai *et al.*, 2015; Karimi *et al.*, 2015; Shiobara *et al.*, 2015; Wenpeng Luan *et al.*, 2013; Budka *et al.*, 2014; Balachandran *et al.*, 2014; Aiello and Pagani, 2014).

The analysis presented in this section is based on the most common transmission characteristics for smart meters with average transmission time (T) of 15 minutes and a payload of 8 bytes. The chosen payload is intended for meters that send basic consumption

information without data aggregation (Andreadou *et al.*, 2018; Wang *et al.*, 2018; Barai *et al.*, 2015; Karimi *et al.*, 2015; Balachandran *et al.*, 2014; Shiobara *et al.*, 2015; Budka *et al.*, 2014).

Figure 5.37 shows the power consumption for Weightless-N and Sigfox with smart meters transmission characteristics using three different message copies. As the standard number of message copies utilised by both technologies is (m = 3), the percentage change in power consumption using other numbers of message copies can be calculated as follows:

$$P_{ch}\% = \frac{P_{std} - P_{new}}{P_{std}} \times 100 \qquad 5.18$$

Where P_{ch} is the percentage change in power consumption, P_{std} is the standard power consumption with three message copies, and P_{new} presents the new value for power consumption using other values of message copies m.

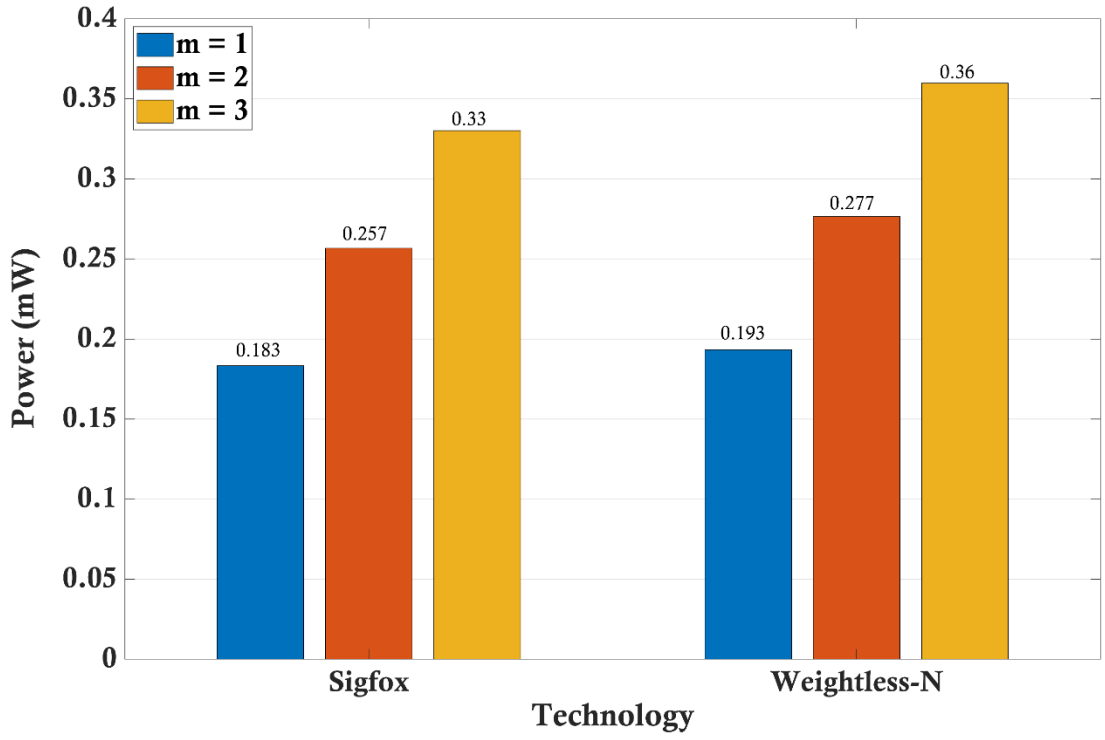

Figure 5.37: Power consumption of smart meters for Weightless-N and Sigfox technologies with three different numbers of message copies *m*, where *PL* = 8 bytes, *T* = 15 min., and *m* = 1, 2, and 3.

It is evident from Figure 5.37 that using two message copies decreases the power consumption by 23.06 per cent in comparison with three message copies for the Weightless-N technology. Moreover, using a single message copy declines the power consumption by 46.39 per cent in comparison with three message copies. On the other hand, using two message copies cuts the power consumption by 22.12 per cent in comparison with three message copies for the Sigfox technology. Using a single message copy lessens the power consumption by 44.55 per cent for Sigfox in comparison with three message copies. Furthermore, it is clear that Weightless-N consumes more power than Sigfox since it utilises a larger message header, as discussed in the previous sections.

Figure 5.38 depicts a comparison of the message lost ratio (MLR) versus the number of connected devices for both technologies including all utilised bands by Weightless-N. The analysis presented in this figure is based on the single group scenario assuming that all devices are smart meters. A massive number of smart meters, of up to one million, are presumed to be connected to a single base station. It is clear from Figure 5.38 that utilising the bands of 1200 and 1500 channels presents a noticeably higher MLR than other bands for all numbers of message copies. Therefore, it is sensible to avoid using these two band for the smart meters. In addition, as Sigfox utilises only 1920 channels, it is reasonable that it provides a higher MLR than Weightless-N, provided that Weightless-N using the four bands of 2499, 3000, 9990, and 15000 channels.

It is clear from Figure 5.38 that Weightless-N with the bands of 9990 and 15000 channels provides a significantly lower MLR than other bands including Sigfox for all employed message copies. Moreover, it is evident from Figure 5.38 that as the number of message copies increases, other bands provide a noticeably higher MLR. As a comparison between Weightless-N with 15000 channels and Sigfox, Weightless-N offers a message lost ratio of 10 per cent if the number of connected smart meters is 700000 devices while Sigfox provides a considerably higher message lost ratio of 95 per cent with the same number of connected smart meters. Furthermore, the MLR surges up to 100 per cent using Sigfox when the connected devices increase to one million while Weightless-N still provides a low MLR as little as 20 per cent only.

According to this analysis, it is reasonable to infer that the must adequate bands for the application of smart meters are the 9990 and 15000 channels bands, which are utilised by the Weightless-N technology. In the following two sections, the analysis employs the 15000 channels band to determine the optimum number of message copies for smart meters using two scenarios: a single group scenario and a multiple group scenario.

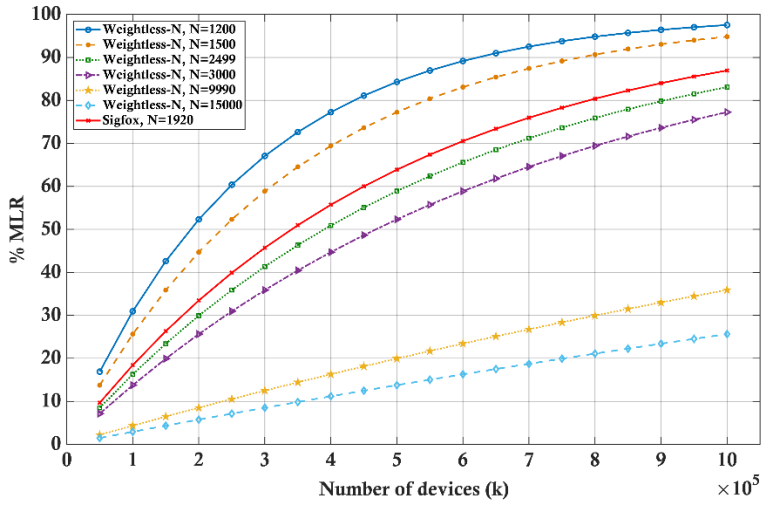

a) $m = 1$.

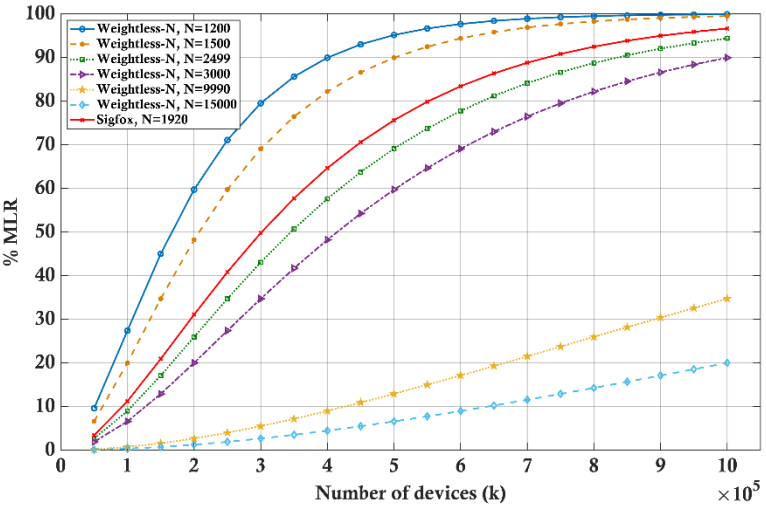

b) $m = 2$.

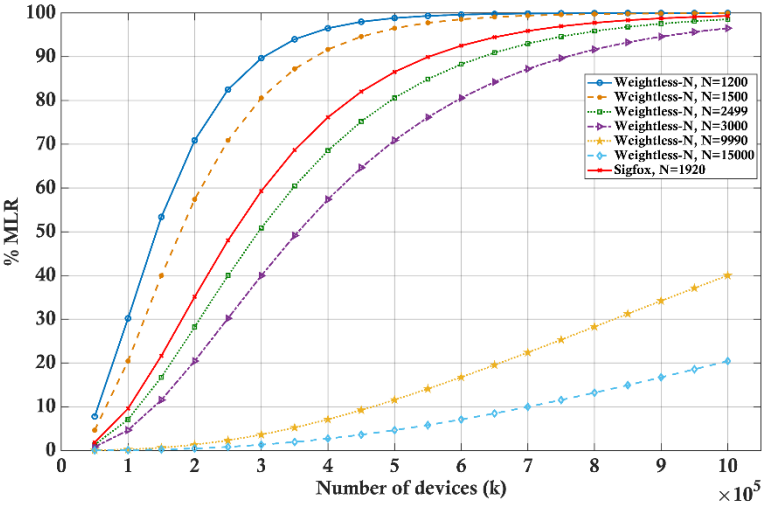

c) $m = 3$.

Figure 5.38: The MLR as a function of the number of smart meters for Weightless and Sigfox with different numbers of channels, where *PL* = 8 bytes, *T* = 15 min., and *N* = 1200, 1500, 1290, 2499, 3000, 9990, and 15000.

5.6.1 Smart Meters with a Single Group Scenario

This section focuses on the optimum number of message copies that ought to be used for smart meters to offer a balance performance between the power consumption and the message lost ratio. The analysis presented in this section utilises the Weightless-N technology with 15000 channels assuming that all connected devices are smart meters with T = 15 minutes and PL = 8 bytes. It is reasonable that a relatively high MLR is adequate in smart meters since small gaps of data do not affect network reliability and sometimes gaps of hours or even days are acceptable (Lloret *et al.*, 2016). Accordingly, the study offered in this section presumes that a message lost ratio of up to 20 per cent is suitable for smart meters.

Figure 5.39 illustrates the effect of increasing the number of smart meters on the MLR using three different numbers of message copies. Despite that using a single message copy drops the power consumption up to 46.39 per cent in comparison with three message copies, it is not preferred in this case since it provides a noticeably high MLR. On the other hand, using two or three message copies offers a lower MLR than using a single message copy with up to one million smart meters. If the number of smart meters exceeds one million meters, the system provides a higher MLR than the acceptable limit of 20 per cent. Therefore, one million smart meters denotes the maximum limit of the number of connected devices for the considered scenario.

It is evident from Figure 5.39 that using three message copies does not offer a perceptible improvement on the system performance in comparison with two message copies. Moreover, using three message copies offers a lower MLR than using two message copies only when the number of connected meters is equal to or less than 900000 meters. Exceeding this limit raises the MLR and there are no beneficial effects of using three message copies over the use of two message copies.

According to the analysis presented in this section and the pervious section, it is sensible to select the two message copies as the optimum number of the message copies that can be used for the smart meters. Using two message copies made no significant difference to the message lost ratio in comparison with three message copies. Moreover, it maintains the MLR within the acceptable range even with an enormous number of smart meters. In addition, it reduces the power consumption by 23.06 per cent, which substantially saves valuable battery energy and prolongs network lifetime.

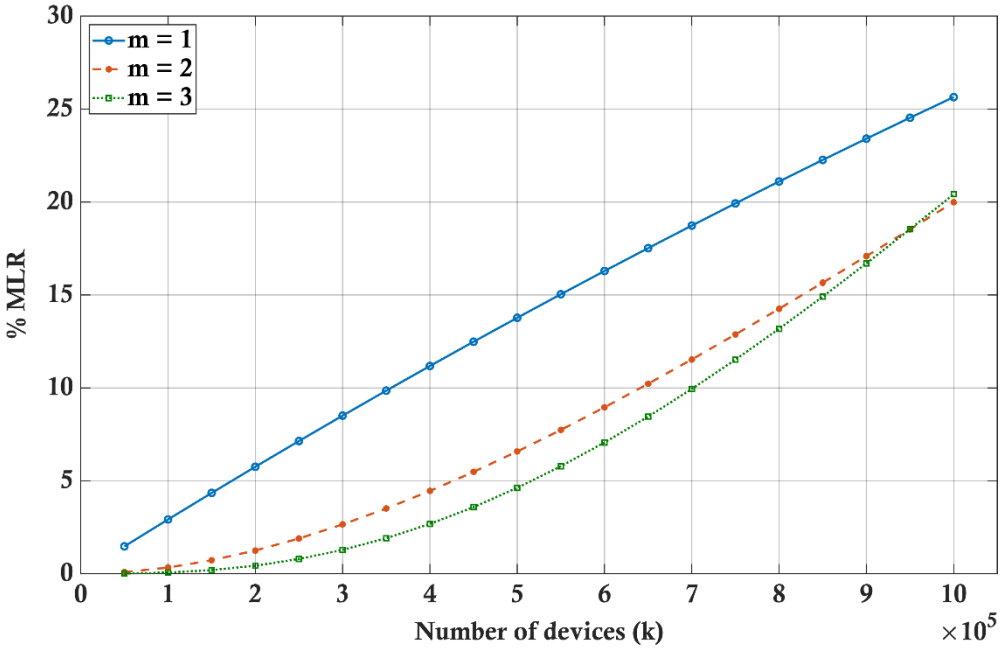

Figure 5.39: The MLR with a varying number of smart meters *k* for Weightless-N with a single group scenario and three different numbers of message copies *m*, where *PL* = 8 bytes, *T* = 15 min., *N* = 15000, and *m* = 1, 2, and 3.

5.6.2 Smart Meters with a Multiple Group Scenario

This section studies a more realistic working instance where different devices from multiple applications work simultaneously and share the medium with the smart meters. The analysis presented in this section focuses on the effect of using different numbers of message copies for the smart meters on the overall system MLR and the individual groups MLR. Again, the analysis is intended to determine the optimum number of message copies for the smart meters. It is also important to highlight that other applications are assumed to employ the standard three message copies in all cases.

The analysis is based on the four groups scenario where the first group *G1* represents the smart meters with a constant number of 800000 smart meters. Other connected devices are divided among the three other groups with various transmission characteristics, where *G2* represents 40% of the connected devices while each of the other two groups represents 30%, as reported in Table 5.2. The analysis is implemented by varying the number of devices in *G2*, *G3*, and *G4* while keeping the number of smart meters in *G1* constant. As the MLR for each group can be calculated separately, this can be helpful to infer the maximum number of devices that can be connected to the same base station with the smart meters and maintains the MLR in the smart meters group within the sufficient range. In addition, the optimum number of message copies is also obtained from this analysis.

Table 5.2: Groups characteristics.

Group name	Number of devices	Percentage of total devices (%)	Transmission scheme	Transmission time (minutes)	Payload (Byte)
G1	800000	NA	Periodic	$t_0 = 15$	8
G2	Variable	40	Periodic	$t_0 = 2$	10
G3	Variable	30	Random	$t_1 = 2$ and $t_2 = 4$	12
G4	Variable	30	Periodic	$t_0 = 4$	14

Figure 5.40 shows the overall system MLR versus a variable number of devices in *G2*, *G3*, and *G4* using three different numbers of message copies for *G1*. On the other hand, Figure 5.41 illustrates the MLR for the smart meters group *G1* and *G2*. It is apparent from Figure 5.40 and Figure 5.41 that using a single message copy is not adequate for smart meters in this scenario since it provides a considerable higher MLR than using two or three message copies. Moreover, the MLR for *G1* is always larger than 20 per cent, which is not preferred in smart meters application.

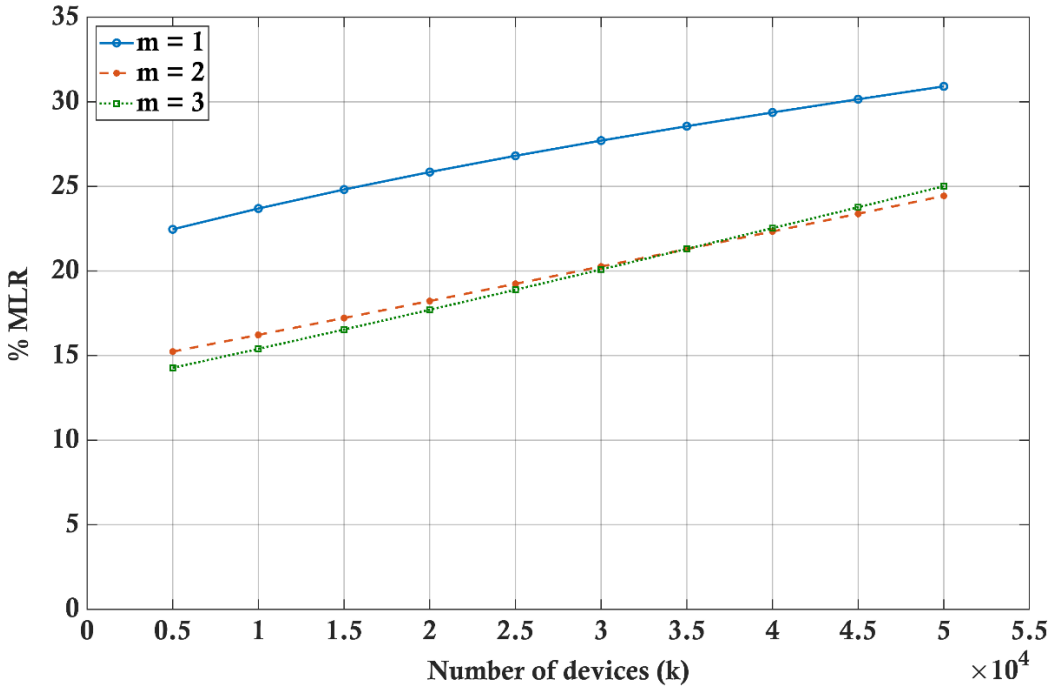

Figure 5.40: The MLR with a varying number of devices *k* in *G2*, *G3*, and *G4* for Weightless-N with a multiple group scenario and three different numbers of message copies *m*, where *G1* devices = 800000, *G2*, *G3*, and *G4* devices = variable. *m* = 3 for *G2*, *G3*, and *G4* and *m* = 1, 2, and 3 for *G1*. *N* = 15000.

It is also evident from Figure 5.40 that using three message copies offers only a slight improvement in the total system performance, given that the number of connected devices is less than 35000 devices. As the number of devices exceeds this limit, the system provides a higher MLR in comparison with the two message copies case. This rise of MLR is due to the escalation of collisions in groups *G2*, *G3*, and *G4*, where using three message copies reduces the MLR in smart meters group *G1*, as illustrated in Figure 5.41.

Figure 5.41 depicts the MLR versus the number of connected devices for the smart meters group *G1* and *G2* for the same working scenario. This allows us to estimate the system limits and the maximum number of devices that can be connected to the same base station with the smart meters and preserve the MLR within the acceptable boundaries. In this analysis, *G2* was selected to evaluate the effect of employing different numbers of message copies in *G1*. More specifically, as *G2* includes the largest number of connected devices and utilises the shortest transmission time *T*, it offers the highest MLR in comparison to other groups. Accordingly, changing the number of message copies in *G1* has a higher impact on *G2* in comparison with *G3* and *G4*.

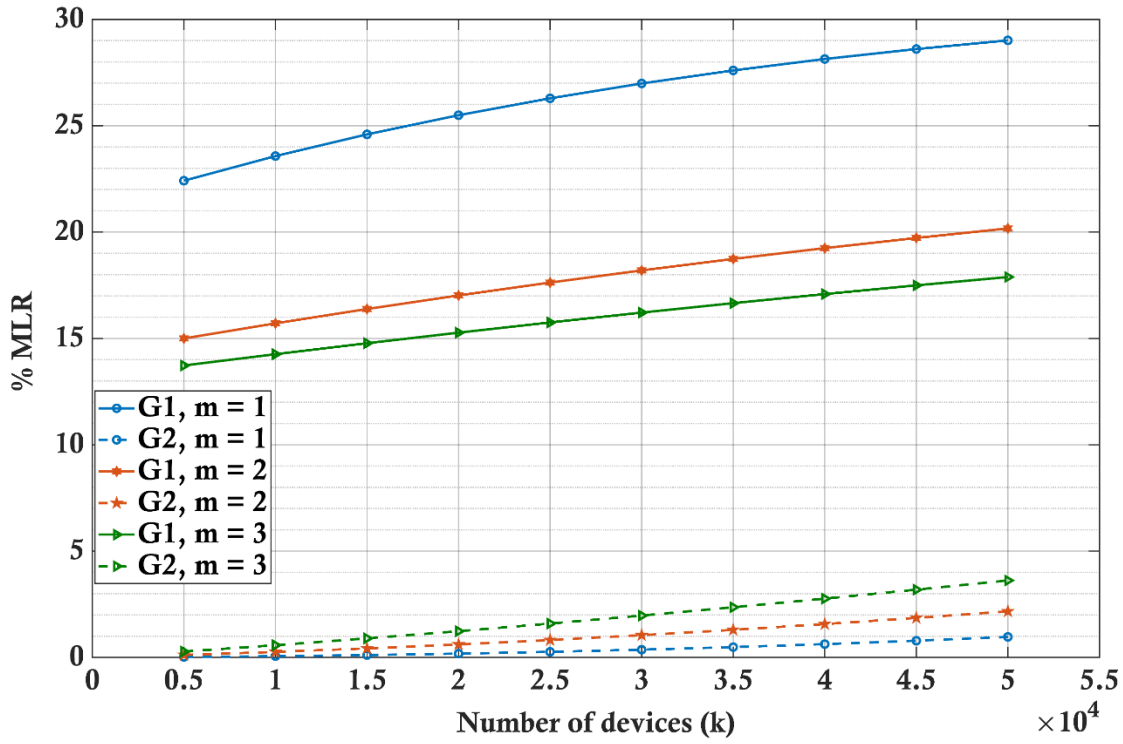

Figure 5.41: The MLR of *G1* and *G2* with a varying number of devices *k* with three different numbers of message copies *m*, where *G1* devices = 800000, *G2*, *G3*, and *G4* devices = variable. *m* = 3 for *G2*, *G3*, and *G4* and *m* = 1, 2, and 3 for *G1*. *N* = 15000.

It is clear from Figure 5.41 that using three message copies reduces the MLR in comparison with two message copies for the smart meters. However, this has an adverse effect on other groups where the MLR noticeably increases in these groups. To obtain a reasonable evaluation of the impact of the change of message copies on each group, the percentage change of the MLR in each group will be calculated as follows, assuming that (k = 50000):

$$MLR_{ch}\% = \frac{MLR_3 - MLR_2}{MLR_3} \times 100 \qquad 5.19$$

$$MLR_{ch}\% = \frac{17.89 - 20.17}{17.89} \times 100 = -12.7\% \quad for\ G1 \qquad 5.20$$

$$MLR_{ch}\% = \frac{3.62 - 2.17}{3.62} \times 100 = 40\% \quad for\ G2 \qquad 5.21$$

Where MLR_{ch} represents the percentage change in the MLR, MLR_2 is the MLR with two message copies, and MLR_3 represent the MLR using three message copies. It is clear that using three message copies in *G1* has a significant impact on the MLR in *G2*, where an increase of 40 per cent is seen in comparison with two message copies. In contrast, using two message copies slightly increases the MLR in the smart meters group *G1* by 12.7 per cent. Also, *G1* still provides a suitable MLR for smart meters with up to 50000 devices. Again, using two message copies reduces the power consumption in Weightless-N devices by 23.06 per cent in comparison with three message copies, which has a substantial impact on battery lifetime.

From this analysis, we can infer that the optimum number of message copies that should be used for smart meters in the case of multiple applications is two message copies. In addition, the maximum number of devices that can be connected to the base station for the current scenario is 50000 devices. However, this maximum limit is related to other system characteristics like transmission time and payload. Therefore, this number is intended to change according to other applications that share the medium with the smart meters.

5.7 Summary

This chapter presents a thorough and comprehensive study of the LPWANs performance in terms of collisions and power consumption employing two candidate technologies namely: Weightless-N and Sigfox. The analysis performed in this chapter involves various working scenarios with different transmission characteristics including the number of devices, the number of message copies, the payload size, the transmission time, and the number of channels. It also provides a systematic evaluation for practical systems with different applications that work simultaneously and connected to the same base station. In addition, the analysis is based on the novel channel selection algorithm (URCAT) described in Chapter 3 and the novel mathematical model presented in Chapter 4. The URCST algorithm is implemented in this chapter since it offers a lower probability of collisions and improves system performance in comparison with the standard algorithm.

The chapter offers an extensive simulation environment for the LPWANs by providing three different simulation testbeds, which offer a detailed analysis of both technologies. The analysis provides by these simulators covers the LPWANs evaluation in terms of the channel histogram, the probability of collision, and the mathematical model. These simulators facilitate the system analysis for various working scenarios with high flexibility to change different transmission characteristics. The simulators were developed using the MATLAB software and used to evaluate the LPWANs using both Weightless-N and Sigfox technologies.

Results show that the multiple message copies approach utilised by the nominated technologies can significantly reduce the message lost ratio (MLR) and improve system performance with certain limits. These limits are connected to other transmission characteristics, like the number of devices and the payload, utilised by the same application and other applications that are connected to the same base station. Exceeding these limits can substantially escalate the MLR and degrades system performance. Therefore, using a high number of message copies is not always beneficial to LPWANs performance. Moreover, increasing the number of message copies escalates the power consumption, which has another unfavourable impact on the system reliability and shortens network lifetime.

The chapter also provides a detailed evaluation of both technologies with the smart meters, which plays a key factor in the IoT and comprise the majority of connected devices in smart cities. The analysis involves two scenarios: a single group scenario and a multiple group scenario where other applications can be added to the same base station and share

the medium with the smart meters. Results show that using the two lower bands utilised by Weightless-N with 9990 and 15000 channels respectively represents the best bands for smart meters. A significantly higher number of smart meters can be connected using these two bands in comparison with Sigfox and other frequency bands employed by Weightless-N. In addition, the analysis reveals that using two message copies for smart meters offers the optimum system performance as it provides a balance between the MLR and the power consumption.

Chapter 6

Conclusions and Future Work

6.1 Conclusions

The collision problem remains one of the most critical challenges that face M2M communication, especially with the growth of the IoT and the tremendous number of devices expected to be connected to M2M systems. It is evident from the literature and the analysis presented in this thesis that data collisions have a substantial impact on the performance of M2M communication and can significantly affect network reliability.

This thesis covers different perspectives of the collision problem in M2M communication and provides technical solutions for the key issues caused by collisions. To investigate the influence of data collisions on the performance of M2M communication systems, two candidate M2M technologies, namely Weightless-N and Sigfox, were chosen as case studies for this research. Neither technologies employ acknowledgements, synchronisation, or any channel sense mechanism and only rely on a random time-frequency access protocol. On the other hand, both technologies utilise the frequency hopping technique with the multiple message copies approach to mitigate the collision problem. The study presented in this thesis shows that these two technologies can support several hundreds of thousands of devices per base station based on other transmission characteristics and the number of utilised UNB channels. More importantly, supporting such a massive number of connected devices has been achieved by employing the new developed channel selection algorithm, URCST, which significantly reduces the probability of collisions in comparison with the standard algorithm. Using URCST can reduce the message lost ratio (MLR) to 62% with three message copies in Weightless-N and up to 92% with eight message copies.

Another key strength of the presented study is the design and development of a comprehensive analysis and evaluation environment by utilising simulation testbeds which can demonstrate the performance of both technologies. Likewise, a general mathematical model has been developed to calculate the probability of lost messages for different ALOHA-based wireless communication technologies. Both, testbeds and the mathematical model, support multiple groups of devices with various transmission characteristics and support the multiple message copies approach. This was advantageous to provide a detailed and extensive study of the performance of Weightless-N and Sigfox and investigate the effects of different system parameters on the probability of collisions.

Subsequently, some important insights into the performance of M2M communication have been provided in this research. For instance, using multiple message copies is only beneficial for system performance within specific limits of transmission characteristics. Conversely, it might significantly increase the probability of collisions and degrade system performance. This contributes to the understanding of the limits of M2M technologies and applications connected to these technologies.

Along with concluding remarks, the main contributions of this research can be summarised in the following sections.

6.2 Channel Selection Technique

This research presents a novel channel selection algorithm called a Uniform Randomisation Channel Selection Technique (URCST), which can be implemented by different M2M technologies that employ the frequency hopping technique. URCST can mitigate the collision problem and maintain low complexity, low power consumption, and low cost requirements for successful M2M communication technologies. It offers a lower probability of collisions in comparison to the standard Weightless-N channel selection algorithm. Moreover, the URCST algorithm provides better performance as the number of message copies increases while the standard algorithm provides the best performance at four message copies. This might be very useful for applications requiring a high QoS.

In addition, URCST provides a uniform channel distribution comparable to the standard uniform random number generator, the MT19937 algorithm. On the other hand, the URCST algorithm can be implemented using simple microcontrollers with much lower hardware resources and much less complexity, computational time, and power consumption in comparison to the MT19937 algorithm.

6.3 System Model

The work presented in this thesis offers a rigorous and general mathematical model for the random time-frequency access protocol utilised by different M2M technologies in terms of the probability of lost messages. The model is flexible and easy to implement for different systems and various working scenarios. It is designed to support the multiple message copies approach with multiple groups of devices that are connected to the same base station and employ different transmission characteristics. To the best of the author's knowledge, this is the first study that considers multiple groups of devices with various numbers of message copies. The model is based on the Poisson distribution to model the time-

frequency access and the Binomial distribution to calculate the final probability of lost messages with the multiple message copies approach.

6.4 Simulation Testbeds

In this research, extensive testbeds have been provided to evaluate Weightless-N and Sigfox M2M technologies in terms of data collisions and study the effects of different transmission characteristics on the probability of collisions. Three different simulation testbeds were developed by the author to evaluate the impact of data collision on system performance from various aspects with high flexibility to change different transmission characteristics. These simulation testbeds cover the channel histogram, the probability of collisions, and the mathematical model. The testbeds were designed to support the multiple message copies approach with various groups of devices that are connected to the same base station and employ different transmission characteristics. To the best of the author's knowledge, these testbeds are the first simulators that offer a complete analysis for the collision problem for both Weightless-N and Sigfox with multiple groups of devices and various numbers of message copies.

6.5 LPWANs Performance Evaluation

With the employment of Weightless-N and Sigfox M2M technologies as case studies, this research provides a comprehensive study of the LPWANs performance in terms of data collision problem and power consumption. The analysis presented in this research offers a systematic evaluation of practical systems with different applications that work simultaneously and connected to the same base station. The analysis involves various working scenarios with different transmission characteristics including the number of devices, the number of message copies, the payload size, the transmission time, and the number of channels.

The results show that Weightless-N and Sigfox can support a massive number of devices (up to 1 million devices) using the URCST algorithm with the multiple message copies method. With certain limits, the multiple message copies can significantly reduce the message lost ratio and improve system performance. These limits are connected to other transmission characteristics, like the number of devices and the payload, and exceeding these limits can substantially increase the MLR and degrade system performance. Therefore, increasing the number of message copies can be disadvantageous to LPWANs performance. Furthermore, using a high number of message copies increases power

consumption, which has another adverse impact on system performance and reduces the network lifetime.

The thesis also provides a detailed analysis of both technologies with the case of smart meters. The analysis considers two scenarios: a single group scenario, where all the connected devices are smart meters, and a multiple group scenario, where devices from other applications share the medium with the smart meters and connected to the same base station. The results show that using Weightless-N with 9990 and 15000 channels can be the optimum choice for smart meters, where a significantly higher number of smart meters can be supported in comparison with Sigfox and other frequency bands employed by Weightless-N. Utilising the 15000 channels band and the URCST algorithm, Weightless-N can support up to one million smart meters with the single group scenario and up to 800 thousand smart meters with the multiple group scenario. Moreover, another 50 thousand devices from other applications can be connected to the same base station in the case of the multiple group scenario. These enormous numbers of devices can be supported by Weightless-N with only two message copies. This number of message copies is lower than the standard number of three message copies utilised by the standard algorithm. Using two message copies maintains the MLR within an acceptable range and reduces the power consumption in Weightless-N devices by 23 per cent in comparison with three message copies. This significantly saves valuable battery energy and prolongs the network lifetime.

6.6 Future Work

This thesis addresses some of the fundamental challenges in M2M communication and offers the foundation for several important future research directions, which can be highlighted in this section as follows:

1. URCST is a general channel selection algorithm and can be implemented by other technologies that employ frequency hopping technique to mitigate the collision problem. For example, LoRaWAN, NB-IoT, and CAT-M2 employ ALOHA access protocol with the frequency hopping technique, and it would be interesting to investigate the implementation of URCST in these technologies. Also, it can be used to perform the time slot selection in EnOcean technology, where EnOcean utilises the time hopping technique over 40 time slots with three message copies.
2. The presented mathematical model can be further developed to evaluate the performance of LPWANs with the time slotted ALOHA, which implemented by

other technologies, and study its effect on the probability of collision with multiple message copies.

3. Investigate the effects of different power levels of the received packets and the capture effect on the probability of collisions and extend the mathematical model to include these parameters which offers a better understanding of the real system performance.
4. Investigate the effect of interference between devices from different cells and study the impact of this interference on the probability of lost messages.

References

Abbas, R.A., Al-Sherbaz, A., Bennecer, A., Picton, P. (2017) A new channel selection algorithm for the weightless-n frequency hopping with lower collision probability. In *2017 8th International Conference on the Network of the Future (NOF)*. London: IEEE, pp. 171–175.

Abouzar, P., Shafiee, K., Michelson, D.G., Leung, V.C.M. (2011) Action-based scheduling technique for 802.15.4/ZigBee wireless body area networks. In *2011 IEEE 22nd International Symposium on Personal, Indoor and Mobile Radio Communications*. IEEE, pp. 2188–2192.

Abramson, N. (1970) THE ALOHA SYSTEM. In *Proceedings of the November 17-19, 1970, fall joint computer conference on - AFIPS '70 (Fall)*. New York, New York, USA: ACM Press, pp. 281–285.

Abramson, N. (2009) The alohanet-surfing for wireless data. *IEEE Communications Magazine*. 47(12), 21–25.

Adame, T., Bel, A., Bellalta, B., Barcelo, J., Oliver, M. (2014) IEEE 802.11AH: the WiFi approach for M2M communications. *IEEE Wireless Communications*. 21(6), 144–152.

Adelantado, F., Vilajosana, X., Tuset-Peiro, P., Martinez, B., Melia-Segui, J., Watteyne, T. (2017) Understanding the Limits of LoRaWAN. *IEEE Communications Magazine*. 55(9), 34–40.

Aiello, M., Pagani, G.A. (2014) The Smart Grid's Data Generating Potentials. *Proceedings of the 2014 Federated Conference on Computer Science and Information Systems*. 2, 9–16.

Aijaz, A. (2014) *Protocol Design for Machine-to-Machine Networks*. University of London.

Ajah, S., Sherbaz, A. Al, Turner, S., Picton, P. (2015) Machine-to-machine communications energy efficiencies: the implications of different M2M communications specifications. *International Journal of Wireless and Mobile Computing*. 8(1), 15.

Al-Fuqaha, A., Guizani, M., Mohammadi, M., Aledhari, M., Ayyash, M. (2015) Internet of Things: A Survey on Enabling Technologies, Protocols, and Applications. *IEEE Communications Surveys & Tutorials*. 17(4), 2347–2376.

Al-Kaseem, B.R., Al-Raweshidy, H.S. (2016a) Energy efficient MAC protocol with smart sleep scheduling for cluster-based M2M networks. In *2016 6th International Conference on Information Communication and Management (ICICM)*. IEEE, pp. 227–232.

Al-Kaseem, B.R., Al-Raweshidy, H.S. (2016b) Scalable M2M routing protocol for energy efficient IoT wireless applications. In *2016 8th Computer Science and Electronic Engineering (CEEC)*. IEEE, pp. 30–35.

Al-Shammari, B.K.J., Al-Aboody, N., Al-Raweshidy, H.S. (2018) IoT Traffic Management and Integration in the QoS Supported Network. *IEEE Internet of Things Journal*. 5(1), 352–370.

Alavikia, Z., Ghasemi, A. (2018) Random multiple data packets transmission scheme in LTE-based machine-type communications. *Computer Communications*. 129(August), 152–165.

Alghamdi, A.S., Ali, M.N., Zohdy, M.A. (2015) Robust Non-Coherent Demodulation Scheme for Bluetooth Voice Transmission Using Linear, Extended, and Unscented Kalman Filtering. *Journal of Signal and Information Processing*. 06(01), 9–27.

Ali, A., Shah, G.A., Arshad, J. (2016) Energy efficient techniques for M2M communication: A survey. *Journal of Network and Computer Applications*. 68, 42–55.

Ali, A., Shah, G.A., Farooq, M.O., Ghani, U. (2017) Technologies and challenges in developing Machine-to-Machine applications: A survey. *Journal of Network and Computer Applications*. 83(September 2016), 124–139.

Ali, S., Li, Y., Chen, S., Lin, F. (2018) Narrowband Internet of Things : Repetition-Based Coverage Performance Analysis of Uplink Systems. *Journal of Communications*. 13(6), 293–302.

Ali, Z., Misic, J., Misic, V.B. (2019) Performance Evaluation of Heterogeneous IoT Nodes with Differentiated QoS in IEEE 802.11ah RAW Mechanism. *IEEE Transactions on Vehicular Technology*. 9545(c), 1–1.

Amini, A., Mohajerin Esfahani, P., Ghavami, M., Marvasti, F. (2019) UWB orthogonal pulse design using Sturm–Liouville boundary value problem. *Signal Processing*. 159, 147–158.

de Andrade, T.P.C., Astudillo, C.A., da Fonseca, N.L.S. (2016) Allocation of Control Resources for Machine-to-Machine and Human-to-Human Communications Over LTE/LTE-A Networks. *IEEE Internet of Things Journal*. 3(3), 366–377.

Andreadou, N., Kotsakis, E., Masera, M. (2018) Smart Meter Traffic in a Real LV Distribution Network. *Energies*. 11(5), 1156.

Andres-Maldonado, P., Ameigeiras, P., Prados-Garzon, J., Navarro-Ortiz, J., Lopez-Soler, J.M. (2017) Narrowband IoT Data Transmission Procedures for Massive Machine-Type Communications. *IEEE Network*. 31(6), 8–15.

Andres-Maldonado, P., Lauridsen, M., Ameigeiras, P., Lopez-Soler, J.M. (2019) Analytical Modeling and Experimental Validation of NB-IoT Device Energy Consumption. *IEEE Internet of Things Journal*. PP(X), 1–1.

ANT+ Alliance (2019a) ANT / ANT+ DEFINED. [online]. Available from: https://www.thisisant.com/developer/ant-plus/ant-antplus-defined [Accessed March 24, 2019].

ANT+ Alliance (2019b) ANT Ecosystem. [online]. Available from: https://www.thisisant.com/business/why-ant/ecosystem/ [Accessed March 24, 2019].

ANT+ Alliance (2019c) ANT history. [online]. Available from: https://www.thisisant.com/company/d1/history/ [Accessed March 24, 2019].

ANT+ Alliance (2019d) ANT WIRELESS GO BEYOND. [online]. Available from: https://www.thisisant.com/company/ [Accessed March 24, 2019].

Anteur, M., Deslandes, V., Thomas, N., Beylot, A.-L. (2014) Ultra Narrow Band Technique for Low Power Wide Area Communications. In *2015 IEEE Global Communications Conference (GLOBECOM)*. IEEE, pp. 1–6.

Anton-Haro, C., Dohler, M. (2015) Introduction to machine-to- machine (M2M) communications. In C. Anton-Haro & M. Dohler, eds. *Machine-to-machine (M2M) Communications Architecture, Performance and Applications*. Cambridge, UK: Woodhead Publishing, pp. 1–23.

Aravind, P.S., Shah, J., Kurup, D.G. (2018) Bit Error Rate (BER) Performance Analysis of DASH7 Protocol in Rayleigh Fading Channel. In *2018 International Conference on Advances in Computing, Communications and Informatics (ICACCI)*. IEEE, pp. 695–698.

Arcari, F.D., Costa, C., Pereira, C.E., Netto, J.C., Torres, G., Souza, M., Muller, I. (2017) Development of a WirelessHART - EnOcean Adapter for Industrial Applications. In *2017 VII Brazilian Symposium on Computing Systems Engineering (SBESC)*. IEEE, pp. 181–186.

Aust, S., Prasad, R.V., Niemegeers, I.G.M.M. (2015) Outdoor Long-Range WLANs: A Lesson for IEEE 802.11ah. *IEEE Communications Surveys & Tutorials*. **17**(3), 1761–1775.

Ayoub, W., Mroue, M., Nouvel, F., Samhat, A.E., Prevotet, J. (2018) Towards IP over LPWANs technologies: LoRaWAN, DASH7, NB-IoT. In *2018 Sixth International Conference on Digital Information, Networking, and Wireless Communications (DINWC)*. IEEE, pp. 43–47.

Ayoub, W., Nouvel, F., Samhat, A.E., Prevotet, J.-C., Mroue, M. (2018) Overview and Measurement of Mobility in DASH7. In *2018 25th International Conference on Telecommunications (ICT)*. IEEE, pp. 532–536.

Ayoub, W., Samhat, A.E., Nouvel, F., Mroue, M., Prevotet, J. (2018) Internet of Mobile Things: Overview of LoRaWAN, DASH7, and NB-IoT in LPWANs standards and Supported Mobility. *IEEE Communications Surveys & Tutorials*. (April 2016), 1–1.

Badenhop, C.W., Graham, S.R., Ramsey, B.W., Mullins, B.E., Mailloux, L.O. (2017) The Z-Wave routing protocol and its security implications. *Computers & Security*. 68, 112–129.

Baker, S.B., Xiang, W., Atkinson, I. (2017) Internet of Things for Smart Healthcare: Technologies, Challenges, and Opportunities. *IEEE Access*. 5, 26521–26544.

Balachandran, K., Olsen, R.L., Pedersen, J.M. (2014) Bandwidth analysis of smart meter network infrastructure. In *16th International Conference on Advanced Communication Technology*. Global IT Research Institute (GIRI), pp. 928–933.

Bao, L., Wei, L., Jiang, C., Miao, W., Guo, B., Li, W., Cheng, X., Liu, R., Zou, J. (2018) Coverage Analysis on NB-IoT and LoRa in Power Wireless Private Network. *Procedia Computer Science*. 131, 1032–1038.

Barai, G.R., Krishnan, S., Venkatesh, B. (2015) Smart metering and functionalities of smart meters in smart grid - a review. In *2015 IEEE Electrical Power and Energy Conference (EPEC)*. IEEE, pp. 138–145.

Baviskar, A., Baviskar, J., Wagh, S., Mulla, A., Dave, P. (2015) Comparative Study of Communication Technologies for Power Optimized Automation Systems: A Review and Implementation. In *2015 Fifth International Conference on Communication Systems and Network Technologies*. pp. 375–380.

Bel, A., Adame, T., Bellalta, B. (2018) An energy consumption model for IEEE 802.11ah

WLANs. *Ad Hoc Networks*. 72(9), 14–26.

Bembe, M., Abu-Mahfouz, A., Masonta, M., Ngqondi, T. (2019) A survey on low-power wide area networks for IoT applications. *Telecommunication Systems*.

Benhiba, B.E., Madi, A.A., Addaim, A. (2018) Comparative Study of The Various new Cellular IoT Technologies. In *2018 International Conference on Electronics, Control, Optimization and Computer Science (ICECOCS)*. IEEE, pp. 1–4.

Berkvens, R., Bellekens, B., Weyn, M. (2017) Signal strength indoor localization using a single DASH7 message. In *2017 International Conference on Indoor Positioning and Indoor Navigation (IPIN)*. IEEE, pp. 1–7.

Biral, A., Centenaro, M., Zanella, A., Vangelista, L., Zorzi, M. (2015) The challenges of M2M massive access in wireless cellular networks. *Digital Communications and Networks*. 1(1), 1–19.

Bluetooth SIG (2014a) Specification Volume 0: Master Table of Contents & Compliance Requirements. In *Specification of the Bluetooth System*. Washington, USA, pp. 1–154.

Bluetooth SIG (2014b) Specification Volume 1: Architecture & Terminology Overview. In *Specification of the Bluetooth System*. Washington, USA, pp. 155–308.

Bluetooth SIG (2014c) Specification Volume 2: Core System Package [BR/EDR Controller volume]. In *Specification of the Bluetooth System*. Washington, USA, pp. 310–1691.

Bonato, V., Mazzotti, B.F., Fernandes, M.M., Marques, E. (2013) A mersenne twister hardware implementation for the Monte Carlo localization algorithm. *Journal of Signal Processing Systems*. 70(1), 75–85.

Bonnefoi, R., Maciel, T.F., Fernandes, C.E.R. (2018) Latency Efficient Request Access Rate for Congestion Reduction in LTE MTC. In *2018 25th International Conference on Telecommunications (ICT)*. IEEE, pp. 481–485.

Bor, M., Vidler, J., Roedig, U. (2016) LoRa for the Internet of Things. In *Proceedings of the 2016 International Conference on Embedded Wireless Systems and Networks*. pp. 361–366.

Botter, G., Alonso-Zarate, J., Alonso, L., Granelli, F., Verikoukis, C. (2012) Extending the lifetime of M2M wireless networks through cooperation. In *2012 IEEE International Conference on Communications (ICC)*. pp. 6003–6007.

Budka, K.C., Deshpande, J.G., Thottan, M. (2014) *Communication Networks for Smart Grids*. London: Springer London.

Burns, J., Kirtay, S., Marks, P. (2015) *Future use of Licence Exempt Radio Spectrum*. London, UK: UK Spectrum Policy Forum.

Carlsson, A., Kuzminykh, I., Franksson, R., Liljegren, A. (2018) Measuring a LoRa Network: Performance, Possibilities and Limitations. In *International Conference on Next Generation Wired/Wireless Networking Conference on Internet of Things and Smart Spaces*. Springer International Publishing, pp. 116–128.

Casals, L., Mir, B., Vidal, R., Gomez, C. (2017) Modeling the Energy Performance of

LoRaWAN. *Sensors*. 17(10), 2364.

Cendo´n, B. (2015) M2M interworking technologies and underlying market considerations. In C. Anton-Haro & M. Dohler, eds. *Machine-to-machine (M2M) Communications Architecture, Performance and Applications*. Cambridge, UK: Woodhead Publishing, pp. 79–92.

Centenaro, M., Vangelista, L., Saur, S., Weber, A., Braun, V. (2017) Comparison of Collision-Free and Contention-Based Radio Access Protocols for the Internet of Things. *IEEE Transactions on Communications*. 65(9), 3832–3846.

Centenaro, M., Vangelista, L., Zanella, A., Zorzi, M. (2016) Long-range communications in unlicensed bands: the rising stars in the IoT and smart city scenarios. *IEEE Wireless Communications*. 23(5), 60–67.

Chang, K.-H. (2014) BLUETOOTH:A VIABLE SOLUTION FOR IOT. *IEEE Wireless Communications*. 21(December), 6–7.

Chang, T.-C., Lin, C.-H., Lin, K.C.-J., Chen, W.-T. (2019) Traffic-Aware Sensor Grouping for IEEE 802.11ah Networks: Regression Based Analysis and Design. *IEEE Transactions on Mobile Computing*. 18(3), 674–687.

Chen, C.-Y., Huang, A.C.-S., Huang, S.-Y., Chen, J.-Y. (2018) Energy-saving scheduling in the 3GPP narrowband Internet of Things (NB-IoT) using energy-aware machine-to-machine relays. In *2018 27th Wireless and Optical Communication Conference (WOCC)*. IEEE, pp. 1–3.

Chen, M, Wan, J., González, S. (2013) A survey of recent developments in home M2M networks. *IEEE Communications Surveys and Tutorials*. 16(1), 98–114.

Chen, Wang, Gao, Q., Xiong, H., Fei, L., Li, Q. (2013) TH-UWB RECEIVER BASED ON TWO PDFS APPROXIMATION IN MULTIUSER SYSTEMS. *Progress In Electromagnetics Research*. 137, 101–116.

Chen, X. (2013) *Low-Power MAC design for M2M Communications in Cellular Networks: Protocols and Algorithms*. Royal Institute of Technology (KTH).

Chung, Y., Ahn, J.Y., Du Huh, J. (2018) Experiments of A LPWAN Tracking(TR) Platform Based on Sigfox Test Network. In *2018 International Conference on Information and Communication Technology Convergence (ICTC)*. IEEE, pp. 1373–1376.

Collotta, M., Pau, G., Talty, T., Tonguz, O.K. (2018) Bluetooth 5: A Concrete Step Forward toward the IoT. *IEEE Communications Magazine*. 56(7), 125–131.

Croce, D., Gucciardo, M., Mangione, S., Santaromita, G., Tinnirello, I. (2018) Impact of LoRa Imperfect Orthogonality: Analysis of Link-Level Performance. *IEEE Communications Letters*. 22(4), 796–799.

Csibi, S., Gyorfi, L. (1996) Random time and frequency hopping for unslotted asynchronous access. In *Proceedings of ISSSTA'95 International Symposium on Spread Spectrum Techniques and Applications*. IEEE, pp. 1123–1127.

Cuomo, F., Della Luna, S., Cipollone, E., Todorova, P., Suihko, T. (2008) Topology

formation in IEEE 802.15.4: Cluster-tree characterization. In *6th Annual IEEE International Conference on Pervasive Computing and Communications, PerCom 2008*. pp. 276–281.

Damayanti, W., Kim, S., Yun, J.-H. (2016) Collision chain mitigation and hidden device-aware grouping in large-scale IEEE 802.11ah networks. *Computer Networks*. 108, 296–306.

DASH7 Alliance (2014) *DASH7 Alliance Protocol*. Paris, France.

DASH7 Alliance (2017) *DASH7 Alliance Protocol - WHERE RFID MEETS WSN*. Paris, France.

DASH7 Alliance (2015) *DASH7 Alliance Wireless Sensor and Actuator Network Protocol VERSION 1.0*. Brussels, Belgium.

Dawaliby, S., Bradai, A., Pousset, Y. (2016) In depth performance evaluation of LTE-M for M2M communications. In *2016 IEEE 12th International Conference on Wireless and Mobile Computing, Networking and Communications (WiMob)*. IEEE, pp. 1–8.

Dawaliby, S., Bradai, A., Pousset, Y. (2017) Scheduling optimization for M2M communications in LTE-M. In *2017 IEEE International Conference on Consumer Electronics (ICCE)*. IEEE, pp. 126–128.

Dawaliby, S., Bradai, A., Pousset, Y., Chatellier, C. (2018) Joint Energy and QoS-Aware Memetic-Based Scheduling for M2M Communications in LTE-M. *IEEE Transactions on Emerging Topics in Computational Intelligence*. PP, 1–13.

Department for Business Energy and Industrial Strategy (2018) *Smart Meters Quarterly report to End March 2018*. Great Britain.

Deshpande, K.V., Rajesh, A. (2017) Investigation on IMCP based clustering in LTE-M communication for smart metering applications. *Engineering Science and Technology, an International Journal*. 20(3), 944–955.

Dias, J., Grilo, A. (2018) LoRaWAN multi-hop uplink extension. *Procedia Computer Science*. 130, 424–431.

Digital Technology Poland (2019) Machine to Machine (M2M). [online]. Available from: https://dtpoland.com/what-we-do/machine-to-machine-m2m/ [Accessed April 16, 2019].

Ding, W., Jing, X., Yan, Z., Yang, L.T. (2019) A survey on data fusion in internet of things: Towards secure and privacy-preserving fusion. *Information Fusion*. 51(2), 129–144.

Do, M.-T., Goursaud, C., Gorce, J.-M. (2014) On the benefits of random FDMA schemes in ultra narrow band networks. In *2014 12th International Symposium on Modeling and Optimization in Mobile, Ad Hoc, and Wireless Networks (WiOpt)*. IEEE, pp. 672–677.

Domazetovic, B., Kocan, E. (2017) Packet error rate in IEEE 802.11ah use case scenarios. In *2017 25th Telecommunication Forum (TELFOR)*. IEEE, pp. 1–4.

Domazetovic, B., Kocan, E., Mihovska, A. (2016) Performance evaluation of IEEE 802.11ah systems. In *2016 24th Telecommunications Forum (TELFOR)*. IEEE, pp. 1–4.

Dynastream Innovations Inc. (2016a) *ANT Channel Search*. Alberta, Canada.

Dynastream Innovations Inc. (2014a) *ANT Message Protocol and Usage*. Alberta, Canada.

Dynastream Innovations Inc. (2013) *ANT USB2 Stick*. Alberta, Canada.

Dynastream Innovations Inc. (2016b) *Burst Transfers*. Alberta, Canada.

Dynastream Innovations Inc. (2014b) *C7 RF Transceiver Module*. Alberta, Canada.

Dynastream Innovations Inc. (2016c) *Continuous Scanning Mode for Asynchronous Topologies*. Alberta, Canada.

Dynastream Innovations Inc. (2018) HIGH NODE COUNT AND IOT SOLUTIONS. [online]. Available from: https://www.dynastream.com/solutions/high-node-count/ [Accessed March 24, 2019].

Dynastream Innovations Inc. (2010) *Interfacing with ANT General Purpose Chipsets and Modules*. Alberta, Canada.

Dynastream Innovations Inc. (2015) *Multi-Channel Design Considerations*. Alberta, Canada.

Dynastream Innovations Inc. (2011) *RSSI Extended Information*. Alberta, Canada.

Echeverría, P., López-Vallejo, M. (2013) High performance FPGA-oriented mersenne twister uniform random number generator. *Journal of Signal Processing Systems*. **71**(2), 105–109.

ElNashar, A., El-saidny, M. (2018) *Practical Guide to LTE-A, VoLTE and IoT*. A. ElNashar & M. El-saidny, eds. Chichester, UK: John Wiley & Sons, Ltd.

Elsaadany, M., Ali, A., Hamouda, W. (2017) Cellular LTE-A Technologies for the Future Internet-of-Things: Physical Layer Features and Challenges. *IEEE Communications Surveys & Tutorials*. 19(4), 2544–2572.

Elsaadany, M., Ali, A., Hamouda, W. (2018) Fast-Decoding Channel Estimation Technique for Downlink Control Channel in LTE-MTC Systems. In *2018 14th International Wireless Communications & Mobile Computing Conference (IWCMC)*. IEEE, pp. 1437–1442.

Enocean Alliance (2015a) *902 MHz – Next Generation Energy Harvesting Wireless Communication for North America*. Oberhaching, Germany.

Enocean Alliance (2019a) Energy Harvesting. [online]. Available from: https://www.enocean.com/en/technology/energy-harvesting/ [Accessed March 24, 2019].

Enocean Alliance (2015b) *Energy Harvesting Wireless Power for the Internet of Things*. Oberhaching, Germany.

Enocean Alliance (2016a) *EnOcean – The World of Energy Harvesting Wireless Technology*. Oberhaching, Germany.

Enocean Alliance (2012) *EnOcean Image Brochure*. Oberhaching, Germany.

Enocean Alliance (2016b) *EnOcean Radio Approval Overview*. Oberhaching, Germany.

Enocean Alliance (2017) *EnOcean Radio Protocol 2, Version 1.2*. Oberhaching, Germany.

Enocean Alliance (2016c) *EnOcean Serial Protocol 3 (ESP3)*. Oberhaching, Germany.

Enocean Alliance (2011) *EnOcean Technology – Energy Harvesting Wireless*. Oberhaching, Germany.

Enocean Alliance (2018a) EnOcean Wireless Standard. [online]. Available from: https://www.enocean-alliance.org/what-is-enocean/enocean-wireless-standard/ [Accessed March 24, 2019].

Enocean Alliance (2018b) *EnOcean Wireless Systems – RANGE PLANNING GUIDE*. Oberhaching, Germany.

Enocean Alliance (2016d) *Introducing the EnOcean ecosystem*. California.

Enocean Alliance (2019b) Patents. [online]. Available from: https://www.enocean.com/en/technology/patents/ [Accessed March 24, 2019].

Enocean Alliance (2019c) Radio Technology. [online]. Available from: https://www.enocean.com/en/technology/radio-technology/ [Accessed March 24, 2019].

Enocean Alliance (2015c) *The Easy Way to Energy Harvesting Wireless Products*. Oberhaching, Germany.

Enocean Alliance (2015d) *The Ecosystem of the EnOcean Alliance*. California.

Enocean Alliance (2019d) Ultra-low Power Management. [online]. Available from: https://www.enocean.com/en/technology/energy-harvesting-wireless/ [Accessed March 24, 2019].

Ergeerts, G., Nikodem, M., Subotic, D., Surmacz, T., Wojciechowski, B., Meulenaere, P. De, Weyn, M. (2015) DASH7 Alliance Protocol in Monitoring Applications. In *2015 10th International Conference on P2P, Parallel, Grid, Cloud and Internet Computing (3PGCIC)*. IEEE, pp. 623–628.

Ervin, R., Temple, M., Betances, A., Talbot, C. (2018) Detecting insteon home automation network attacks using a Software Defined Radio (SDR) radio frequency air monitor. In *Proceedings of the 13th International Conference on Cyber Warfare and Security, ICCWS 2018*. pp. 200–207.

Esfahani, A., Mantas, G., Matischek, R., Saghezchi, F.B., Rodriguez, J., Bicaku, A., Maksuti, S., Tauber, M., Schmittner, C., Bastos, J. (2017) A Lightweight Authentication Mechanism for M2M Communications in Industrial IoT Environment. *IEEE Internet of Things Journal*. 6(1), 288–296.

Evans-Pughe, C. (2013) The M2M connection. *Engineering & Technology*. 8(11), 39–43.

Evans, D. (2011) *The Internet of Things - How the Next Evolution of the Internet is Changing Everything*. California.

Fadel, E., Gungor, V.C., Nassef, L., Akkari, N., Malik, M.G.A., Almasri, S., Akyildiz, I.F. (2015) A survey on wireless sensor networks for smart grid. *Computer Communications*.

71, 22–33.

Fadlullah, Z.M., Fouda, M.M., Kato, N., Takeuchi, A., Iwasaki, N., Nozaki, Y. (2011) Toward intelligent machine-to-machine communications in smart grid. *IEEE Communications Magazine*. 49(4), 60–65.

Fan, Z., Tan, S. (2012) M2M communications for e-health: Standards, enabling technologies, and research challenges. In *2012 6th International Symposium on Medical Information and Communication Technology (ISMICT)*. pp. 1–4.

Faridnasr, M., Ghanbari, B., Sassani, A. (2016) Optimization of the moving-bed biofilm sequencing batch reactor (MBSBR) to control aeration time by kinetic computational modeling: Simulated sugar-industry wastewater treatment. *Bioresource Technology*. 208, 149–160.

Farooq, M.J., Zhu, Q. (2018) Optimal dynamic contract for spectrum reservation in mission-critical UNB-IoT systems. In *2018 16th International Symposium on Modeling and Optimization in Mobile, Ad Hoc, and Wireless Networks (WiOpt)*. IEEE, pp. 1–6.

Fawal, A.H. El, Mansour, A., Najem, M., Le Roy, F., Le Jeune, D. (2017) LTE-M adaptive eNodeB for emergency scenarios. In *2017 International Conference on Information and Communication Technology Convergence (ICTC)*. IEEE, pp. 536–541.

El Fawal, A.H., Najem, M., Mansour, A., Le Roy, F., Le Jeune, D. (2018) CTMC modelling for H2H/M2M coexistence in LTE-A/LTE-M networks. *The Journal of Engineering*. 2018(12), 1954–1962.

Fehri, C. El, Kassab, M., Abdellatif, S., Berthou, P., Belghith, A. (2018) LoRa technology MAC layer operations and Research issues. *Procedia Computer Science*. 130(00), 1096–1101.

Ferro, E., Potorti, F. (2005) Bluetooth and wi-fi wireless protocols: a survey and a comparison. *IEEE Wireless Communications*. 12(1), 12–26.

Fuller, J.D., Ramsey, B.W., Rice, M.J., Pecarina, J.M. (2017) Misuse-based detection of Z-Wave network attacks. *Computers & Security*. 64, 44–58.

García-Hernando, A.-B., Martínez-Ortega, J.-F., López-Navarro, J.-M., Prayati, A., Redondo-López, L. (2008) *Problem Solving for Wireless Sensor Networks*. Springer Nature, Switzerland.

Garg, V. (2007a) *Wireless Communications and Networking*. San Francisco: Elsevier.

Garg, V. (2007b) Wireless Personal Area Network - Bluetooth. In *Wireless Communications and Networking*. San Francisco: Elsevier, pp. 653–674.

Ghamari, M., Janko, B., Sherratt, R., Harwin, W., Piechockic, R., Soltanpur, C. (2016) A Survey on Wireless Body Area Networks for eHealthcare Systems in Residential Environments. *Sensors*. 16(6), 1–33.

Ghanaatian, R., Afisiadis, O., Cotting, M., Burg, A. (2019) Lora Digital Receiver Analysis and Implementation. In *ICASSP 2019 - 2019 IEEE International Conference on Acoustics, Speech and Signal Processing (ICASSP)*. IEEE, pp. 1498–1502.

Ghavimi, F., Chen, H.H. (2015) M2M communications in 3GPP LTE/LTE-A networks:

Architectures, service requirements, challenges, and applications. *IEEE Communications Surveys and Tutorials*. 17(2), 525–549.

Gomez, C., Paradells, J. (2015) Urban automation networks: Current and emerging solutions for sensed data collection and actuation in smart cities. *Sensors (Switzerland)*. 15(9), 22874–22898.

Gomez, C., Paradells, J. (2010) Wireless home automation networks: A survey of architectures and technologies. *IEEE Communications Magazine*. 48(June), 92–101.

Gopinath, A.J., Nithya, B. (2018) Mathematical and simulation analysis of contention resolution mechanism for IEEE 802.11ah networks. *Computer Communications*. 124(August 2017), 87–100.

Goursaud, C., Gorce, J.M. (2015) Dedicated networks for IoT: PHY / MAC state of the art and challenges. *EAI Endorsed Transactions on Internet of Things*. **1**(1), 150597.

Goursaud, C., Mo, Y. (2016) Random unslotted time-frequency ALOHA: Theory and application to IoT UNB networks. In *2016 23rd International Conference on Telecommunications (ICT)*. IEEE, pp. 1–5.

Grabia, M., Markowski, T., Mruczkiewicz, J., Plec, K. (2017) Design of a DASH7 low power wireless sensor network for Industry 4.0 applications. In *2017 IEEE International Conference on RFID Technology & Application (RFID-TA)*. IEEE, pp. 254–259.

Gratton, D.A. (2013) *The Handbook of Personal Area Networking Technologies and Protocols*. Cambridge: Cambridge University Press.

GSM Association (2018) *LTE-M Deployment Guide to Basic Feature Set Requirements*. London, UK.

Gupta, H.V., Kling, H. (2011) On typical range, sensitivity, and normalization of Mean Squared Error and Nash-Sutcliffe Efficiency type metrics. *Water Resources Research*. 47(10).

Guvenc, I., Gezici, S., Sahinoglu, Z., Kozat, U. (2011) *Reliable communications for short-range wireless systems*. Cambridge: Cambridge University Press.

Harwahyu, R., Cheng, R.-G., Tsai, W.-J., Hwang, J.-K., Bianchi, G. (2019) Repetitions v.s. Retransmissions: Trade-off in Configuring NB-IoT Random Access Channels. *IEEE Internet of Things Journal*. PP(c), 1–1.

Hauer, J., Handziski, V., Wolisz, A. (2009) Experimental study of the impact of WLAN interference on IEEE802.15.4 body area networks. In *6th European Conference ,EWSN 2009*. pp. 17–32.

Hazmi, A., Rinne, J., Valkama, M. (2012) Feasibility study of 802.11ah radio technology for IoT and M2M use cases. In *2012 IEEE Globecom Workshops*. IEEE, pp. 1687–1692.

Hongli Zhao, Hailin Jiang (2016) LTE-M system performance of integrated services based on field test results. In *2016 IEEE Advanced Information Management, Communicates, Electronic and Automation Control Conference (IMCEC)*. IEEE, pp. 2016–2021.

Hsieh, P.-C., Jia, Y., Parra, D., Aithal, P. (2018) An Experimental Study on Coverage Enhancement of LTE Cat-M1 for Machine-Type Communication. In *2018 IEEE*

International Conference on Communications (ICC). IEEE, pp. 1–5.

Hunn, N. (2010a) Bluetooth. In *Essentials of Short-Range Wireless*. Cambridge: Cambridge University Press, pp. 81–114.

Hunn, N. (2010b) IEEE 802.15.4, ZigBee PRO, RF4CE, 6LoWPAN and WirelessHART. In *Essentials of Short-Range Wireless*. Cambridge: Cambridge University Press, pp. 147–175.

Huq, M.Z., Islam, S. (2010) Home Area Network technology assessment for demand response in smart grid environment. In *2010 20th Australasian Universities Power Engineering Conference*. pp. 1–6.

IEEE 802.3 (2008) *Part 3: Carrier sense multiple access with Collision Detection (CSMA/CD) Access Method and Physical Layer Specifications*.

IEEE Computer Society (2017) IEEE Standard for Information technology--Telecommunications and information exchange between systems - Local and metropolitan area networks--Specific requirements - Part 11: Wireless LAN Medium Access Control (MAC) and Physical Layer (PHY) Specifications. *IEEE Std 802.11ah-2016 (Amendment to IEEE Std 802.11-2016, as amended by IEEE Std 802.11ai-2016)*, 1–594.

Ingenu (2015a) *An Educational Guide : How RPMA Works*. San Diego, California, USA.

Ingenu (2016a) *How RPMA Handles Interference*. San Diego, California, USA.

Ingenu (2016b) *HOW RPMA WORKS: The Making of RPMA*. San Diego, California, USA: eBOOK BY INGENU.

Ingenu (2015b) *RPMA Technology for the Internet of Things*. San Diego, California, USA.

Insteon (2019) Insteon: The Technology. [online]. Available from: www.insteon.com/technology/#ourtechnology [Accessed March 22, 2019].

Insteon (2013a) *INSTEON WHITEPAPER : The Details*. Irvine, California.

Insteon (2013b) *Insteon Whitepaper: Compared*. Second Edi. Irvine, California.

International Telecommunication Union (2012) *Short range narrow-band digital radiocommunication transceivers – PHY and MAC layer specifications*. Geneva.

Irwin, D., Barker, S., Mishra, A., Shenoy, P., Wu, A., Albrecht, J. (2011) Exploiting home automation protocols for load monitoring in smart buildings. In *Proceedings of the Third ACM Workshop on Embedded Sensing Systems for Energy-Efficiency in Buildings - BuildSys '11*. New York, New York, USA: ACM Press, pp. 7–12.

ISO, IEC (2012) *INTERNATIONAL STANDARD ISO/IEC DIS 14543-3-10*.

Jha, S.C., Koc, A.T., Gupta, M., Vannithamby, R. (2013) Power Saving mechanisms for M2M communication over LTE networks. In *2013 1st International Black Sea Conference on Communications and Networking, BlackSeaCom 2013*. pp. 102–106.

Ji, B., Chen, S., Song, K., Li, C., Chen, H., Li, Z. (2015) Throughput enhancement schemes for IEEE 802.11ah based on multi-layer cooperation. In *2015 International Wireless Communications and Mobile Computing Conference (IWCMC)*. IEEE, pp. 1112–1116.

Jia, M., Komeily, A., Wang, Y., Srinivasan, R.S. (2019) Adopting Internet of Things for the development of smart buildings: A review of enabling technologies and applications. *Automation in Construction*. 101(January), 111–126.

Kail, E., Banati, A., Laszlo, E., Kozlovszky, M. (2018) Security Survey of Dedicated IoT Networks in the Unlicensed ISM Bands. In *2018 IEEE 12th International Symposium on Applied Computational Intelligence and Informatics (SACI)*. IEEE, pp. 000449–000454.

Karimi, B., Namboodiri, V., Jadliwala, M. (2015) Scalable Meter Data Collection in Smart Grids Through Message Concatenation. *IEEE Transactions on Smart Grid*. **6**(4), 1697–1706.

Kartsakli, E., Lalos, A., Antonopoulos, A., Tennina, S., Renzo, M., Alonso, L., Verikoukis, C. (2014) A Survey on M2M Systems for mHealth: A Wireless Communications Perspective. *Sensors*. 14(10), 18009–18052.

Kartsakli, E., Lalos, A., Antonopoulos, A., Tennina, S., Renzo, M., Alonso, L., Verikoukis, C. (2015) Machine-to-machine (M2M) communications for e-health applications. In C. Anton-Haro & M. Dohler, eds. *Machine-to-machine (M2M) Communications Architecture, Performance and Applications*. Cambridge, UK: Woodhead Publishing, pp. 375–397.

Kaur, A., Gregory, M. a (2011) Performance analysis of random multiple access protocols used in wireless communication. In *7th International Conference on Broadband Communications and Biomedical Applications*. IEEE, pp. 12–17.

Kaynia, M., Jindal, N. (2008) Performance of ALOHA and CSMA in Spatially Distributed Wireless Networks. In *2008 IEEE International Conference on Communications*. IEEE, pp. 1108–1112.

Khan, B.M., Ali, F.H., Stipidis, E. (2010) Improved backoff algorithm for IEEE 802.15.4 wireless sensor networks. In *2010 IFIP Wireless Days*. IEEE, pp. 1–5.

Khorov, E., Lyakhov, A., Krotov, A., Guschin, A. (2015) A survey on IEEE 802.11ah: An enabling networking technology for smart cities. *Computer Communications*. 58(May 2014), 53–69.

Kim, H., Cho, S., Oh, J., Jo, G. (2018) Uplink Scheduling Technique for the LTE System to Improve the Performance of the NB-IoT System. *International Conference on Ubiquitous and Future Networks, ICUFN*. 2018-July, 613–615.

Kim, Jaewoo, Lee, J., Kim, Jaeho, Yun, J. (2014) M2M service platforms: Survey, issues, and enabling technologies. *IEEE Communications Surveys and Tutorials*. 16(1), 61–76.

Kocan, E., Domazetovic, B., Pejanovic-Djurisic, M. (2017) Range Extension in IEEE 802.11ah Systems Through Relaying. *Wireless Personal Communications*. 97(2), 1889–1910.

Korte, K.D., Tumar, I. (2009) Evaluation of IPv6 over Low-Power Wireless Personal Area Networks Implementations. In *2009 IEEE 34th Conference on Local Computer Networks*. Zurich, pp. 881–888.

Kos, A., Milutinović, V., Umek, A. (2019) Challenges in wireless communication for connected sensors and wearable devices used in sport biofeedback applications. *Future Generation Computer Systems*. 92, 582–592.

Koubaa, A., Cunha, A., Alves, M., Tovar, E. (2008) TDBS: A time division beacon scheduling mechanism for ZigBee cluster-tree wireless sensor networks. *Real-Time Systems*. 40(3), 321–354.

Kraemer, R., Katz, M.D. (2009) *Short-Range Wireless Communications. Emerging Technologies and Applications*. Chichester, UK: John Wiley & Sons Ltd.

Kshetrimayum, R.S. (2009) An introduction to UWB communication systems. *IEEE Potentials*. 28(2), 9–13.

Kumar, T., Mane, P.B. (2016) ZigBee topology: A survey. In *2016 International Conference on Control, Instrumentation, Communication and Computational Technologies (ICCICCT)*. IEEE, pp. 164–166.

Latvakoski, J., Iivari, A., Vitic, P., Jubeh, B., Ben Alaya, M., Monteil, T., Lopez, Y., Talavera, G., Gonzalez, J., Granqvist, N., Kellil, M., Ganem, H., Vaisanen, T. (2014) A Survey on M2M Service Networks. *Computers*. 3(4), 130–173.

Lauridsen, M., Kovacs, I.Z., Mogensen, P., Sorensen, M., Holst, S. (2016) Coverage and Capacity Analysis of LTE-M and NB-IoT in a Rural Area. In *2016 IEEE 84th Vehicular Technology Conference (VTC-Fall)*. IEEE, pp. 1–5.

Lauridsen, M., Nguyen, H., Vejlgaard, B., Kovacs, I.Z., Mogensen, P., Sorensen, M. (2017) Coverage Comparison of GPRS, NB-IoT, LoRa, and SigFox in a 7800 km^2 Area. In *2017 IEEE 85th Vehicular Technology Conference (VTC Spring)*. IEEE, pp. 1–5.

Lavric, A., Petrariu, A.I., Popa, V. (2019) Long Range SigFox Communication Protocol Scalability Analysis under Large-Scale, High-Density Conditions. *IEEE Access*. 7, 1–1.

Lavric, A., Popa, V. (2017a) Internet of Things and LoRa™ Low-Power Wide-Area Networks: A survey. In *2017 International Symposium on Signals, Circuits and Systems (ISSCS)*. IEEE, pp. 1–5.

Lavric, A., Popa, V. (2017b) LoRa™ wide-area networks from an Internet of Things perspective. In *2017 9th International Conference on Electronics, Computers and Artificial Intelligence (ECAI)*. IEEE, pp. 1–4.

Lavric, A., Popa, V., Males, C., Finis, I. (2012) A performance study of ZigBee wireless sensors network topologies for street lighting control systems. In *International Conference on Selected Topics in Mobile and Wireless Networking*. pp. 130–133.

Laya, A., Alonso, L., Alonso-Zarate, J. (2014) Is the random access channel of LTE and LTE-A suitable for M2M communications? A survey of alternatives. *IEEE Communications Surveys and Tutorials*. 16(1), 4–16.

Laya, A., Wang, K., Alonso, L., Alonso-Zarate, J., Markendahi, J. (2015) Supporting machine-to-machine communications in long-term evolution networks. In C. Anton-Haro & M. Dohler, eds. *Machine-to-machine (M2M) Communications Architecture, Performance and Applications*. Cambridge, UK: Woodhead Publishing, pp. 109–129.

Lee, H.-C., Ke, K.-H. (2018) Monitoring of Large-Area IoT Sensors Using a LoRa Wireless Mesh Network System: Design and Evaluation. *IEEE Transactions on Instrumentation and Measurement*. 67(9), 2177–2187.

Lee, H., Chung, S.-H., Lee, Y.-S., Ha, Y. (2013) Performance Comparison of DASH7 and ISO/IEC 18000-7 for Fast Tag Collection with an Enhanced CSMA/CA Protocol. In *2013 IEEE 10th International Conference on High Performance Computing and Communications & 2013 IEEE International Conference on Embedded and Ubiquitous Computing*. IEEE, pp. 769–776.

Lee, J., Su, Y., Shen, C. (2007) A Comparative Study of Wireless Protocols : Bluetooth, UWB, ZigBee, and Wi-Fi. In *33rd Annual Conference of the IEEE Industrial Electronics Conference (IECON)*. Taipei, pp. 46–51.

Lee, W. (2005) *Wireless and cellular communications*. Third Edit. New York: McGraw-Hill.

Legates, D.R., McCabe Jr., G.J. (2005) Evaluating the Use of 'Goodness of Fit' Measures in Hydrologic and Hydroclimatic Model Validation. *Water Resources Research*. 35(1), 233–241.

Li, Xiaohui, Chen, G., Zhao, B., Liang, X. (2014) A kind of intelligent lighting control system using the EnOcean network. In *2014 International Conference on Computer, Information and Telecommunication Systems (CITS)*. IEEE, pp. 1–5.

Li, Yi-Chang, Hong, S.H., Li, X.H., Kim, Y.C., Alam, M. (2014) Implementation of a BACnet-EnOcean gateway in buildings. In *2014 International Conference on Intelligent Green Building and Smart Grid (IGBSG)*. IEEE, pp. 1–7.

Li, Y., Jiang, J., Cheng, H., Zhang, M., Wei, S. (2012) An Efficient Hardware Random Number Generator Based on the MT Method. In *2012 IEEE 12th International Conference on Computer and Information Technology*. IEEE, pp. 1011–1015.

Li, Z., Zozor, S., Drossier, J.-M., Varsier, N., Lampin, Q. (2017) 2D time-frequency interference modelling using stochastic geometry for performance evaluation in Low-Power Wide-Area Networks. In *2017 IEEE International Conference on Communications (ICC)*. IEEE, pp. 1–7.

Lien, S.Y., Chen, K.C., Lin, Y. (2011) Toward ubiquitous massive accesses in 3GPP machine-to-machine communications. *IEEE Communications Magazine*. 49(April), 66–74.

Lin, X., Adhikary, A., Eric Wang, Y.-P. (2016) Random Access Preamble Design and Detection for 3GPP Narrowband IoT Systems. *IEEE Wireless Communications Letters*. 5(6), 640–643.

Liu, Y., Guo, J., Orlik, P., Nagai, Y., Watanabe, K., Sumi, T. (2018) Coexistence of 802.11ah and 802.15.4g networks. In *2018 IEEE Wireless Communications and Networking Conference (WCNC)*. IEEE, pp. 1–6.

Lloret, J., Tomas, J., Canovas, A., Parra, L. (2016) An Integrated IoT Architecture for Smart Metering. *IEEE Communications Magazine*. 54(12), 50–57.

LoRa Alliance (2015) *A technical overview of LoRa and LoRaWAN*. San Ramon, California, USA.

LoRa Alliance (2017) *LoRaWAN™ 1.1 Specification*. Beaverton, orlando, Florida, USA.

LoRa Alliance (2019) What is the LoRaWAN™ Specification? - Classes. [online]. Available from: https://lora-alliance.org/about-lorawan [Accessed March 31, 2019].

Lumpkins, W. (2015) Home Automation: Insteon (X10 Meets Powerline) [Product Reviews]. *IEEE Consumer Electronics Magazine*. 4(4), 140–144.

Martinez, B., Adelantado, F., Bartoli, A., Vilajosana, X. (2019) Exploring the Performance Boundaries of NB-IoT. *IEEE Internet of Things Journal*. PP(c), 1–1.

Martolos, J., Anděl, P. (2013) Distances between Vehicles in Traffic Flow and the Probability of Collision with Animals. *Transactions on Transport Sciences*. 6(2), 97–106.

MathWorks (2019) LTE-M Uplink Waveform Generation. *MathWorks UK*. [online]. Available from: https://uk.mathworks.com/help/lte/examples/ltem-uplink-waveform-generation.html?searchHighlight=LTE-M uplink channels&s_tid=doc_srchtitle [Accessed April 7, 2019].

Matlab (2018) Poisson probability density function. [online]. Available from: https://uk.mathworks.com/help/stats/poisspdf.html [Accessed July 28, 2018].

Matsumoto, M., Nishimura, T. (1998) Mersenne twister: a 623-dimensionally equidistributed uniform pseudo-random number generator. *ACM Transactions on Modeling and Computer Simulation*. 8(1), 3–30.

Mehboob, U., Zaib, Q., Usama, C. (2016) *Survey of IoT Communication Protocols Techniques, Applications, and Issues*. Pakistan: xFlow Research Inc.

Mehmood, N.Q., Culmone, R., Mostarda, L. (2016) A Flexible and Scalable Architecture for Real-Time ANT+ Sensor Data Acquisition and NoSQL Storage. *International Journal of Distributed Sensor Networks*. 12(5), 3651591.

Mekki, K., Bajic, E., Chaxel, F., Meyer, F. (2019) A comparative study of LPWAN technologies for large-scale IoT deployment. *ICT Express*. **5**(1), 1–7.

Mendes, T., Godina, R., Rodrigues, E., Matias, J., Catalão, J. (2015) Smart Home Communication Technologies and Applications: Wireless Protocol Assessment for Home Area Network Resources. *Energies*. 8(7), 7279–7311.

Mikhaylov, K., Petäjäjärvi, J. (2016) Analysis of Capacity and Scalability of the LoRa Low Power Wide Area Network Technology. In *22th European Wireless Conference - European Wireless 2016*. Oulu, Finland, pp. 119–124.

Mroue, H., Nasser, A., Hamrioui, S., Parrein, B., Motta-Cruz, E., Rouyer, G. (2018) MAC layer-based evaluation of IoT technologies: LoRa, SigFox and NB-IoT. In *2018 IEEE Middle East and North Africa Communications Conference (MENACOMM)*. IEEE, pp. 1–5.

Myers, T., Howard, D., On-rampWireless, Lampe, J. (2009) *Ultra-Link Processing Preliminary Proposal to 802.15.4TG4g SUN*.

Nash, J.E., Sutcliffe, J.V. (1970) River flow forecasting through conceptual models part I — A discussion of principles. *Journal of Hydrology*. 10(3), 282–290.

Nielsen, J.J., Madueño, G.C., Pratas, N.K., Sørensen, R.B., Stefanovic, C., Popovski, P. (2015) What can wireless cellular technologies do about the upcoming smart metering traffic? *IEEE Communications Magazine*. 53(9), 41–47.

Nolan, K.E., Guibene, W., Kelly, M.Y. (2016) An evaluation of low power wide area network technologies for the Internet of Things. In *2016 International Wireless Communications and Mobile Computing Conference (IWCMC)*. IEEE, pp. 439–444.

Nugraha, A.T., Wibowo, R., Suryanegara, M., Hayati, N. (2018) An IoT-LoRa System for Tracking a Patient with a Mental Disorder: Correlation between Battery Capacity and Speed of Movement. In *2018 7th International Conference on Computer and Communication Engineering (ICCCE)*. IEEE, pp. 198–201.

O'Dwyer, E., Pan, I., Acha, S., Shah, N. (2019) Smart energy systems for sustainable smart cities: Current developments, trends and future directions. *Applied Energy*. 237(November 2018), 581–597.

Obaid, T., Abou-Elnour, A., Rehan, M., Muhammad Saleh, M., Tarique, M. (2014) Zigbee Technology and Its Application in Wireless Home Automation Systems: a Survey. *International Journal of Computer Networks & Communications (IJCNC)*. 6(4), 115–131.

Obaidat, M., Misra, S. (2014) *Principles of Wireless Sensor Networks*. Cambridge: Cambridge University Press.

Ofcom (2014) *M2M application characteristics and their implications for spectrum Final Report*. London.

Oh, J., Song, H. (2018) Study on the Effect of LTE on the Coexistence of NB-IoT. *International Conference on Ubiquitous and Future Networks, ICUFN*. 2018-July, 610–612.

Pan, G., He, J., Wu, Q., Fang, R., Cao, J., Liao, D. (2018) Automatic stabilization of Zigbee network. In *2018 International Conference on Artificial Intelligence and Big Data (ICAIBD)*. IEEE, pp. 224–227.

Park, C.W., Hwang, D., Lee, T.-J. (2014) Enhancement of IEEE 802.11ah MAC for M2M Communications. *IEEE Communications Letters*. 18(7), 1151–1154.

Park, M. (2014) IEEE 802.11ah: Energy efficient MAC protocols for long range wireless LAN. In *2014 IEEE International Conference on Communications (ICC)*. IEEE, pp. 2388–2393.

Park, M. (2015) IEEE 802.11ah: sub-1-GHz license-exempt operation for the internet of things. *IEEE Communications Magazine*. 53(9), 145–151.

Park, P. (2011) *Modeling, Analysis, and Design of Wireless Sensor Network Protocols*. KTH Electrical Engineering.

Pau, G., Collotta, M., Maniscalco, V. (2017) Bluetooth 5 Energy Management through a Fuzzy-PSO Solution for Mobile Devices of Internet of Things. *Energies*. 10(7), 992.

Pereira, C., Aguiar, A. (2014) Towards Efficient Mobile M2M Communications: Survey and Open Challenges. *Sensors*. 14(10), 19582–19608.

Persia, S., Rea, L. (2016) Next generation M2M Cellular Networks: LTE-MTC and NB-IoT capacity analysis for Smart Grids applications. In *2016 AEIT International Annual Conference (AEIT)*. IEEE, pp. 1–6.

Piromalis, D.D., Arvanitis, K.G., Sigrimis, N. (2013) DASH7 Mode 2: A Promising Perspective for Wireless Agriculture. *IFAC Proceedings Volumes*. 46(18), 127–132.

Ploennigs, J., Ryssel, U., Kabitzsch, K. (2010) Performance analysis of the EnOcean wireless sensor network protocol. In *2010 IEEE 15th Conference on Emerging Technologies & Factory Automation (ETFA 2010)*. IEEE, pp. 1–9.

Punj, R., Kumar, R. (2019) Technological aspects of WBANs for health monitoring: a comprehensive review. *Wireless Networks*. 25(3), 1125–1157.

Purkovic, D., Honsch, M., Meyer, T.R.M.K. (2019) An Energy Efficient Communication Protocol for Low Power, Energy Harvesting Sensor Modules. *IEEE Sensors Journal*. 19(2), 701–714.

Qadir, Q.M., Rashid, T.A., Al-Salihi, N.K., Ismael, B., Kist, A.A., Zhang, Z. (2018) Low Power Wide Area Networks: A Survey of Enabling Technologies, Applications and Interoperability Needs. *IEEE Access*. 6, 77454–77473.

Qian, Y., Yan, J., Guan, H., Li, J., Zhou, X., Guo, S., Jayakody, D.N.K. (2017) Design of Hybrid Wireless and Power Line Sensor Networks with Dual-Interface Relay in IoT. *IEEE Internet of Things Journal*. 6(1), 1–1.

Qiao, L., Zheng, Z., Cui, W., Wang, L. (2018) A Survey on Wi-Fi HaLow Technology for Internet of Things. In *2018 2nd IEEE Conference on Energy Internet and Energy System Integration (EI2)*. IEEE, pp. 1–5.

Rao, S.N., Akhil, P., Kumaravelu, V.B., Arthi, M. (2018) Dual —Hop Relaying for Quality of Service Improvement in IEEE 802.11ah - Downlink. In *2018 International Conference on Communication and Signal Processing (ICCSP)*. IEEE, pp. 0249–0253.

Rashid, K.M., Louis, J., Fiawoyife, K.K. (2019) Wireless electric appliance control for smart buildings using indoor location tracking and BIM-based virtual environments. *Automation in Construction*. 101(January), 48–58.

Ratasuk, R., Mangalvedhe, N., Bhatoolaul, D., Ghosh, A. (2017) LTE-M Evolution Towards 5G Massive MTC. In *2017 IEEE Globecom Workshops (GC Wkshps)*. IEEE, pp. 1–6.

Ratasuk, R., Vejlgaard, B., Mangalvedhe, N., Ghosh, A. (2016) NB-IoT system for M2M communication. *2016 IEEE Wireless Communications and Networking Conference Workshops, WCNCW 2016*. (Wd5g), 428–432.

Rawat, P., Singh, K.D., Chaouchi, H., Bonnin, J.M. (2014) Wireless sensor networks: a survey on recent developments and potential synergies. *Journal of Supercomputing*. 68(1), 1–48.

Ray, P.P., Agarwal, S. (2016) Bluetooth 5 and Internet of Things: Potential and architecture. In *2016 International Conference on Signal Processing, Communication, Power and Embedded System (SCOPES)*. IEEE, pp. 1461–1465.

Raza, U., Kulkarni, P., Sooriyabandara, M. (2017) Low Power Wide Area Networks: An Overview. *IEEE Communications Surveys & Tutorials*. 19(2), 855–873.

Reynders, B., Meert, W., Pollin, S. (2016) Range and coexistence analysis of long range unlicensed communication. In *2016 23rd International Conference on Telecommunications (ICT)*. IEEE, pp. 1–6.

Roberts, L.G. (1975) ALOHA packet system with and without slots and capture. *ACM SIGCOMM Computer Communication Review*. 5(2), 28–42.

Rohini, S., Venkatasubramanian, K. (2015) Z-Wave based Zoning Sensor for Smart Thermostats. *Indian Journal of Science and Technology*. 8(20), 1–6.

Rong, N. iu F., Xin, Y.Y. (2016) Study on ANT-based Wireless Network for Wearable Medical Monitoring. *International Journal of Future Generation Communication and Networking*. 9(3), 37–46.

Sahinoglu, Z., Gezici, S., Guvenc, I. (2009) *Ultra-wideband Positioning Systems Theoretical Limits, Ranging Algorithms, and Protocols*. Cambridge University Press.

Sahinoglu, Z., Guvenc, I. (2011) ZigBee networks and low-rate UWB communications. In I. Guvenc, S. Gezici, Z. Sahinoglu, & U. Kozat, eds. *Reliable Communications for Short-range Wireless Systems*. Cambridge: Cambridge University Press, pp. 139–167.

Saito, M., Matsumoto, M. (2013) Variants of Mersenne Twister Suitable for Graphic Processors. *ACM Transactions on Mathematical Software*. 39(2), 1–20.

Sanchez-Iborra, R., Cano, M.D. (2016) State of the art in LP-WAN solutions for industrial IoT services. *Sensors (Switzerland)*. 16(5).

Savaux, V., Kountouris, A., Louet, Y., Moy, C. (2017) Modeling of Time and Frequency Random Access Network and Throughput Capacity Analysis. *EAI Endorsed Transactions on Cognitive Communications*. 3(11), 152555.

Semtech (2015) *LoRa Modulation Basics*. California, USA.

Semtech (2017) *Wireless & RF Selection Guide*. Camarillo, California, USA.

Sethi, P., Sarangi, S.R. (2017) Internet of Things: Architectures, Protocols, and Applications. *Journal of Electrical and Computer Engineering*. 2017, 1–25.

Severino, R.A.R. da S. (2008) *On the use of IEEE 802.15.4/ZigBee for Time-Sensitive Wireless Sensor Network Applications*. Polytechnic Institute of Porto.

Shahid, M.H., Masud, S. (2015) Improved low power scheduler for OSS-7: An open source DASH7 stack. In *2015 IEEE International Conference on Electronics, Circuits, and Systems (ICECS)*. IEEE, pp. 645–648.

Shao, H., Beaulieu, N.C. (2011) Direct sequence and time-hopping sequence designs for narrowband interference mitigation in impulse radio UWB systems. *IEEE Transactions on Communications*. 59(7), 1957–1965.

Sharma, H., Sharma, S. (2014) A review of sensor networks: Technologies and applications. In *2014 Recent Advances in Engineering and Computational Sciences (RAECS)*. IEEE, pp. 1–4.

Shende, S.F., Deshmukh, R.P., Dorge, P.D. (2017) Performance improvement in ZigBee cluster tree network. In *2017 International Conference on Communication and Signal Processing (ICCSP)*. IEEE, pp. 0308–0312.

Shin, E., Jo, G. (2017) Structure of NB-IoT NodeB system. In *2017 International Conference*

on Information and Communication Technology Convergence (ICTC). IEEE, pp. 1269–1271.

Shiobara, T., Palensky, P., Nishi, H. (2015) Effective metering data aggregation for smart grid communication infrastructure. In *IECON 2015 - 41st Annual Conference of the IEEE Industrial Electronics Society*. IEEE, pp. 002136–002141.

Sierra Wireless (2017) *Coverage Analysis of LTE-M Category-M1*. Richmond, British Columbia, Canada.

Sigfox (2019a) *Sigfox connected objects : Radio specifications*. Laberge, France.

Sigfox (2019b) Sigfox Radio Configurations. [online]. Available from: https://build.sigfox.com/sigfox-radio-configurations-rc [Accessed April 2, 2019].

Sigfox (2017a) Sigfox Radio Technology Keypoints. [online]. Available from: https://www.sigfox.com/en/sigfox-iot-radio-technology [Accessed April 1, 2019].

Sigfox (2017b) *Sigfox Technical Overview*. Laberge, France.

Sigfox (2017c) Sigfox Technology Overview. [online]. Available from: https://www.sigfox.com/en/sigfox-iot-technology-overview [Accessed April 1, 2019].

Silicon LABS (2018) *AN1141 : Thread Mesh Network Performance*. Austin, Texas, USA.

Sinha, R.S., Wei, Y., Hwang, S.-H. (2017) A survey on LPWA technology: LoRa and NB-IoT. *ICT Express*. 3(1), 14–21.

Sivasankari, A., Sudarvizhi, S., Sarala, L. (2014) A Comparative Study of Wireless Technologies Based on Home Automation Bluetooth Low Energy , Zigbee , Insteon and ENOCEAN. *International Journal of Computer Science and Information Technology Research*. 2(3), 255–259.

Soares, S.M., Carvalho, M.M. (2019) Throughput Analytical Modeling of IEEE 802.11ah Wireless Networks. In *2019 16th IEEE Annual Consumer Communications & Networking Conference (CCNC)*. IEEE, pp. 1–4.

Song, M., Shetty, S., Gopalpet, D. (2007) Coexistence of IEEE 802.11b and bluetooth: An integrated performance analysis. *Mobile Networks and Applications*. 12(5–6), 450–459.

Song, Y., Lin, J., Tang, M., Dong, S. (2017) An Internet of Energy Things Based on Wireless LPWAN. *Engineering*. 3(4), 460–466.

Spadacini, M., Savazzi, S., Nicoli, M. (2014) Wireless home automation networks for indoor surveillance: technologies and experiments. *EURASIP Journal on Wireless Communications and Networking*. 1(6), 1–17.

Sun, Q., Li, H., Ma, Z., Wang, C., Campillo, J., Zhang, Q., Wallin, F., Guo, J. (2016) A Comprehensive Review of Smart Energy Meters in Intelligent Energy Networks. *IEEE Internet of Things Journal*. 3(4), 464–479.

Sun, W., Choi, M., Choi, S. (2017) IEEE 802.11ah: A Long Range 802.11 WLAN at Sub 1 GHz. *Journal of ICT Standardization*. 1(1), 83–108.

Talbot, C.M., Temple, M.A., Carbino, T.J., Betances, J.A. (2018) Detecting rogue attacks

on commercial wireless Insteon home automation systems. *Computers & Security*. 74, 296–307.

Thonet, G., Allard-jacquin, P., Colle, P. (2008) *ZigBee – WiFi Coexistence White Paper and Test Report*. Grenoble.

Tian, L., Khorov, E., Latré, S., Famaey, J. (2017) Real-Time Station Grouping under Dynamic Traffic for IEEE 802.11ah. *Sensors*. 17(7), 1559.

Tian, X., Benkrid, K. (2009) Mersenne Twister random number generation on FPGA, CPU and GPU. In *2009 NASA/ESA Conference on Adaptive Hardware and Systems, AHS 2009*. pp. 460–464.

Tuna, G., Gungor, V.C., Gulez, K. (2013) Wireless Sensor Networks for Smart Grid Applications: A Case Study on Link Reliability and Node Lifetime Evaluations in Power Distribution Systems. *International Journal of Distributed Sensor Networks*. 9(2), 796248.

Tuset-Peiró, P., Anglès-Vazquez, A., López-Vicario, J., Vilajosana-Guillén, X. (2014) On the suitability of the 433 MHz band for M2M low-power wireless communications: propagation aspects. *Transactions on Emerging Telecommunications Technologies*. 25(12), 1154–1168.

U., S., A. V., B. (2019) Performance analysis of IEEE 802.11ah wireless local area network under the restricted access window-based mechanism. *International Journal of Communication Systems*. 32(4), e3888.

Umar, P.R., Gupta, P. (2016) The Capacity of Wireless Networks. *IEEE/ACM Transactions on Networking*. 24(3), 1518–1532.

Usman, A., Shami, S.H. (2013) Evolution of Communication Technologies for Smart Grid applications. *Renewable and Sustainable Energy Reviews*. 19, 191–199.

Vejlgaard, B., Lauridsen, M., Nguyen, H., Kovacs, I.Z., Mogensen, P., Sorensen, M. (2017) Coverage and Capacity Analysis of Sigfox, LoRa, GPRS, and NB-IoT. In *2017 IEEE 85th Vehicular Technology Conference (VTC Spring)*. IEEE, pp. 1–5.

Verma, P.K., Verma, R., Prakash, A., Agrawal, A., Naik, K., Tripathi, R., Alsabaan, M., Khalifa, T., Abdelkader, T., Abogharaf, A. (2016) Machine-to-Machine (M2M) communications: A survey. *Journal of Network and Computer Applications*. 66(March), 83–105.

Vermesan, O., Friess, P. (2014) *Internet of Things - From Research and Innovation to Market Deployment*. M. Ruggieri & H. Nikookar, eds. Aalborg: River Publishers.

Vilajosana, X., Tuset-Peiro, P., Vazquez-Gallego, F., Alonso-Zarate, J., Alonso, L. (2014) Standardized Low-Power Wireless Communication Technologies for Distributed Sensing Applications. *Sensors*. 14(2), 2663–2682.

Vlajic, N., Stevanovic, D. (2009) Performance Analysis of ZigBee-Based Wireless Sensor Networks with Path-Constrained Mobile Sink(s). In *2009 Third International Conference on Sensor Technologies and Applications*. IEEE, pp. 61–68.

Vodafone Group (2017) *Narrowband-IoT: pushing the boundaries of IoT*. Newbury, Berkshire,

UK.

Waidner, M., Kasper, M. (2016) Security In Industrie 4.0 — Challenges and Solutions for the Fourth Industrial Revolution. In *Proceedings of the 2016 Design, Automation & Test in Europe Conference & Exhibition (DATE)*. Singapore: Research Publishing Services, pp. 1303–1308.

Wan, L., Zhang, Z., Wang, J. (2019) Demonstrability of Narrowband Internet of Things technology in advanced metering infrastructure. *Eurasip Journal on Wireless Communications and Networking*. 2019(1).

Wang, Y.-P.E., Lin, X., Adhikary, A., Grovlen, A., Sui, Y., Blankenship, Y., Bergman, J., Razaghi, H.S. (2017) A Primer on 3GPP Narrowband Internet of Things. *IEEE Communications Magazine*. 55(3), 117–123.

Wang, Y., Chen, Q., Hong, T., Kang, C. (2018) Review of Smart Meter Data Analytics: Applications, Methodologies, and Challenges. *IEEE Transactions on Smart Grid*. 3053(June 2017), 1–1.

Watteyne, T. (2015) Lower-power wireless mesh networks for machine-to-machine communications using the IEEE802.15.4 standard. In C. Anton-Haro & M. Dohler, eds. *Machine-to-machine (M2M) Communications Architecture, Performance and Applications*. Cambridge, UK: Woodhead Publishing, pp. 63–77.

Webb, W. (2012a) On using white space spectrum. *IEEE Communications Magazine*. 50(8), 145–151.

Webb, W. (2012b) The Role of Networking Standards in Building the Internet of Things. *Communications & Strategies*. Third Quar(87), 57–66.

Webb, W. (2012c) *Understanding Weightless: Technology, Equipment, and Network Deployment for M2M Communications in White Space*. Cambridge: Cambridge University Press.

Webb, W. (2013) *Weightless : A bespoke technology for the IoT*. Cambridge.

Webb, W. (2015) Weightless machine-to-machine (M2M) wireless technology using TV white space. In C. Anton-Haro & M. Dohler, eds. *Machine-to-machine (M2M) Communications Architecture, Performance and Applications*. Cambridge, UK: Woodhead Publishing, pp. 93–108.

Weightless-SIG (2015a) Developing with Weightless. [online]. Available from: http://www.weightless.org/about/developing-with-weightless [Accessed April 3, 2019].

Weightless-SIG (2015b) *LPWAN Technology Decisions: 17 critical features*. Cambridge, UK.

Weightless-SIG (2015c) *Weightless-N System specification v1.0*. Cambridge, UK.

Weightless-SIG (2015d) Weightless-P Standard is Designed for High Performance, Low Power, 2-Way Communication for IoT. [online]. Available from: http://www.weightless.org/news/weightlessp-standard-is-designed-for-high-performance-low-power-2way-communication-for-iot [Accessed April 3, 2019].

Weightless-SIG (2015e) *Weightless-P System specification v1.0*. Cambridge, UK.

Weightless-SIG (2013) *Weightless Core Specification v1.0*. Cambridge, UK.

Weightless-SIG (2015f) Weightless Expands Wide-Area IoT Spec. [online]. Available from: http://www.weightless.org/news/weightless-expands-widearea-iot-spec [Accessed April 3, 2019].

Weightless-SIG (2015g) Weightless Specification. [online]. Available from: http://www.weightless.org/about/weightless-specification [Accessed April 3, 2019].

Wenpeng Luan, Sharp, D., LaRoy, S. (2013) Data traffic analysis of utility smart metering network. In *2013 IEEE Power & Energy Society General Meeting*. IEEE, pp. 1–4.

Weyn, M., Ergeerts, G., Berkvens, R., Wojciechowski, B., Tabakov, Y. (2015) DASH7 alliance protocol 1.0: Low-power, mid-range sensor and actuator communication. In *2015 IEEE Conference on Standards for Communications and Networking (CSCN)*. IEEE, pp. 54–59.

Weyn, M., Ergeerts, G., Wante, L., Vercauteren, C., Hellinckx, P. (2013) Survey of the DASH7 Alliance Protocol for 433 MHz Wireless Sensor Communication. *International Journal of Distributed Sensor Networks*. 2013, 1–9.

Win, M.Z., Pinto, P.C., Shepp, L.A. (2009) A Mathematical Theory of Network Interference and Its Applications. *Proceedings of the IEEE*. 97(2), 205–230.

Win, M.Z., Scholtz, R.A. (2000) Ultra-wide bandwidth time-hopping spread-spectrum impulse radio for wireless multiple-access communications. *IEEE Transactions on Communications*. 48(4), 679–691.

Wiriaatmadja, D.T., Choi, K.W. (2015) Hybrid Random Access and Data Transmission Protocol for Machine-to-Machine Communications in Cellular Networks. *IEEE Transactions on Wireless Communications*. 14(1), 33–46.

Wu, X., Shi, J. (2007) Anti-Interference Performance Analysis in Bluetooth Frequency Hopping System. In *2007 International Workshop on Anti-Counterfeiting, Security and Identification*. pp. 328–331.

Xiong, X., Zheng, K., Xu, R., Xiang, W., Chatzimisios, P. (2015) Low power wide area machine-to-machine networks: Key techniques and prototype. *IEEE Communications Magazine*. 53(9), 64–71.

Xu, J., Yao, J., Wang, L., Ming, Z., Wu, K., Chen, L. (2018) Narrowband Internet of Things: Evolutions, Technologies, and Open Issues. *IEEE Internet of Things Journal*. 5(3), 1449–1462.

Xu, T., Darwazeh, I. (2018) Non-Orthogonal Narrowband Internet of Things: A Design for Saving Bandwidth and Doubling the Number of Connected Devices. *IEEE Internet of Things Journal*. 5(3), 2120–2129.

Yin, R., Yu, G., Maaref, A., Li, G.Y. (2016) LBT-Based Adaptive Channel Access for LTE-U Systems. *IEEE TRANSACTIONS ON WIRELESS COMMUNICATIONS*. 15(10), 6585–6597.

Yu, C., Yu, L., Wu, Y., He, Y., Lu, Q. (2017) Uplink Scheduling and Link Adaptation for Narrowband Internet of Things Systems. *IEEE Access*. 5, 1724–1734.

Z-Wave Alliance (2019) About Z-Wave Technology. *Z-Wave Alliance*. [online]. Available from: https://z-wavealliance.org/about_z-wave_technology/ [Accessed March 22, 2019].

Z-Wave Alliance (2016) *Z-Wave Frequency Coverage*. California.

Z-Wave Alliance (2018) *Z-Wave Transceivers – Specification of Spectrum Related Components*. California.

Zhang, B., Zuo, J., Mao, W. (2019) SmartWAZ: Design and implementation of a smart WiFi access system assisted by Zigbee. *IEEE Access*. PP(c), 1–1.

Zhang, M., Hu, Q. (2017) A hybrid network smart home based on Zigbee and smart plugs. In *2017 7th International Conference on Communication Systems and Network Technologies (CSNT)*. IEEE, pp. 389–392.

Zhang, W., Shen, H., Kwak, K.S. (2007) Improved Delay-Locked Loop in a UWB Impulse Radio Time-Hopping Spread-Spectrum System. *ETRI Journal*. 29(6), 716–724.

Zhu, X., Tao, X., Gu, T., Lu, J. (2015) Target-Aware, Transmission Power-Adaptive, and Collision-Free Data Dissemination in Wireless Sensor Networks. *IEEE Transactions on Wireless Communications*. 14(12), 6911–6925.

ZigBee Alliance (2016) ZiBee IP and 920IP. [online]. Available from: http://www.zigbee.org/zigbee-for-developers/network-specifications/zigbeeip/ [Accessed March 26, 2019].

ZigBee Alliance (2014) *ZigBee IP Specification*. California, USA.

ZigBee Alliance (2018) ZigBee Pro. [online]. Available from: https://www.zigbee.org/zigbee-for-developers/zigbee-pro/ [Accessed March 26, 2019].

ZigBee Alliance (2012) *ZigBee Specification*. California, USA.